Organic and inorganic biohybrid assemblies of the Cowpea Chlorotic Mottle Virus

Een wetenschappelijke proeve op het gebied van de
Natuurwetenschappen, Wiskunde en Informatica

Proefschrift

ter verkrijging van de graad van doctor
aan de Radboud Universiteit Nijmegen
op gezag van de rector magnificus prof. mr. S.C.J.J. Kortmann,
volgens besluit van het College van Decanen
in het openbaar te verdedigen op vrijdag 21 augustus 2009
om 13.30 uur precies

door

Friso Doetze Sikkema
geboren op 27 juli 1976
te Ellecom

Promotores

Prof. dr. R.J.M. Nolte
Prof. dr. J.J.L.M. Cornelissen

Manuscriptcommissie

Prof. dr. A.-J. Schouten (Rijksuniversiteit Groningen)
Prof. dr. J.C.M. van Hest
Dr. A. de la Escosura Navaso (Universidad Autónoma Madrid, Spanje)

Realisatie: Ipskamp Print Partners

Omslag: Wouter Sikkema

ISBN: 978-90-9024450-1

Opgedragen aan Inès en Aurélie

Contents

Chapter 1

General introduction

1.1 Complexity in chemistry

Over the last hundred and fifty years, the development of the chemical sciences has shown an interesting and rapid trend towards molecules and molecular systems of ever increasing complexity. Ever since what is generally considered to be the first chemical synthesis of an organic compound, i.e. urea, the size and complexity of the substances under investigation have vastly increased. For example, the molecule on the right in Figure 1.1, brevetoxin 1, a toxin isolated from a species of plankton, has been synthesized in the laboratory[1a-g], by a sequence of 123 steps and a total yield of 9.10^{-4} percent.

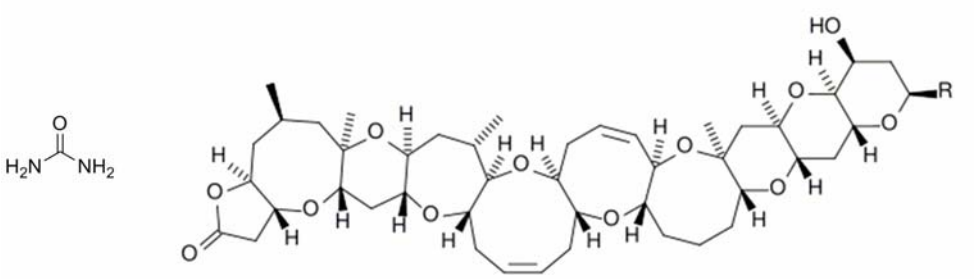

Figure 1.1. *The structures of urea (left) and Brevetoxin 1, where R = $CH_2C(=CH_2)CHO$ (right).*

As a comparison, the structures of urea and brevetoxin 1 are depicted in Figure 1. A protein structure is even more complex than the brevetoxin molecule. Thus, although incredible progress has been made in the synthesis of complex compounds, synthetic chemists are still outclassed by the abilities of natural systems. Because of this, chemists are increasingly looking at biological systems for inspiration and a gradual merging of molecular biology/biochemistry and "classical" chemistry is currently noticeable.

At the beginning of the twentieth century, novel methods became available to determine the relative molecular weight of compounds. One of the species measured was rubber, which was found to possess a very high molecular weight. At that time, the prevailing idea was that the measured high molecular weight was only an apparent phenomenon; it was thought to be caused by the presence of colloïdal particles. In a landmark paper in 1920, Staudinger proposed that rubber (and other polymeric substances such as starch) consisted of small molecules, which were repeatedly covalently linked to form a long chain[2]. This idea was rejected by many of his contemporary colleagues, among which eminent scientists such as Emil Fischer, mainly because the understanding of the molecular structure of compounds and the bonding interactions at that time were inconsistent with the existence of such long molecules. However, only Staudingers explanation fitted all the data that had been generated, leading to the general acceptance of the concept of "*makromoleküle*". Nowadays, polymers are part of everyday life, both in synthetic and natural form. It is remarkable, that such an important class of compounds was only conceived one hundred years after the first synthesis of a chemical compound. Nevertheless, an entire new world of molecular complexity had been opened.

There are several types of polymers that are essential for life, such as DNA, proteins, and polysaccharides. DNA is one of the most precisely defined polymers known. Each of its four different monomeric units (nucleobases) is placed at an exact position in the polymeric chain. In fact, the alteration of just one of these bases (known as a Single Nucleotide Polymorphism, or SNP) in a chain containing millions of bases can lead to substantial changes in the living species. It is, therefore, not surprising that nature has evolved various highly effective SNP-detection and repair mechanisms, so that spontaneous mutations are suppressed. Another such class of highly important polymers are the proteins, which are built up from twenty-odd different monomers, i.e. the amino acids. The DNA-chain contains information about the sequence of these amino acid monomers, i.e. the sequence in which they are incorporated into the protein chain. A very important difference between DNA and proteins is that in the latter biopolymers, it is not the exact sequence of monomers (amino acids) that defines the function of the protein, but rather the three-dimensional shape. This shape, with various sites at which for example a charge is present, is defined by the sequence of the monomers, as they appear in the protein. The nature of the interaction of a protein with another molecule, e.g., a substrate, is mediated through a series of weak, non-covalent forces, e.g. van der Waals forces, dipole-dipole interactions and hydrogen bonding. The sum of these relatively modest forces can be reasonably high. For instance, the binding of the low molecular weight compound biotin to the protein streptavidin is nearly as strong as a covalent bond[3]. The study of all these interactions falls within the realm of supramolecular chemistry. Supramolecular interactions are also encountered in another class of compounds important in everyday life, the surfactants.

1.2 Surfactant self-assemblies

Surfactants, or amphiphiles, are a special class of compounds in which two important features are combined, i.e. hydrophobic properties in the form of a hydrophobic “tail” and hydrophylic properties in the form of a “head”. This makes that when they are dissolved in water, self-assembly into well-defined structures, such as micelles, in which the hydrophobic tails coagulate inside a spherical structure takes place

(Figure 1.2). An inverted micelle is obtained when the surfactants are dissolved in an apolar solvent. The ordering process of micellization is partly the result of an increase in entropy which occurs when water molecules around the hydrophobic tails are set free. A competitive force in micellization is the repulsion between the head groups, which are closely packed at the interface[4,5].

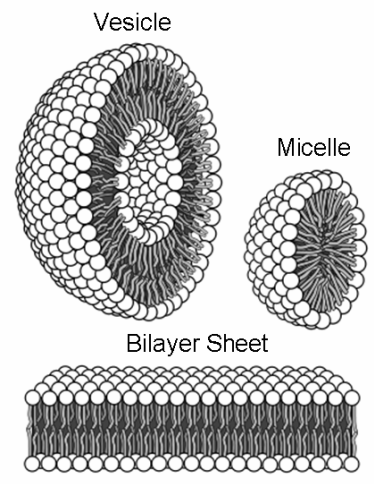

	*v*/*al*<1/3	spherical micelles
	1/3<*v*/*al*	cylindrical micelles
	1/2<*v*/*al*<1	vesicles, flexibile bilayers
	*v*/*al* ≈1	lamellae, planar bilayers
	*v*/*al*>1	inverse cylindrical and spherical micelles

Figure 1.2. *Left: The structures of a micelle, a vesicle and a bilayer sheet. In this example, assemblies from double chain surfactants are depicted. Right: packing parameter range for different types of surfactants.*

As a result of these interactions, micelles typically contain between 50 and 80 surfactant molecules. The shape and size of a micelle is thus a function of the molecular geometry of its surfactant molecules and solution conditions such as surfactant concentration, temperature, pH, and ionic strength. For instance, oval shapes and hexagonal arrays can be obtained. A rough prediction of the supramolecular structure of a surfactant self-assembly can be made by inspection of the relative areas of the polar head groups and the lipophilic tails. The packing parameter *v/(al)*, with *v* and *l* describing the volume and length of the hydrocarbon tails and *a* describing the effective headgroup area, encompasses these parameters[6]. For large polar headgroups *v/al* < ⅓ implying the formation of spherical micelles, whereas the presence of longer hydrocarbon tails (*v/al* > 1) gives rise to inverse spherical and micellar structures (Figure 1.2). The parameters *v* and *l* can be readily calculated from the van der Waals radii, whereas *a* also depends on external parameters such as pH, ionic strength, and temperature.

1.3 Large amphiphilic architectures

A very important class of surfactant self-assemblies is the vesicle (Figure 1.2). These aggregates, which are also called liposomes, are used as synthetic models of cells. Vesicles have been applied as nano-vessels, in which chemical reactions take place. These aggregates have also been used to store enzymes and to enable biomineralization[7]. An important aspect of these complex structures is that they are synthetically accessible, and that they can be prepared from other than low molecular weight amphiphilic molecules. A number of polymeric amphiphilic structures have been prepared in our group. Vriezema et al. have shown that a synthetic AB type block copolymer, consisting of a polystyrene and a polyisocyanide block, self assembles in a THF/water mixture to generate vesicles that possessed diameters in the order of micrometers[8]. It was possible to encapsulate an enzyme that performed a catalytic reaction inside the vesicle. Furthermore, the unique character of the polyisocyanide block allowed the crosslinking of the vesicles, once they had formed. In this way, the porosity of the vesicles could be controlled. These so-called "super amphiphiles" had a molecular volume of approximately 5 nm^3, compared to just 0.5 nm^3 for a phosphatidylcholine molecule, a common natural small amphiphile (see Figure 1.3). In another study, Velonia et al. showed that the covalent attachment of a lipase enzyme to a polystyrene lipophylic block yielded so-called giant amphiphiles, which have an even larger molecular volume, i.e. ca. 25 nm^3. It was found, that these biohybrid block copolymers formed catalytically active micellar rods[9], and that these micellar rods aggregated in solution to generate long bundles of fibers.

It has thus been shown that (biohybrid) amphiphilic structures can self-assemble in solution to produce supramolecular structures[10]. As part of the amphiphile project it was envisaged that an even larger amphiphilic structure, i.e. the mega-amphiphile, as shown on the right hand side of Figure 1.3 should be accessible.

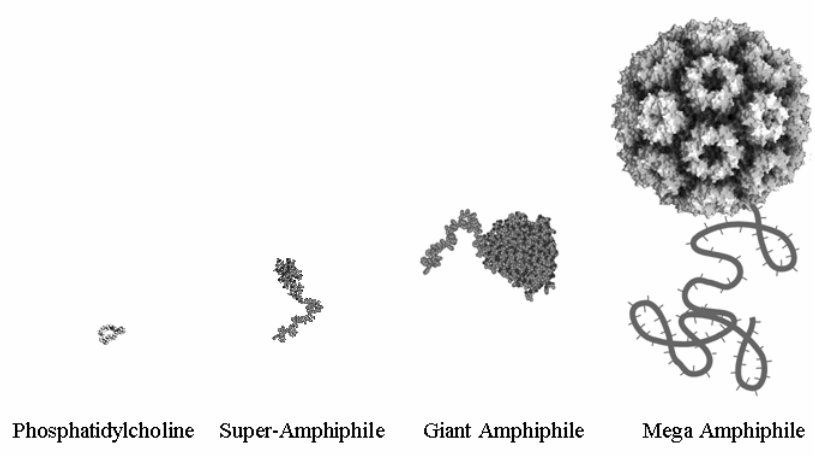

Figure 1.3. *From left to right: phosphatidylcholine, a common natural small molecular amphiphile; a super amphiphile, prepared from polystyrene and polyisocyanide; a giant amphiphile, obtained from a large protein and polystyrene; and a mega amphiphile, which is prepared from a viral cage and a very large hydrophobic polymer.*

In order to construct such a mega amphiphile, the polar headgroup must be very large, much larger than a large protein. As a comparison, the head group of this architecture alone would have a molecular volume of circa 11,000 nm^3. A virus particle was thought to be a suitable candidate for the headgroup. In this thesis, efforts in the pursuit of such a mega amphiphile are described.

1.4 Outline of the thesis

In **Chapter 1**, several concepts that are important in connection with the scope of this thesis are introduced.

Chapter 2 reviews the properties of the Cowpea Chlorotic Mottle Virus (CCMV), which is aimed to be used as the polar head group in the preparation of the mega-amphiphile. It is explained that the unique properties of this virus enable the inclusion of several non-natural species.

Chapter 3 deals with the synthesis of isocyanides with pendant lipophylic arms to form large, bulky and stiff linear aliphatic polymers. These polymers were intended to be applied as tails in the preparation of the above-mentioned mega-amphiphiles. Since the polar head group consists of a virus in this approach, the aliphatic tail must be very large indeed.

In **Chapter 4**, efforts are described to synthesize an anionic polymer that can be used to construct a mega amphiphile, which is envisaged to be built up from a block copolymer consisting of a polyanionic block and a very long aliphatic polymer (see Chapter 3). The CCMV protein subunits are expected to exert an attractive force on the polyanion, such that self-assembly in the presence of the block copolymer may result in the formation of the desired mega amphiphile (Figure 1.4).

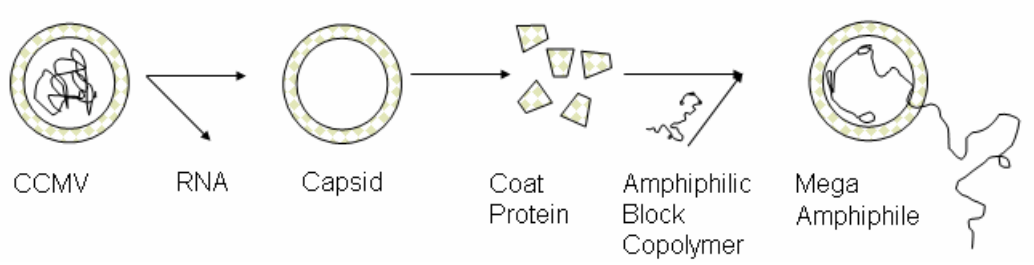

Figure 1.4. *Envisaged strategy for the preparation of the mega amphiphile. From left to right: Natural CCMV with RNA. Removal of the RNA yields the empty capsid, which can be disassembled into free Coat Protein (CP). The block copolymer that is depicted will be a negatively charged polystyrene sulfonate, combined with a long hydrophylic tail. Self-assembly of this amphiphilic block copolymer with the coat protein leads to the creation of a Mega Amphiphile.*

In this chapter also, efforts to synthesize a fluorescent initiator for Atom Transfer Radical Polymerization (ATRP) and the use of this initiator in ATRP reactions of styrene sulfonate ethyl ester are described. The fluorescent initiator is expected to facilitate the detection of the polymers.

In **Chapter 5**, the synthesis of various block-copolymers of polystyrene sulfonate is reported. Both organic polymers and enzymes have been coupled to polystyrene sulfonate with the objective to prepare various types of block-copolymers.

Chapter 6 describes the effects of homopolymers of polystyrene sulfonate on the assembly behavior of the CCMV protein subunits. Unusual behavior was found in these cases.

In **Chapter 7**, the interactions of several block copolymers on the assembly of the protein subunits of CCMV are described. The synthesis of the block copolymers was reported in Chapter 5.

Chapters 8 and 9 describe initial efforts to photopolymerize a water-soluble monomer inside the cavity of the CCMV, and the inclusion inorganic nanoparticles. In these experiments, the cavity of the CCMV virus is used as a nano-reaction space.

1.5 Notes and references

[1] (a) K.C. Nicolaou, M.E. Duggan and C.-K. Hwang, *J. Am. Chem. Soc.* **1989**, *111*, 6666; (b) K.C. Nicolaou, M.E. Duggan and C.-K. Hwang, *J. Am. Chem. Soc.* **1989**, *111*, 6676; (c) K.C. Nicolaou, C.-K. Hwang and M.E. Duggan, *J. Am. Chem. Soc.* **1989**, *111*, 6682; (d) K.C. Nicolaou, D.A. Nugiel, E. Couladouros and C.-K. Hwang, *Tetrahedron* **1990**, *46*, 4517; (e) G. Matsuo, H. Matsukura, N. Hori and T. Nakata, *Tetrahedron Lett.* **2000**, *41*, 7673; (f) G. Matsuo, N. Hori, H. Matsukura and T. Nakata, *Tetrahedron Lett.* **2000**, *41*, 7677; (g) H. Matsukura, N. Hori, G. Matsuo and T. Nakata, *Tetrahedron Lett.* **2000**, *41*, 7681.

[2] H. Staudinger, *Ber. Deut. Chem. Ges.* **1920**, *53*, 1073.

[3] K.J. Hamblett, B.B. Kegley, D.K. Hamlin, M.-K. Chyan, D.E. Hyre, O.W. Press, D.S. Wilbur and P.S. Stayton, *Bioconjugate Chem.* **2002**, *13*(3), 588.

[4] C. Tanford, *The Hydrophobic Effect*, (John Wiley & sons, New York), **1973**.

[5] J.M. Seddon and R.H. Templer, *Polymorphism of Lipid-Water Systems*, from the Handbook of Biological Physics, Vol. 1, ed. R. Lipowsky, and E. Sackmann (c), Elsevier Science, **1995**.

[6] J. Israelachvili, *Intermolecular & Surface Forces*, 2nd Ed. (Academic Press, London), **1992**, pp. 341.

[7] D.M. Vriezema, M.C. Aragonés, J.A.A.W. Elemans, J.J.L.M. Cornelissen, A.E. Rowan and R.J.M. Nolte, *Chem. Rev.* **2005,** *105*, 1445.

[8] D.M. Vriezema, J. Hoogboom, K. Velonia, K. Takazawa, P.C.M. Christianen, J.C. Maan, A.E. Rowan and R.J.M. Nolte, *Angew. Chem., Int. Ed.* **2003**, *42*, 772.

[9] K. Velonia, A.E. Rowan and R.J.M. Nolte, *J. Am. Chem. Soc.* **2002**, *124*, 4224.

[10] See for example: J.-M, Lehn, *Chem. Soc. Rev,* **2007**, *36*, 151; H.M. Keizer and R.P. Sijbesma, *Chem. Soc. Rev*. **2005**, *34*, 226; M.B. Linder, G.R. Szilvay, T. Nakari-Setäla. and M.E. Penttilä, *FEMS Microbiology Reviews* **2005**, *29*, 877.

Chapter 2

Literature Survey

2.1 General introduction

For thousands of years, viruses have been foes of mankind. These non-living particles can be regarded as toxins that self-replicate upon the infection of a host cell. They continue to claim lives to this day. Research has classically focused on the biological and medical properties of viruses, yielding a large diversity of life-saving vaccines. However, not a single viral disease can nowadays be cured by medical science. These issues make the understanding of viral structure, assembly and interactions highly important.

During the fabrication of virus particles in a host cell, exceedingly complex interactions successfully direct the self-assembly of protein subunits around the RNA/DNA core into a predefined structure. Similar to normal protein folding, this process must therefore describe some thermodynamic minimum or kinetic trap. A difference between virus assembly and protein folding is that the self-assembly of virus

particles often involves self-assembly of dozens of subunits, whereas quaternary folding of proteins involves no more than a few proteins, which can also rely on the assistance of chaperone proteins to assist the folding process. Seemingly without fundamental insight in the forces that govern such assemblies, e.g. the formation of salt bridges, the occurrence of dipole interactions, hydrogen bonding, pi-pi-stacking and van der Waals interactions, nature applies all of these forces simultaneously, in endless variation. To this day, no chemist has succeeded in duplicating some of the beautiful icosahedral shapes that are seen in viruses, using only synthetic materials.

Only during the last 15 years or so, an increasing interest in the chemical and physical aspects of viruses is discerned. Viruses are of interest because they are *(i)* nanosized, *(ii)* monodisperse, *(iii)* (mostly) readily accessible, and *(iv)* possess identical and predictable structures. Many efforts have been directed toward the use and modification of the natural material (the virus or capsid) itself. This review will try to highlight the recent research in this area.

Most viruses used for modification in a chemical and/or microbiological manner belong to the class of plant viruses. The reason behind this is their easy availability and their non-pathogenic behavior towards humans. The main subject of this review, i.e. CCMV, can be grown with the help of simple equipment within two weeks. Other readily available viruses are the Tobacco Mozaic Virus (TMV)[1] and the Cowpea Mozaic Virus, (CPMV)[2].

Viruses reproduce only within a living cell, which they control after infection. Thus, after entering the cell, the protein and RNA/DNA synthetic machinery is used to generate the materials needed for the production of the virus particles. Typically, one cell can produce thousands of virus particles. From a microbiological point of view, this is a very interesting phenomenon; modification of the viral gene directs the synthesis of designer proteins, provided that this process does not interfere with the folding of the protein molecules. In many examples, encoding viral proteins in the DNA of a plasmid yields virus-like-particles (VLP's or capsids), i.e. protein shells without any genetic material. Despite the sensitive nature of the self-assembly process of the viral protein, relying on subtle interactions with the genetic material, some viruses have the interesting property that capsids can be obtained from the complete virion (complete infectious

particle). One of the viruses that possess this property is the *Cowpea Chlorotic Mottle Virus* (CCMV). CCMV is a well studied plant virus; the first report on the isolation and various assembly states of CCMV dates from the sixties[3,4]. The CCMV consists of 90 identical dimeric coat proteins (CP) enveloping a central RNA strand, yielding a 28 nm icosahedral virion[5-7] The various surfaces and the cavity of CCMV give the materials scientist a multitude of possibilities for modification (Figure 2.1)

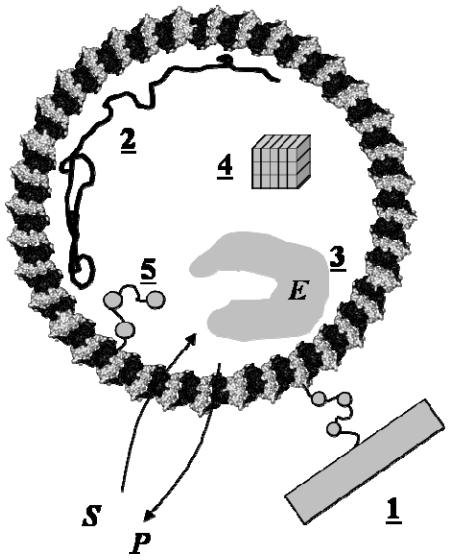

1. **Covalent modification of the exterior surface allowing attachment to a solid surface.**

2. **Self assembly around foreign templates**

3. **Encapsulation of enzymes (*E*) and other species**

4. **Growth of crystalline materials**

5. **Covalent modification of the interior surface**

Figure 2.1. *CCMV as a modifiable nanoscopic object.*

In an ongoing effort to understand and manipulate the assembly of viruses, many efforts have been aimed at the modification of the CCMV capsid (Figure 2.1). This review will focus on the use of several procedures to achieve this:

(i) covalent (chemical) modification of the exterior surface. A great variety of functional groups present on the outside of the protein shell can be used to attach useful moieties.

(ii) The unique assembly-disassembly properties of CCMV allowing induction of self-assembly of the protein subunits by a polymeric species.

(iii) Incubation of the virus coat protein with another protein or enzyme, followed by a change in pH, leading to a statistical inclusion of the protein or enzyme.

(iv) Inclusion of inorganic salts and subsequent reaction to yield inorganic solid (crystalline) materials inside the viral cage.

(v) Chemical or microbiological approaches to covalently modify the inside of the viral capsid.

(vi) Careful and selective (covalent) functionalization of the exterior surface of the virus followed by attachment of the whole virus to a solid surface.

All these techniques will be discussed in some detail. However, before doing so, it is first necessary to obtain insight into the assembly behavior of CCMV and the reversibility of the assembly process.

2.2 Assembly behavior of CCMV

The icosahedral shape of the virus can be described according to the Caspar-Klug T (triangulation) numbers. The number of protein subunits required to form the icosahedron is 60 x T. In CCMV 180 coat protein (CP) subunits (figure 2, right) give rise to a T=3 particle, consisting of 12 pentameric and 20 hexameric faces. The monomeric 20 kDa CP consists of 189 amino acids with nine basic residues at the N-terminus. In its free form, the CP is dimeric. It is believed that ionic interactions between the RNA and these basic residues enhance the structural integrity of the virus, so that capsid assembly in the presence of RNA is even possible at *neutral* pH[8].

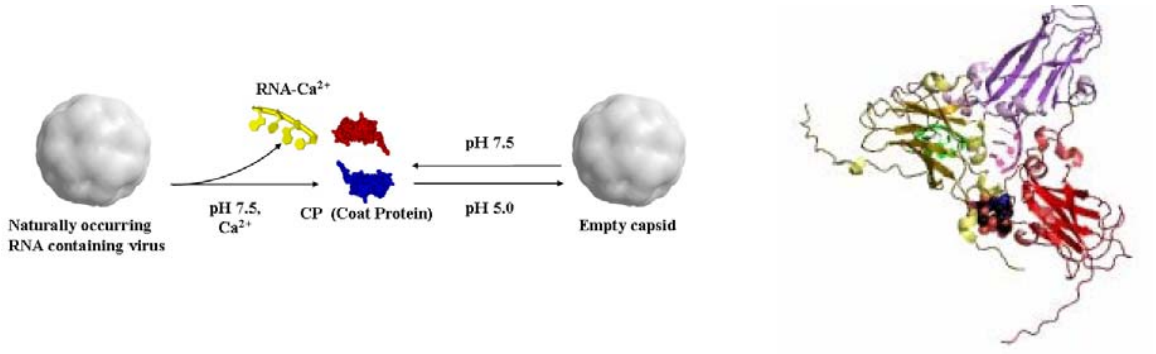

Figure 2.2. *Left: disassembly of the CCMV into the coat protein (CP) after removal of RNA by precipitation with calcium ions and the assembly of CP into empty capsids by changing the pH. Right: view from the inside of the virus to the outside protein wall. Picture is taken from PDB ID 1CWP.*

Removal of the RNA by precipitation with calcium ions yields pure CP which can be assembled by lowering the pH to ~5, yielding mainly empty T=3 capsid molecules[9]

(Figure 2.2). In practice, this means that dialysis of a sample of virus with a 0.5 M $CaCl_2$ buffer, followed by ultracentrifugation yields a solution of free CP at "high" pH (7.5).

In the absence of RNA, very little or no empty capsid will form under these conditions. Simple addition of small amounts of acid to the protein solution, however, will assemble the protein molecules into a particle. It is clear from these data that the step, in which the pH is lowered to 5.0, can be used to include certain species in the empty capsid. It has been shown that incubation of the coat protein with RNA yields infectious particles again[5]. However, by removing the stabilizing force of the RNA other morphologies than spherical capsids can be formed as well. It has been shown that these morphologies strongly depend on the pH and ionic strength of the medium. The subunits can assemble in larger, smaller, tubular and multi-shelled structures, all depending on the precise conditions (Figure 2.3)[5].

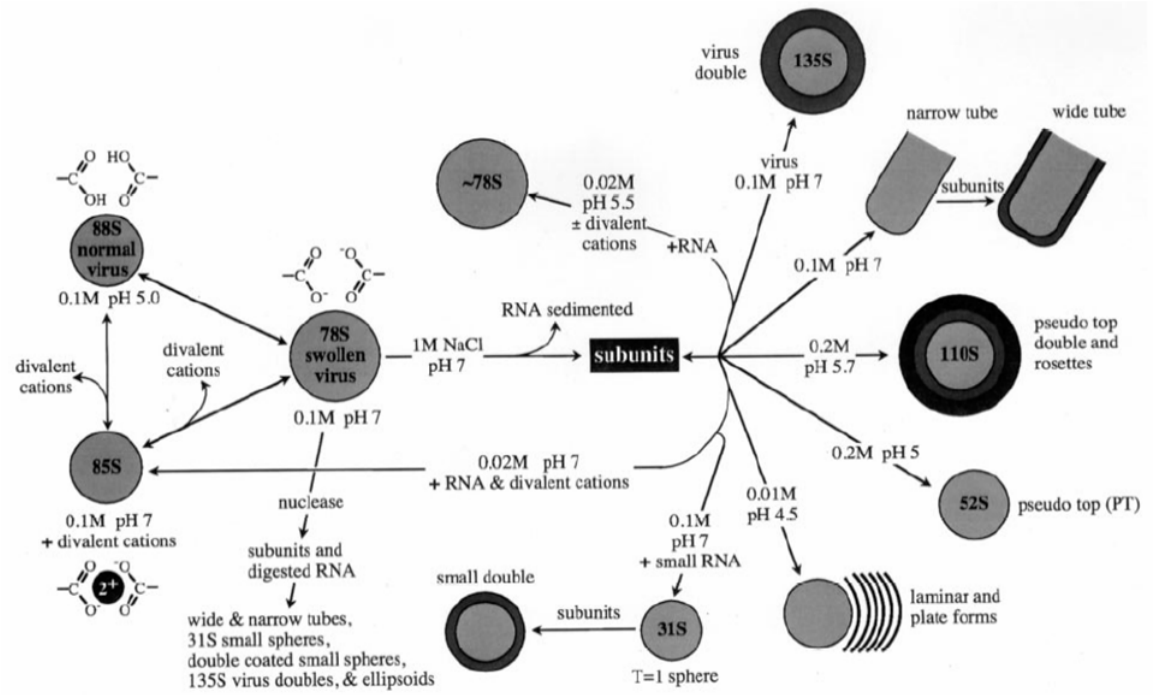

Figure 2.3. *The various assembly morphologies of the CCMV coat protein as dependent on pH and salt concentration. The S-numbers indicate the centrifugation sedimentation rate.*

The most remarkable properties of the CP assembly process are its dependence on the presence of divalent cations, the formation of multi-shelled species and the formation of tubular structures A further striking observation is that the protein subunits are only

observed as dimers and never as monomeric species, implying very strong binding interactions between the two subunits. A large variety of icosahedral quasi-symmetries can be observed in Figure 2.3: although the natural particle only exists as the T=3 species, smaller ("T=1", "T=2") and larger ("multi-shelled") particles have been observed as well. Whether or not the larger particles exhibit icosahedral symmetry is unknown, but seems likely. The virus also exhibits a gating mechanism, in which the removal of divalent cations such as Ca^{2+}, followed by a slight increase of pH to ca. 6.5, creates a coulombic repulsion between the carboxylates at the pseudo threefold axis. This, in turn, gives rise to holes of ca. 2 nm each in the structure and an increase in the particle size by ca. 10%[10].

These interesting properties, combined with the non-toxicity of CCMV and its relatively easy isolation have made that this virus is extensively used as a model virus to study assembly, infection, RNA packaging and a host of other processes. Other factors have also contributed to the ease at which the viral shell and the cavity can be manipulated, but most of all, both the ease and accuracy of spectroscopic detection of the various structures have greatly increased. For example, the relatively recent development of highly porous water based size-exclusion chromatography columns, such as Superose 6™, in combination with FPLC fractionating devices and highly sensitive UV detection, have greatly increased the precision and efficiency of detection of the virus particles. A short review on the development of these separation media can be found in the literature[11]. Not only do the new columns allow the separation of smaller quantities, the process is also much faster; whereas gradient density centrifugation typically requires one day and in general also larger sample volumes, these analytical columns already give results within a few hours. A highly essential tool in the characterization of these particles remains transmission electron microscopy, combined with negative staining. This powerful tool can visualize individual particles as well as arrays of particles.

2.3 Covalent modification of the exterior and interior surface of CCMV

The functional groups present in the amino acid residues on the outside of the virus particle are precisely arranged in space. This is important for one of the two

methods, that is used to modify this surface; modification by covalent organic chemistry. Bioconjugation is a well-known tool in the field of virus modification. Other viruses than CCMV have been extensively modified in this manner[12]. Douglas and Young have investigated the chemical modification of the exterior of both native and engineered CCMV (see below) with fluorescent molecules and small peptides[13]. They report on the use of carbodiimide chemistry in the activation of the surface carboxylates, present in the glutamic and aspartic acid residues on the surface of the protein shell. The assumed presence of these residues was based upon inspecting a space filling model based on the CCMV crystal structure. They treated the activated esters with an amine containing fluorophore to generate the amides, and the product was analyzed by UV-VIS. Interestingly, even when using 1000 equivalents of fluorophore per monomeric subunit, only 500-600 dye molecules were detected after reaction. Analysis of the capsid structure was also performed by dynamic light scattering (DLS), which showed a 10 nm increase in the particle diameter, which the authors attributed to the swelling of the capsid. Similar results were obtained by functionalization of the amines, present on the surface. In the same paper, the use of the molecular biology toolkit is reported to generate a mutant that displays two cysteines per subunit on the surface of the protein shell. Subsequent reaction with a thiol containing small polypeptide yielded a peptide functionalized virus. The authors estimate that 25% of the subunits are functionalized in this way.

In another publication, the same authors describe the use of similar techniques to synthesize protein subunits that possess, in assembled form, 180 free thiols on the surface of the capsid. Subsequently, the capsid was bound to the solid phase of a sulfur-functionalized resin and all non-bound sulfur groups were protected. After isolation of the thus obtained, capsid mostly mono-functionalized with thiols, it was deposited onto a gold surface. The authors were able to show that the number of thiols, present on the surface of the capsid, needs to be well controlled in order to obtain a moderately well defined monolayer. They could not determine the number of thiols that remained on the surface of the capsid after this treatment.

The examples above illustrate the molecular biological way of modifying the surface of a virus and this is the second method by which a virus is covalently modified. The isolation of the viral RNA, followed by reverse transcriptase and a polymerase chain

reaction (PCR), yields DNA which can subsequently be incorporated into a plasmid (circular double stranded DNA). Molecular biological methods then provide a plethora of possibilities, so that different amino acids or amino acid sequences can be inserted at virtually any site in the protein. This is done by manipulation of the plasmid. Briefly, the plasmid is cut open at specific sites using restriction enzymes. Short double stranded DNA fragments can then be inserted, after which the plasmid is closed. These plasmids can then be inserted into the DNA of a bacteria, a process which the bacteria will undertake all by itself given the proper conditions, and the DNA will be read and translated into (a) protein(s), which can be isolated afterward.

When performing such alterations to the structure of the protein, it is important to keep in mind the normal folding and binding patterns. If these are not respected, the engineered protein may behave completely different from the original one.

The *P. Pastoris* yeast-based expression system has been used to synthesize various mutants of the CCMV CP[14]. The inside of the capsid was altered by modifying the N-termini of the individual proteins; basic amino acid residues (lys, arg), which are positioned on the inside, were replaced by acidic ones (glu) to alter the binding properties of the capsid (see below)[15]. Furthermore, other mutants were designed to possess the same polypeptide, as mentioned above. In this case, however, these polypeptides were attached to the C-terminus in a molecular-biological fashion. As a final effort, CP was engineered to lack the interior residues 4-37 from the N-terminus (NΔ34). The proteins synthesized were subjected to assembly conditions and studied by TEM, DLS and size exclusion chromatography. All the mutant CP's were found to exhibit capsid formation, except the NΔ34 mutant, which showed a variety of different structures.

Other researchers have undertaken efforts to genetically decorate the outside of the capsid with non-natural amino acids, to generate unique functionalities in a precise manner. The growth of bacteria in a medium that contained the chemically synthesized amino acid azidohomoalanine[16], instead of the natural equivalent methionine, combined with the ability to grow methionine auxothroph bacteria (i.e. bacteria that cannot produce methionine themselves) that accept this amino acid as a substitute, leads to the biosynthesis of externally azide-functionalized coat protein[17]. These coat proteins exhibit normal assembly behavior, and the presence of the azide functionality was proven by

reaction with an acetylene[18]. Genetic engineering was also used to display fusion proteins onto the surface of the capsid. Alternatively, a protein could be attached to the (engineered) surface proteins of the virus through chemical means.

2.4 Supramolecular self-assembly of CP with polymeric species

The presence of RNA induces the self assembly of the coat protein around this biomacromolecule; a T=3 particle is obtained which is indistinguishable from the natural species. However, detailed information about the assembly behavior and the interactions between the RNA and the protein is hardly available, although data suggest that the growth commences with the association of a pentamer of dimers with some part of the RNA. It is known, that the 3' side of RNA molecule 4 (there are 4 different RNA's) is folded in a tRNA –like structure. Although there is conflicting data on the function of this assembly (see below), it has been generally accepted that it is important in the assembly of the complete virion. However, incubation of CCMV CP with RNA's lacking the 3' terminal T-RNA-like structure results in T=3 particle formation in high yield. It is also possible, then, that the tRNA structure is simply a very efficient manner of packing the RNA tightly.

All these observations imply very subtle mechanisms and demonstrate the overall lack of knowledge regarding the assembly process, since other morphologies are also known to exist (see above). It is of interest, therefore, to study the interaction of CP with other (bio)polymers than RNA. Already thirty years ago, Bancroft et al. incubated CP with various polyanionic species[19]. Upon incubation of the CP with various single stranded polyribonucleotides, they found evidence for the formation of spherical structures. However, when the protein sample was incubated with poly I or poly IG, which possess considerably more self-structure than the other polymers, the aggregates precipitated from solution. They concluded that the rigidity and aggregation state of the polymers played a significant role in the assembly process. Whether or not, the RNA strands used in these experiments contained tRNA-like structures remains unanswered. When synthetic polyvinyl sulfate was used in the incubation experiments, spherical

particles were found as well, but, in this case, the spheres were not constant in size. The authors attributed this to the heterogeneity in the starting polyanion, which is, however, contradicted by data reported in this thesis (Chapter 6). These observations are further complicated by the formation of long tubes, when the CP was incubated with *ds*-DNA. Mixing of the CP with low molecular weight anionic species (e.g. AMP, ATP) did not result in the formation of particles. The conclusion was drawn that polyanionic species are essential for the formation of shelled structures. The incubation of viral protein with *ds*-DNA has recently been thoroughly studied by Zlotnick et al. It was found that the migration of the DNA in an agarose gel electrophoresis was hampered by the addition of CP[20]. Electron microscopy studies revealed the presence of long 17 nm diameter tubes, which may be identical to those obtained by Bancroft[21]. It was found that the lengths of the tubes was strongly dependent on the ratio of DNA base pair to CP: very long tubes (>5 μm) were obtained when the bp:CP ratio was 7:1. The authors speculate that the CP binds nonspecifically to multiple DNA strands, so that one cross-section of the assembly contains multiple DNA strands. Douglas and Young showed that spherical particles are formed when CP is incubated with an anionic polymer, i.e. polyanetholesulfate, when the pH of the preparation is lowered to 5[22,23]. They concluded that the polymer was incorporated into the viral capsid because part of the UV absorption of the isolated particle was identical to that of the polymer. Also, in Transmission Electron Microscopy experiments, using uranyl acetate, no inclusion of this staining agent into the particle was observed. They proposed that the presence of the polymer prevents this, a phenomenon which is in agreement with previous observations.

Zlotnick and Johnson have shown that CP lacking the non crystalline N-terminal sequence (where 34 amino acid residues are missing, hence the name NΔ34) assembles into a statistical mixture of T=1,2 and 3 assemblies. In this study, it was reported that in preparations containing the non-degraded CP, the T=1 particle is never observed[24].

More recently, CCMV CP has been exposed to polystyrene sulfonate samples of high molecular weight[25]. This has resulted in the formation of two discrete particles: when a relative low-molecular weight polystyrene sulfonate polymer was used, particles of ca. 22 nm ("T=2") arose. Use of a higher molecular weight polystyrene sulfonate

polymer resulted in the formation of T=3 particles. These data are in contrast to the results reported in this work (Chapter 6).

2.5 Inclusion of chemical or enzymatic species in order to create a nanoreactor

The capsid can be considered as a porous nanoreactor which opens very interesting possibilities for applications. For example, the inclusion of a chemical catalyst, followed by incubation with several substrates, might yield a (size-selective) catalytic system. After all, reactants have to diffuse in and out of the capsid via its pores or via a closed protein membrane depending on the pH. Since the pores of the capsid membranes are chiral, a dual selectivity might in principle be achieved in the sense that the catalyst inside the capsid will only carry out a reaction with species of a certain chirality and size.

The inclusion of enzymes in a CCMV capsid has been reported by M. Comellas of our group[26]. In this work, the protein subunits, which are dimeric at pH 7.5, are incubated with a certain concentration of a protein or enzyme, e.g. Horse Radish Peroxidase, after which the pH is lowered by dialysis. The authors were able to demonstrate the incorporation of the enzyme in the viral capsid. A very detailed investigation using confocal fluorescence microscopy was carried out in order to prove that the enzyme remained active on the inside the capsid; it was even possible to study the activity of one single enzyme in a single viral cage. It was determined that the enzyme was, in fact, active and that the activity was controlled by the diffusion of the substrate in and out the capsid. The pH dependency of the enzymatic reaction was studied and it was concluded that the enzymatic reaction was faster, when the pH was higher, which was in line with the expectation; the capsid is known to possess pH dependent holes in the wall structure, (see above) with holes $\geq$ 2 nm when the pH is above ~5.8. Substrate and product diffusion are thus much faster. It was thus shown that the substrates could penetrate the viral shell, react, and diffuse out of the capsid again.

2.6 Inclusion of inorganic species in viral capsids

The preparation of monodisperse inorganic nanoparticles has been a long standing goal in materials chemistry and a wide variety of methods has been used to achieve this goal[27-31]. Reports on the use of biological materials as templates for nanoparticle synthesis only began to appear ten years ago. Especially supramolecular aggregates of ferritin have been used to confine mineralization reactions. Also, CCMV might be an ideal candidate for such reactions. It has been reported that incubation of the CCMV CP or the open (gated) structure (see above) with WO_4^{2-} water soluble species, followed by lowering of the pH simultaneously induced two effects[32]. Initially, the tungstate species underwent oligomerization, forming large oxometallate species such as $H_2W_{12}O_{42}^{10-}$, that crystallized out of solution as the ammonium salts. Secondly, the capsid assembly took place at this point, leading to the selective crystallization of the polyoxotungstate species inside the capsid. The authors claim that the affinity of the water soluble species for the ammonium groups present on the inside of the capsid enhances the binding of the salts, both in soluble and insoluble state, to the inside of the cavity. Furthermore, they conclude that the crystallization of the tungsten species is induced by the presence of the lysine/ammonium endgroups present on the inside of the capsid. In this way, an elegant method to prevent the crystallization of bulk polyoxotungstate in bulk was developed.

Young et al. have prepared iron oxide nanoparticles in CCMV capsids[10]. In order to achieve this, the CP needed to be genetically modified (see above) to generate N-terminal glutamic acid rich capsid proteins. The interior of capsids, formed from these proteins, becomes strongly attractive to ferrous and ferric ions, thus generating a favorable environment for oxidative hydrolysis reactions, leading to iron oxide formation inside the capsid. It was determined that treatment of the capsid with higher amounts of iron precursors led to a larger type of particles, such that the complete particle cavity was filled with the iron species.

Wright et al. have used CCMV to reduce $AuCl_4^-$ with the help of the tyrosine residues present on the surface of the virus to obtain a viral species that is decorated on the outside with gold[33]. The same authors also engineered a capsid protein with carboxylic acid rich N-terminus, in accordance with the work by Young et. al, described

above, in the hope of complexing the gold before it was reduced. It was found that the reductive power of the tyrosines prevented this, creating capsids with only gold particles on the outside. Thus, the complexation strength of the carboxylic acids was not strong enough to prevent the reduction of the gold species, even for a short time.

In preliminary investigations, the CCMV CP has also been incubated with Gd^{3+} salts to generate a MRI contrast agent[34]. It was found that the species generated in this way exhibited unusually high relaxation times, an effect that was attributed to both the high amount of Gd bound to the protein and the presence of water molecules bound to the metal.

2.7 Conclusions

This chapter has reviewed the highly interesting possibilities to use the CCMV capsid as a chemical scaffold and container. Both the inner and outer surface of the virus as well as its cavity are accessible, due to the assembly-disassembly nature of the virus particle. Several examples have been presented in which the capsids and virions are functionalized in different ways. It is striking that despite the fact that CCMV has been studied thoroughly and is one of the simplest viruses available, detailed knowledge of the assembly of the protein cage, as well as specific information on interactions that exist between the RNA and the inside of the capsid, are not available in the literature. The rather recently developed view that viruses can be chemical starting materials, as opposed to dangerous pathogens, may lead to new applications in both chemistry and medicine. For instance, the use of the CCMV capsid, decorated with protein receptors and containing a medicinal species, may yield novel medical applications. Extensive further research is needed, however, in order to ascertain the effects of such particles *in vivo*. The possibilities to include compounds, combined with the now available techniques to modify the capsid surface using synthetic-organic or molecular biology techniques could lead to the synthesis of capsids containing medicinal species that might be directed toward specific cells. An important conclusion of this chapter is that the assembly processes and the interactions that lead to the assembly, are not understood in detail. This

lack of understanding makes the rational design of modified capsid protein very difficult. It is not possible, for example, to design a protein species that assembles *specifically* in tubes or in larger spherical species.

2.8 Notes and references

[1] K. Brandner, A. Sambade, E. Boutant, P. Didier, Y. Mely, C. Ritzenthaler and M. Heinlein, *Plant Physiol.* **2008,** *147*, 611 and references stated therein.

[2] K.T. Kareem and M.A. Taiwo, *Virology Journal* **2007**, *4*, 15.

[3] C.W. Kuhn, *Phytopathology* **1964**, *54*, 853E.

[4] E. Hiebert, J.B. Bancroft and C.E. Bracker, *Virology***1968**, *34*, 492.

[5] J.E. Johnson and J.A. Speir, *J. Mol. Biol*. **1997**, 665.

[6] A. Zlotnick, R. Aldrich, J.M. Johnson, P. Ceres and M. Young, *Virology* **2000,** 450.

[7] E. Hiebert, J.B. Bancroft and C.E. Bracker, *Virology* **1968**, *34*, 492.

[8] L.O. Liepold, J. Revis, M. Allen, L. Oltrogge, M. Young and T. Douglas, *Phys. Biol.* **2005**, *2*, S166.

[9] J.B. Bancroft, C.E. Bracker and G.W. Wagner, *Virology* **1969**, *38*, 324.

[10] J.A. Speir, S. Munshi, G.J. Wang, T.S. Baker and J.E. Johnson, *Structure* **1995**, *3*, 63.

[11] M. Eisenstein, *Nature Methods* **2006**, *3*, 410.

[12] E. Strable and M.G. Finn, *Current topics in microbiology and immunology; Viruses and nanotechnology* **2008,** DOI *10.1007/978-3-540-69379-6.*

[13] E. Gillitzer, D. Willits, M. Young and T. Douglas, *Chem. Commun.* **2002**, 2390.

[14] S. Brumfield, D. Willits, L. Tiang, J.E. Johnson, T. Douglas and M. Young, *Journal of general virology* **2004**, *85*, 1049.

[15] T. Douglas, E. Strable, D. Willits, A. Aitouchen, M. Libera and M. Young, *Adv. Mat.* **2002**, *14*, 415.

[16] K.L. Kiick, E. Saxon, D. Tirrell and C.R. Bertozzi, *PNAS* **2002**, 19.

[17] L.A. Hendriks, M. Lambermon and J.C.M. van Hest, *manuscript in preparation.*

[18] Known as the copper catalyzed azide-alkyne click reaction. See e.g. H.C. Kolb, M.G. Finn and K.B. Sharpless, *Angew. Chem. Int. Ed.* **2001**, *40*, 2004.

[19] J.B. Bancroft, E. Hiebert and C.F. Bracker, *Virology* **1969**, *39*, 924.

[20] S. Mukherjee, C.M. Pfeifer, J.M. Johnson, J. Liu and A. Zlotnick, *J. Am. Chem. Soc.* **2006**, *128*, 2538.

[21] J.B. Bancroft, E. Hiebert and C.E. Bracker, *Virology* **1969**, *39*, 924.

[22] T. Douglas and M. Young, *Nature* **1998**, *393*, 152.

[23] T. Douglas and M. Young, *Adv. Mater.* **1999**, *11*, 679.

[24] J. Tang, J.M. Johnson, K.A. Dryden, M.J. Young, A. Zlotnick and J.E. Johnson, *J. Struc. Biol.* **2006**, *154*, 59.

[25] Y.F. Hu, R. Zandi, A. Anavitarte, C.M. Knobler and W.M. Gelbart, *Biophys. J.* **2008**, *94*, 1428.

[26] M. Comellas-Aragonès, H. Engelkamp, V. Claessen, N.A.J.M. Sommerdijk, A.E. Rowan, P.C.M. Christianen, J.C. Maan, B.J.M. Verduin, J.J.L.M. Cornelissen and R.J.M. Nolte, *Nature Nanotechnology*, submitted.

[27] a) K.J. Klabunde and R.S. Mulukutla in *Nanoscale Materials in Chemistry* (Wiley-interscience, New York) **2001**. b) B.F.G. Johnson, *Top Catal.* **2003**, *24*, 147.

[28] J. Turkevich, P.S. Stevenson and J. Hillier, *Discuss. Faraday Soc.* **1951**, 5, 209.

[29] B.L. Cushing, V.L. Kolesnichenko and C.J. Connor, *Chem. Rev*, **2004**, *104*, 3893.

[30] L.L. Hench and J.K. West, *Chem. Rev*. **1990**, *90*, 33.

[31] V.T. Liveri in *Nano-surface chemistry*, M. Rosoff (Dekker, New York) **2001**.

[32] a) T. Douglas and M. Young, *Nature* **1998**, *393*, 152; b) T.Douglas and M. Young, *Adv. Mater.* **1999**, *11*, 679.

[33] J.M. Slocik, R.R. Naik, M.O. Stone and D.W. Wright, *J. Mat. Chem.* **2005,** *15*, 749.

[34] M. Allen, J.W. Bulte, L. Liepold, G. Basu, H.A. Zywicke, J.A. Frank, M. Young and T. Douglas, *Magnetic Resonance in Medicine* **2005**, *54*, 807.

Chapter 3

Synthesis of novel lipophylic polyisocyanides

3.1 Introduction

In Chapter 1, the initial goal of the research reported in this thesis has been presented. The CCMV capsid is to be used as a host for an anionic polymer species (A) that is part of a very high molecular weight AB-type block copolymer. The other block (B) would consist of a hydrophobic polymer, so that after self-assembly of the capsid around the anionic block of the block copolymer, an amphiphilic species arises. One of the many problems in this approach is the need for a very bulky apolar polymer chain. This necessity is caused by the fact that a given molecular structure will only be amphiphilic if the ratio of hydrophylic/hydrophobic bulk is reasonably close. Since the volume of the CCMV virus is considerable (ca. $1.1 \cdot 10^5$ nm^3), the volume of the hydrophobic group needs to be of the same order of magnitude. The preparation of such a structure can in principle be achieved in two ways, the first being the preparation of an exceedingly long polymer. Such polymers are known in synthetic polymer chemistry and are commercially available: the dyneema fiber, for example, consists of ultra high molecular weight polyethylene (UHMWPE). The manipulation of such polymers,

however, is difficult, because of solubility-, viscosity- and other problems. It is also very problematic to functionalize the end groups of such a long polymer. The second method, by which polymers with sufficient steric bulk are accessible, is via the preparation of a highly branched, "bottle brush" -type of polymer. Ample experience with polyisocyanides in our group has revealed that the polymerization of isocyanides can be a route to synthesize very long polymeric chains[1]. This possibility combined with the fact that functional isocyanides are easily accessible (vide infra) made us decide to focus on the preparation of an isocyanide monomer that is equipped with a very long aliphatic chain, which is subsequently polymerized to yield a hydrophobic polymer that is both long and bulky. In line with one of the goals of this thesis, the preparation of a mega-amphiphile, it was envisaged to use this large block copolymer in the preparation thereof. This chapter reports on the results of these investigations.

3.1.1 Polyisocyanides

Polyisocyanides are obtained by the polymerization of isocyanides and are polymers that have a remarkable feature: each carbon atom present in the backbone of the polymer possesses a side group. This leads to considerable steric hindrance in the polymer chain, even with relatively small side chains. This steric hindrance is such that the polymeric backbone twists and adopts a 4_1 (4 repeat units per turn) helical structure, as first proposed by Millich et al. on the basis of theoretical models. Millich also stumbled upon the first catalyst for the polymerization of isocyanides, namely acid coated glass2. A study into a more practical transition metal catalyst was undertaken by Nolte, who found that Ni(II) species are particularly effective in mediating polymerization[3] (Scheme 3.1). Several complicated aspects of this nickel(II) mediated polymerization have been discovered, for example by Novak, who found that the addition of an excess of *tert*-butyl isocyanide (10 eq.) to $NiCl_2$ causes the reduction of this salt to nickel (I), which does not catalyze the polymerization. Molecular oxygen from air can reoxidize the metal to Ni(II), thereby regenerating the catalyst. However, the use of pure oxygen can also prevent polymerization because the nickel catalyses as a side reaction the oxidation of the isocyanide to the isocyanate.

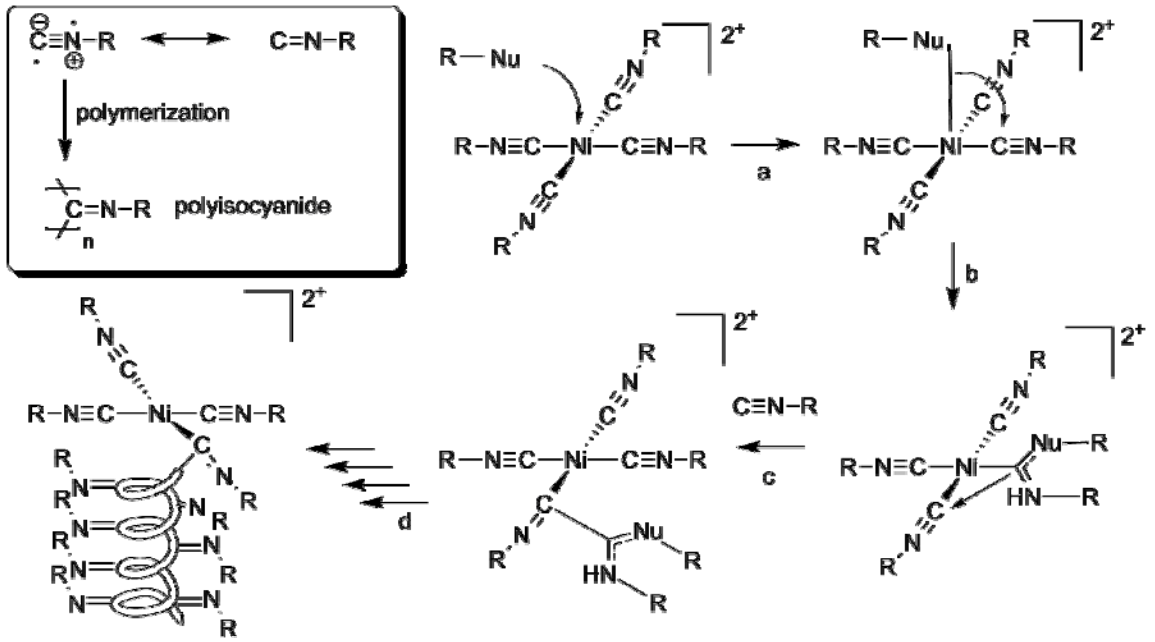

Scheme 3.1. Polymerization of isocyanides (inset) and the nickel(II) catalyzed polymerization via the "merry-go-round" mechanism. Attack of the nucleophilic initiator (a) (e.g. an amine or alcohol) onto the nickel activates one of the isocyanide ligands, which is converted into a carbene-like species (b). The nucleophilicity of this activated isocyanide is sufficient to attack a neighboring isocyanide, after which a new monomer occupies the vacant site (c) and the polymerization continues (d).

In the nickel(II) catalyzed polymerization, the first step involves coordination of isocyanides around the metal ion in a square-planar fashion. The resulting complex can be isolated, provided that a bulky isocyanide is used, e.g. *tert*-butyl isocyanide. An initiating nucleophile then coordinates to the metal and attacks the electrophilic carbon of a coordinated isocyanide, effectively migrating to this atom (a). The produced carbene-like species is now nucleophilic enough to attack one of its neighbors (b), which becomes electron richer and hence the nucleophile (c). The helical structure as first proposed by Millich et al.[4], is often found in polyisocyanides, and is primarily caused by steric factors. Once a direction of the helix has been chosen (randomly), the helix will continue to grow in that same direction, as long as there is monomer present (d). Polymerization of isocyanides that possess modest bulk still leads to a helical conformation that is lost over time. This was shown by for example Rosen et al., who synthesized poly(phenylisocyanide) and observed a slow loss of helical conformation in solution[5], in contrast to for example poly(tert-butylisocyanide), which was found to yield two separate helical polymers, viz. right handed (P) and left handed (N)[6]. After separation of these two

different stereoisomers it was shown that they possessed optical activity, although no chiral centers were present in the monomeric species. The optical activity arises from the two different helical conformations. The chirality in these types of polymers is induced by a restricted rotation around the C-C bonds in the polymer backbone, called atropisomers. Other studies[7,8] have shown that the helical structure is mostly governed by steric interactions in the side chains of the polymer, giving rise to an equimolar mixture of a right- and left handed helix. The use of chiral isocyanides, however, can induce a preference for one helical morphology (*vide infra*) which is kinetically controlled at the nickel centre. Several other interesting observations have been made in the study of polyisocyanides. Yashima has prepared polyisocyanides from 4-carboxyphenyl-isocyanide, which show a random coil conformation[9]. The steric bulk of the phenyl group is not sufficient to cause a kinetic trapping of the helical conformation during the polymerization. Upon treatment of the polymers with optically active amines, a circular dichroism effect was found, after a long incubation time. It was concluded that the amines induced the formation of a helical structure. This helical structure was also memorized in the polymer, when the chiral amines were removed. A general conclusion of the authors was that the polymer exists in an equilibrium state, which contains helical segments of differing sense, as well as random coil domains.

The polymerization of isocyanides has produced fundamental insight into polymer folding and behavior. However, only a comparatively small amount of papers has been published. A SciFinder search (keyword: isocyanide AND polymer) yields just 215 hits.

3.1.2. Polyisocyanopeptides

The examples above describe the kinetic trapping and stabilization of the polyisocyanide helix by bulky side chains. It has been found that intramolecular hydrogen bonds can also stabilize the helix after polymerization. This was discovered when chiral dipeptide isocyanide monomers derived from glycine and alanine were investigated by Cornelissen et al.[10] (Scheme 3.2.)

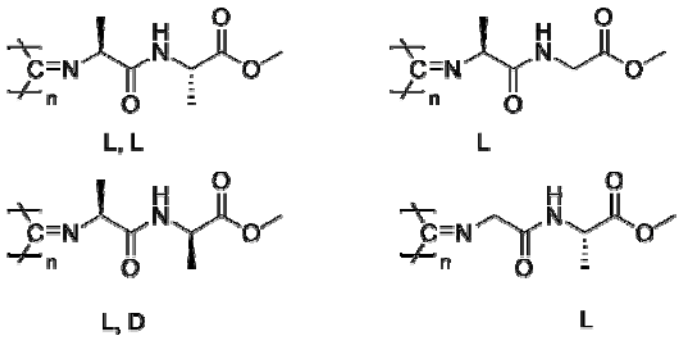

Scheme3.2. *Dipeptide derived isocyanides.*

All the polymers shown in Scheme 3.2, except isocyano-L-alanine-glycine-methyl ester, displayed the ability to stabilize the helical conformation of the polyisocyanide by formation of a hydrogen bond between the amides, present at position n and n+4, which are situated nearly above one another. Thus, the introduction of chirally oriented steric bulk, and the introduction of amide bonds that can form hydrogen bonds together determine the helical shape. Interestingly, a right-handed helix was found for most of the polymers in Scheme 3.2[11].. Thus, both L,L-IAA (L,L isocyano-alanine-alanine methyl ester, the derived polymer is shown in Scheme 3.2, top left), and L,D-IAA, (the bottom left structure) give rise to a right handed helix when polymerized. The enantiomer of both L,D-IAA, and L,L-IAA should consequentially give rise to predominantly left-handed helices (Scheme 3.3). Block- and copolymerizations of L,D- and D,L- IAA's have been investigated and have shown to be slow and unfavorable. These observations are probably caused by the morphology of the final helix. If in a copolymerization reaction, say, a left-handed helix has been formed by polymerization of one stereoisomer, coordination of the other stereoisomer to the nickel ion and polymerization thereof would require the helical sense to invert, leading to considerable steric strain[11].

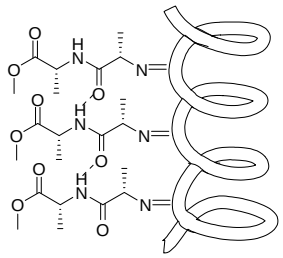

Scheme 3. *Helical 4_1 conformation in D,L PIAA.*

Detailed analysis of the polymer D,L-PIAA has shown the presence of hydrogen bonds between amide groups present in side chains n and n+4, which act as an extra stabilization of the helix. The shifts typical for hydrogen bonded N-H vibrational levels were observed in IR. When the optical rotation was divided by the number of monomers, an amplification in D,L-PIAA and in PIGA was observed, but not in PIAG. This led to the conclusion that the secondary helical structure is present in PIGA, even though the chiral centre is further removed from the backbone.

Metselaar has found that the formation of helices in polyisocyanopeptides is also catalyzed by acid: Upon polymerization of L,D-IAA with acid, helix formation was observed as well[12]. Conversely, when L,L-IAA was subjected to acid catalyzed polymerization, no polymer could be obtained. From this study, it was proposed that the formation of the hydrogen bonded conformation in the polymer is a cooperative process in which an isocyanide monomer is complexed to the growing helical polymer chain through the formation of a hydrogen bond between peptide bonds in the polymer chain and the monomer. It was shown that the isocyanide conformation is vital to the polymerization efficiency. Interestingly, when LL-IAA was added to a growing polymer chain of LD-IAA, the former monomer could be readily polymerized. It was thus concluded that the formation of the initial helical structure, at the beginning of the polymerization, is a highly subtle interplay between different forces, and is essential to the entire polymerization reaction. In general it was concluded that after polymerization to form oligomers of about 8 monomers, the polymerization pauses until the folding in the oligomer is suitable for helix formation and subsequent continuation of polymerization. Not all monomers can adjust in such a fashion, explaining the non-reactivity of L,L-IAA towards acid. It was shown[13] that the polymerization of LL-IAA, when catalyzed by a minute trace of trifluoroacetic acid, yields rigid polymers of several micrometers length. As explained in Section 3.1 and in Chapter 1, the research performed in this thesis requires a very bulky hydrophobic polymer. It was therefore decided to synthesize polyisocyanopeptides with long aliphatic tails, since the size of the amphiphilic structure, which we intend to create, demands a very bulky hydrophobic part indeed, and also because the length of such a lipophilic tail should be considerable.

3.2 Synthesis of polyisocyanides bearing long aliphatic tails

In order to prepare isocyanides with long aliphatic tails, it was conceived to prepare DL-IAA bearing two different aliphatic tails, a C12 and a C20 carbon chain. The stereochemistry was chosen in such a way, that the nickel-catalyzed polymerization would proceed readily[14]. Thus, Boc-*L*-alanine was condensed with 1-icosanol under Mitsunobu conditions. This procedure did not yield satisfactory quantities of product, so it was decided to attempt the condensation of *L*-alanine and 1-icosanol under classical esterification conditions (Scheme 3.4). To this end, an excess of p-toluenesulfonic acid was added in excess to a mixture of **1** and **2**, followed by addition of a small amount of water, in order to solubilize the alanine. Refluxing in toluene employing a Dean-Stark apparatus yielded **3**. It was found that longer refluxing times yielded byproducts, as detected by TLC. The purification of **3** was complicated due to its amphiphilic character. It was found that the most straightforward route was to exchange the p-toluenesulfonic acid salt for HCl, followed by crystallization. Subsequently, the obtained HCl-L-Ala-O-C_{20} was condensed employing EDC[15] with **4**, yielding **5**. Subsequent deprotection and formylation, using HCl/EtOAc and $NaHCO_2$/HCO_2Et respectively yielded formamide **6,** which was dehydrated with diphosgene to yield isocyanide **7**. It was found that this isocyanide could be readily polymerized with nickel(II) perchlorate, yielding polymer **8**.

In order to prevent purification problems with the analogous alanine with a C_{12} lipophilic side group, which was synthesized at another point in time, it was decided to condense Boc-L-Ala with 1-dodecanol under the agency of EDC. The protection of the amine imparts a hydrophobic character on the amine, thus dispensing with any amphiphilic character. It was found that the use of a DMF/hexane mixture was vital for the coupling reaction to proceed. Further manipulations were very similar to the synthesis of the C_{20} isocyanide and are therefore omitted from the scheme. In all reactions leading to the formation of both isocyanides, the use of ninhydrin as a staining agent for TLC turned out to be very useful, since several different colorations could be observed for every step. The C_{12} and the C_{20} isocyanides were used in the preparation of the corresponding polymers (vide infra).

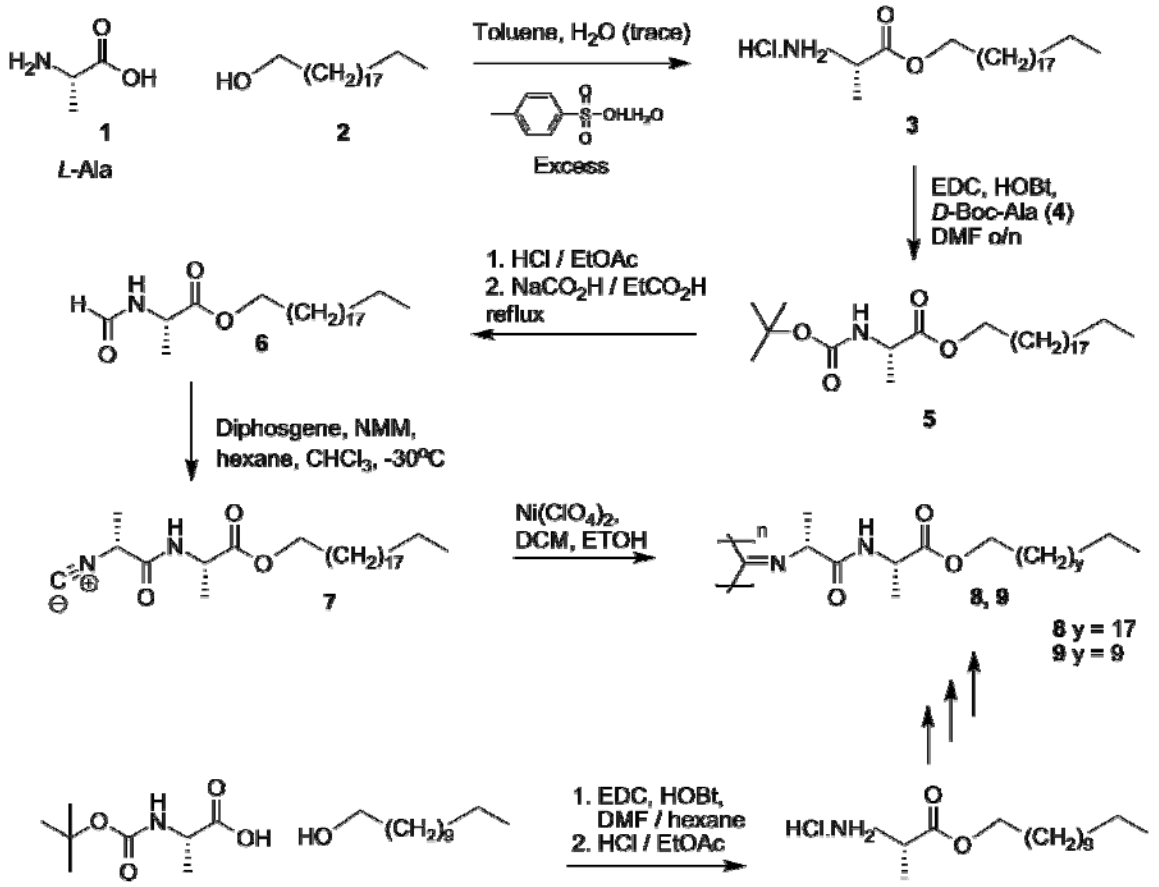

Scheme 3.4. *Synthesis and polymerization of isocyano-D-Ala-L-Ala-C_{20}- and C_{12} ester.*

Since the synthesis and purification of both the C_{12} and the C_{20} isocyanides was more troublesome than expected, it was envisioned to synthesize a monomer with a synthetic handle that would allow the functionalization of that monomer itself, opening the possibility to synthesize a small isocyanide, which is conceivably easy to purify by crystallization and the functionalization of this monomer with any desired group. Furthermore, facile functionalization of the *poly*isocyanide by grafting would be possible in this way. The functional group selected for this procedure should be *(i)* small in order to prevent steric effects on the polymer structure. The size of the functional group on the monomer cannot be allowed to interfere in the determination of the final polymer structure. *(ii)* The functionality should also be inert to several synthetic manipulations. *(iii)* The functional group should still be reactive enough so that coupling is possible. The allyl group was thought to be a viable candidate, for it is known to be a good substrate for the ruthenium catalyzed olefin cross methathesis[16] (Scheme 3.5). It is feasible to attempt

the metathesis, using a second group of choice (e.g. 1-hexene) on **12**, although there may be a fair chance that it will be polymerized, so that the Grubbs catalyst, intended for the cross metathesis actually polymerizes the isocyanide. Should it be successful, then the allyl functionalized isocyanodipeptide would be a valuable synthon indeed towards easily prepared functional isocyanides. The Grubbs catalyst could also be used for the crosslinking of the polymer, which may be useful for other work. Thus, *N*-Boc-*L*-alanine was reacted with allyl bromide and silver carbonate to yield *L*-Ala-OAllyl after deprotection in good yield. Further reaction towards formamide **11** was carried out according to previously described routes, see the experimental section. The synthesis of **11** did not require any chromatographic purification, and pure product was obtained by crystallization alone.

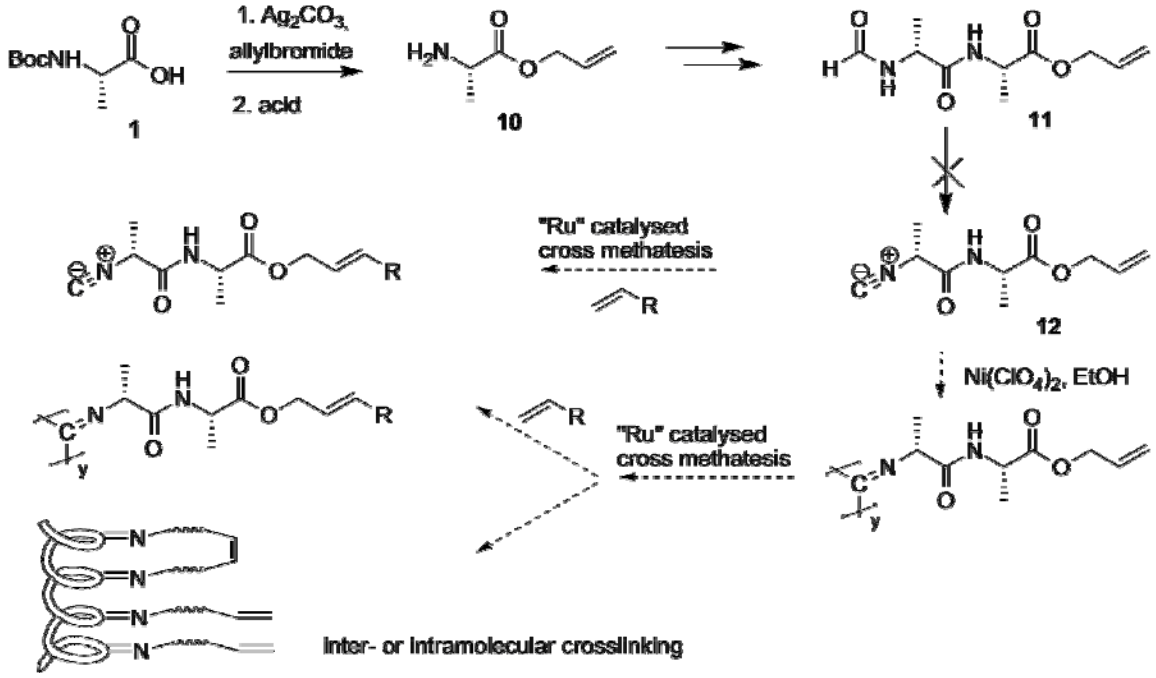

Scheme 3.5. *Synthetic route towards isocyano-D-Ala-L-Ala-Allyl-ester (D,L-IAAOAllyl).*

Upon treatment of formamide **11** with diphosgene to generate **12**, TLC showed the formation of a multitude of products. The predominantly formed product was an apolar one, which was isolated by column chromatography. Figure 3.1 shows an NMR experiment in time, performed to test the stability of this presumed isocyanide. Considerable degradation was observed over time.

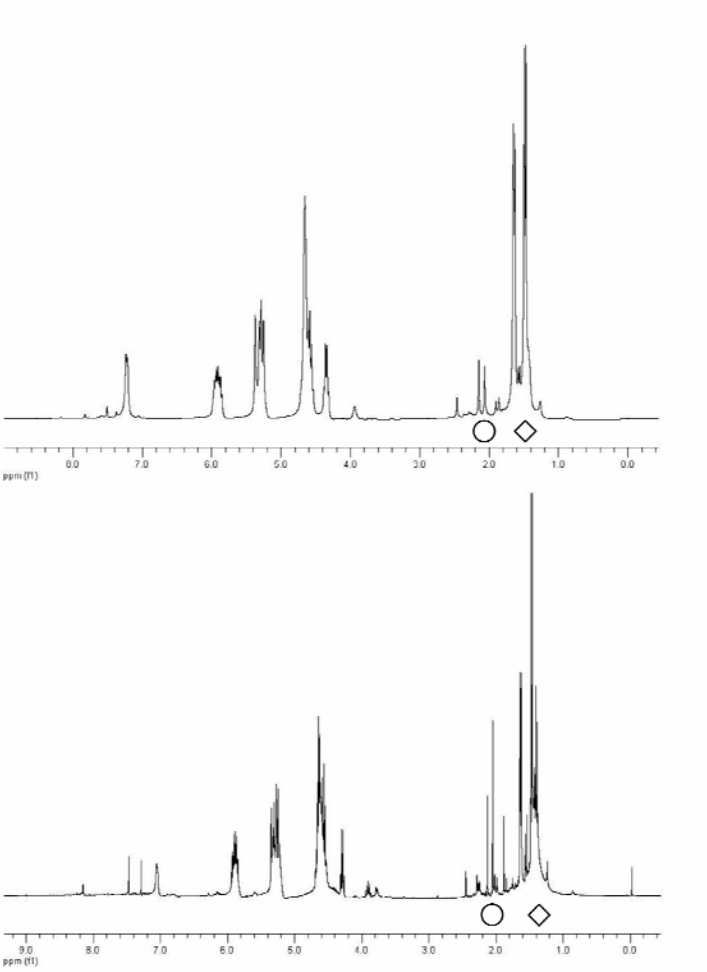

Figure 3.1. *NMR spectra of freshly purified (above) and partially degraded isocyano-D-Ala-L-Ala-Allyl-ester (below). (D,L-IAAOAllyl).*

Numerous new peaks appeared in the spectrum. When the signals for the methyl groups of the alanines are considered (diamond, top spectrum), both symmetrical doublets disappear to yield a cluster of peaks in the aliphatic region of the spectrum (diamond and circle, lower spectrum). Further research is required to investigate the nature of these compounds. A literature search on possible side reactions in the preparation of the allyl derivative did not provide any reason why this should be so; in fact, the first isocyanide ever prepared more than one hundred years ago was allyl isocyanide[17].

Isocyanides *D,L*-$IAAC_{12}$ and *D,L*-$IAAC_{20}$ (Scheme 3.4) but not *D,L*-IAAOAll showed a distinct infrared absorption at 2153 cm^{-1}, typical for an isocyanide. Thus, the

nature of the compound, resulting from the dehydration of the formamide remains elusive.

Polymerization reactions were carried out by dissolving one of the above described monomers in dichloromethane and adding a small amount of $Ni(ClO_4)_2$, dissolved in ethanol. Polymerization of the C_{20} and the C_{12} isocyanides yielded **8** and **9** (Scheme 3.4). Fast reactions were observed for both polymerizations. After several hours, infrared analysis revealed the absence of the characteristic peak at 2153 cm^{-1}, indicating full consumption of the isocyanide.

In the analyses of the polymeric structures by ^1H NMR, only parts of the alkyl tails could be visualized, presumably the part furthest away from the polymeric backbone. This effect could be caused by the fact that only the outer shell of the polymer, which contains these methylene- and methyl groups, is dissolved to a certain extent, and that both the steric bulk, as well as the presence of the hydrogen bonded network prevents dissolution. On the other hand, it is also possible that the rigidity of the polymer backbone imposes long relaxation times on the structure. Therefore, spectra were recorded with a very long relaxation time (D_1). Figure 3.2 shows the NMR measurement of *D,L*-$PIAAC_{12}$ with a D_1 relaxation time of 10 seconds.

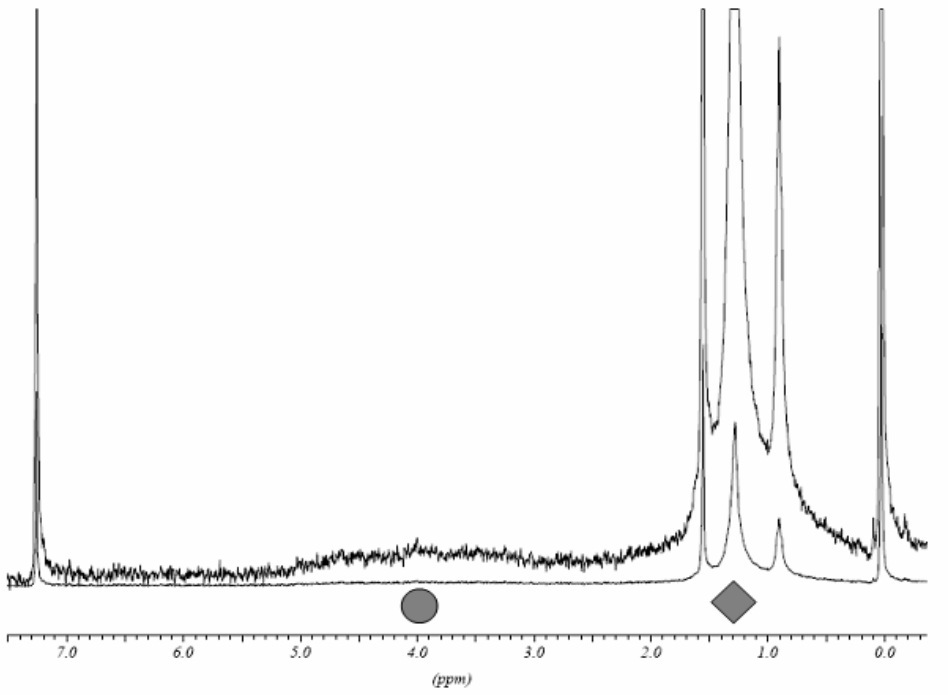

Figure 3.2. *^1H NMR spectrum of D,L-$PIAAC_{12}$, measured with a D_1 of 10 seconds (below), and a magnification (above). Proton NMR on D,L-$PIAAC_{20}$ (not shown) provided similar spectra.*

The clearly visible peaks in the bottom spectrum of Figure 3.2 are the methyl and methylene peaks (diamond), but only upon large magnification of the spectrum the very broad peak(s) between 3 and 5 ppm become visible (circle). This effect is presumably caused by a very large relaxation time which in turn may be caused by the fact that the isocyanide core is not solubilized. When *D,L*-PIAAC$_{20}$ was analyzed in the same manner, similar patterns were observed, and the intensities of the signals between 3 and 5 ppm were found to be even smaller, compared to the signals of the aliphatic part.

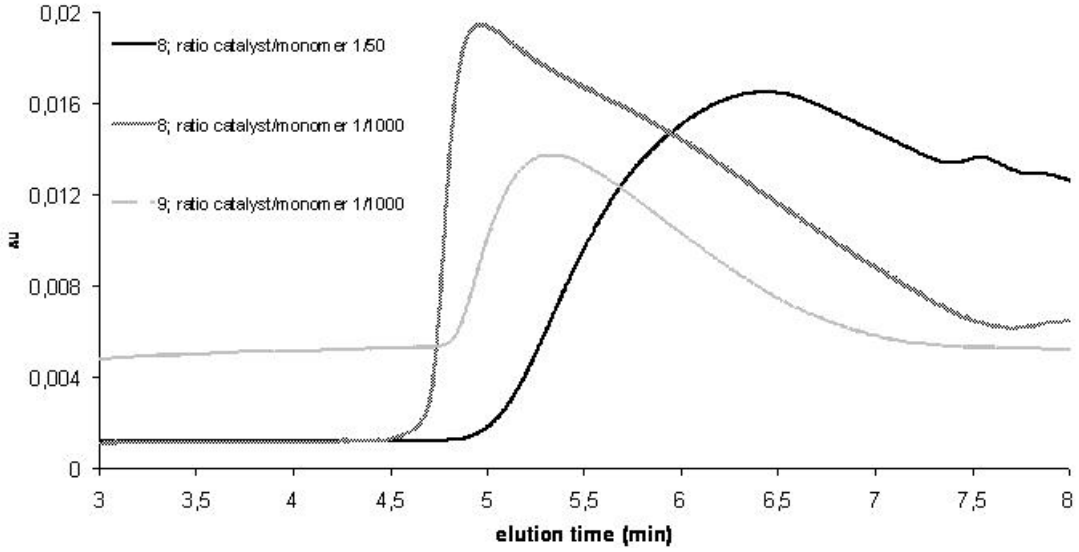

Figure 3.3. *Gel permeation chromatographs of **8** and **9**. Molecular weight data as follows: 8 (1/1000 cat.) Mp >3,000,000. 8 (1/50 cat.) Mp = 60,000. **9** (1/1000 cat.): Mp = 720,000.*

Figure 3.3 shows the GPC analysis of the polymers. Although the polymerization using more (1/50; ratio of catalyst to monomer) catalyst did yield a polymer of lower molecular weight than a reaction carried out at the ratio of 1/1000, the observed molecular weights in GPC did not correlate linearly to the ratios of nickel to monomer. The nickel concentration used was much lower than the initiator (EtOH) concentration, therefore the polymer length is primarily influenced by the amount of nickel used. During the polymerization reaction, the monomer concentration decreases. Therefore, a competing reaction, in which the catalyst complex dissociates from the growing polymer starts to play a role. Subsequently, these catalytically active nickel complexes can start a novel polymerization reaction. The large tails, observed in the GPC spectra, are the result

of this competing reaction. However, since the molecular weight of the polymers was very high, the range of this competing reaction is limited. The dissociation of the catalyst from the progressing polymerization reaction is therefore energetically not favored.
It may be possible to prevent the smaller molecular weigth fractions by maintaining a constant monomer concentration throughout the reaction. However, control is difficult since more complex mechanisms, such as the reduction/oxidation of the catalyst play a role as well.

The hydrodynamic radius of **8** (prepared with a catalyst/monomer ratio of 1/1000) is too large for the GPC column: the molecular weight is in excess of the range of the GPC column. (>3,000,000). There are two distinct possibilities when performing GPC on rigid polymers: *(i)* the rigidity of the polymer increases the net hydrodynamic volume, in that way reducing the elution time, effectively simulating the presence of a larger polymer, or *(ii*) the rigidity of the polymer causes the polymer to be withheld in the beads of the polystyrene matrix, since penetration of the nanoscopic channels requires a certain degree of flexibility. Molecular weight analysis of rigid-rod polymers by gel permeation chromatography is known to give overestimated values if polystyrene samples are used for calibration, which is the case here. However, the opposite has also been observed in the literature[18]. Fractions of higher molecular weight may be observed; a molecular weight of 3,000,000, however, seems to be excessive. Upon inspection of the GPC-curve of the *D,L*-PIAAC$_{12}$ (1/50 cat.) a considerable amount of lower molecular weight fractions are observed. This phenomenon is in accordance with the mechanism of initiation; the polymerization reaction is much faster than the formation of the initiator complex from the nickel salt, resulting in high molecular weight polymers and a large polydispersity. This is a second mechanism that increases the polydispersity.

Metselaar from our group has shown that calamitic rod-shaped polyisocyanide molecules can form cholesteric phases, when these polymers are present in high concentration[11]. Since these polymers required a solvent to obtain a lyotropic crystalline polymer solution, we envisaged that the alkyl tails in the presently discussed polymers may have two functions, i.e. they act as *(i)* a solvent and *(ii*) as an isotropic microphase. Thus, it was expected that these polymers might exhibit liquid-crystalline behavior in the melted phase.

Samples of L,D-PIAAC$_{12}$ and C$_{20}$ were therefore studied using a microscope with crossed polarizers, so that any liquid-crystalline behavior would be detected. Upon heating of the neat samples, however, no liquid-crystalline behavior was observed. The tell-tale ribbons that would indicate LC behavior remained absent throughout the melt.

A polymer sample of L,D-PIAAC$_{12}$ was studied by DSC. An exothermic peak was detected, which had an onset of 195^{o}C and a calculated heat of - 45 J/gram. A similar but much smaller peak was observed in the DSC trace, obtained from L,D-PIAAC$_{20}$. In both cases, the observed process was irreversible, leading to either one of the following possibilities: *(i)* destruction of the hydrogen bonding network or *(ii)* thermolysis of the ester bond. The former possibility seems unlikely, since *(i)* hydrogen bond breaking would take place more gradually and *(ii)* ester bond saponification is expected to be more exothermic. Other factors may also play a role, such as the absence of solvent and the presence of long tails, which possibly protect the hydrogen-bonded network. Still, an exothermal reaction is not to be expected in such a case. No further attempts were undertaken to elucidate the structures of the compounds that resulted after the thermal treatment.

3.3 Conclusions

Polymers L,D-PIAAC$_{12}$ and L,D-PIAAC$_{20}$ have been synthesized successfully, showing that it is possible to prepare very long rigid rod brush-like polymers with lipophilic side groups. GPC analysis has shown that the molecular weight of L,D-PIAAC$_{20}$, when polymerized using 1/1000 eq. of catalyst and initiator, exceeds the maximum of the GPC column, indicating a very high hydrodynamic radius of the polymer. Thus, the goals of the work described in this chapter have been reached; a simple polymerization method yields very long polymers with considerable hydrophobic bulk. Since the preparation of block copolymers of polyisocyanides has been described before, synthesis of the block copolymer as described in Chapter 1 is possible, at least in principle. The polydispersity of the polymers was very high, as is expected from the applied polymerization method. DSC data showed that the polymers possessed

considerable stability, since only at high temperatures degradation was found to take place.

The synthesis of the allyl functionalized isocyanide was not successful. As a reaction product *D,L*-formyl-alanylalanine allyl ester (**11**) was obtained in good yields. It seems likely that conversion of the formamide into the isocyanide yields the correct product, but that this reaction is subject to a number of side reactions, so that the yield of the desired product is low. IR analysis of the product did not show the isocyanide absorption.

3.4 Experimental Section

3.4.1 General experimental procedures

All organic solvents were of analytical quality or distilled before use. All reagents were used as received, unless otherwise stated. Silica gel chromatography was performed using J.T. Baker silica gel 20-70 um particle size and was pressurized. GPC was recorded on a Polymer Labs PLgel 5 μm column with chloroform as the eluent on a Shimadzu 10A LC system and was calibrated with monodisperse polystyrene samples obtained from Polymer Labs. NMR spectra were taken on a Bruker DMX 300 MHz or on a Varian DPX 400 MHz machine with TMS as the internal standard. DSC was carried out on a Perkin Elmer Diamond DSC apparatus, calibrated with indium standards.

3.4.2 Synthetic procedures

L-Alanine-icosanyl ester (*L*-A-C_{20}) (3)

In a 250 ml round bottom flask, equipped with a cooler and a Dean-Stark setup, p-TsOH.1H_2O (4.18 g, 22 mmol) and *L*-Alanine (**1**) (1.78 g, 20 mmol) were placed. To this, 5 ml water and 150 ml toluene were added, and the mixture was stirred until all compounds had dissolved. 1-Eicosanol (CH_3-$(CH_2)_{19}$-OH, 5.35 g., 19 mmol) was then added to the mixture. The reaction mixture was refluxed for 20 hrs, after which the calculated amount of water was collected in the Dean Stark trap. All solvents were

evaporated *in vacuo* and the remaining waxy mass was dissolved in chloroform. This solution was washed with an aqueous saturated $NaHCO_3$ solution (2x), water (1x) and the organic phase was dried and evaporated. During these work-up procedures, formation of emulsions was observed, rendering these procedures impractical. Silica gel column chromatography (eluent: MeOH/$CHCl_3$, 5 → 20 %) could not separate the product from the 1-eicosanol. Therefore, the solid was dissolved in acetone, and acetone/HCl (prepared by bubbling gaseous HCl through acetone) was added until the pH was ~2. The pure product was then crystallized from hot chloroform, yielding **3** in 80 % yield (6.4 g, 17 mmol), TLC Rf 0.6 ($CHCl_3$/MeOH/AcOH 89/10/1) ^{1}H-NMR (MeOH, 300 MHz): δ 4.2 (m, 2H, CH_2–O); 3.95 (q, 1H, *J* = 9.6 Hz, Cα-Ala) 1.69 (m, 2H, C$\underline{H}_2$-CH_2–O); 1.56 (d, *J* = 7.2 Hz, CH_3 alanine); 1.26-1.24 (m, 33 H, CH_2 icosanyl); 0.87 (t, *J* = 7 Hz, 3H, CH_3 icosanyl).

HCl.*D*-Alanine-*L*-Alanine-1-eicosanol ester (HCl.H-*D*-A-*L*-A-C_{20})

L-Ala-C_{20} ester (0.9 g, 2.4 mmol) and Boc-*D*-Ala (0.5 g, 2.7 mmol) were placed in a round-bottom flask, and co-evaporated twice with dry toluene. The mixture was then dissolved in DMF (30 ml) and HOBt (0.41 g, 2.7 mmol), and Et_3N (0.8 ml, 5.2 mmol) were added to the mixture. After stirring the mixture for 30 min. EDC (0.52 g, 2.7 mmol) was added. Not all components dissolved in the provided solvent, so more DMF was added, up to a volume of 70 ml. When this amount of solvent was not sufficient to dissolve all reagents, DCM was added (50 ml). The reaction was then observed to give complete conversion of the starting material into a slightly less polar compound. Silica gel column chromatography (Eluent: MeOH/DCM, 0 → 3%) afforded the slightly impure product. Subsequently, the product was co-evaporated twice with 1,4-dioxane, dissolved in dry EtOAc, and dry HCl gas was bubbled through the solution until complete deprotection had taken place. (~ 30 min.) All solvents were then evaporated and the product was co-evaporated twice with *tert*-butanol. Rf 0.1 (5% MeOH/DCM) ^{1}H-NMR (MeOD, 300 MHz): δ 4.43 (m, 1H, Cα-Ala); 4.14 (m, 2H, CH_2–O); 3.91 (m, 1H, Cα-Ala); 1.66 (m, 2 H, C$\underline{H}_2$-CH_2–O); 1.51 (d, *J* = 7.0 Hz, CH_3 alanine); 1.44 (d, *J* = 7.2 Hz, CH_3 alanine); 1.30 (m, 35 H, CH_2 icosanyl); 0.91 (t, *J*=6.6 Hz, CH_3 icosanyl).

_N_-Formamido-D-Alanine-L-Alanine-1-icosanol ester (_D,L_-Formyl- _(D)_-A-_(L)_-A-C_{20}) (6)

HCl.H-_D,L_-AA-C_{20} (1.6 g, 3.3 mmol) was placed in a round bottom flask, co evaporated with 1,4-dioxane (2x) and dissolved in a minimal amount of dry $CHCl_3$ (5-10 ml). Ethyl formate (100 ml) and sodium formate (1.4 g, 20 mmol) were added and the mixture was refluxed overnight. Since only small amounts of product could be obtained after this time, the mixture was evaporated to dryness, more ethyl formate was added and the reaction was refluxed again for ~20 hrs. After this time, TLC (10% MeOH/$CHCl_3$) showed complete conversion of the starting material into a slightly less polar product. (Rf 0.4 in this solvent) After evaporation of all solvents *in vacuo* the solid was extracted with warm chloroform (~200 ml) and a part of this solution was subjected to several standard washing steps. The amphiphilic character of the product, however, made this procedure very inefficient. Silica gel column chromatography on the crude mixture (Eluent: MeOH/DCM, 0 → 5%) afforded pure product in 70 % yield (1.1 g, 2.3 mmol). ^{1}H-NMR($CDCl_3$, 300 MHz): δ 8.16 (s, 1H, H-formyl); 6.54 (d, *J*=6.7Hz, NH formyl); 6.23 (d, *J* = 6 Hz, NH amide); 4.61 (m, 2H, 2 x Cα-Ala); 4.14 (m, 2H, CH_2–O); 1.65 (m, 2 H, C$\underline{H_2}$-CH_2–O); 1.43 (d, *J*=7 Hz, 6H, 2 x CH_3 alanine); 1.30 (m, 35 H, CH_2 icosanyl); 0.87 (t, *J* = 6 Hz, 3H, CH_3 icosanyl). ^{13}C-NMR ($CDCl_3$, 50 MHz DEPT): δ 160.2 (HCO); 65.8 (CH_2–O); 48.3 (Cα-Ala); 47.5 (Cα-Ala); 32.0 ($\underline{C}H_2$-CH_2–O); 29.82, 29.70, 29.63, 29.49, 29.32 (all CH_2 icosanyl); 28.63 ($\underline{C}H_2$- CH_2- CH_2-CH_3); 25.92 ($\underline{C}H_2$- CH_2-CH_3); 22.84 ($\underline{C}H_2$-CH_3); 18.6 (CH_3-Ala); 18.43 (CH_3-Ala); 14.30 (CH_3-icosanyl). Mp (uncorrected) 95-98 ^{o}C. ESI-MS: M/Z 468. calc.: 468.71.

_N_-Isocyano-(_D_)-Alanine-(_L_)-Alanine-1-eicosanol ester (_D,L_-IAA-C_{20}) (7)

_N_-Formyl-(_D_)-Ala-(_L_)-Ala-C_{20} ester (0.95 g, 2.0 mmol) was co-evaporated with 1,4 dioxane (3 x 30 ml) and dissolved in dry chloroform (50 ml). To this mixture, distilled petroleum ether 80-100 ^{o}C was added (40 ml), as well as _N_-methyl morpholine (0.46 ml, 4.2 mmol). The flask was cooled to -30 ^{o}C, after which diphosgene (0.12 ml, 1 mmol) in chloroform (5 ml) was added dropwise over 1 hr. TLC showed complete conversion of the starting material into an apolar product (Rf 0.9, 10 % MeOH/$CHCl_3$). The reaction was quenched by the addition of 10 ml ice-cold saturated aqueous $NaHCO_3$

solution and stirring was continued for 15 min. Separation of phases, washing the organic phase with brine (2x) and drying the organic phase with $MgSO_4$ yielded a solution that was evaporated to dryness *in vacuo*. Subsequently, the mixture was subjected to silica gel column chromatography (eluent MeOH/$CHCl_3$/Et_3N, 0/99/1 → 3/96/1). This procedure yielded pure (**7)** in 95 %. (0.88 g, 1.9 mmol). ^{1}H-NMR ($CDCl_3$, 300 MHz): δ 6.90 (br.s., 1H, NH); 4.53 (quintet, *J* = 7 Hz, 1H, Cα-Ala); 4.23 (q, *J*=6.4 Hz, 1H, Cα-Ala); 4.14 (m, 2H, CH_2–O); 1.66 (m, 5H, CH_3 Ala and C$\underline{H_2}$-CH_2–O); 1.47 (d, *J*=7.0 Hz 3H, CH_3 Ala); 1.25 (m, 37 H, CH_2 icosanyl); 0.87 (t, *J* = 6.0 Hz, 3H, CH_3 icosanyl). ^{13}C-NMR ($CDCl_3$, 50 MHz DEPT and FID (quaternary peaks from FID): δ 171.8 (C=O q); 165.4 (C=O q) 66.2 (CH_2–O); 53.6 (Cα-Ala); 48.9 (Cα-Ala); 32.24 ($\underline{C}H_2$-CH_2–O); 29.8, 29.7, 29.6, 29.5, 29.3, (all CH_2 icosanyl); 28.6 ($\underline{C}H_2$- CH_2- CH_2-CH_3); 25.92 ($\underline{C}H_2$- CH_2-CH_3); 22.84 ($\underline{C}H_2$-CH_3); 19.8 (CH_3-Ala); 18.3 (CH_3-Ala); 14.30 (CH_3-icosanyl). FTIR (neat) 2153.15 (C≡N stretch)

Poly(*N*-isocyano-(*D*)-Alanine-(*L*)-Alanine-1-eicosanol ester) *(D,L*-PIAA-C_{20}) (8)

In a round bottom flask, *D,L*-IAA-C_{20} (50mg, 0.11 mmol) was dissolved in $CHCl_3$ (2 ml) and to this solution, a solution of $Ni(ClO_4)_2$. 6 H_2O (5 mM in $CHCl_3$, 0.44 ml) was added. The presence of EtOH in commercial chloroform was ensured by NMR. The ethanol acts as the nucleophilic initiator in the polymerization reaction. The solution turned brown immediately upon the addition of the nickel salt, and the reaction was allowed to stir over night. TLC showed the disappearance of the starting isocyanide. After one night of stirring, no monomer could be detected by TLC. The reaction mixture was poured into methanol (50 ml, 2x) and dried in vacuo, yielding an off-white powder (16 mg, 32%). ^{1}H-NMR ($CDCl_3$, 300 MHz): δ 4.0 (very broad and small multiplet, presumably Cα-Ala); 1.25 (m, 1H, 9H, CH_2 icosanyl); 0.49 (m, 3H, CH_3 icosanyl). ^{13}C-NMR ($CDCl_3$, 50 MHz) no signals. $[\alpha]^{20}_{D\text{-}Na}$ +28.2^o . FTIR (neat) *absent*: 2153.15 (C≡N stretch). GPC see text.

***N*-Boc-(*L*)-Alanine-dodecanol ester (*L*-A-C_{12})**

In a round bottom flask, Boc-(*L*)-alanine (2.84 g, 15 mmol) and 1-dodecanol (1.86 g, 10 mmol) were placed. The compounds were dissolved in dry DMF (100 ml) and

HOBt (2.0 g, 15 mmol) and Et_3N (2.1 ml, 15 mmol) were added. This mixture was allowed to stir for 30 mins, until all components had dissolved. Then, EDC (2.87 g, 15 mmol) was added to the mixture and the reaction was allowed to react for 16 hrs. After this time, not all reagents had reacted therefore hexane (50 ml) was added to the reaction in order to solubilize the dodecanol and the product; the reaction was stirred for an additional 16 hrs. Subsequently, the reaction mixture was placed into a separation funnel and water (200 ml) was added, after which the hexane solution, containing the product, was separated from the DMF/water mixture. The DMF/water layer was then extracted with more hexane (4 x 30 ml), dried, evaporated. TLC showed only the presence of product, and this was of such purity that column chromatography was not required. (Rf 0.4; 5%MeOH/DCM). ^{1}H-NMR($CDCl_3$, 300 MHz): δ 5.36 (d, J = 7.8 Hz, 1H, NH); 4.18 (m, 1H, Cα-Ala); 4.12 (m, 2H, CH_2–O); 1.63 (m, 2 H, C$\underline{H_2}$-CH_2–O); 1.43 (d, *J*=7.2 Hz, 6H, 2 x CH_3 ala); 1.30 (m, 18 H, CH_2 dodecanyl); 0.85 (t, *J* = 6.3 Hz, 3H, CH_3 dodecanyl). ^{13}C-NMR ($CDCl_3$, 50 MHz): δ 172.5 (Cq CO Boc); 154.4 (Cq ester); 78.8 $\underline{C}(CH)_3$; 64.8 (CH_2–O); 48.9 (Cα-Ala); 31.99 (C$\underline{H_2}$-CH_2–O); 29.73, 29.71, 29.65, 29.59, 29.43, 29.32, 28.68 (all (all CH_2 dodecanyl); 28.36 (CH_3 Boc) 25.93 ($\underline{C}H_2$- CH_2-CH_3); 22.77 ($\underline{C}H_2$- CH_3); 18.50 (CH_3 Ala); 14.10 (CH_3 dodecanol).

HCl salt of (*L*)-Alanine-dodecanol ester (*L*-A-C_{12})

This compound was prepared in two ways, either via the route described for the analogous synthesis using the icosanol alcohol in a Dean Stark reflux setup, followed by HCl treatment, or by deprotection of the above compound: N-Boc-(*L*)-A-C_{12} was co-evaporated with 1,4 dioxane (2 x) and dissolved in EtOAc. Through this solution HCl gas was led, until all Boc had been deprotected, as observed by TLC (½ hour). The mixture was then co-evaporated with *tert* butanol (2x) and dried. ^{1}H-NMR ($CDCl_3$, 300 MHz): δ 8.75 (s, 1.5 H, HCl.NH_2); 4.17 (m, 3H, Cα-Ala and CH_2–O); 1.72 (d, 3 H, CH_3 ala); 1.64 (t, J=6.2 Hz, C$\underline{H_2}$-CH_2–O); 1.25 (m, 18 H, CH_2 dodecanyl); 0.85 (t, *J* = 6.3 Hz, 3H, CH_3 dodecanyl).

HCl salt of (*D*)-Alanine-(*L*)-alanine-dodecanol ester (HCl.*D*-A-*L*-A-C_{12})

HCl.H-(*L*)-alanine-dodecanol ester (9.9 g, 34 mmol) was co-evaporated with 1,4-dioxane (2x50 ml) and dissolved in DMF/hexane (4/1, 200 ml), after which HOBt (5.7 g, 38 mmol), Et_3N (10 ml, 72 mmol) and *N*-Boc-D-Ala-OH (7.1 g, 38 mmol) were added. EDC (7.2 g, 38 mmol) was then added to the mixture and TLC showed complete conversion after 16 hrs of stirring. The solvents were evaporated *in vacuo* after which the resulting slurry was redissolved in DCM, and extracted with aqueous $NaHCO_3$ (satd.) (2x 100 ml), water (1x 100 ml), 0.5 M HCl (2x 100 ml), dried over $MgSO_4$ and evaporated *in vacuo*. Silica gel column chromatography (eluent MeOH/DCM, 0/100 → 5/95) afforded pure product. Rf 0.85 (10% MeOH/$CHCl_3$). The product was subsequently dissolved in EtOAc (100 ml) and HCl gas was bubbled through until completion of the reaction (½ hr.). Rf 0.3 (5% MeOH/DCM). ^{1}H-NMR ($CDCl_3$, 300 MHz): δ 8.3 (d, J = 5.7 Hz, 1H, NH amide); 6.4 (br. s., 4 H, NH+); 4.55 (t, J = 7.2 Hz, 1H, Cα-L-Ala); 4.26 (m, 1H, Cα-D-Ala); 4.10 (m, 2H, CH_2–O); 1.66 (m, 6 H, C$\underline{H}_2$-CH_2–O and CH_3 alanine); 1.44 (d, *J* = 7.0 Hz, CH_3 alanine); 1.25 (m, 20 H, CH_2 dodecanyl); 0.87 (t, *J*=6.3 Hz, CH_3 icosanyl).

***N*-Formyl-(*D*)-Alanine-(*L*)-alanine-dodecanol ester (*D,L*-FAA-C_{12})**

HCl.H-(*D*)-(*L*)-AA-C_{12} (7.95 g, 22mmol) was dissolved in ethyl formate (200 ml) and sodium formate (8.9 g, 132 mmol) was added to this solution, which was subsequently refluxed for 16 hrs. TLC showed complete conversion after this time, so all solvents were evaporated *in vacuo* and the white solid was extracted with chloroform. The chloroform solution was then evaporated and the product was co-evaporated with 1,4-dioxane. Crystallization from acetone/Et_2O yielded the desired product in 70% yield (5.15 g, 14 mmol). ^{1}H-NMR ($CDCl_3$, 300 MHz): δ 8.17 (s, 1H, H-formyl); 6.50 (d, *J* = 6.6 Hz, NH formyl); 6.23 (m, 1H, NH amide); 4.55 (m, 2H, 2 x Cα-Ala); 4.12 (m, 2H, CH_2–O); 1.63 (m, 2 H, C$\underline{H}_2$-CH_2–O); 1.43 (d, *J*=7.2 Hz, 6H, 2 x CH_3 ala); 1.30 (m, 18 H, CH_2 dodecanyl); 0.85 (t, *J* = 6.3 Hz, 3H, CH_3 dodecanyl). ^{13}C-NMR ($CDCl_3$, 50 MHz DEPT): δ 160.5 (HCO); 66.0 (CH_2–O); 48.5 (Cα-Ala); 47.6 (Cα-Ala); 32.2 (C$\underline{H}_2$-CH_2–O); 29.9, 29.6, 28.8, 26.0, (all CH_2 dodecanyl); 23.0 (C$\underline{H}_2$-CH_3); 18.6 (CH_3-dodecanyl).

Isocyano-(*D*)-Alanine-(*L*)-alanine-dodecanol ester (*D,L*-IAA-C_{12})

D,L-Formyl-AA-C_{12} (5.15 g, 14.4 mmol) was co-evaporated with 1.4 dioxane (2 x 100ml) and dissolved in chloroform/hexane 75/25, v/v, 200 ml. To this solution, NMM was added (3.32 ml, 30 mmol) and the reaction mixture was cooled to -30 ^{o}C. Over a period of 1 hr, DPP (0.87 ml, 7.2 mmol) was added, and the reaction mixture was allowed to stir for 2 hrs. After this time, the reaction was quenched by the addition of aqueous $NaHCO_3$ (sat.) (30 ml) and the layers were separated. The organic layer was washed twice with brine and once with water. Crystallization of the product from EtOAc/Et_2O yielded the product in good yield (4.37 g, 12.9 mmol, 90 %). Rf 0.9 (10%MeOH/$CHCl_3$) M.p. 73^{o}C (uncorrected) b.p. (dec.) 240 ^{o}C. ^{1}H-NMR ($CDCl_3$, 300 MHz): δ 6.91 (br.s., 1H, NH amide); 4.53 (quintet, *J* = 7.2 Hz, 1H, Cα-L-Ala); 4.26 (q, *J*=6.4 Hz, 1H, Cα-D-Ala); 4.14 (m, 2H, CH_2–O); 1.64 (m, 5H, CH_3 Ala and C$\underline{H}_2$-CH_2–O); 1.47 (d, *J*=7.0 Hz, 3H, CH_3 Ala); 1.25 (m, 19 H, CH_2 dodecanyl); 0.87 (t, *J* = 6.0 Hz, 3H, CH_3 dodecanyl). ^{13}C-NMR ($CDCl_3$, 50 MHz): δ 171.8 (C=O q); 165.4 (C=O q);161.4 (Cq isocyanide) 66.2 (CH_2–O); 53.6 (Cα-D-Ala); 48.9 (Cα-L-Ala); 32.24 ($\underline{C}H_2$-CH_2–O); 29.9, 29.8, 29.8, 29.6, 29.5 (all CH_2 dodecanyl); 28.8 ($\underline{C}H_2$- CH_2- CH_2-CH_3); 26.1 ($\underline{C}H_2$- CH_2-CH_3); 23.0 ($\underline{C}H_2$-CH_3); 20.0 (CH_3-Ala); 18.5 (CH_3-Ala); 14.5 (CH_3-dodecanyl) FTIR (neat) 2153.12 (C≡N stretch)

Poly(*N*-isocyano-(*D*)-Alanine-(*L*)-Alanine-dodecanol ester) . *(D,L*-PIAA-C_{12}) (9)

In a round bottom flask, *D,L*-IAA-C_{12} (400 mg, 1.18 mmol) was dissolved in $CHCl_3$ (10 ml) and to this solution, a solution of $Ni(ClO_4)_2$. 6 H_2O (5 mM in $CHCl_3$, 0.236 ml, 0.1% relative to monomer concentration) was added. The presence of EtOH in commercial chloroform, which functions as the nucleophilic initiator in the polymerization reaction, was ensured by NMR. The solution turned brown immediately upon addition of the nickel salt, and the reaction was allowed to stir over night. TLC showed the disappearance of the starting isocyanide; after one night of stirring, no monomer could be detected anymore by TLC. The reaction mixture was poured into methanol (50 ml, 2x) and dried *in vacuo*, yielding an off-white powder (16 mg, 32%). ^{1}H-NMR ($CDCl_3$, 300 MHz): δ 5.0 - 3.0 (very broad and small multiplet, presumably Cα-

Ala); 1.25 (m, 6H, CH_2 dodecanyl); 0.87 (m, 3H, CH_3 dodecanyl). ^{13}C-NMR ($CDCl_3$, 50 MHz) no signals. FTIR (neat) *absent*: 2153.12 (C≡N stretch). GPC see text.

L-Alanine-allyl ester (10)

N-Boc-*L*-Alanine (10 g, 52 mmol) was co-evaporated with 1,4-dioxane (3 x 200 ml) and dissolved in DMF (150ml), after which the flask was cooled in a ice bath and covered in aluminum foil to shield the mixture from light. Next, Ag_2CO_3 (18.9 g, 67 mmol) was added and the stirred mixture was allowed to warm up to room temperature. Allyl bromide (20.6 ml, 235 mmol) was added and the reaction was allowed to proceed for 4 hours, after which TLC (eluent: 10% MeOH/$CHCl_3$ Rf 0.9) showed complete conversion of the starting material to a more apolar compound. The mixture was filtered and the resulting solid was washed with ETOAc (3x 100 ml), after which the filtrate was evaporated *in vacuo.* The product was then re-dissolved in Et_2O, which was washed with cold aqueous 0.5 M HCl (100 ml, 2x) and brine (1 x 100 ml). The solvent was evaporated, yielding crude *N*-Boc-*L*-Alanine Allyl ester, which was subsequently co-evaporated twice with toluene (100 ml) and dissolved in dry EtOAc (200 ml). HCl gas was passed through this solution until TLC showed complete conversion into a new product. The solution was evaporated *in vacuo* and co-evaporated twice with *tert*-butanol (2 x 150 ml), yielding 12 g. (72 mmol) of impure product. At least part of the impurity was remaining *tert*-butanol, as determined by NMR.

***N*-Boc-D-Alanyl-L-alanine-allyl ester (*N*-Boc-(*D*)-A-(*L*)-A-OAll)**

HCl.(*L*)-Ala-OAll (12 g, all of the above yield) was dissolved in DMF (200 ml) and *N*-Boc-*D*-Alanine (11 g, 58 mmol), HOBt, (9 g, 58 mmol), and Et_3N (18.5 ml, 132 mmol) were added to the mixture, after which it was cooled in an icebath. Subsequently, EDC was added (11 g, 59 mmol), and the reaction was allowed to stir overnight. After this period, a complete reaction had occurred, as shown by TLC. The solvent was evaporated *in vacuo*. The slurry was redissolved in EtOAc (300 ml) and washed subsequently with aqueous $NaHCO_3$ (satd.) (2 x 100 ml), water (1x 100 ml), 0.5 M citric acid (2 x 100 ml) and brine (2 x 100 ml) yielding the crude title compound (15.2 g, 56 mmol), which was reacted in the next step without further purification.

_(D)_-Alanyl-(_L_)-alanine-allyl ester HCl salt (HCl.D,L-AA-OAll)

N-Boc-(*D*)-A-*(L)*-A-OAll (15.2 g, 56 mmol) was treated in dry EtOAc (300 ml) with dry HCl gas, that was passed through the mixture. Circa 2 hrs of bubbling the gas appeared to be sufficient for complete conversion of the starting material into a very apolar compound. The product was then extracted from the EtOAc into a water-layer by repeated extraction (5 x 50 ml) with water and this solution was evaporated *in vacuo* and co-evaporated with 1,4 dioxane (3 x 100 ml) to yield 12.8 g (55 mmol, 95%) of the title compound as an off-white oil. ^{1}H-NMR ($CDCl_3$, 300 MHz): δ 8.68 (d, *J*=6.6 Hz, 1H, NH amide); 8.09 (s, 3 H, NH_2^+); 5.90 (m, 1H, CH_2-C<u>H</u>=CH_2); 5.34 (d, *J*=17 Hz, 1H, CH_2-CH=C<u>H</u>$_2$); 5.24 (d, *J*=10.2 Hz, 1H, CH_2-CH=C<u>H</u>$_2$); 4.62 (m, 4H, CH_2–O and 2x Cα); 1.67 (d, *J*= 6.6 Hz, 3H, CH_3 *D*-ala); 1.48 (d, *J*= 7.2 Hz, 3 H, CH_3 *L*-ala).

***N*-Formyl-(*D*)-alanyl-(*L*)-alanine-allyl ester (D,L – FAA-Oall)**

HCl.H-*D,L*-AA-OAll (0.54 g, 2.2 mmol) was dissolved in ethyl formate (50 ml) and sodium formate (0.6 g, 8.8 mmol) was added to this mixture, which was subsequently refluxed for 18 hrs. TLC showed complete conversion after this time. The solvent was evaporated *in vacuo* and the resulting white solid was dissolved in EtOAc and this solution was filtered. Crystallization from EtOAc/Et_2O yielded the desired product in 70% yield (0.4 g, 1.5 mmol). TLC (EtOAc 100%) Rf 0.85. ^{1}H-NMR ($CDCl_3$, 300 MHz): δ 8.15 (s, 1H, H-formyl); 6.80 (d, *J* = 6.0 Hz, NH formyl); 6.45 (m, 1H, NH amide); 5.90 (m, 1H, CH_2-C<u>H</u>=CH_2); 5.26 (2 x d, *J*=9.3 Hz, 2H, CH_2-CH=C<u>H</u>$_2$); 4.61 (m, 4H, CH_2–O and 2x Cα); 1.47 (m, 6 H, 2 x CH_3 ala). ^{13}C-NMR ($CDCl_3$, 50 MHz): δ 164.0 (Cq); 160.7 (C=O formyl); 131.1 (CH_2-<u>C</u>H=CH_2); 118.5 (CH_2 allyl); 65.95 (CH_2-O Allyl); 48.27, 47.37 (2x Cα); 18.5, 18.07 (2 x CH_3 Ala).

Isocyano-(*D*)-alanyl-(*L*)-alanine-allyl ester (*D,L* – IAA-OAll)

D,L–FAA-OAll (0.4 g, 1.5 mmol) was co-evaporated with toluene (2 x 30 ml) and subsequently dissolved in DCM (30 ml). To this solution, NMM was added (1.7 ml, 1.5 mmol) and the reaction mixture was cooled to -30 ^{o}C. Over a period of 1 hr, DPP (0.09 ml, 0.75 mmol) was added, and the reaction was allowed to stir for 2 hrs, during which the mixture was allowed to heat up to room temperature. TLC showed a multitude

of spots at this stage. The reaction was quenched by the addition of $NaHCO_3$ (satd., 30 ml,) and the layers were separated. The organic layer was washed twice with brine and once with water. Silica gel column chromatography (toluene/acetone 100/0 to 90/10, v/v) afforded slightly impure title compound. The yield was not determined since the compound was found to be unstable.

Poly(isocyano-(*D*)-alanyl-(*L*)-alanine-allyl ester (*D,L* – PIAA-OAll)

The product obtained from the previous reaction, *D,L* – IAA-Oall, was dissolved in DCM (10 ml) and to this solution, a solution of $Ni(ClO_4)_2$. 6 H_2O (5 mM in DCM/MeOH 80/20, v/v, 2.1 ml, 0.5 % relative to monomer concentration) was added. TLC showed the disappearance of the starting isocyanide; after one night of stirring, no monomer could be detected anymore by TLC. Subsequently, the reaction mixture was precipitated in methanol (50 ml, 1x) and analyzed by ^{1}H-NMR; no polymer could be detected by this method.

3.5 Notes and references

[1] M.B.J. Otten, G.A. Metselaar, J.J.L.M. Cornelissen, A.E. Rowan and R.J.M. Nolte, Polyisocyanides: Stiffened Foldamers, *Ed*. S. Hecht, I. Huc **2007**, 367.

[2] F. Millich, *Chem. Rev.*, **1972**, *72*, 101.

[3] R.J.M. Nolte, *Chem. Soc. Rev.* **1994**, *23*, 11.

[4] F. Millich and G.K. Baker, *Macromolecules* **1969**, *2*, 122.

[5] J. T. Huang, J. X. Sun, W. B. Euler and W. Rosen, *J. Pol. Sci. A.* **1997**, *35*, 439.

[6] R.J.M. Nolte, A.J.M. van Beijnen and W. Drenth, *Recl. Trav. Chim. Pays-Bas,* **1980,** *99,* 121.

[7] Y. Yamada, T. Kawai, J. Abe, T. Iyoda, *J. Pol. Sci. A.* **2002**, *40*, 399.

[8] M. Ishikawa, K. Maeda, E. Yashima, *J. Am. Chem. Soc.* **2002,** *124,* 7448.

[9] M. Ishikawa, K. Maeda, K. Mitsusuji and E. Yashima, *J. Am. Chem. Soc.* **2004,** *126,* 732.

[10] J.J.L.M. Cornelissen, J.J.J.M. Donners, R. de Gelder, W.S. Graswinckel, G.A. Metselaar, A.E. Rowan, N.A.J.M. Sommerdijk and R.J.M.Nolte, *Science* **2001**, *293*, 676.

[11] G.A. Metselaar, *Ph. D. Thesis, Radboud University Nijmegen* **2006**, 64.

[12] G.A. Metselaar, J.J.L.M. Cornelissen, A.E. Rowan and R. J. M. Nolte, *Angewandte Chemie* **2005**, *117*, 2026.

[13] G.A. Metselaar, *Ph. D. Thesis, Radboud University Nijmegen* **2006**, 98.

[14] J.J.L.M. Cornelissen, J.J.J.M. Donners, R. de Gelder, W.S. Graswinckel, G.A. Metselaar, A.E. Rowan, N.A.J.M. Sommerdijk and R.J.M. Nolte, *Science*, **2001**, *293*, 676.

[15] EDC = N-ethyl-N'-dimethylaminopropyl carbodiimide HCl salt.

[16] H.E. Blackwell, D.J. O'Leary, A.K. Chatterjee, R.A. Washenfelder, D.A. Bussmann and R.H. Grubbs, *J. Am. Chem. Soc.* **2000**, *122*, 58.

[17] W. Lieke, "*Über das Cyanallyl". Annalen der Chemie und Pharmacie* **1859**, *112*, 316.

[18] Y. Tian, Y. Li, T. Iyoda, *J. Pol. Sci. Part A: Pol. Chem.* **2003**, *41*, 1871.

Chapter 4

Synthesis of polystyrene sulfonate by ATRP

4.1 Introduction

In Chapter 1, the objectives of the work described in this thesis have been explained. It is the intention to use a specific virus (CCMV) as a host for a negatively charged polymer. This polymer is part of a block copolymer. The other part of this copolymer is very bulky and hydrophobic giving the block copolymer an amphiphilic character. Thus, inclusion of the negatively charged part of the block copolymer into the viral host would yield a mega amphiphile, of which the polar head consists of the viral cage and the tail of the large hydrophobic polymer. Several conditions must be met in order to be able to such a structure. First of all, the inclusion of the negatively charged polymer into the viral cage must be understood in some detail. Secondly, the inclusion process must somehow be followed, implying that some analytical tool must be employed. For the latter, the use of fluorescence spectroscopy was envisaged. These demands lead to the following requirements: *(i)* the ability to synthesize well-defined, negatively charged polymers and *(ii)* the possibility to functionalize these polymers with a fluorescent probe. This chapter describes our efforts to prepare such polymers. The

development of new, fluorescent initiators for Atom Transfer Radical polymerization (ATRP) is reported in this chapter, as well as the preparation of deuterated polystyrene sulfonate by ATRP using deuterated styrene, followed by sulfonation of the polymer. The deuterated polystyrene is required in order to be able to study the interaction of polystyrene sulfonate with the protein shell of the CCMV virus, employing small angle neutron scattering. The latter research is described in Chapter 6.

In this chapter, furthermore, the use of a new monomer for ATRP, i.e. styrene-4-sulfonate ethyl ester, will be described, as well as a novel deprotection technique. The methodologies presented here allow unprecedented control over the molecular weight, polydispersity, and end functionality of polystyrene sulfonate polymers.

4.2 Literature overview

The design and synthesis of polymers possessing well defined lengths, functionalities, polydispersities, and architectures have been a long standing ambition of polymer chemists. Until ca. 10 years ago, cationic, anionic and ring-opening polymerizations were the prevalent methods of choice to achieve this ambition. Disadvantages of these methods are the high sensitivity of the process to monomer functionality and impurities, the elaborate laboratory set ups that in most cases are required, and the inapplicability of these procedures to a large variety of monomers. Matyjaszewski was the first to report[1] the use of the Atom Transfer Radical Addition (ATRA) technique (Scheme 4.1.) in controlled/'living' polymer synthesis.

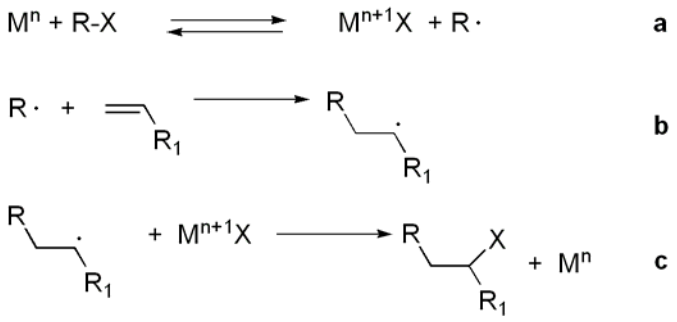

Scheme 4.1. *Mechanisms of Atom Transfer Radical Addition.*

ATRA[2] is a process in which a transition metal species M^n abstracts a halide atom X from an organic halide RX in a homolytic bond dissociation (reaction a), yielding $M^{n+1}X$ and a radical R·. This radical then adds to an alkene, yielding an intermediate radical species (reaction b). The key step to prevent bimolecular termination of this species, and to favor addition to another alkene, is the fast reaction between the intermediate radical species and $M^{n+1}X$ to regenerate the catalyst M^n and the product (reaction c). ATRA is thus an efficient method to create carbon-carbon bonds from alkyl halides and alkenes. The presence of a halogen in the product is useful for further manipulations and reactions. For ATRA, it is imperative that the reaction conditions inhibit the abstraction of this halide from the product. However, for ATRP (see below), the halogen atom must be abstracted from this product in order to create a propagating species.

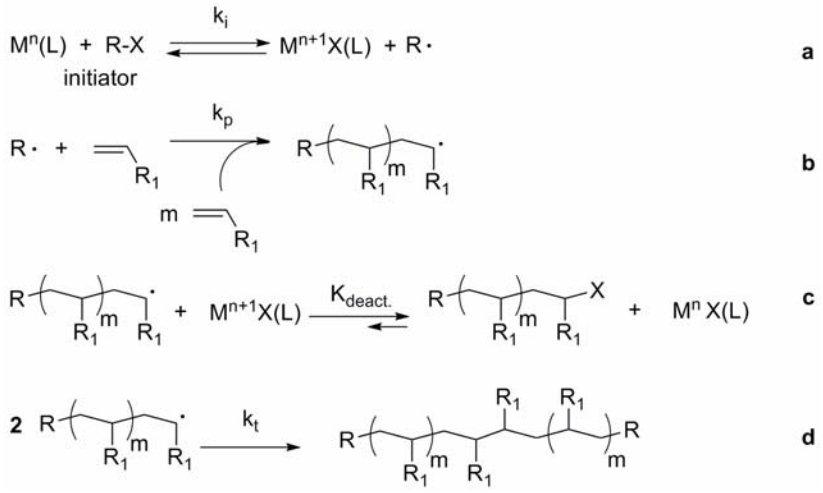

Scheme 4.2. *Mechanisms of Atom Transfer Radical Polymerization.*

ATRP like ATRA acts by abstracting a halide atom from an initiator species (Scheme 4.2, reaction a). Again, as in the case of ATRA, the created radical reacts with an alkene bond to yield a new radical (Scheme 4.2, reaction b). However, a ligand (L) is now used to promote the shuttling of the halogen between the growing polymer chain and the metal-ligand complex (Scheme 4.2, reaction c). The temporarily deactivated polymer chain subsequently reacts with the catalyst again to regenerate the radical. As the equilibrium constant of this reaction $K_{deact.}$ is very large, termination reactions such as

radical coupling (Scheme 4.2, reaction d) are kept at a minimum due to the low concentrations of the radical species. The magnitude of $K_{deact.}$ is imperative to the control of the reaction: if $K_{deact.}$ is too high, no or very little reaction will occur, if it is too low, the termination reaction will have a too large effect. Another part of the reaction in which delicate control can be obtained in ATRP is the propagation step. If abstraction of the halogen atom is fast, the concentration of radicals is very high during the polymerization reaction. This, in turn, implies that the equilibrium constant, K_{deact}, will not be very large (the equilibrium lies to the left) and this condition leads to the occurrence of a number of side reactions, such as bimolecular termination. It also is also important that the rate constant of the initiation step (k_i) is faster than the rate constant of the propagation step. If this is not the case, polymer chains resulting from an effective initiation in the reaction mixture will continue to grow whereas unreacted initiator molecules will only react at a later point in time. Slow initiation will therefore increase the polydispersity. In summary, the complex interplay of all the rate and equilibrium constants in Scheme 4.2 can give rise to a polymerization that is "just right", meaning that initiation is fast with respect to propagation and that the process is not too fast, keeping radical concentrations in the reaction mixture to a minimum and thus reducing the occurrence of side reactions. In this chapter, a polymerization reaction of styrene sulfonate ethyl ester is described that is tuned such that it reaches ca. 70% conversion in 4 hours. A fluorescent initiator is synthesized and used in the polymerization reaction to yield well-defined fluorescent polystyrene sulfonate. This methodology affords the polyanionic polymer species that is required for the study of the interaction with the virus capsid. These results are reported in Chapter 6.

4.2.1 Initiators for ATRP

As considerable effort in this chapter is directed towards the synthesis of a suitable initiator compound, an overview of ATRP initiators reported in the literature is appropriate. As discussed above, the rate of initiation needs to be fast in comparison to the rate of propagation in order to obtain a monodisperse polymer. In ATRP, the amount of initiator added to the reaction mixture determines the final molecular weight of the

polymer. Macromolecular or multifunctional initiators may be used in ATRP polymerization reactions in order to obtain different types of polymeric architectures. The most frequently used initiators for ATRP are halogenated alkanes. Chloroform and tetrachloromethane, for example, are two of the first initiators studied in the polymerization of methyl methacrylate (MMA)[3]. Mono-, and dichloromethane are not able to polymerize MMA. In general, the use of polyhalogenated initiators is not very efficient, since control over their reactions is not always optimal. In the ATRP of styrene, CCl_4 acts as a bifunctional initiator, as opposed to the ATRP of MMA[4]. Other initiator systems, such as benzylic halides, have been shown to be efficient initiators for styrene and its derivatives due to the structural and electronic resemblance of the initiator structures to the monomers. 1-Phenylethyl chloride is an efficient initiator for the polymerization of styrene, however, in the polymerization of MMA, this compound fails to act as desired, resulting in a polymer displaying a bimodal molecular weight distribution[3,4]. This is in contrast to more stabilized initiators such as benzhydryl chloride (Ph_2CHCl), which are capable of promoting an efficient polymerization reaction. Exchange of the chlorine for a bromine atom in the initiator (1-phenylethyl bromide) yields an efficient initiator species as well, apparently because radical generation is much faster for a bromine than for a chlorine derivative[6]. α-Haloesters have found widespread use in ATRP, which can be attributed to their efficient initiation, both in styrene- and acrylate-based systems. In general, α-haloisobutyrates initiate better than α-haloisopropionates, due to the better stabilization of the generated radicals from the first mentioned compounds. Functionalization of the ester is very well tolerated, and as such, many ATRP-generated polymers have been synthesized using a variety of functional groups, e.g. alcohols, epoxides, vinyl groups, lactones, and benzoic acids. Figure 4.1 shows a small although representative selection of proprionate initiators.

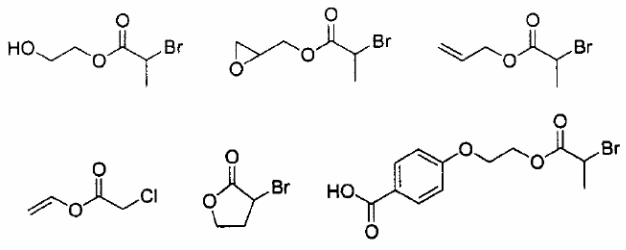

Figure 4.1. *Various ester based functional initiators used in ATRP.*

It has been shown, that when the isopropionate esters shown in Figure 4.1 are replaced by their isobutyrate analogs, the initiation efficiency is higher. This is related to the higher stability of the generated radical species. On the other hand, the stabilization of the carbon atom cannot be allowed to be too high, since the carbon-halogen bond may then be split heterolytically to generate two ions. This may be the case in the ATRP reaction of p-methoxystyrene, which only yields oligomers, and mainly dimers[7]. Apparently, in this polymerization, the electron donating methoxy group on the styrene promotes the heterolysis of the carbon-bromine bond to generate a cation instead of a radical. It is not clear why the polymerization reaction then does not proceed cationically. Another explanation for this phenomenon could be that the radical is formed first, but is then oxidized by the Cu(II) species to form the cation.

The easy functionalization of the ester moiety, combined with the relative insensitivity of ATRP to functional groups have allowed the straightforward synthesis of a vast number of polymeric architectures. For example, functionalization of PEG with one or two initiator ester moieties yields di- (AB) or triblock (ABA) copolymers when polymerized with a second monomer[8]. It is also possible to prepare block copolymers by post polymerization functionalization of the polymers with initiator groups. For instance, condensation of a dendritic species with isobromobutyric acid followed by polymerization has been shown to yield core-shell structures[9].

In general, the success of ATRP strongly depends on a proper balance between all the rate and equilibrium constants depicted in Scheme 4.2. These constants are determined by the nature of the monomer, the solvent, the reaction temperature, the initiator, and the catalyst. The proper combination of all these factors have made the development and understanding of ATRP a challenging process, in which catalyst and initiator design have been steadily improved over the last decade to give reactions in which the monomer in good approximation reacts in a first order kinetic process and in which the molecular weight of the polymer increases linearly with conversion.

4.2.2 Preparation of polystyrene sulfonate

Poly(sodium 4-styrene sulfonate) (PSS) is a versatile polymer and crosslinked PSS has found widespread use in ion-exchange applications[10]. It is furthermore used as a super-plastifier in cement[11], as a dye improving agent for cotton[12], and as proton exchange membranes in fuel cell applications[13]. Pharmaceutical applications of PSS include its use as a treatment for abnormally high levels of potassium in the blood (hyperkalemia)[14]; it is also an effective topical microbicide and spermicide, inhibiting the genital transfection of, among others, HIV[15]. Finally, PSS is used as a convenient model system for the study of the physical properties of RNA and DNA, provided that it is synthesized in a completely reproducible manner (see below)[16]. Although the behavior of PSS in solution has been a topic of intense studies over the last years, its synthesis has not been investigated in great detail[17]. PSS is mostly prepared by post-polymerization sulfonation of polystyrene, see Scheme 4.3[18].

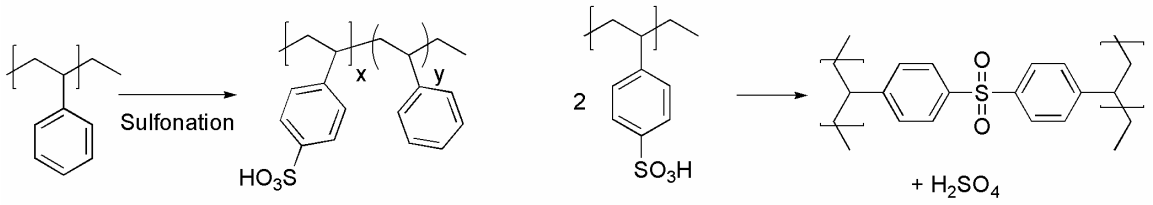

Scheme 4.3. *The sulfonation of polystyrene to yield polystyrene sulfonate, PSS. The ratio x/y defines the sulfonation degree. Right: crosslinking reaction in the sulfonation of polystyrene.*

The harsh conditions used in this approach lead to the occurrence of a number of side reactions. Double substitutions of the phenyl rings are known to occur, even at conversions well below 100%. Crosslinking reactions between two sulfonic acid groups which yield a sulfonyl crosslink are also found. The reproducible determination of a number of properties (e.g. the influence of ion density on thermal, optical and electrical properties) of these polymers is therefore hampered, because these side reactions lead to irreproducible ion content and large and/or multimodal size distributions[5,19]. It has been shown that even when applying carefully selected identical conditions, repeated for several sulfonation reactions, no reproducible results are obtained. Especially, in the application as ion exchange membranes, this is a serious problem during the production;

no two membranes will have the same properties, if they are produced from different batches of polymerization. Furthermore, should one desire to use polystyrene sulfonate in medical applications, it is also highly desirable to produce identical materials at any given time.

In order to synthesize polystyrene sulfonate with reproducible length *and* ion content (and thus properties) sodium styrene sulfonate has been polymerized by nitroxide-mediated polymerization (NMP). This was achieved by Keoshkerian et al.[20], who homo-polymerized sodium styrene sulfonate (NaStS) at 125°C using a 3:1 v/v ethylene glycol/water mixture and potassium persulfate as the initiator in combination with 2,2,6,6-tetramethyl-1-piperidinyloxy (TEMPO). Number-average molecular weights ranged from 7200 to 762,000, polydispersities varied from 1.12 to 1.33, and conversions as high as 97% could be reached. However, the temperatures required for this reaction were very high, and the reaction was slow.

Other groups have continued this research and have synthesized block-copolymers of styrene and styrene sulfonate[21] as well as block-copolymers of NaStS and 4-vinylbenzoic acid[22] with the objective to prepare micelles that show a dependence of pH in their aggregation behavior. Reverse Addition-Fragmentation chain Transfer polymerization (RAFT) has been carried out with NaStS, using a 4,4′-azobis(4-cyanopentanoic acid) as initiator in combination with 4-cyanopentanoic acid dithiobenzoate as a chain transfer agent in water at 70 °C. This work by Chiefari et al.[23] yielded polymers with a polydispersity of 1.13 and a molecular weight M_n of 8,000. Several groups have independently reported the use of NaStS in an ATRP reaction in water. Tsarevski et al. have investigated the ATRP of NaStS in a 1:1 v/v water/pyridine mixture at 30°C and obtained a conversion of 70%, a molecular weight M_n of 10,900 and a polydispersity of 1.26 (Scheme 4.4)[24].

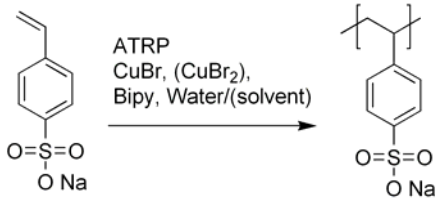

Scheme 4.4. *Atom Transfer Radical Polymerization of sodium styrene sulfonate in water. The use of methanol and/or $CuBr_2$ significantly increases the control over the reaction. Solvents that have been used include pyridine and methanol.*

Polymerization of NaStS in pure water under the same conditions produced poly(NaStS) with a much higher polydispersity of 2.06, and a conversion of only 32% was achieved. Armes and Iddon have reported the use of ATRP in a water/methanol solvent system[25]. They reported that if pure water is used, no good control over the polymerization reaction is obtained. The reaction in pure water yielded a polymer with a higher polydispersity and lower conversion, which is in agreement with the results obtained by Tsarevski, and also with the studies performed by Choi et al. who reported that $CuBr_2$ has a stabilizing effect on the polymerization of NaStS in water, and that the polymerization of NaStS in pure water yields polymers with not only a high polydispersity index but also with a bimodal distribution. Armes and Iddon suggested that the emergence of a higher molecular weight fraction is due to the occurrence of fast side reactions such as the coupling of growing radical chains at the initial stages of reaction. It is of interest to note that the reactions in pure water are extremely fast, even if they are carried out at room temperature. The investigations by Choi also showed that the reaction is exothermic, increasing the reaction temperature by several degrees, when it is carried out in pure water with the following combination of reagents: NaStS:CuBr:$CuBr_2$:Bipy[26]:initiator = 60:1:1:2:1 (in moles) at 25^{o}C and a monomer concentration of 1M.

Although the production of polystyrene sulfonate is feasible in this way, several important drawbacks are still present for our applications. First of all, the initiator that is used needs to be water soluble. In the examples presented above, water-soluble initiators such as 2-bromo-2-methyl propionate, functionalized with a short PEG, as well as 1-bromoethylbenzoic acid are used. However, since one our goals in this work is the preparation of fluorescent (block-co)polymers of polystyrene sulfonate, this would imply the use of a fluorescent, water soluble initiator. The synthetic challenges in the preparation of such a compound are not trivial. Furthermore, in the preparation of a block copolymer of polystyrene sulfonate-*b*-(aliphatic polymer) the solubility problems would be very hard to overcome. Another problem arises with the analysis of such water-soluble polymers. It is known, for example, that the strong ionic bonding between and within the polystyrene sulfonate chains greatly hamper mass spectrometry analysis. MALDI-TOF analysis of polystyrene sulfonate has been reported, but only on polymers that had first

been polymerized using anionic techniques to prepare polystyrene, and then modified by sulfonation[27]. As explained above, the ion content in these sulfonation techniques is not reliable, and therefore such polymers are not suitable for our purpose.

For the reasons explained above, it was decided to develop a strategy, in which a protected styrene sulfonate, which is soluble in organic solvents, is polymerized using a fluorescent or multifunctional initiator. The resulting polymers are easily analyzed relative to water-soluble polystyrene sulfonates. They can be analyzed by GPC using an organic eluent. Furthermore, an initiator that is soluble in organic solvents can be used (see below), allowing a range of synthetic strategies to be employed.

4.2.3 Click chemistry

As is explained in the introduction of this chapter, as well as in the main introduction of this thesis, one of our main goals is the preparation of block copolymers comprising a hydrophilic (anionic) block and a hydrophobic block. One of the methods to achieve this is the coupling of terminally functionalized polymers. Advantage of this methodology is the fact that the two blocks can be prepared separately according to different chemical syntheses and the ability to follow the formation of the desired product by GPC. A disadvantage of this method is the fact that the end groups of the prepared polymers will have reduced reactivity. Therefore, exceedingly efficient reactions must be used that provide highly reactive functionalities. A consequence of the use of such functionalities is the occurrence of side reactions. For this reason, “click” chemistry may be highly suitable to achieve the coupling of the two blocks.

Much attention has recently been directed towards chemical reactions which possess, amongst others, the following properties: *(i)* high specificity, *(ii)* favorable enthalpy of formation and *(iii)* high tolerance with respect to functionalities. One such reaction, the copper(I) catalyzed azide-alkyne 1+3 dipolar Huisgen[28] cycloaddition, better known as “click” reaction, is shown in Scheme 4.5.

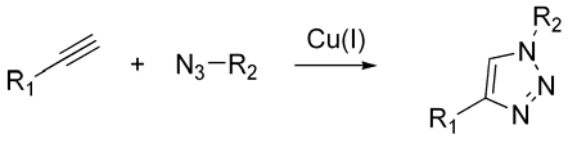

Scheme 4.5. *Copper (I) catalyzed "click" reaction.*

It involves the reaction of a terminal azide and an acetylene moiety under the agency of Cu (I) species to generate 1,2,3-triazoles. The reaction proceeds in high yields and without any side products[29]. The latter is due to the highly energetic nature of the coupling reaction. It is conspicuous, that despite the fact that each moiety is highly reactive, both functional groups are insensitive to most manipulations. It has been found that click reactions proceed best in aqueous conditions, even when the reactants are very sparingly soluble in this medium. Further advantages are that in many cases, the synthesized small compounds are crystalline in nature and that the catalyst can be easily removed from the reaction mixture by extraction[30].

The advantages described above have made research efforts on click chemistry to increase dramatically over the last few years. Various block copolymers[31], dendrimers[32], star polymers[33], and graft copolymers[34] have been prepared by this methodology. Since the copper(I) catalyzed azide-alkyne cycloaddition reaction is compatible with the presence of many functional groups, including groups present in biological systems, it is also a perfect tool to be employed in the preparation of protein-polymer bioconjugates[35].

4.3 Results and discussion

4.3.1 Synthesis of fluorescent initiator

The polymerization of styrene sulfonate ethyl ester using ATRP is described in this chapter. As explained in the introduction section, a halogen functionalized initiator is required for ATRP. In order to detect, by fluorescence, the presence of a polymer it was decided to synthesize a fluorescent ATRP initiator. In a first series of experiments, the functionalization of coumarin 343 was attempted. Despite several reactions employing a variety of methods, such functionalization proved impossible. Subsequently, L-Lysine

was chosen as it can be orthogonally functionalized on three synthetic handles. Several reaction conditions were employed in the synthesis of a compound that was designed to possess three-fold functionality: An ATRP initiator, a fluorescent group for detection and a synthetic handle to enable block copolymer synthesis at a later stage. Such functionalization was shown to be unsuccessful.

In an attempt to use the ester based initiator for ATRP, bromoisobutyric acid bromide was reacted with propargyl alcohol to yield **2** (Scheme 4.6).

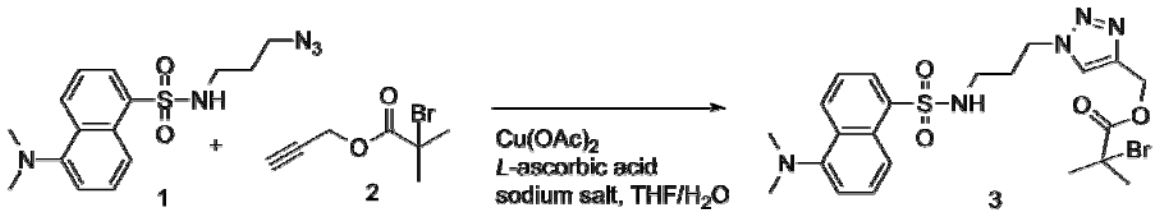

Scheme 4.6. *Synthesis of a fluorescent, ester- based initiator.*

In a separate experiment it was found that polymerization of **2** ethyl styrene sulfonate ethyl ester initiated by **2** yielded well-defined poly(styrene sulfonate ethyl ester) with a propargyl functionality. Reaction of **1** with **2** under copper(I) catalyzed conditions yielded the fluorescent initiator **3** in quantitative yield. When used in an ATRP reaction, initiator **3** led to a polymerization reaction that showed good kinetic control, both for styrene and for ethyl styrene sulfonate as monomers. However, it was found that treatment with the relatively weak base $(NH_4)_2CO_3$, used to deprotect the ethyl functionalities of poly(styrene sulfonate ethyl ester), quantitatively hydrolyzed the bromoisobutyryl end group of the polymer, rendering the fluorescent label useless (see below).

From the work presented above it was concluded that the bromoisobutyryl group is quite labile. No valuable initiator has been prepared, despite efforts to maintain conditions as mild as possible, and the reaction times as short as possible. Therefore, the use of the bromoisobutyric ester was discarded, notwithstanding the fact that it is known to be a very efficient initiator[36]. Thus, it was decided to prepare a non-ester based initiator system To this end, the benzoic acid initiator **4** was employed (Scheme 4.7). In order to couple it with the readily available compound **1** (see Scheme 4.6)**,** 1-bromoethyl benzoic

acid **4** was reacted with propargyl amine using 1-ethyl-3-(3-dimethylaminopropyl) carbodiimide hydrochloride (EDC) and hydroxybenzotriazole **(**HOBt) as coupling reagents.

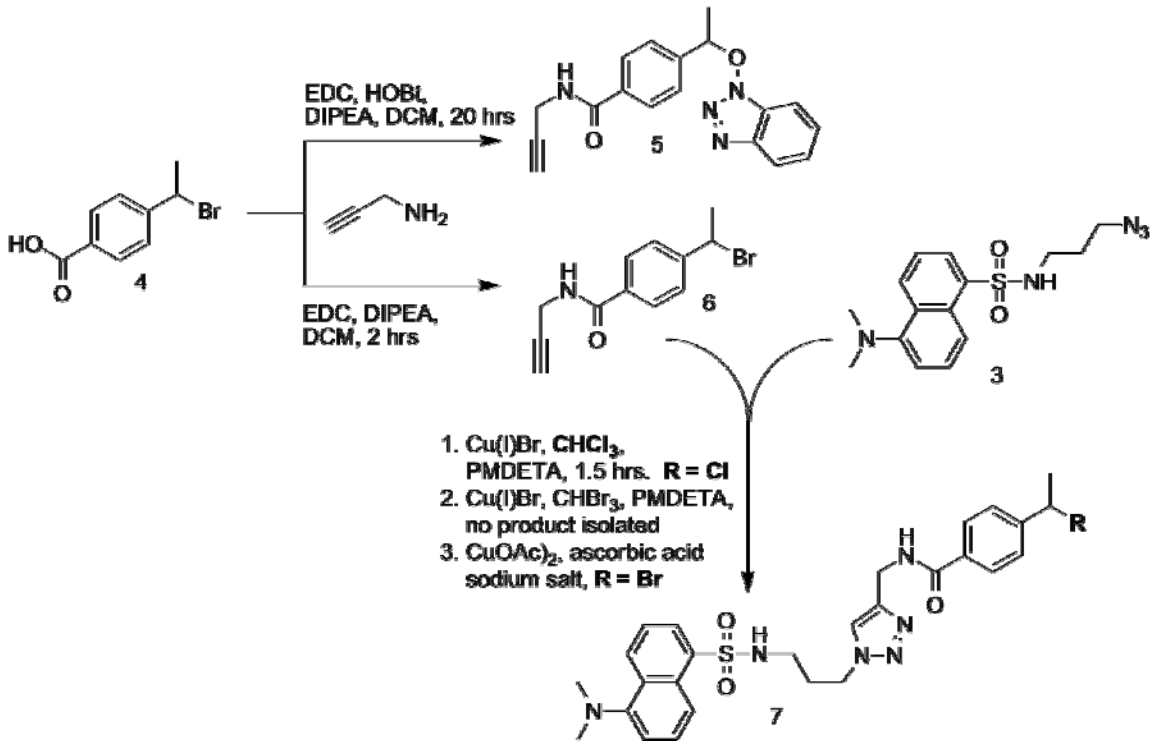

Scheme 4.7. *"Click" chemistry synthesis of the fluorescent, amide-based initiator* ***7****.*

The overnight reaction yielded a product that could be isolated in high yield, however, its ^{1}H-NMR spectrum showed various unexpected signals in the aromatic region, corresponding to an ortho-substituted benzene ring. Careful NMR and LCMS analysis showed that compound **5** was obtained, and that a multicomponent reaction (MCR) had occurred; apparently, the hydroxyl functionality on the nitrogen atom of HOBt was nucleophilic enough to displace the bromine in **4**.

When the reaction was carried out without the presence of HOBt (Scheme 4.7), compound **6** could be isolated in high yields. Separate ATRP reactions using **6** revealed moderate control of the kinetic parameters of the reaction[37] (see below). Several attempts were undertaken to react **1** with **6** in order to obtain **7** (R=Br). Initially, Cu(I)Br was employed as a catalyst in chloroform, with PMDETA as the ligand. This procedure, however, yielded a compound similar to **7** in which the bromine atom was quantitatively displaced by chlorine, presumably by an exchange reaction with chloroform. Therefore,

$CHBr_3$ was used as the solvent for this reaction, however, two separate attempts, employing this freshly distilled solvent yielded no product. The more standard procedure using $Cu(OAc)_2$ and sodium ascorbate, however, gave the desired product in high yields. Subsequently, **7** was used as the initiator in ATRP, however, the attempted reactions were not successful, probably because the triazole group, present in the initiator, coordinates to the copper catalyst required for ATRP.

It was then decided to employ dansyl chloride in the synthesis of a fluorescent initiator for ATRP, based on stable amide bonds and an alkyl spacer, with enough molecular flexibility to exhibit good solubility properties. (Scheme 4.8).

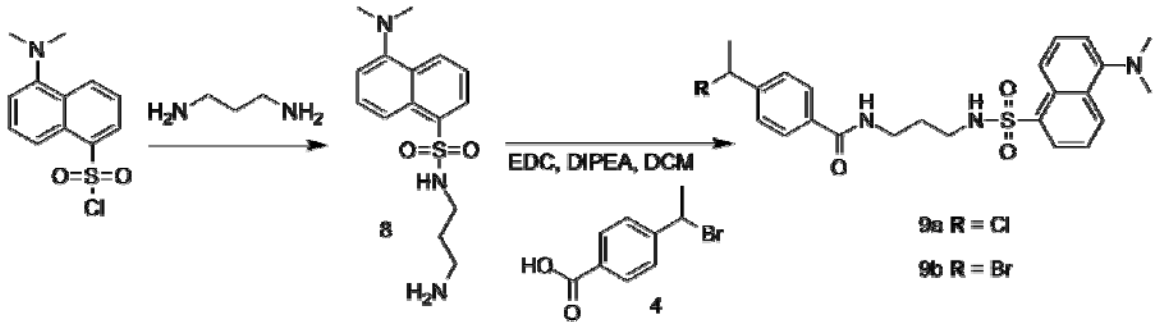

Scheme 4.8. *Synthesis of a non-ester based fluorescent ATRP initiator.*

Thus, a reaction of dansyl chloride with excess 1,3-propyldiamine was carried out, yielding **8** in good yield. This compound was subsequently condensed with initiator **4** using EDC to give **9b**. When the reaction times were too long (*i.e.* overnight) **9a** was obtained; apparently the chlorine atom, present in EDC slowly exchanges with the bromine atom under these conditions. Although such halogen exchange reactions are known in the literature, they often require transition-metal catalysis or very high temperatures[38]. Compound **9b** was found to possess suitable properties for initiation of an ATRP reaction (vide infra).

4.3.2 ATRP of styrene sulfonate ethyl ester

Monomer synthesis

Several articles cite the preparation of ethyl styrene-4-sulfonate (ESS). Rostociev et al. have reacted potassium styrene-4-sulfonate with PCl_5 to obtain 4-styrene sulfonyl chloride, subsequently reacting it with ethanol to obtain the ethyl ester[39] (Scheme 4.9, reaction A). Peculiarly, no solvent for the reaction was mentioned in this publication, although all the reacting compounds in the first step are solids. In our laboratory, purification of the monomer turned out to be difficult; separation of the monomer from unreacted sulfonyl chloride was highly problematic. Purification also required a vacuum distillation at relatively high temperature, inevitably leading to oligomerization.

Complete p-toluenesulfonic ethyl ester formation has been reported to occur upon treatment of the corresponding acid with triethyl orthoacetate[40]. We therefore decided to treat sodium styrene sulfonate with $HClO_4$ to give the sulfonic acid (Scheme 4.9, reaction B). Subsequent reaction of the acid with triethyl orthoacetate yielded the ethyl ester in reasonable yields, as shown by TLC. NMR analysis of the reaction mixture revealed, however, that the intensities of the double bond protons had decreased significantly during the reaction, leading to the conclusion that oligomerization had also taken place in this case. Although vacuum distillation should be possible to obtain pure product, the resulting yields would be quite low. Chromatographic purification is not a viable option in the present case, since the difference in polarity of the monomer and (short) oligomers is very small. As such, the synthesis of a sizeable quantity (e.g. 20 g) is problematic.

A more efficient procedure turned out to be an adaptation of a literature procedure published by Wegner et al.[41], in which sodium styrene sulfonate is reacted at room temperature with silver nitrate in water (Scheme 4.9, reaction C). Isolation and desiccation of the resulting product, followed by reaction with ethyl bromide yielded the desired compound. It was found that dropwise addition of a solution of silver nitrate, instead of addition of the solid, gave better yields of the monomer. We also found that a capacious condenser was required in the reaction with ethyl bromide. The combination of these measures made column chromatography as applied in the literature procedure

redundant, requiring only two filtration steps, which is very useful for the preparation of larger quantities. Ethyl 4-styrene sulfonate therefore is accessible in high quantities, yields and purity.

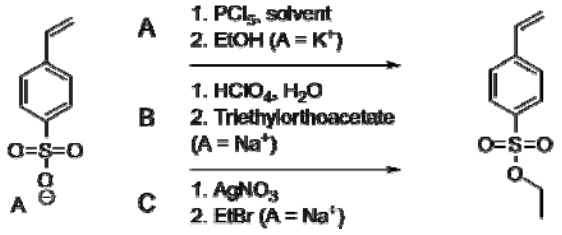

Scheme 4.9. *Three strategies for the synthesis of SSEt.*

ATRP of styrene sulfonate ethyl ester

In a first series of experiments, several test reactions were carried out employing the prepared monomer in bulk. The monomer reactivity was found to be much higher than that of styrene; a reaction performed at 100°C (SSEt:CuBr:PMDETA[42]:initiator, 100:1:1:1 (molar ratios) where initiator = ethyl bromoisobutyrate, Figure 4.2, no solvent) yielded a solid and brittle glass within one hour. This glass could only be dissolved after lengthy stirring with dichloromethane or chloroform.

Lowering the temperature to 90°C, and subsequently to 80°C still gave reactions that proceeded too fast for ^{1}H-NMR analysis of the progress of the polymerization. Practically, the process of taking sufficient samples and analyzing these with NMR, followed by mathematical analysis is difficult if the polymerization reaches 90 % conversion within one hour.

A change to a ligand that is known to bind the copper species less strongly, *viz.* 2,2'-bipyridine gave reactions that could be reasonably followed in time. Unrelated to the ligand species, the ATRP reactions of SSEt in bulk have in common, that the kinetic plots obtained generally deviate significantly from a straight line, *i.e.* only by crude approximations they obey first order kinetics[43]. Polydispersities are also higher. Figure 4.2 shows results obtained from the polymerization of SSEt at 80°C, with the following ratio of compounds: SSEt:Bipy:CuBr:Init = 800:2:0.5:1. The large amount of

SSEt (800 equiv.) was used to eliminate the influence of monomer concentration on the kinetic processes at higher conversions.

Figure 4.2 shows that a reasonably straight line can be fitted through the data points up to ca. 90 minutes. After this time, the reaction kinetics deviate from the linear trend. Two effects were visible during the reaction: first, the viscosity had increased, and secondly, the mixture had turned inhomogeneous; upon the collection of a sample, areas of larger and smaller viscosity could be discerned. This led us to postulate that the polymer was barely soluble in the monomer, and that the concentration of polymer could not be allowed to reach a certain critical value. Indeed, further experiments yielded well-defined polymers with low polydispersity, when the conversion was kept below ~ 40%. Although this procedure was used to some extent in our experiments, it was nevertheless decided to search for a more efficient procedure.

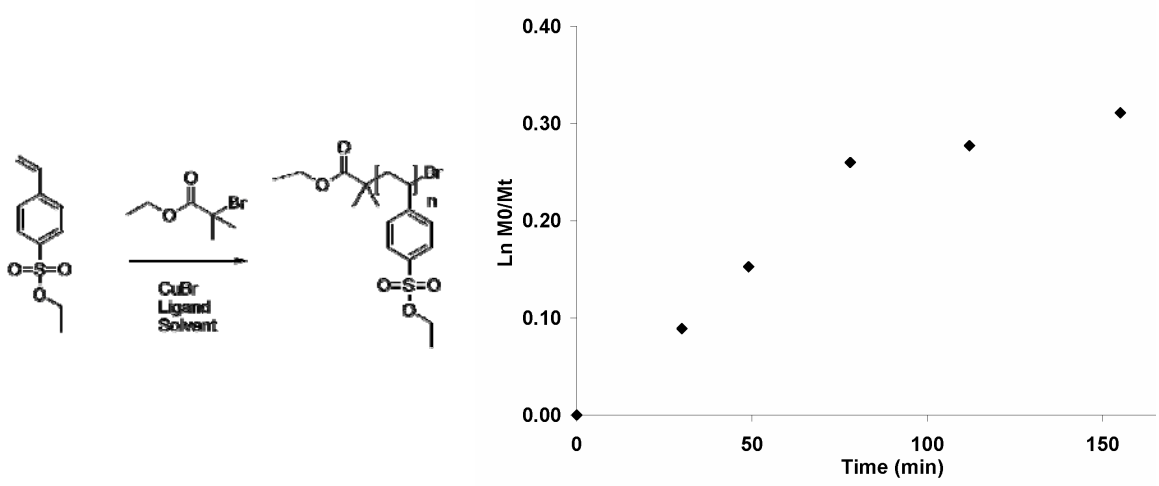

Figure 4.2. *Plot of ln(M0/Mt), where M0 and Mt are the relative concentrations of the monomer at time 0 and time t, respectively, versus time in the ATRP of SSEt in bulk. Reagents and conditions: SSEt: Bipy: CuBr: Init = 800:2:0.5:1, no solvent, 80°C.*

Inherent to a kinetically efficient procedure is the use of a solvent to reduce viscosity (thereby increasing the mobility of the reactive chain endgroup) and to increase polymer solubility, so that conversion can be allowed to reach higher levels.

However, a solvent needs to comply with the following conditions as well: *(i)* the solvent should be chemically inert; *(ii)* it should have a boiling point much higher than the reaction temperature; *(iii)* preferably, the copper complex should dissolve in the

solvent; *(iv)* the solvent should be practically manageable, i.e. it should for example be liquid at room temperature and not be excessively toxic or hygroscopic.

Table 4.1 summarizes the results of polymerization reactions carried out in several solvents.

Table 4.1. *ATRP of SSEt in several solvents. Reagents and conditions: SSEt :CuBr :PMDETA :initiator are 100: 1: 1: 1 (molar ratios) where initiator = ethyl bromoisobutyrate, monomer concentration 1 or 2 M in the solvent.*

Solvent	Ligand	Inert	Homogeneous reaction mixture	Practical	Result[a]
DCM	Bipy	No	Yes	Yes	M
DMSO (wet)	Bipy	No	Yes	Yes	M
DMSO (dry)	PMDETA	Yes	Yes	No	No
Toluene	PMDETA	Yes	No	Yes	K
Anisole	PMDETA	Yes	No	Yes	K
Acetone	PMDETA	Yes	Yes	No	K
THF	PMDETA	No	No	Yes	K
DMF	PMDETA	No	Yes	Yes	H
Ethylene carbonate	Bipy	Yes	Yes	No	G
1,2-dichloroethane	PMDETA	No	Yes	No	M
Propylene carbonate	Bipy	Yes	Yes	Yes	G

[a]*M = multimodal polymer molecular weight, H = monomer hydrolysis, No = no reaction observed, K = unsatisfactory kinetics, G = desired results*

Although it is known that dichloromethane (DCM) itself acts as an initiator for ATRP, we applied this solvent (entry 1) because of the necessity to dissolve the fluorescent initiator (**9b**) for later experiments. This initiator at first only appeared to be soluble in DCM or chloroform (see below). It was thought likely that the bromide of the initiator would be much more active in efficiently initiating the reaction than dichloromethane at the moderate temperatures used (room temperature). The result, however, was a low-molecular weight polymer with a multimodal molecular weight distribution, as observed by GPC, leading us to conclude that DCM indeed gives rise to

initiation. The use of DMSO was then investigated, but moderately wet DMSO was observed to give rapid hydrolysis of the monomer. Upon drying and distillation of the solvent, no polymerization reaction was observed. Although this reaction was only attempted once, the use of very dry DMSO was considered to be unpractical and too cumbersome. Toluene and anisole as solvents led to unsatisfactory kinetic behavior, because the resulting polymers were insoluble. However, we have exploited the insolubility of the polymer in the purification of the polymer in toluene; it is used as a precipitation medium, in which the monomer dissolves, but the polymer precipitates.

Although acetone is able to dissolve both the monomer and polymer, as well as the copper complex, the reaction at 30^{o}C was too sluggish to be efficient (higher temperatures will boil-off the acetone). The solvent must also be very dry to prevent hydrolysis of the monomer at the longer reaction times, required in this case. Further investigations led to the use of THF, in which the polymer unfortunately was found to be only sparingly soluble. Subsequently, DMF was investigated as a solvent. Figure 4.3 shows a plot of ln Mo/Mt versus the time, and as can be seen a clear linear dependence is observed at lower conversions, whereas higher conversions lead to a deviation from this linearity.

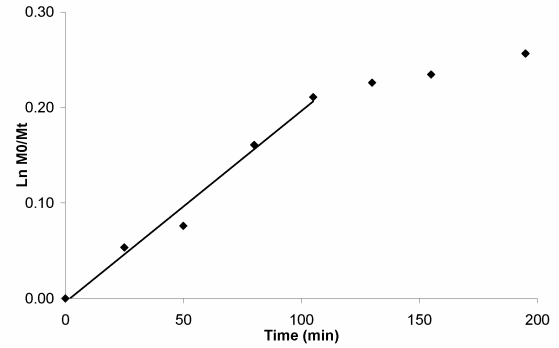

Figure 4.3. *Plot of ln(M0/Mt) versus time in the ATRP of SSEt in DMF.*

Inspection of the NMR spectra at high conversions revealed the origin of this deviation; a second set of vinylic protons was present, as well as peaks that could likely be an ethyl group attached to a polar moiety such as an amine or alcohol. These data point to hydrolysis or aminolysis (see below), which will cause a decrease in reaction rate because of solubility reasons; both monomer and polymer must be affected similarly by

this hydrolysis and the resulting amines and sulfonates are likely to poison the catalyst as well. Because the DMF used had been freshly distilled, the presence of water in significant quantities was excluded as the hydrolytic agent. Scheme 4.10 shows a possible hydrolysis mechanism, in which DMF is hydrolyzed, possibly catalyzed by copper. The dimethylamine obtained can then displace the ethyl functionality from the monomer and polymer. However, this mechanism was not proven.

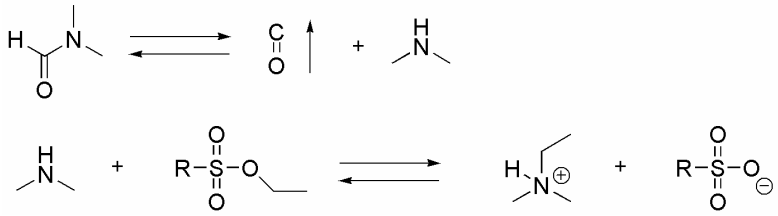

Scheme 4.10. *Degradation of DMF and corresponding aminolysis reactions. R = monomer or polymer.*

No further efforts were undertaken to investigate the reaction patterns in more detail.

In a subsequent series of experiments, the use of ethylene carbonate as a solvent was tried. Concentrations of 1 or 2 M of were used in the reaction and the ethylene carbonate has been shown before to be efficient in ATRP[44] (Scheme 4.11).

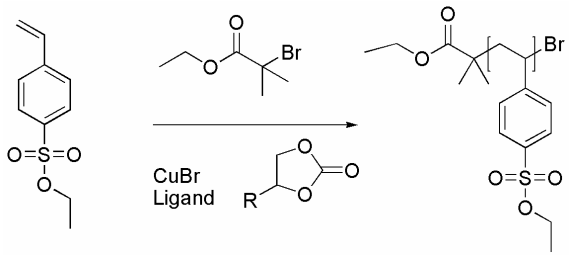

Scheme 4.11. *ATRP of SSEt in ethylene carbonate (R=H) or in propylene carbonate (R=Me).*

Figure 4.4 shows the kinetic plots of a ATRP reaction carried out in ethylene carbonate at 60^{o}C. As can be seen from the graphs, the polymerization reactions approach first order kinetics to a high degree.

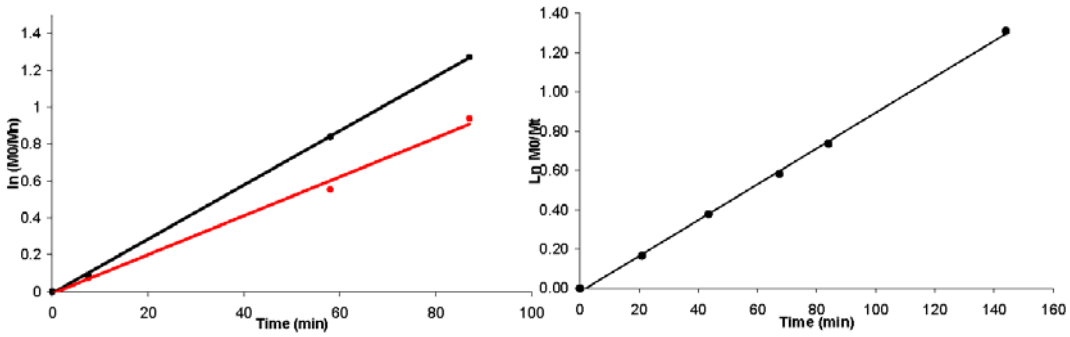

Figure 4.4. *First order kinetic plots for the ATRP of SSEt in ethylene carbonate. Left: in black the data points as obtained from a comparison of the integrals of the solvent signals and the peaks of the vinylic protons; in grey the comparison of the vinylic protons with the proton signals in the aromatic region. Right: duplo ATRP reaction. Solvent integral peaks are compared with the vinylic protons.*

Since ethylene carbonate is a solid at room temperature, it was decided to switch to propylene carbonate, which is a liquid at room temperature. Kinetic evaluation yielded similar results for both solvents at two different temperatures; 60 and 70°C. As a control experiment, the ATRP reaction was also carried out in the absence of initiator in ethylene carbonate (reaction time of several hours). It appeared that no conversion took place, excluding the occurrence of side reactions. Only when initiator was added did the reaction commence (Figure 4.5). For the reaction beginning at that point a good kinetic control was obtained.

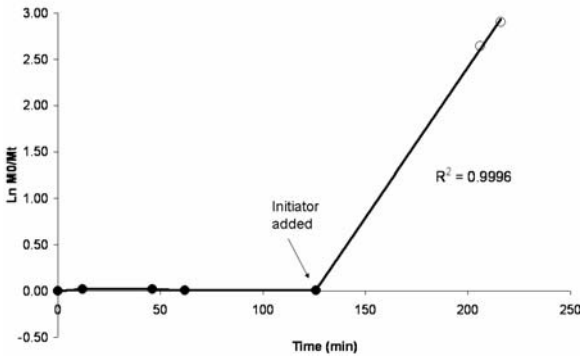

Figure 4.5. *Analysis of the autopolymerization reaction of SSEt in ethylene carbonate at 60°C. The reaction only starts when the initiator is added.*

In certain polymerization reactions, probably those in which some water was present in the solvent, a conspicuous effect was observed in the GPC analysis of the polymer product, viz. the presence of a high molecular weight peak, besides the expected

lower molecular weight peak (Figure 4.6). However, if the pESS was hydrolyzed and the resulting polymer analyzed by water-based GPC (FPLC, superose columns), only one peak was visible. Since the polymerization of styrene sulfonate ethyl ester was shown to be possible, several polymerization experiments were carried out using fluorescent photoinitiator **9b**. After polymerization and purification (*vide infra*), the polymer showed a distinct yellow coloring. Figure 4.6 shows representative GPC chromatograms, as obtained in the analyses of several batches of dansyl-pESS (obtained by the initiation of the ATRP reaction with **9b**), as well as an FPLC chromatogram, obtained after deprotection of the ethyl functions.

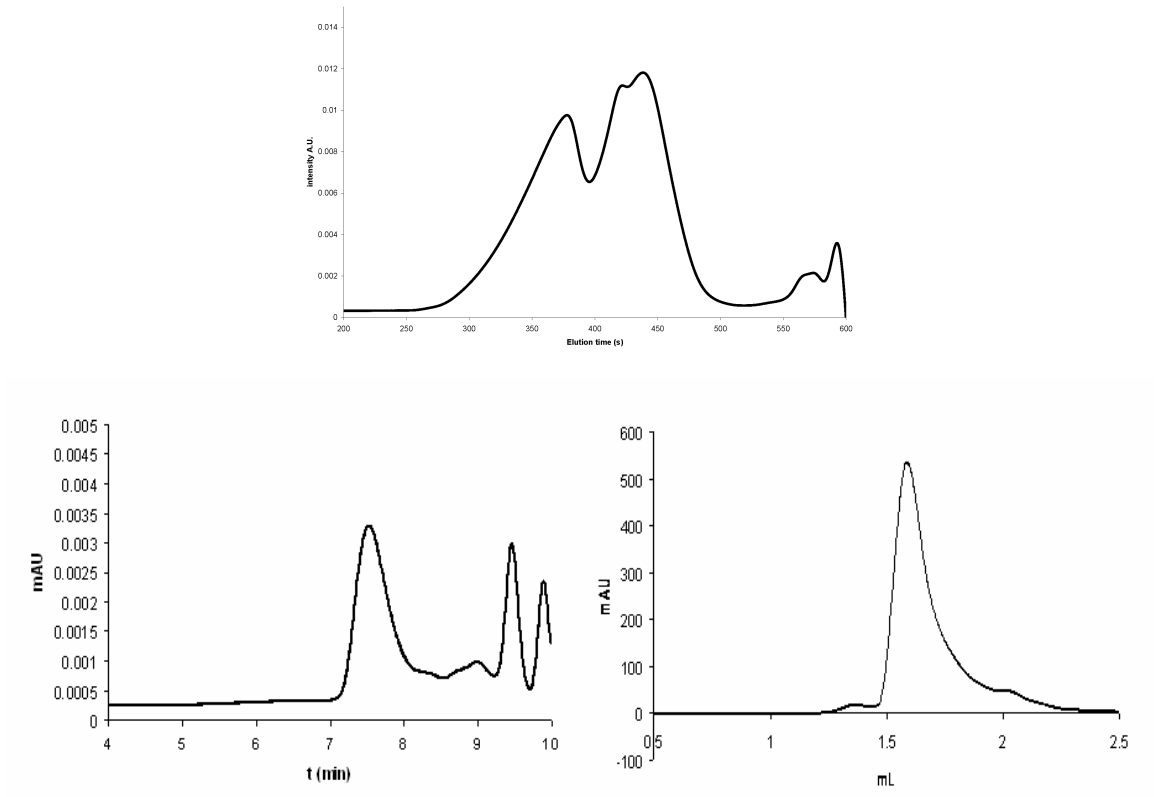

Figure 4.6. *Analysis of ATRP of SSEt in propylene carbonate (Molar ratios of reagents: SSET:Bipy:CuBr:Init = 100:2:1:1 molar ratios, monomer concentration 1M). Top panel: a GPC analysis of the multimodal molecular weight distribution is visible in the GPC spectrum. The left peak corresponds to Mn=300,000. Lower left panel: GPC analysis of similar polymerization reaction, now taken with great care to maintain dry conditions. The peak corresponds to Mn=11,000. Lower right panel: FPLC analysis of the same polymer after deprotection (see text).*

As can be seen in Figure 4.6, there is a multimodal peak elution present in the GPC, while the FPLC analysis shows only one peak. The only reason for this behavior can be the partial hydrolysis of the polymer ethyl ester functions. Even if only few of the ester groups are hydrolyzed in a polymer of e.g. 10,000 Da molecular weight, the effect on the polarity of this polymer will be considerable. The GPC column, with its cross-linked polystyrene solid phase, could then act as a reverse phase column, in which the most polar compound elutes first, leading to the emergence of the higher molecular weight peak as observed in Figure 4.6.

Standard calibration of the GPC column is carried out with near-monodisperse samples of polystyrene. In order to investigate if such GPC calibration can be correctly applied for the polymers prepared in this work, MALDI-TOF[45] experiments were carried out. Figure 4.7 shows the resulting curves obtained during the polymerization of ESS in similar conditions as used to obtain samples for GPC and FPLC analysis, see Figure 4.6.

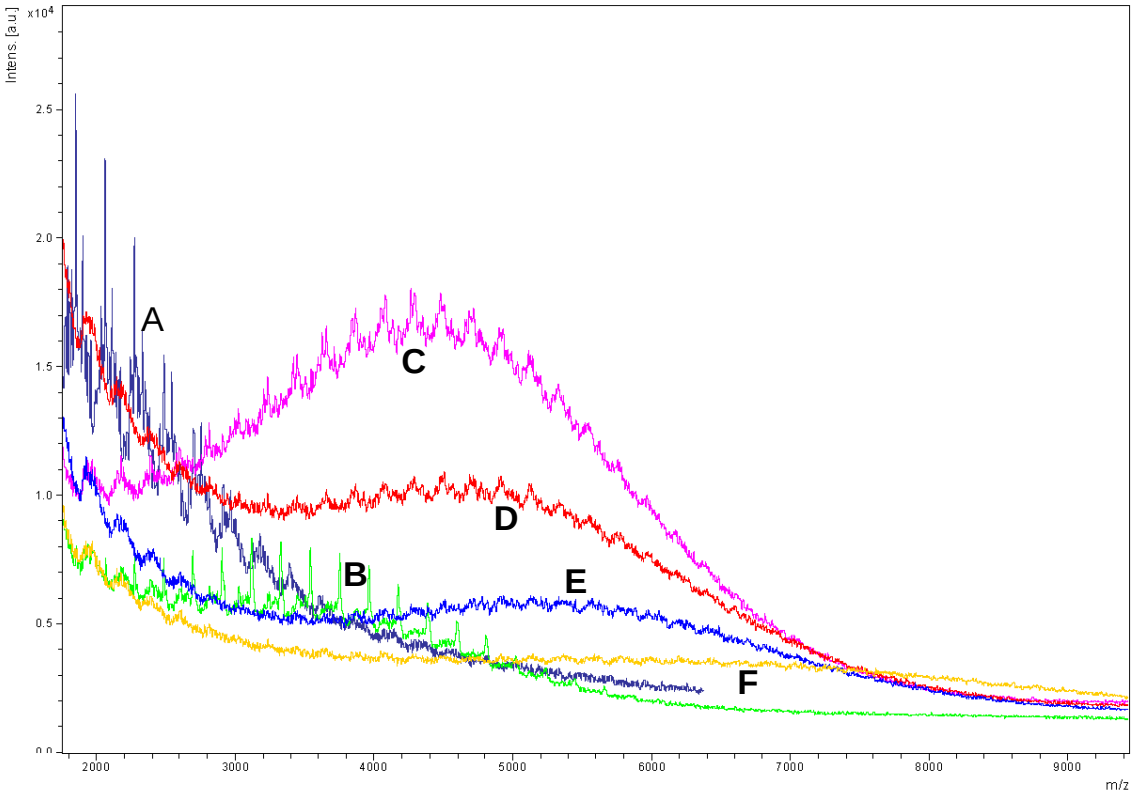

Figure 4.7. *MALDI-TOF spectra of pESS, showing singular Gauss curves of increasing mass. MALDI-TOF data for the polymerization reaction of ethyl styrene sulfonate. For reaction conditions see Figure 4.7. A,B,C etc. indicate increasing conversion. Spectra taken from polymerizations with higher conversions did not yield any peaks. It can be concluded from these graphs that the level of polymerization, as indicated by curve F, is on the edge of detection.*

No high molecular weight peaks are observed in the MALDI –TOF spectra, probably because the higher molecular weight polymers are too large to fly. Therefore, the presence of a higher molecular weight pESS, which is not hydrolyzed can not be excluded from this data. In Figure 4.8 the MALDI-TOF and the GPC-derived molecular weight data are compared. The molecular weight of the maximum peak (Mn)[46] of each MALDI-TOF spectrum is manually obtained and the degree of polymerization is deduced by subtracting the molecular weight of the initiator and dividing by the monomer molecular weight. Similar techniques afford the degree of polymerization for the GPC data.

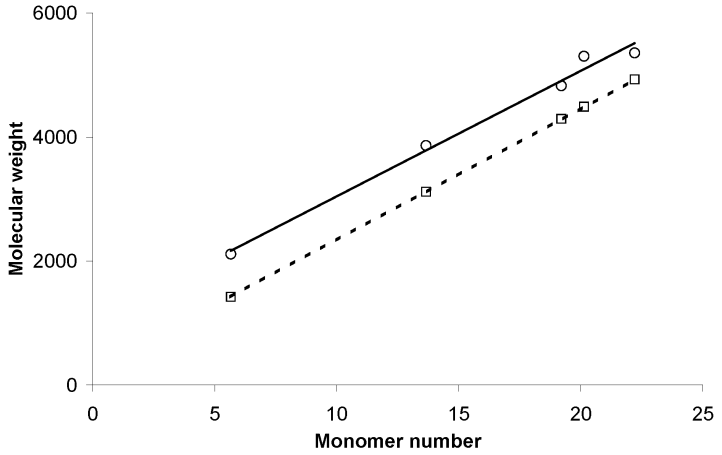

Figure 4.8. *Plots of GPC- (circles and continuous line) and MALDI-TOF (squares and dotted line) derived molecular weight of samples taken from the ATRP of styrene sulfonate ethyl ester, versus the number of monomers incorporated into the polymer. The parallel nature of the lines indicates that GPC measurements are accurate for the determination of the molecular weight.*

It is clear from these data that the molecular weights, as measured by GPC, are quite reliable. Although there is a deviation of ca. 500 Da, this deviation is independent of molecular weight. Therefore, GPC is an accurate tool in the determination of the molecular weight of these polymers. The discrepancy is probably caused by the fact that polystyrene sulfonate ethyl ester possesses a different polarity than polystyrene.

4.3.3 Deprotection procedures

In order to obtain polystyrene sulfonate, the ethyl ester functions of the protected polymer described in the previous section must be removed. The literature procedure to

perform this reaction is a base catalyzed hydrolysis[47]. In order to facilitate purification this hydrolysis is usually carried out with ammonium carbonate, which can be thermally degraded after the reaction (Scheme 4.12 top). Other standard bases, such as NaOH, KOH, and Na_2CO_3 can be applied as well. The use of bases at higher temperatures, however, will also hydrolyze the ester functionality of the ethyl bromoisobutyrate, and in the case of a nucleophilic base, also substitute the bromine end functionality.

In order to test the retain of the bromine end group, several possibilities were evaluated. No mass spectrometry technique was available that could analyze such polar, high molecular weight samples to such a degree. Detection of the bromine end group in ^{1}H NMR was also attempted, but was not successful. In the end, it was decided to perform the base catalyzed deprotection procedure on a polymer sample to yield **10,** which was subsequently used as a macroinitiator in a water-based ATRP[48]. This procedure did not yield any ATRP product, indicating the absence of the bromine group in **10** (Scheme 4.12).

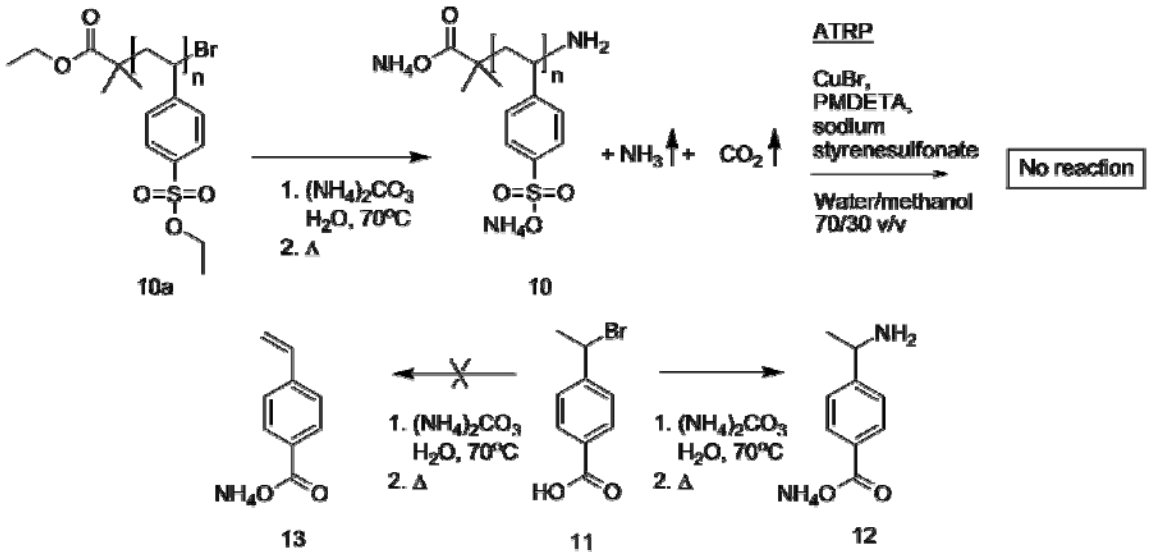

Scheme 4.12. *Top: basic deprotection of pSSEt (**10a**) employing ammonium carbonate, yielding **10** which was tested as a macroinitiator in an ATRP reaction. Bottom: test experiments on model compound **11**: see text.*

Apparently, the NH_3 present in ammonium carbonate is sufficient in order to displace the bromine. It is possible that the use of this weak base also leads to elimination of the bromine end functionality, and the formation of an alkene compound **13**, but this possibility could not be verified and seems unlikely in view of the fact that E1 and E2

elimination reactions usually require strongly basic conditions, such as sodium ethoxylate. As mentioned above, techniques such as NMR and IR were not sufficiently sensitive to determine the end-group functionality in **10**, since end-group signals are too small to be discerned. Therefore, 2-bromoethylbenzoic acid **11** was used as a model compound in a control experiment, in which it was exposed to the same hydrolytic conditions as compound **10a**. Mass spectrometry revealed that compound **12** was obtained in virtually quantitative yield, whereas alkene **13** and the corresponding alcohol could not be detected.

Thus, a procedure was desired that would deprotect the ethyl esters of the sulfonate groups in **10a** and at the same time substitute the bromine end-functionality. Such a reagent should also leave the carboxylate ester functionality intact, so that for the formation of **10a**, ester functionalized initiators could still be used. Several nucleophilic agents were considered, and finally sodium azide was chosen as the deprotection nucleophile. This reagent fulfilled all three conditions for proper deprotection and functionalization, *i.e. (i*) full deprotection of the ethyl sulfonate moieties, *(ii)* full conversion of the bromine atom into a functional group, and *(iii*) inertness toward the carboxyl ester moiety (*vide infra*). Scheme 4.13 shows the deprotection procedure, as applied on several polymers in this work.

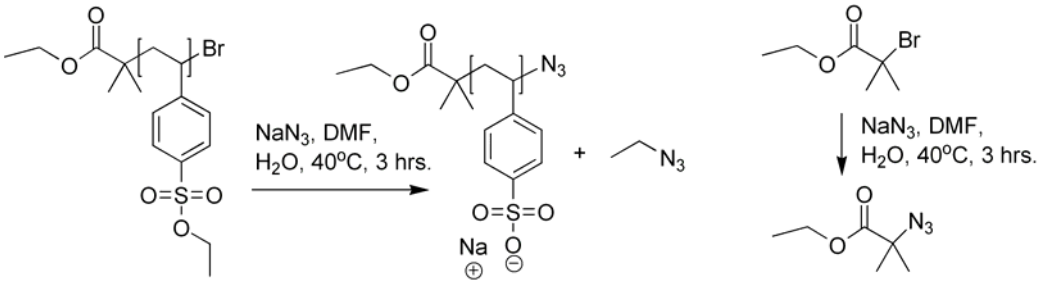

Scheme 4.13. *Use of sodium azide to deprotect the ethyl sulfonate groups in PSSEt polymer 30a with concomitant functionalization of the polymer end-group. Treatment of ethyl bromoisobutyrate with sodium azide yields the substituted product without carboxylate ester hydrolysis (right).*

Dissolution of pSSEt in DMF, followed by the addition of water and sodium azide yielded the deprotected and functional polymer. No ester hydrolysis was detected when the model compound ethyl bromoisobutyrate was exposed to similar conditions

(Scheme 4.13). In summary, Scheme 4.14 shows the preparation of fluorescent polystyrene sulfonate sodium salt, functionalized with an azide moiety.

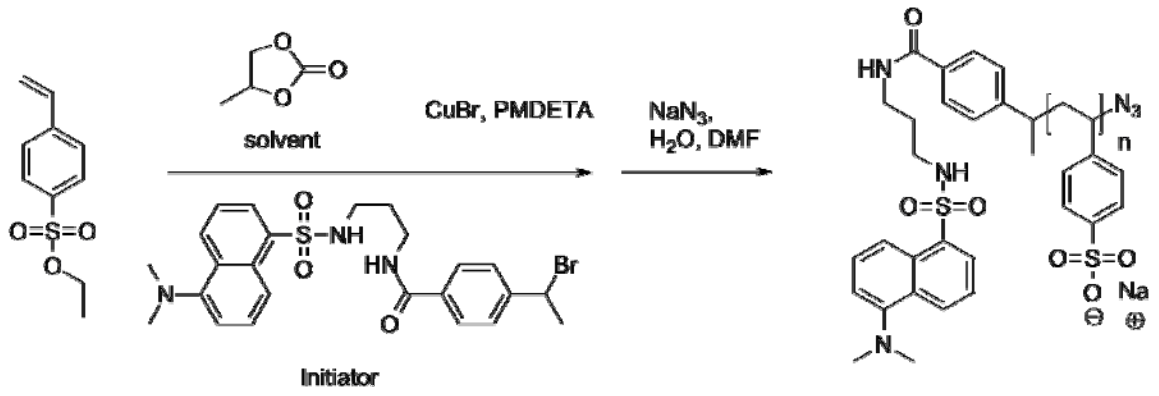

Scheme 4.14. *Summary of polymer synthesis and deprotection.*

We may conclude that the above procedure allows the use of ester-based initiators in the ATRP reaction of ethyl styrene sulfonate without the loss of the carboxylate ester moiety upon deprotection. This property was used to produce highly fluorescent, water-soluble polymers and applied in the bio-conjugation of a protein, using the azide moiety (see Chapter 5). The main motivation for the production of these polyanionic species, however, was the study of their interaction with the CCMV coat protein (see Chapter 6).

The purification of the obtained poly(sodium-4-styrenesulfonate) was first attempted by precipitation in polar solvents, such as methanol and THF. Two problems were encountered in this procedure: *(i)* the sodium azide often did not dissolve in these solvents, leading to an impure product, and *(ii)* precipitation often yielded a very fine dispersion of the product, which was difficult to isolate by filtration or centrifugation. However, since we were dealing with the purification of water soluble and fairly high molecular weight polymers, dialysis was a viable option. To this end, the deprotected polymer solution was first concentrated and the resulting product dissolved in water. This solution was then brought into a dialysis tube and dialyzed. The purity of the dialyzate was checked by performing conductivity measurements. Several observations were made when performing this purification: the dialysis proceeded only quite slowly making that several hours were typically needed for complete equilibrium of the system. Furthermore, the use of *demineralized* water in the dialysis setup gave rise to the formation of a small

amount of precipitate. At first it was thought that this solid was the Ca^{2+} salt of the polymer, but further experiments revealed that this was not the case: when $CaCl_2$ was added to a solution of the polymer, no precipitate was formed, even after a long period of time. Subsequently, $Ca(N_3)_2$ was considered as an option, but similar tests proved that this was not formed either: addition of $CaCl_2$ to a solution of NaN_3 did not yield a precipitate. The use of ultrapure (MilliQ) water, however, prevented the formation of these precipitates. However, since the purification of the polymers by dialysis was very slow, i.e. it took up to three days to obtain the pure polymer, a more facile and faster method was explored. Initially, a set-up that combines a Soxhlet continuous extraction with a dialysis step was considered. It was noted, however, that such a set-up would have two drawbacks: first, it would take too long to fill the reservoir of the Soxhlet extractor, during which time the dialysis membrane would be left dry, which is highly unfavorable. Secondly, since the solvent is water, the set-up would be subjected to high (vapor) temperatures, which is incompatible with the use of dialysis membranes. Therefore, a continuous counter-current dialysis set-up that would use a relatively small volume of ultrapure water, which is continuously replenished, was conceived. Figure 4.9 shows the set-up in detail.

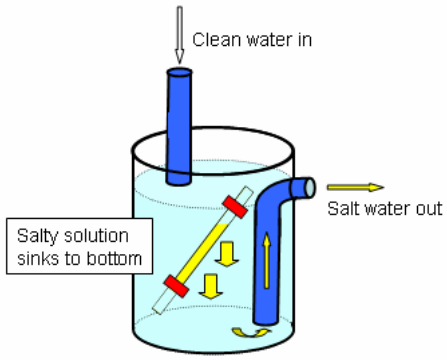

Figure 4.9. *A continuous dialysis setup as used to purify the polystyrene sulfonate synthesized in this work.*

The vessel was filled with the dialysis bag as shown in Figure 4.9, and a continuous stream of water was added dropwise. The contents of the dialysis vessel was ca. 75 ml. The solution was only stirred very slowly or not at all, allowing the heavier salt solution to sink to the bottom such that it can be transported out of the exit tube. Approximately 10 L. of ultrapure water was used for the dialysis over a period of ca.

10 hours. The polymers treated in this way showed high purity and their solutions had conductivities in the range of demineralized water. This procedure can also be used to purify polymers of more apolar nature, it is for example conceivable to use a solution of 20% THF in water, instead of pure water.

4.3.4 Synthesis of deuterated polystyrene sulfonate

In Chapter 6, the interaction of polystyrene sulfonate with CCMV coat protein is described in detail. For these and future studies, in particular small angle neutron scattering, also samples of fully deuterated polystyrene sulfonate were required. In this section, the synthesis of this polymer is reported. As discussed in the introduction section of this chapter, polystyrene sulfonate can be synthesized by sulfonation of polystyrene. De Paoli found that upon using acetyl sulfate, only a degree of 30% sulfonation could be achieved, after which no more sulfonation took place[49]. It is also known that treatment of polystyrene with liquid SO_3 in cyclohexane yields high degrees of sulfonation, but also of crosslinking[50]. The practical applicability of this method for the preparation of a deuterated sample, therefore, is questionable, since the synthesis of pure SO_3 is not a trivial exercise, requiring several sequential distillations of fuming sulfuric acid. SO_3 also polymerizes in the presence of traces of water, requiring another cracking/distillation reaction. In a method described by Vink et al.[51] the sulfonation reaction is performed using sulfuric acid and phosphorus pentoxide. This more practical approach yields polymers that are highly sulfonated, but no comments on the percentage of crosslinking were made. It was decided, therefore, to prepare deuterated polystyrene by means of ATRP, employing ethyl bromoisobutyrate acid as the initiator and styrene-*d*8 as the monomer, which provided polystyrene-d8 in good yields. Subsequently, the procedure of Vink was used to sulfonate the deuterated polymer. Scheme 4.15 shows the reactions involved.

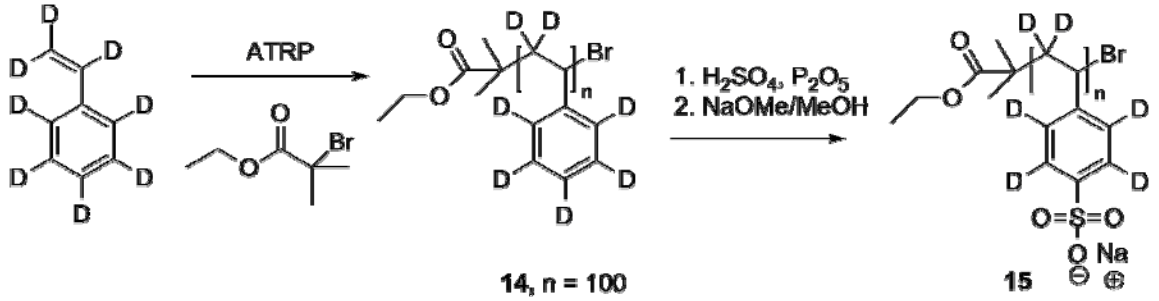

Scheme 4.15. *Synthesis of polystyrene-d8 (**14**) and subsequent sulfonation, yielding **15**.*

Purification of the polymers was performed using the same dialysis set-up as described above. It is possible, that these polymers were crosslinked to a small extent. The sulfonation grade was not determined, but the literature[51] suggests that up to 80% can be achieved. The sulfonation grade of the polymers obtained was not investigated further. The yields of the sulfonation reactions were quite low: only 20% of sulfonated polymer was obtained. This low yield arises from the fact that the procedure employs a two phase system of cyclohexane and sulfuric acid. After reaction, the sulfonated polymer "floats" in the cyclohexane layer. A relatively large amount of polystyrene sulfonate is dissolved in the sulfuric acid layer, and not recovered.

4.4 Conclusions

In the previous sections, the synthesis of polystyrene sulfonate was described. In the first section, several types of initiators are synthesized. After several experiments employing an ester based initiator, it was decided to discard the use of the ester function altogether, also because the basic deprotection of the aimed polystyrene sulfonate ethyl ester leads to carboxylate ester hydrolysis, rendering all initiator functionalities useless. Subsequently, several initiators, based upon "click chemistry" were prepared, but all proved to be ineffective for different reasons. Then, a non-ester-based functionalized initiator was found to possess the right properties for the synthesis of fluorescent polystyrene sulfonate ethyl ester by ATRP. In the ATPR of styrene sulfonate ethyl ester a series of organic solvents was attempted, using standard ethyl isobromoibutyrate. For several reasons, such as solubility, stability, suitability of boiling point considerations and

practicability, all but one solvent proved inefficient, i.e. propylene carbonate. The latter was found to be an efficient medium because it is easily purified and degassed, and virtually non-toxic.

Subsequently, a novel deprotection method that simultaneously deprotects the sulfonic acid ethyl ester functions and substitutes the end-functional bromine atom for an azide was developed. This method uses non-basic conditions, which were also shown not to affect the carboxylic acid ester functions. Our work shows that isobromobutyric acid ester as initiator for ATRP is not a viable option, when basic conditions are required in the synthesis. Although a base catalyzed hydrolysis is expected to take place, it was surprising to see that the ester function was so sensitive. Several observations have been made in the past with respect to the alkaline hydrolysis of ethyl bromoisobutyrate[52], the most important ones being that *(i)* during hydrolysis, the bromine atom is also displaced by water or OH^- leading to an alcohol; *(ii)* both reactions are accelerated by a high ionic strength of the medium; *(iii*) the reactions accelerate one other since the solubility in water increases dramatically in either step.

After having optimized the initiator system, compound **9b** was finally used for the polymerization of styrene sulfonate ethyl ester by ATRP. The reaction proceeded well-controlled and rapidly. The obtained polymers were analyzed by NMR, GPC and MALDI-TOF. The data obtained from MALDI-TOF and GPC were different but it was concluded that the deviation between the two sets of data was the result of the calibration problems with the GPC column. Our study shows that it may be possible to calibrate the GPC column with polystyrene sulfonate ethyl ester (pESS) samples and MALDI-TOF. The prepared polystyrene sulfonate ethyl ester was deprotected and simultaneously functionalized with an azide end-group by reaction with sodium azide to displace the bromine atom. Other deprotection agents can be used as well, e.g. the use of ammonia in water will yield an amine at the end of the polymer chain. A new continuous dialysis set-up was designed allowing for the rapid and efficient purification of the polymers, using relatively modest amounts of MilliQ water. All these efforts have led to a strategy in which monodisperse fluorescent polystyrene sulfonate sodium salt with an azide end group is accessible.

We also prepared deuterated polystyrene sulfonate polymers by sulfonation of deuterated polystyrene. The obtained deuterated polymer was purified by dialysis. The yields of the sulfonation reaction were low, i.e. only ca. 20%. This might be improved by the neutralization of the whole reaction mixture immediately after reaction, so that all polymer can be isolated by dialysis. However, this would imply the purification of a polymer that contains a large amount of salts. It may also be feasible to neutralize the reaction mixture with a base allowing the reacted (sulfate) salt to precipitate out. This would greatly shorten the dialysis time or even dispense the need for it. $Ca(OH)_2$ or CaO may be good candidates for this purpose.

4.5 Experimental section

4.5.1 General methods and materials

All organic solvents were of analytical quality or distilled before use. All reagents were used as received, unless otherwise stated. Flash silica gel chromatography was performed using J.T. Baker silica gel 20-70 um particle size. Eluent systems are give in v/v. GPC was taken on a Polymer Labs PL gel 5 μm column with chloroform or THF as the eluent on a Shimadzu 10A LC system and was calibrated with monodisperse polystyrene samples obtained from Polymer Labs. NMR was taken on a Bruker DMX 300 MHz or on a Varian DPX 400 MHz machine with TMS as the internal standard. DSC was carried out on a Perkin Elmer Diamond DSC apparatus, calibrated with indium standards. Dialysis was carried out using Spectra Por dialysis tubing (MWCO 3,000) and ultrapure water. (Deuterated) styrene was distilled in vacuo and stored at -20^{o}C only for short periods of time (~1 month). FPLC was carried out with the help of a superose 6 column in an Amersham (GE) Ettan LCMS system, using several solutions of various salt concentrations to prevent polar interactions with the column material.

4.5.2. Synthesis of fluorescent initiators

(1-(3-(Dansyl)propyl)-1H-1,2,3-triazol-4-yl)methyl isobromobutyrate (3)

Compounds **1** and **2** were synthesized according to literature procedures[53,54]. *N*-dansyl-3-azidopropane (0.121 g, 0.36 mmol) and propargyl isobromobutyrate (0.08 g, 0.38 mmol) were dissolved in THF (5 ml) and PMDETA (8 µl, 0.02 mmol) and CuBr (~ 10 mg) were added to the reaction mixture. After 1 h., TLC showed the complete disappearance of starting materials. The reaction mixture was therefore evaporated, after which column chromatography (MeOH/$CHCl_3$ 0/100 → 0.9/99.1) afforded the title compound in pure form. Rf 0.3 (5% MeOH/DCM) FTIR analysis showed the absence of the azide peak (2094 cm^{-1}) in the product. Experiments in which copper sulfate and ascorbic acid in a THF water mixture were used, gave similar results. ^{1}H NMR ($CDCl_3$): δ 8.55 (d, *J*=8.6 Hz, 1H, CH arom.), 8.30, (d, *J*=8.6 Hz, 1H, CH arom.), 8.21 (d, *J*=7.2 Hz, 1H, CH arom.), 7.55 (m, 3H, CH arom. and CH triazole), 7.19 (m, 1H, CH arom.), 5.64 (m, 1H, NH), 5.26 (s, 2H, CH_2-O), 4.36 (t, *J*= 8.8 Hz, 2H, N-CH_2), 2.89 (m, 8 H, 2x CH_3 and CH_2) 2.08 (m, 2H, CH_2-C$\underline{H_2}$-CH_2), 1.90 (s, 6 H, 2xCH_3). ^{13}C NMR ($CDCl_3$): δ 171.5, 152.16, 142.20, 134.4, 131.0, 130.7, 129.9, 129.7, 129.5, 128.7, 124.4, 123.3, 118.6, 115.4 (all CH arom. and Cq), 76.7 (CH_2), 59.17, 55.8, 47.16, 45.48, 39.9, 30.7. ESI-MS 538.2 (M+H).

4-(1-(1H-Benzo[d][1,2,3]triazol-1-yloxy)ethyl)-N-(prop-2-ynyl)benzamide (5)

1-(Bromoethyl)benzoic acid (0.2 g, 0.87 mmol) (**4**) was dissolved in DCM (50 ml) and propargylamine (0.1 g, 1.7 mmol) was added. Subsequently, HOBt (0.23 g, 1.7 mmol), DIPEA (0.3 ml, 1.7 mmol) and EDC (0.33 g, 1.7 mmol) were added and the reaction mixture was allowed to stir for 40 hrs. TLC analysis showed the emergence of one spot, which was isolated by column chromatography (1st column MeOH/$CHCl_3$ 0/100 → 1/99, then acetone/toluene 5/95 → 20/80). Rf 0.55 (10% MeOH/$CHCl_3$) Yield 0.29 g, 0.9 mmol, 100%) ^{1}H NMR ($CDCl_3$): δ 7.9 (d, 1H, CH arom.); 7.8 (d, 2H, CH arom.); 7.41 (d, 2H, CH arom.); 7.3 (m, 3H, CH arom. and $CHCl_3$); 7.05 (t, *J* = 5.5 Hz, 1H, NH); 5.82 (q, *J* = 6.6 Hz, 2H, CH); 4.20 (dd, *J* = 7.3 Hz, 2H, CH_2); 2.23 (t, *J* = 2.4 Hz, 1H, CH alkyn); 1.83 (d, *J* = 6.6 Hz, 3H, CH_3). ^{13}C NMR ($CDCl_3$): δ 168 (Cq, C=O);

144, 142, 135 (Cq, arom.); 128,127 (CH arom.); 120 (CH arom.); 109 (C propargyl); 88 (CH ethyl); 80 (CH propargyl); 72(Cq); 30 (CH_2-N); 20 (CH_3). MS (LCMS) 361.2 (M + CH_3CN).

4-(1-Bromoethyl)-N-(prop-2-ynyl)benzamide (6)

1-(Bromoethyl)benzoic acid (0.4 g, 1.74 mmol) (**4**) was dissolved in DCM (50 ml) and propargylamine (0.1 g, 1.65 mmol) was added. Subsequently, DIPEA (0.45 ml, 2.6 mmol) and EDC (0.37 g, 1.9 mmol) were added and the reaction mixture was allowed to stir for 2 hrs, after which TLC showed complete conversion. Column chromatography (MeOH/$CHCl_3$ 0/100 → 4/96) afforded the title compound in 90 % yield (0.41 g, 1.58 mmol) Rf 0.8 (10% MeOH/$CHCl_3$). ^{1}H NMR ($CDCl_3$): δ 7.77 (d, *J* = 6.15 Hz, 2 H, CH arom.); 7.52 (d, *J* = 6.5 Hz, 2 H, CH arom.); 6.2 (s, 1H, NH), 5.22 (q, *J*= 5.2 Hz, 1H, CH); 4.27 (q, *J*= 1.9 Hz, 2H, CH_2 propargyl); 4.14 (m, 1H, CH propargyl); 2.05 (d, *J* = 6.2 Hz, 3H, CH_3). ^{13}C NMR ($CDCl_3$): MS (LCMS) M 307.1 (M+CH_3CN) M 186.2 (M-Br).

4-(1-Chloroethyl)-N-((1-dansyl-propyl)-1H-1,2,3-triazol-4-yl)methyl)benzamide (7, R=Cl or Br)

N-Dansyl-3-azidopropane (30 mg, 0.09 mmol) (**1**) and propargyl amine (26 mg, 0.1 mmol) were dissolved in freshly distilled $CHCl_3$, after which PMDETA (tip of pipette) and CuBr (point of spatula) were added to the mixture. After 3 hrs no reaction was observed, hence more catalyst and ligand were added (similar quantities) after which the reaction proceeded rapidly. Evaporation of the solvent followed by chromatography afforded the pure title compound (**7, R=Cl**). Yield: 40 mg (0.07 mmol, 80%) The following procedure leads to the brominated product: The same amounts of starting materials were dissolved in THF/H_2O 80/20 and small amounts of $Cu(OAc)_2$ and sodium ascorbate were added. LCMS showed that the latter procedure was more efficient in the preparation of **7, R=Br**. ^{1}H NMR ($CDCl_3$): 8.496 (d, *J*=8.4 Hz, 1H, CH arom.), 8.299, 8.277 (d, *J*=8.8 Hz, 1H, CH arom.), 8.166, 8.148 (d, *J*=7.2 Hz, 1H, CH arom.), 7.87 (m, 1H, NH), 7.746 (m, 2H, CH arom.), 7.334, (m, 4H, CH arom.), 5.109 (q, *J*=7.2 Hz, 1H, CH-Br) (this peak changes slightly depending on the nature of the halogen atom, being

either chlorine or bromine), 4.659 (d, *J*=5.6 Hz, 2H, CH_2), 4.289 (m, 2H, CH_2), 2.933 (d, *J*=6 Hz, 2H, CH_2), 2.827 (s, 6H, 2 x CH_3), 2.027 (dt, 2H, CH_2-C$\underline{H_2}$-CH_2), 1.950, 1.932 (d, *J*=7.2 Hz, 3H, CH_3).

N-(3-aminopropyl)-5-(dimethylamino)naphthalene-1-sulfonamide) (Dansylpropylamine) (8)

To a vigorously stirred solution of 1,3-propyldiamine (2.8 ml, 33 mmol) in DCM (150 ml) at 0^{o}C, a solution of dansylchloride (0.88 g, 3.3 mmol) in DCM (100 ml) was added dropwise. The reaction was stirred at 0^{o}C for 4 hrs., after which 50 ml of aqueous 1N NaOH was added, and the layers were separated. After extraction of the organic layer with water (2x100 ml), the organic layer was dried over Na_2SO_4 and evaporated under reduced pressure. The obtained oil was then co-evaporated with DMF (3 x 50 ml, for removal of the unreacted 1,3-propylamine) to yield the product as a yellow oil. (1.07 g, 100%) ^{1}H NMR ($CDCl_3$): δ 1.46 (dt, 2H, *J*=6 Hz, CH_2 alkyl); 2.64 (m, 2H, C$\underline{H_2}$-NH_2); 2.87 (s, 6H, NMe_2, dansyl); 2.99 (t, 2H, *J*=6 Hz, CH_2-NH); 7.14 (d, 1H, *J*=7.5 Hz, CH arom.); 7.50 (dd, 2H, CH arom.); 8.22 (d, 1H, *J*=7.2 Hz, CH arom.) 8.31 (d, 1H, *J*=8.7 Hz, CH arom.) 8.52 (d, 1H, *J*=7.2 Hz, CH arom.).

4-(1-Bromoethyl)-N-(dansyl)propyl)benzamide (9, R=Br)

A solution of dansyl chloride (0.86 g, 3.1 mmol) in THF (200 ml) was added dropwise over a period of 1 h. to a solution of 1,3 diaminopropane (13 ml, 155 mmol) at 0^{o}C. Then, as TLC showed complete consumption of the starting material, 20 ml aqueous 1N NaOH was added and the solvent was evaporated *in vacuo*. Subsequently, the reaction slurry was separated between aqueous 1 N. NaOH and DCM, and the water layer was extracted with DCM (2x 50 ml). The organic layer was washed twice with aqueous 1N NaOH, dried and evaporated, yielding crude *N*-3-dansyl-1-aminopropane (**8**), which was used in the following experiment without further purification. *N*-3-Dansyl-1-aminopropane (0.6 g, 1.9 mmol) (**8**) and 1-bromoethyl benzoic acid (**4**) were dissolved in DCM (100 ml) and to this solution, N-diisopropylethylamine (DIPEA) (0.34 ml, 2 mmol) and EDC (0.38 g, 2 mmol) were added. If this reaction is allowed to stand overnight, virtually all bromine atoms is exchanged for chlorine atoms (**9, R=Cl**). After 2 hrs,

however, the reaction turned out to be finished, as observed by TLC, and the solvent was evaporated after which column chromatography ($MeOH/CHCl_3$ 0/100 → 2/98) yielded pure (**9**, **R=Br**) (0.22 g, 46 %). Rf 0.47 (10% $MeOH/CHCl_3$). ^1H NMR (400 MHz, $CDCl_3$): δ 1.63 (dt, 2H, *J*=6 Hz, CH_2 alkyl); 1.96 (d, 3H, *J*=7.04 Hz, CH_3 ethyl); 2.93 (m, 2H, $C\underline{H_2}$-NH-SO_2); 3.44 (m, 2H, $C\underline{H_2}$-NH-CO); 5.14 (q, 1H, *J*= 7 Hz, CH-Br); 6.27 (t, 1H, *J* =6.4 Hz, NH); 7.00 (t, 1H, *J*= 6.1 Hz, NH); 7.14 (d, 1H, *J*=7.5 Hz, CH arom.); 7.35 (d, 2H, *J*=8.4 Hz, CH arom. phenyl); 7.50 (dd, 2H, CH arom.); 7.67 (d, 2H, *J*= 8.3 Hz, CH arom. phenyl); 8.17 (d, 1H, *J*=7.2 Hz, CH arom.); 8.33 (d, 1H, *J*=8.7 Hz, CH arom.); 8.51 (d, 1H, *J*=7.2 Hz, CH arom.) ^{13}C NMR ($CDCl_3$): δ 167.5, 151.7, 146.4, 135.1, 133.8, 130.4, 129.7, 128.4, 127.5, 127.3, 127.1, 126.9, 126.6, 126.2, 123.2, 118.9, 115.3 (14 x CH arom. and Cq), 55.0, 53.8, 48.3, 48.1, 45.4, 40.0, 36.4, 31.7, 29.7, 29.4, 26.5. LCMS (eluent: CH_3CN/10 mM NH_4OH(aq.) 50/50 to 95/5, column Zorbax extent C18) M 518 (M+H ^{79}Br), M 520 (M+H ^{81}Br). Calculated: 517.10. MS (ESI) M 518.1 (M+H), 540.1 (M+Na).

4.5.3 ATRP of ethyl styrene sulfonate

Ethyl p-styrene sulfonate

To a solution of sodium styrene sulfonate (20.6 g, 0.1 mol), in water (150 ml) at 0^oC, a solution of $AgNO_3$ (18.7 g, 0.11 mol) in water (50 ml) was added dropwise over a 15 min period. All reactions were performed under the strict exclusion of light. After complete addition, the mixture was stirred for 2 hrs at room temperature after which the precipitate was filtered off and the solid was washed with water (3x) and with Et_2O (3x). The solid was then re-dissolved in CH_3CN, filtered, evaporated under reduced pressure, and subsequently co-evaporated with 1,4-dioxane (2x). The dry styrene sulfonate silver salt was dissolved in acetonitrile (250 ml) and ethyl bromide was added (20 ml, 0.34 mol). The flask was equipped with a cooler and the mixture was heated to 70^o C overnight, filtered with Hyflo and evaporated under reduced pressure. The resulting greenish oil was dissolved in toluene and filtered over Hyflo again. This procedure yielded product of such high purity, that chromatographic purification was not necessary. Yield: 14 g, 67 mmol, 67%. ^1H NMR ($CDCl_3$): δ 1.31, (t, 3H, *J*=6.9 Hz, CH_3 Et); 4.14

(q, 2H, *J*= 7.2 Hz, O-CH_2); 5.48 (d, 2H, *J*= 11.1 Hz, CH_2 vinyl); 5.93 (d, 2H, *J*=17.7 Hz, CH_2 vinyl); 6.81 (dd, 1H, CH vinyl); 7.57 (d, 2H, *J*=8.4 Hz, CH arom.); 7.88 (d, 2H, *J*=8.4 Hz, CH arom..) ^{13}C NMR ($CDCl_3$): δ 14.96 (CH_3); 66.99 (CH_2) 117.83 (CH Ph) 126.59 (CH arom.) 127.99 (CH arom.) 134.82 (CH vinyl) 134.96 (CH vinyl) 142.57 (Cq). ESI-MS: 213.4 (M+H). Calc.: 212.27 (M).

Polymerization

A degassed and dry Schlenk vessel was charged with CuBr (18 mg, 0.12 mmol), 2,2'-bipyridine (20 mg, 0.12 mmol), ethyl styrene sulfonate (2 ml, 9.4 mmol) and propylene carbonate in sufficient amounts to give a 1M monomer solution. The mixture was degassed by three vacuum/argon cycles and immersed in an ice bath. Initiator (in this case ethyl bromoisobutyric acid) (7.0 mg, 0.063 mmol) was added and the degassing cycle was repeated. Alternatively, fluorescent initiator **9b** was used for the reaction, in similar molar ratios. The reaction vessel was then placed in a thermostated oil bath at 70^{o}C and samples were taken at regular intervals to determine the monomer conversion by ^{1}H NMR. After the desired conversion had been reached (~ 3 hrs.) the polymerization was stopped by exposing the catalyst to air. The resulting slurry was taken up in a large volume of $CHCl_3$ (300 ml), vigorously stirred in a flask with an aqueous 0.1 M citric acid solution (100ml), transferred into a separating funnel, and separated. This procedure was repeated three times, after which the organic phase was washed with water once. After drying the solution over $MgSO_4$ the solvent was evaporated under reduced pressure. The resulting glass was taken up in a minimal amount of $CHCl_3$ and precipitated in toluene, re-dissolved in chloroform, after which the resulting solution was dried by evaporation under reduced pressure yielding a yellow-green glass (1.1 g., ~50 %). GPC-SEC ($CHCl_3$): M_n 22400, PDI 1.12. GPC occasionally showed a peak eluting much earlier from the column; this is attributed to partial hydrolysis of the polymer. See also text. ^{1}H NMR ($CDCl_3$): δ 1.34 (br., CH_3 Et); 1.53 (br., CH_2 backbone); 4.15 (br., O-CH_2); 6.70 (br., 2H, CH arom..); 7.65 (br., 2H, CH arom.), sometimes signals for the initiator can be observed, mostly depending on the molecular weight of the polymer.

Deprotection of poly(ethyl-4-styrenesulfonate)

The polymer (1.0 g) was dissolved in a mixture of DMF/H_2O, 1/1, v/v, 50 ml. To this mixture, NaN_3 (1.1 equiv. per ethyl) was added and the mixture was allowed to stand overnight at 40°C. The volume of the reaction solvents was then reduced to about 1/3 of its original quantity, and the watery solution was transferred into a dialysis tube (MWCO 3,000) and dialyzed against ultrapure water in a countercurrent setup. The solvent was then evaporated, yielding pure polystyrene sulfonate in 95% yield. ^{1}H NMR ($CDCl_3$): δ 1.65 (br., CH_2 backbone); 6.90 (br., 2H, CH arom..); 7.71 (br., 2H, CH arom.).

ATRP of styrene-*d*8 (14)

A degassed and dry Schlenk vessel was charged with 1.6 ml (13 mmol) of styrene-*d*8, CuBr (47 mg, 0.33 mmol), PMDETA (78 µl, 0.45 mmol) and 2 ml of anisole. Each individual addition was followed by degassing *via* three argon/vacuum cycles. Subsequently, ethyl bromoisobutyrate (43 mg, 32 µl, 0.22 mmol) was added to the mixture and the flask was bubbled with argon on an ice bath for 30 min. The reaction was then placed in a temperature-controlled oil bath at 90°C and samples were taken at regular intervals. This reaction was allowed to proceed overnight, after which the product was isolated by dissolving the glassy solid in chloroform (~200 ml) and washing the resulting polymer solution with EDTA solution (0.1 M, 100 ml, 2x) $KHSO_4$ (5 g/L, 100 ml, 2x) and finally with water. Drying and evaporation of the solvent yielded a glassy polymer, which was further purified by precipitation in MeOH. Yield: 1.53 g. GPC: M_n 10,933: PDI 1.25. Other reactions performed at 110°C gave faster polymerization reactions and were quenched at an earlier stage, yielding better defined polymers with lower PDI's. The 98% deuteration grade of the monomer allowed the analysis of the polymers by ^{1}H NMR. ^{1}H NMR ($CDCl_3$): δ 1.53 (br., 2H, CH_2 backbone); 1.80 (br, 1H, CH-Ph backbone); 6.70 (br., 2H, CH arom..); 7.65 (br., 2H, CH arom.).

Sulfonation of polystyrene–*d*8 (15)

A 500 ml flask was charged with 50 ml H_2SO_4 and 11 g. P_2O_5 was added in portions. A solution of polystyrene-*d*8 (0.8 g) in cyclohexane (75 ml) was added and the reaction was stirred at 40°C. In accordance with the literature, after several minutes of

stirring, the mixture became (seemingly) homogeneous, and ca. 20 min. later a separation of layers was observed. The mixture was then cooled in an ice bath and crushed ice was added (~50 g) until the polymer floated on the boundary of the mineral acid and cyclohexane layers. These layers were then separated and the polymer was dissolved in more water, after which the polymer was neutralized with an aqueous 1M NaOH solution. The water layer was filtered and concentrated to a small volume (~20 ml) and dialyzed in the same manner as described above. The final conductivity of the water, after continuous dialysis was between 15 and 20 μS/cm. Yield: 0.15 g. Again, concentrated samples were used for analysis by ^{1}H NMR: (D_2O): δ 1.15 (br., 3H, CH_2 backbone); 6.70 (br., 2H, CH arom..); 7.65 (br., 2H, CH arom.).

4.6 Notes and references

[1] J.-S. Wang and K. Matyjaszewski, *J. Am. Chem. Soc.* **1995**, *117*, 5614.

[2] (a) D.P. Curran, *Comprehensive Organic synthesis* **1988**, 489. (b) J.H. Udding, K.J.M. Tuijp, M.N.A. van Zanden, H. Hiemstra and W.N. Speckamp, *J. Org. Chem.* **1994**, *59*, 1993.

[3] M. Kato, M. Kamigaito, M. Sawamoto and T. Highashimura, *Macromolecules* **1995**, *28*, 1721.

[4] M. Destarac, K. Matyjaszewski and B. Boutevin, *Macromol. Chem. Phys.* **2000**, *201*, 265.

[5] K. Matyjaszewski, J.-L Wang, T. Grimaud and D.A. Shipp, *Macromolecules* **1998**, *31*, 1527.

[6] K. Matyjaszewski and J. Xia, *Chem. Rev.* **2001**, *101*, 2921.

[7] J. Qiu, K. Matajaszewski, Macromolecules 1997, 30, 5643.

[8] M. Even, D.M. Haddleton and D. Kukulj, *Eur. Pol. Journal* **2003**, *39*, 633.

[9] J. Roovers and B. Comanita, *Adv. Pol. Sci.* **1999**, *142*, 180.

[10] P.K. De Bokx and H.M.J. Boots, *J. Phys. Chem.* **1989**, *93*, 8243.

[11] a) S. Biagini, G. Ferrari, V. Maniscalco, M. Casolaro, M. C. Tanzi and L. Rusconi, *Cemento* **1982**, *79*, 345; b) K. Takagi, T. Haraoka and M. Takagi, *Jpn. Kokai Tokkyo Koho* **1999**.

[12] C. Pisuntornsug, N. Yanumet and E.A. O'Rear. *Color Technology* **2002**, *118(2)*, 64.

[13] J.F. Ding, C. Chuy and S. Holdcroft, *Chem. Mater.* **2001**, *13*, 2231.

[14] H.J. Kim, S.W. Han, *Nephron* **2002**, *92*, 33.

[15] N. Bourne, L.D.J. Zaneveld, J.A. Ward, J.P. Ireland and L.R. Stanberry, *Clin. Microbiol. Infect.* **2003**, *9*, 816.

[16] V.F. Kurenkov and V.A Myagchenkov, *"Styrenesulfonic acid and its salts" in S.C. Salmone (Ed) Polymeric materials encyclopedia, CRC Press, Boca Raton, London, Tokyo, New York,* 8025.

[17] a) P. Molyneux, *"Water soluble synthetic polymers", CRC Press Inc., Boca Raton* **1975**; b) A. Eisenberg, M. King, *"Ion containing polymers" in Polymer physics", R. S. Stein, Ed., Academic press, New York* **1977**, ch. III C, 87; c) A. Wilson and H.J. Prosser, *"Developments in ionic Polymers", vol. 2, Appl. Sci. Publ. London* **1989**.

[18] a) H. Vollmann, H. Becker, M. Corell and H. Streeck, *Ann. Chem.* **1937**, *531*, 1; b) H. Vink, *Makromol. Chem.* **1982**, *182*, 279.

[19] F. Kučera and J. Jančář, *Pol. Eng. Sci.* **1998**, *38 (5)*, 783.

[20] B. Keoshkerian, M.K. Georges and D. Boilsboissier. *Macromolecules* **1995**, *28*, 6381.

[21] M. Bouix, J. Gouzi, B. Charleux, J.P. Vairon and P. Guinot, *Macromol. Rapid Comm.* **1998**, *19 (4)*, 209.

[22] L.I. Gabaston, S.A. Furlong, R.A. Jackson and S.P. Armes, *Polymer* **1999**, *40 (16)* 4505–4514.

[23] 1 J. Chiefari, Y.K. Chong, F. Ercole, J. Krstina, J. Jeffery, T.P.T. Le, R.T.A. Mayadunne, G.F. Meijs, C.L. Moad, G. Moad, E. Rizzardo and S.H. Thang, *Macromolecules* **1998**, *31 (16)*, 5559.

[24] N.V. Tsarevsky, T. Pintauer and K. Matyjaszewski, *ACS Polym. Prepr.* **2002**, *224 (2)*, 466.

[25] P.D. Iddon, K.L. Robinson and S.P. Armes, *Polymer* **2004**, *45*, 759.

[26] Bipy = 2,2`bipyridine.

[27] R. Arakawa , S. Watanabe and T. Fukuo, *Rapid Comm. in Mass Spectr.* **1999**, *13*, 1059.

[28] R. Huisgen, *"Cenetary Lecture - 1,3-Dipolar Cycloadditions". Proceedings of the Chemical Society of London* **1963**, 357.

[29] V.V. Rostovtsev, L.G. Green, V.V. Fokin and K.B. Sharpless, *Angew. Chem.* **2002**, *41*, 1053.

[30] V.D. Bock, H. Hiemstra and J.H. Maarseveen, *Eur. J. Org. Chem.*, **2006**, 51.

[31] a) J.A. Opsteen and J.C.M. van Hest, *Chem. Commun.* **2005**, 57; b) D. Quemener, T.P. Davis, C. Barner-Kowollik and M.H. Stenzel, *Chem. Comm.* **2006**, 5051.

[32] P. Wu, M. Malkoch, J.N. Hunt, R. Vestberg, E. Kaltgrad, M.G.Finn, V.V. Fokin, K.B. Sharpless and C.J. Hawker, *Chem. Comm.* **2005**, 5775 and references therein.

[33] R. Hoogenboom, B.C. Moore and U.S. Schubert, *Chem. Comm.* **2006**, 4010.

[34] B. Parrish, R.B. Breitenkamp and T. Emrick, *J. Am. Chem. Soc.* **2005**, *127*, 7404.

[35] See Chapter 5.

[36] K. Matyjaszewski and J. Xia, *Chem. Rev.* **2001**, *101*, 2921.

[37] There is some evidence that in the ATRP reaction with an unprotected acetylene functionality, side reactions do occur. See reference [31a].

[38] K.A. Davis and K. Matyjaszewski, *Chin. J. of Pol. Science* **2004**, *22*, 195.

[39] N.I.Gritsai and O.A. Prib, *Zhurnal Organicheskoi Khimii*, **1967**, *3(9)*, 1597.

[40] M.S. Khajavi, A.A. M, *J. Chem. Res.* **2002**, *3*, 136.

[41] K. Lienkamp, I. Schnell, F. Groehn and G. Wegner, *Macromol. Chem. Phys.* **2006**, *207*, 2066.

[42] PMDETA= Pentamethyl diethylenetriamine, or Bis(dimethylaminoethyl)methylamine.

[43] See Chapter 1.

[44] A.S. Brar and T. Saini, *Eur. Pol. Journal* **2007**, *43*, 1046.

[45] MALDI-TOF = Matrix Assisted Laser Desorption Ionization – Time of Flight mass spectroscopy.

[46] Due to the possiblity of asymmetry in the MALDI-TOF peak (large polymer molecules fly less than short ones) these values may be somewhat flawed. The correlation between the MALDI-TOF and GPC values is however good.

[47] K. Lienkamp, I. Schnell, F. Groehn, G. Wegner, *Macromol. Chem. Phys.* **2006**, *207*, 2066.

[48] Dr. A. de la Escosura is kindly acknowledged for this part.

[49] C. R. Martins, G. Ruggeri, M-A. De Paoli, *J. Braz. Chem. Soc.* **2003**.

[50] Gmelin, *Handbuch der inorganische chemie, Schwefel B, Lieferungen I, II, III, Verlag Chemie, Weinheim, Germany* **1953, 1960, 1963**).

[51] H. Vink, *Macromol. Chem. Phys.* **1981**, *182*, 279.

[52] M-W. Wang and G-K Lam, *Chem. Eng. Comm.* **2004**, *191*, 220.

[53] A.E. Luedtke and J. W. Timberlake, *J. Org. Chem.* **1985**, *50*, 270.

[54] D.D. Diaz, K. Rajagopal, E. Strable, J. Schneider and M.G. Finn, *J. Am. Chem. Soc.* **2006**, *128*, 6056.

Chapter 5

Synthesis of polystyrene sulfonate architectures

5.1 Introduction

The synthesis and properties of copolymers have been a topic of continued interest for many decades. Several types of copolymers exist: one type encompasses the class of random copolymers, in which the monomeric subunits are randomly distributed in the polymer chain. A second type involves alternating copolymers, which posses a (near) perfect alternation of monomeric residues. A third type is obtained when polymer structures are prepared, possessing a gradient in the monomer residues. This is achieved through a variation of the concentration of the respective monomers during the polymerization reaction. As a fourth type, block copolymers in which the monomers are clustered together in two separate blocks can be mentioned. Although other architectures can be envisaged (such as triblock copolymers or alternating multiblock copolymers) the above types are the predominant forms of copolymer structures. It is needless to say that all these compounds have very different and unique properties. In the synthesis of AB block copolymers, several strategies can be employed (Figure 5.1) Modular block coupling involves the separate synthesis of two homopolymers (A and B) which are

coupled afterwards. A serious disadvantage of this method is the low effective concentration of the reactive end groups in solution, which hampers coupling. Also, there are not many polymerization techniques that afford the reactive end groups immediately; further chemical manipulation of the separate blocks is often required to convert the end groups into reactive functionalities. Since the yields of these further manipulations (i.e. the conversion to reactive end groups, as well as the coupling of the polymers) are usually relatively low, the preparation of the final block copolymer is hindered by low yields. Furthermore, the final product is nearly always polluted with the two block constituents. However, a great advantage of this method is the possibility of synthesizing block copolymers that are very heterogeneous in composition. There are many manipulations that one can envisage in order to obtain a reactive end group on a polymer. A disadvantage of end-group manipulation is the difficulties that one encounters in the characterization of the product; the detection of such an end group by standard techniques is not trivial.

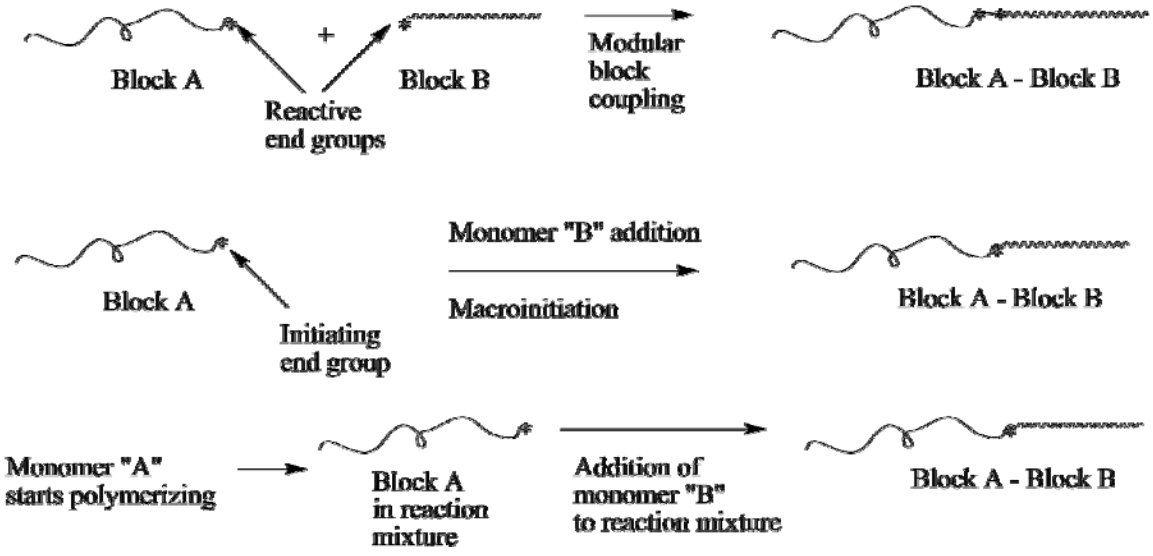

Figure 5.1. *Different approaches toward the preparation of block copolymers. The blocks shown can also be functional on two ends.*

A second strategy is that of macroinitiation. This methodology involves the use of a reactive end-group, present on one of the synthesized homopolymers, as macroinitiator in the preparation of the final architecture. While convenient, this methodology also has a serious weak point, since it places severe restrictions on the composition of the end group

and the polymerization method used. Some kinetic aspects also play an important role. If this methodology is used in combination with ATRP, it is imperative that the rate of initiation far exceeds the rate of propagation, at which the second monomer adds to the growing chain. If not, the polydispersity of the polymer will be large, since some polymer chains are already growing, while others have not yet been initiated. Thus, the monomer, that is intended to react with the macroinitiator, should be chosen such, that the polymerization proceeds relatively slow. The macroinitiator should always be composed of fast polymerizing monomers, compared to the second monomer.

Impurities in the final product include unreacted "block A", which may, however, be chosen such, that it is easily separated from the mixture. Macroinitiators can be readily prepared from homopolymers by chemical post-polymerization modifications.

The third polymerization strategy, which is also very suitable for large scale applications, involves the consecutive addition of monomers to a polymerization mixture. For example, the well-known block copolymer family Kraton is prepared in this manner[1]. This sequential monomer addition is, of course, restricted to monomer combinations that can be polymerized according to the same polymerization principle. If the polymer architecture must be very well defined, this method can not be used, since it will yield block copolymers with a (small) gradient in the transition from one block to the other. However, this procedure is probably the one that is most used because of its practicability and atom efficiency. One interesting class of polymers is that of the amphiphilic block copolymers, which can in principle be prepared using one of the strategies above. The preparation of such block copolymers is of interest since they may exhibit amphiphilic properties and can be used to construct so-called mega-amphiphiles from the CCMV coat protein as outlined in Chapters 1 and 6.

In this chapter, efforts to synthesize well-defined block copolymers of polystyrene sulfonate and several other polymers, will be presented.

5.2 Results and discussion

5.2.1 Synthesis of star shaped polystyrene sulfonate polymers

Chapter 6 describes in detail the interactions of polymers of polystyrene sulfonate with the CP of CCMV. In this connection it would be of interest to see if a non-linear polystyrene sulfonate has a similar effect on the CP assembly as a linear polymer. It was therefore decided to prepare a multivalent ATRP initiator, which could efficiently initiate the ATRP reaction on multiple sites, creating a star polymer. This initiator was made fluorescent for easy detection. To this end, a porphyrin was chosen, since such a compound can be designed to possess 4 or even 8 identical groups, which can all be functionalized (Scheme 5.1).

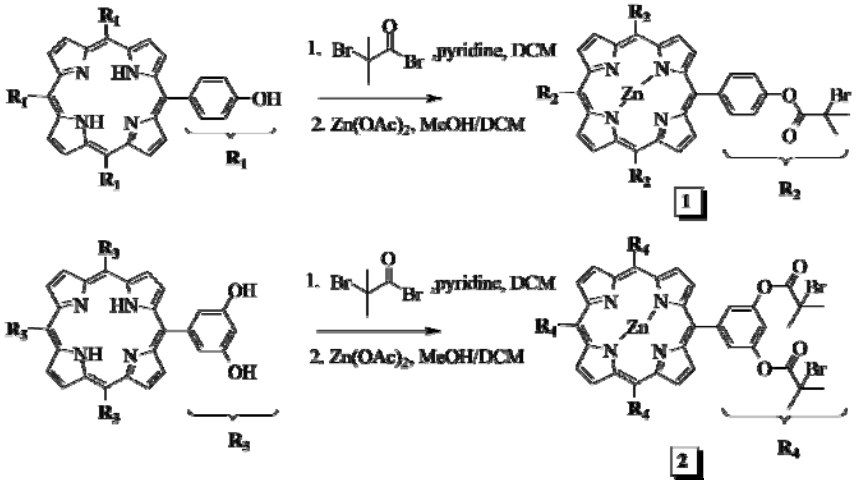

Scheme 5.1. *Synthesis of ATRP porphyrin initiators 1, yield 60 % over two steps, and 2, yield 85% over two steps.*

Porphyrin **1** was chosen as one of the target compounds. Tetrakis(hydroxyphenyl) porphyrine was reacted with bromoisobutyric acid bromide. Subsequently, zinc was inserted in the macrocycle, to prevent interference with the copper ions used in the ATRP reaction. Compound **2** was synthesized in a similar manner. The two multifunctional initiators **1** and **2** were used in ATRP reactions, yielding highly fluorescent dendrimer-like anionic polymers. Kinetic analysis of the polymerization reaction of **1** (molar ratio $SSEt^2$:CuBr:Bipy:**1** = 100:2:2:1) showed linear plots. When the polymer was analyzed by

GPC, the resulting chromatogram showed a large main peak and a decreasing tail (Figure 5.2). The molecular weight of the larger peak corresponded to M_w 43000, implying approximately 50 monomeric units per initiator functionality (i.e. 200 monomer residues per porphyrin), a number that is obviously impossible when the stoichiometry is taken into account.

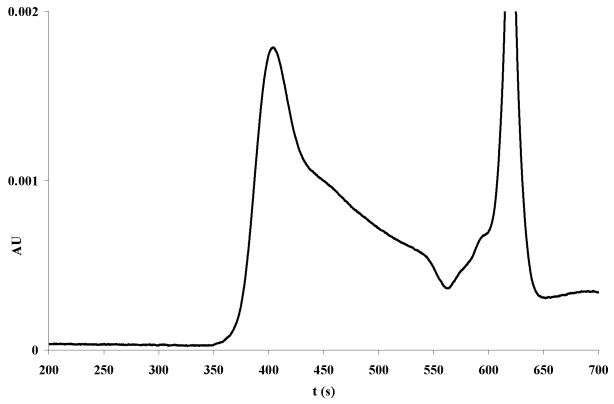

Figure 5.2. *GPC analysis of the polymerization mixture using compound **1** as initiator, and styrene sulfonate ethyl ester. Detection was set at 400 nm (absorption of the porphyrin functionalized polystyrene sulfonate).*

This effect is caused by the well established fact that star-shaped and dendritic polymers appear larger than their corresponding linear polymers in GPC, which in turn is due to their larger hydrodynamic volume. The tailing of the peak could have two causes. It is possible, that not all four chains have a similar degree of polymerization, thus leading to the tailing phenomenon. This may be caused by a subsequent slower initiation of each of the 4 initiator functionalities. In other words, the polymerization rate of the monomer is too high, compared to the initiation rate. Alternatively, it is possible that not all initiator groups have reacted properly, with as a result that some initiator moieties do not contain polymer chains. If, however, the ensuing polymerization runs in a normal fashion, a multimodal distribution would be expected, instead of a peak that displays tailing. It is likely, then, that the larger peak in the GPC chromatogram (polydispersity approximately 1.5) consists of the properly initiated polymer molecules (thus, all four initiators have initiated) and that the "tail" consists of products that were formed by a slower initiation process. Analysis by MALDI-TOF of polymer samples did not clarify these matters greatly, since almost no signal could be obtained. Further studies are needed

to explain the encountered polymerization problems. Purification by repeated precipitation in toluene, in which the lower molecular weight polymers should display higher solubility, were not successful. The obtained polymer (Figure 5.3, left) was deprotected using a sodium azide solution in DMF/water and its effects on the assembly of CCMV CP studied (see Chapter 7).

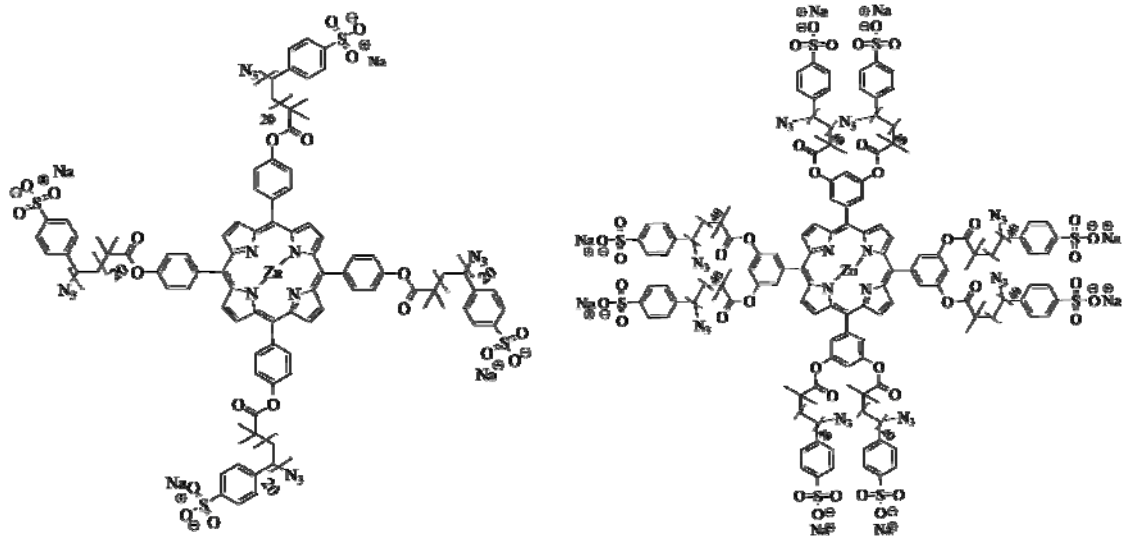

Figure 5.3. *Structure of the polymer obtained after polymerization and deprotection of 1 (left). Successful polymerization of 2 would yield the right-handed structure.*

When compound **2** was used as an initiator in a polymerization reaction applying similar conditions as in the polymerization employing **1**, it was found that this compound did not dissolve in the ethylene- or propylene carbonate solvent. Thus, a small amount of DMF was needed to dissolve this compound. Samples taken from the polymerization reaction mixture always contained precipitated solids, even after these samples had been diluted with chloroform. Although NMR did reveal the disappearance of the double bonds in the monomer, the detection of the polymer was difficult, as it had precipitated out of solution. No kinetic analysis could therefore be carried out. Whether the insoluble product consisted of insoluble polymer, or the polymer had hydrolyzed to a small extent, was not determined. The structure of the hydrolyzed polymer product is presented in Figure 5.3. It is likely that further optimization of the reaction conditions will yield a controllable reaction. Studies with IR spectroscopy may clarify the exact compositions of the reaction products.

In another approach, a porphyrin was functionalized with three aliphatic tails and one initiator group. The polymerization of the single ATRP initiator would yield a polymer which has amphiphilic character, provided that the polystyrene sulfonate part would not be too large (Figure 5.4).

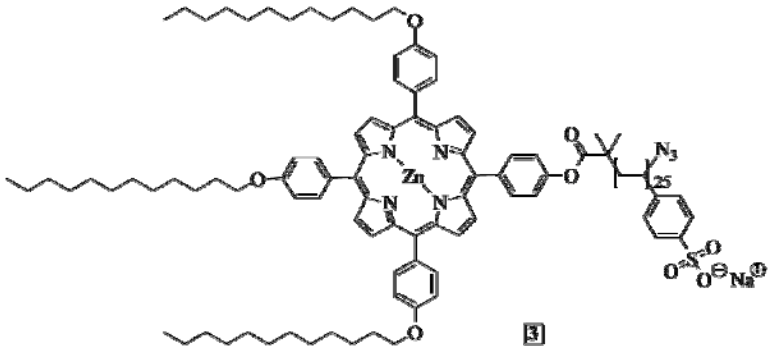

Figure 5.4. *Structure of 3, which has amphiphilic character.*

During the ATRP reaction, using this porphyrin initiator and 100 equivalents of styrene sulfonate ethyl ester, it was found that the initiator did not dissolve in the propylene carbonate solvent, so a small amount of DMF (~0.5 ml) was used as a cosolvent. Although kinetic analysis showed a very rapid consumption of monomer, no high molecular weight polymer was obtained. Since GPC is not a reliable tool to obtain the molecular weight data, MALDI-TOF was applied as a tool to follow the progress of the polymerization reaction. After a long reaction time (6 hours), the presence of only oligomers was detected. These results indicated that some porphyrin molecules had acted as initiator molecules yielding of ca. 10-15 monomer units. In the MALDI-TOF spectra of the samples, a large peak for the initiator compound could still be seen after a long polymerization time. After work-up and deprotection of the oligomer the resulting slurry did not dissolve in water. Extraction with chloroform gave rise to a purple coloration of the chloroform layer. Drying, concentration and TLC analysis of the chloroform layer revealed the presence of the porphyrin initiator. It may therefore be concluded that the initiation efficiency is not very high. This could be caused by a collapse of the hydrophobic alkyl tails on the porphyrin initiator, as a result of the presence of the polar solvent propylene carbonate. This problem might be overcome by the use of a less polar solvent, however, this will lead to other problems. For example, the monomer does not dissolve in hexane or other alkanes. Nevertheless, the water layer that remained after the

extraction with chloroform was concentrated and polymer **3** was isolated and used in experiments with the CCMV CP (Chapter 7). Proton NMR spectra showed the absence of ethyl moieties, which were present in the monomer, but also revealed the presence of the porphyrin and of polystyrene sulfonate. The molecular weight of the polymer could not be determined.

5.2.2 Synthesis of biohybrid block copolymers *via* click chemistry

In order to further investigate the use of polystyrene sulfonate polymers as prepared by ATRP it was thought of interest to prepare biohybrid block copolymers, comprising a polystyrene sulfonate block and a protein. In Chapter 4, the deprotection and simultaneous functionalization of polystyrene sulfonate polymers prepared by ATRP is described. The azide end group functionalization of these polymers make them suitable candidates for the employment of the "click" reaction (see below and Chapter 1). Although bioconjugation of polymers is known, it is often performed using neutral (apolar) polymers. Such biohybrids are known, and have been synthesized in our group.[5] The research presented here represents initial experiments to conjugate a protein with a polyanionic species. It was decided to start with Bovine Serum Albumin (BSA) as the protein component. The use of this protein has several advantages: *(i*) it is readily available, *(ii*) very stable and *(iii*) can be selectively functionalized, since it possesses precisely one cysteine on the surface of the protein. It was decided to prepare the biohybrid *via* the copper(I) catalyzed azide-acetylene cycloaddition. The BSA therefore needs to be functionalized with an acetylene moiety. This can be achieved using the free thiol which is present on its surface. A literature procedure[3] was used to achieve this (Scheme 5.2).

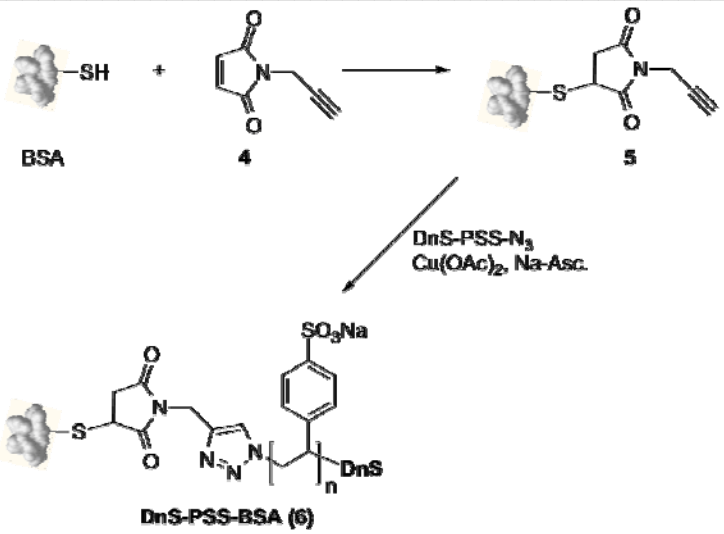

Scheme 5.2. *Functionalization of BSA and subsequent "click" reaction to yield bioconjugate **6**.*

3-Amino-1-propyne functionalized maleimide **4** was prepared according to a literature procedure[4] and allowed to react with BSA, yielding acetylene-functionalized BSA (**5**) Subsequently, in a $Cu(OAc)_2$/sodium ascorbate mediated "click" reaction, the BSA-acetylene was coupled to DnS-PSS (see Chapter 4) yielding conjugate **6**. Figure 5.5 shows the FPLC (Superose 12 column) traces of BSA-acetylene, DnS-PSS and the conjugate, DnS-PSS-BSA.

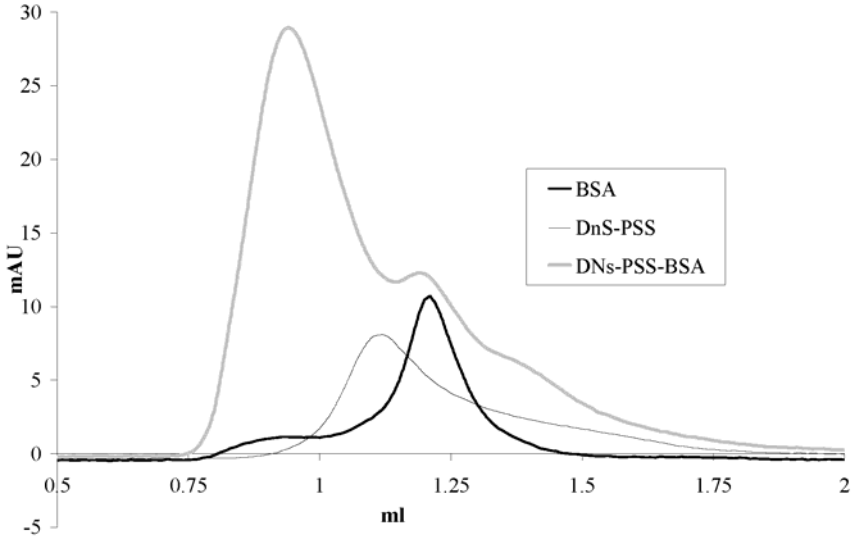

Figure 5.5. *FPLC elution curves of BSA, DnS-PSS and the bioconjugate, detection is at 312 nm.*

The graphs show clearly that the bioconjugate elutes at a smaller volume, implying that it has a larger hydrodynamic radius than both BSA and DnS-PSS. The much larger absorption of the conjugate is caused by a concentration step, which was included in the work-up. The individual fractions were analyzed with UV-VIS spectrometry and SDS-PAGE. UV-VIS spectra of the bioconjugate confirmed the presence of polymer in the fraction that was isolated from the FPLC (~ 0.9 ml). The absorption of the polymer at ~230 nm and the typical absorption of the protein at 260 were both observed in the spectra. Additional absorbance at 310 nm was also visible, which was attributed to the fluorescent dansyl group in the polymer. Figure 5.6 shows an SDS-PAGE analysis of the bioconjugate. Different spots are present in the two traces but the DnS-PSS-BSA bioconjugate cannot be easily detected. This is probably caused by the inability of the complex to penetrate the gel. Unfortunately, the staining of the gel with coomassie brilliant blue may also be impeded by the presence of the polymer; the negatively charged polymer may interfere with the physisorption of the negatively charged dye. Investigations on the behavior of PSS polymers on gels are currently underway. The presence of large amounts of negative charges on the polymer may cause a lengthier migration than might be expected from the molecular weight alone.

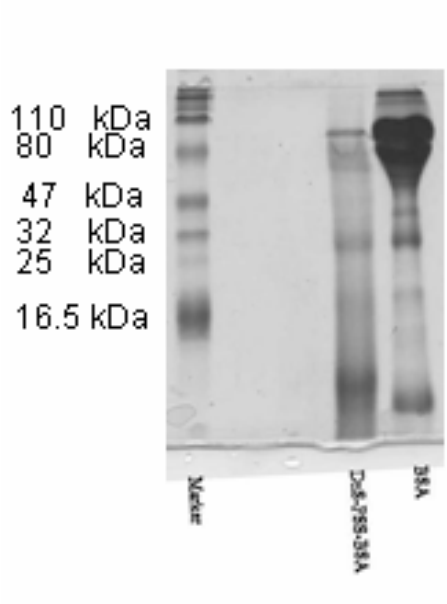

Figure 5.6. *SDS-PAGE analysis of BSA and the bioconjugate. No high molecular adduct is detected.*

In Chapter 7, the effects of this bioconjugate on the CP assembly behavior are presented.

One profound effect on the assembly is the number of negative charges that are present on the polymer. The polymer that is part of the biohybrid structure described here has ~50 negative charges, which was shown to be sufficient to impose assembly of the CCMV CP (see Chapter 6). However, since the above biohybrid polymer consists of only one polystyrene sulfonate chain, its effects on the assembly might be hampered by the hydrophobic/neutral bulk of the protein. It was therefore decided to proceed with another protein, Glucose Oxidase (GOx), which allows functionalization of the amines on the surface of the protein. The successful click chemistry technology was also used in this case. In order to functionalize the eleven amines, present on the surface of GOx, functionalization with 1-pentynoic acid was performed (Scheme 5.3).

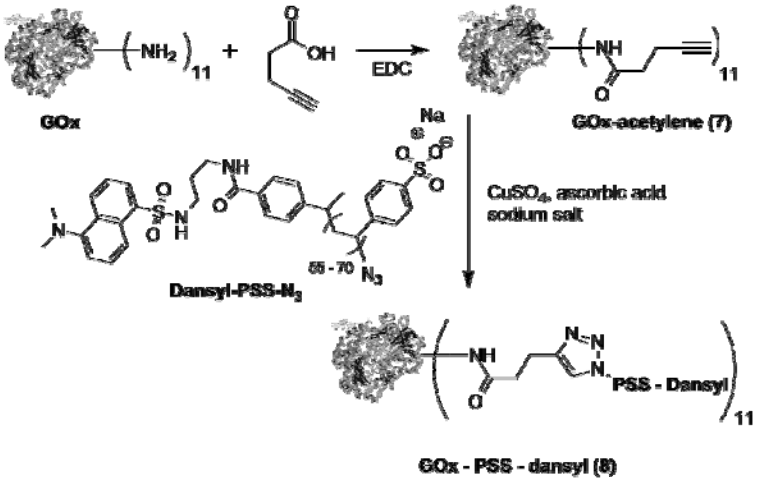

Scheme 5.3. *Chemical strategy for the preparation of a GOx-PSS biohybrid.*

Thus, GOx was reacted in a phosphate pH 7.5 buffer with 14-pentynoic acid under the agency of EDC, yielding **7**. Characterization of **7** by SDS-PAGE or by FPLC was not possible: the migration of the gel did not change dramatically. Subsequently, **7** was reacted with dansyl-PSS-N_3 using the above applied "click" conditions to yield adduct **8**. Two different molecular weight polymers were used for this reaction: one with M_w 12,000 (sample 1) and another with M_w 16,000 (sample 2) corresponding to 55 and 75 repeating monomeric units, respectively. Figure 5.7 shows the FPLC chromatograms, obtained after the reactions.

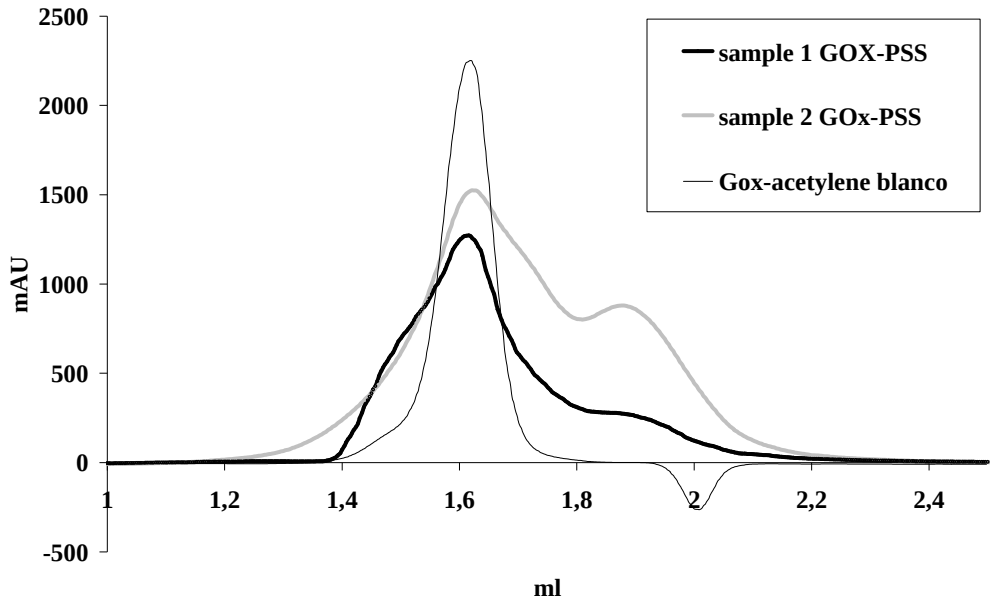

Figure 5.7. *FPLC analysis of GOx and the bioconjugate GOx-PSS. (Superose 6 column, UV detection at 225 nm).*

From Figure 5.8 it is clear that the two different samples do not yield traces that differ significantly, although it is evident that the polydispersities of the products are considerably larger than that of GOx. It is possible, that the broader peaks of the product are indicative of a successful reaction. This would, however, not explain the presence of *lower* molecular weight fractions. It is known, that GOx consists of two identical 80 kDa subunits. Is it therefore possible that the lower molecular weight fractions are the result of dissociation of the protein. Thus, the chromatograms might indicate the presence of dissociated- and non-dissociated enzymes, and both of these could have reacted with polystyrene sulfonate as well. The shoulders at an elution volume of ~1.5 ml elution volume may be assigned to the successful reaction of non-dissociated (160 kDa) species with a varying number of polymer chains. The reaction mixtures were subsequently analyzed with SDS-PAGE (Figure 5.8).

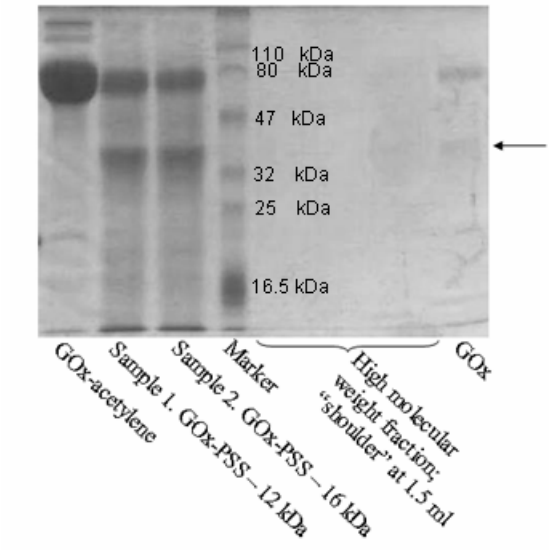

Figure 5.8. *SDS-PAGE analysis of the click reaction between functionalized GOx and polystyrene sulfonate.*

Inspection of the gel revealed that for each of the reactions (samples 1 and 2) a large quantity of unmodified GOx-acetylene had remained. However, below the spots that represent the GOx-acetylene (at ca. 85 kDa, representing a subunit), a spot of lower molecular weight (~ 35 kDa) was observed. It may be that the successful reaction of the GOx and the PSS yields an adduct that is so strongly charged, that it migrates faster through the gel, thus having an apparent lower molecular weight. In that case, however, one would have expected a much broader spot, not only because the polymer is not perfectly monodisperse, but also because the number of polymer chains per enzyme is will display a Gaussian distribution. This idea was, therefore, discarded. Close inspection of the lane representing unmodified GOx revealed a lower molecular weight spot (arrow), probably as a result of disintegration of the GOx subunits. It is thus possible that cleavage of the 80 kDa subunits into two similar fragments occurs. Possibly, these fragments are degraded to a somewhat larger extent, yielding low-molecular weight fractions that are observed at the bottom of the gel. It might thus be possible that the lower molecular weight spots in the gel of the reaction product are caused by the enzyme itself. Furthermore, it is not unlikely that the staining reagent reacts differently with a strongly negatively charged species, since the coomassie brilliant blue that is used for this purpose

is negatively charged itself (Figure 5.9). It may be possible to apply Ag^+ staining for these gels.

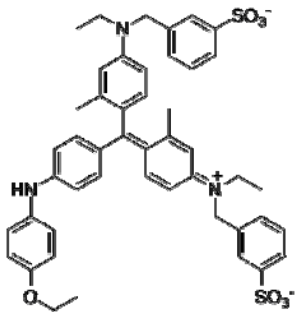

Figure 5.9. *The structure of coomassie brilliant blue.*

These results may be further clarified by the application of SDS-PAGE on a somewhat larger scale, so that the different spots can be isolated and subjected to MALDI-TOF or a related mass spectroscopy technique.

5.2.3 Synthesis of organic block copolymers of PSS *via* ATRP macroinitiation

The elegant methodology of ATRP macroinitiation is limited by two factors: *(i*) a suitable initiator must be present at one end of the starting polymer chain, and *(ii*) the relative polymerization rates of the individual monomers must be appropriate, that is, the rate of initiation (dependent on the electronic structure of the macroinitiator) must be much larger than the propagation rate of the (second block) polymerization. (see also the introduction section of this Chapter.) Since the propagation rate of styrene sulfonate ethyl ester under ATRP conditions is very high, it was envisaged that polystyrene sulfonate ethyl ester (PSS-Et) after polymerization could be used as the macroinitiator for the polymerization of styrene. Subsequent deprotection of the ethyl ester moieties will then yield an amphiphilic block copolymer. Scheme 5.4. clarifies this strategy.

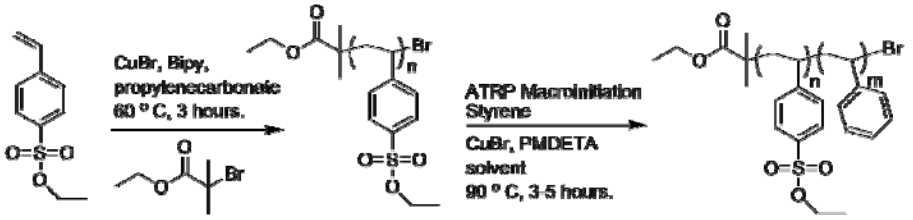

Scheme 5.4. *Use of polystyrene sulfonate ethyl ester as a macroinitiator in the preparation of an amphiphilic block copolymer.*

The most conspicuous practical problem of ATRP macroinitiation is that of solubility. Two different monomers and two polymers (macro-initiator and resulting block copolymer) need to dissolve in quite high concentrations in order to be able to carry out the reaction. In separate experiments, the polystyrene sulfonate ethyl ester was therefore dissolved in various solvents and test macroinitiation reactions were carried out. Unfortunately, the options were limited and it was found, after trying other solvents such as DMF and THF that the PSSEt dissolved slightly in anisole, a solvent commonly used in the ATRP reaction of styrene. Thus, the macroinitiator PSSEt was prepared (See Chapter 4) and dissolved in relatively large volumes of this solvent and the polymerization reaction was carried out. However, since GPC analysis of the polymer product yielded a very broad signal on every attempted reaction, this methodology was not pursued further. A possible reason for this negative result could again be the solubility problems. The polymers obtained were purified anyway (see experimental part) and deprotected. After exhaustive purification, the obtained polymer only dissolved in mixtures of THF and water, which was not unexpected. Analysis of this deprotected block copolymer was hampered by the fact that ^{1}H NMR only showed the presence of polystyrene. It was not possible to distinguish between the sulfonated and the normal polystyrene. GPC analysis of these mixtures also turned out to be impossible due to the amphiphilic character of the material.

In order to circumvent these solubility and analytical problems, *n*-butyl acrylate might be chosen as the monomer to prepare the hydrophobic block of the amphiphilic block copolymer. It is known that n-butyl acrylate polymerizes fast and efficiently in ethylene-, and propylene carbonate[5]. Unfortunately, due to lack of time, experiments with this monomer could not be carried out.

All block copolymers described in this chapter were tested in experiments with CCMV CP as discussed in Chapter 7. Due to the amphiphilic nature of the polymers, their solubilities are severely restricted, requiring the presence of a large proportion of organic solvent, e.g. THF or chloroform[6]. Unfortunately, this requirement is not compatible with the labile character of the coat protein of the CCMV, as was discovered

at this stage of the research. It was therefore decided to also synthesize block copolymers that had a slightly less hydrophobic block.

Hence, an AB type block copolymer that could be prepared starting from a small polyethyleneglycol (PEG, MW 1100) macroinitiator, functionalized at one end with a bromoisobutyric acid moiety, was envisaged. In order to maintain control over the reaction and to test the feasibility of the polymerization reaction, low molecular weight polymers were used. To this end, a small monohydroxy PEG was reacted with bromoisobutyric acid bromide (BiB-Br) in the presence of DIPEA yielding PEG-BiB, after which this product was used in an ATRP reaction with styrene sulfonate ethyl ester (Scheme 5.5.).

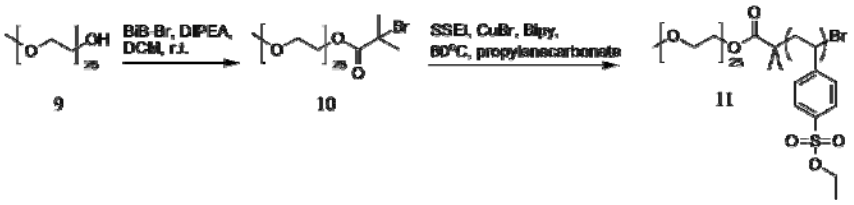

Scheme 5.5. *Preparation of PEG macroinitiator **10** and its reaction with ethyl styrene sulfonate to yield AB-type block copolymer **11**.*

However, despite several attempts, no well-controlled polymerization could be developed. Since the solubility of the PEG initiator in ethylene- and propylenecarbonate was determined to be good, the solvent was kept the same in several experiments. NMR analysis revealed that no conversion had occurred two hours after the reaction was initiated. Figure 5.10 shows the GPC curves, obtained after ~16 hours of reaction.

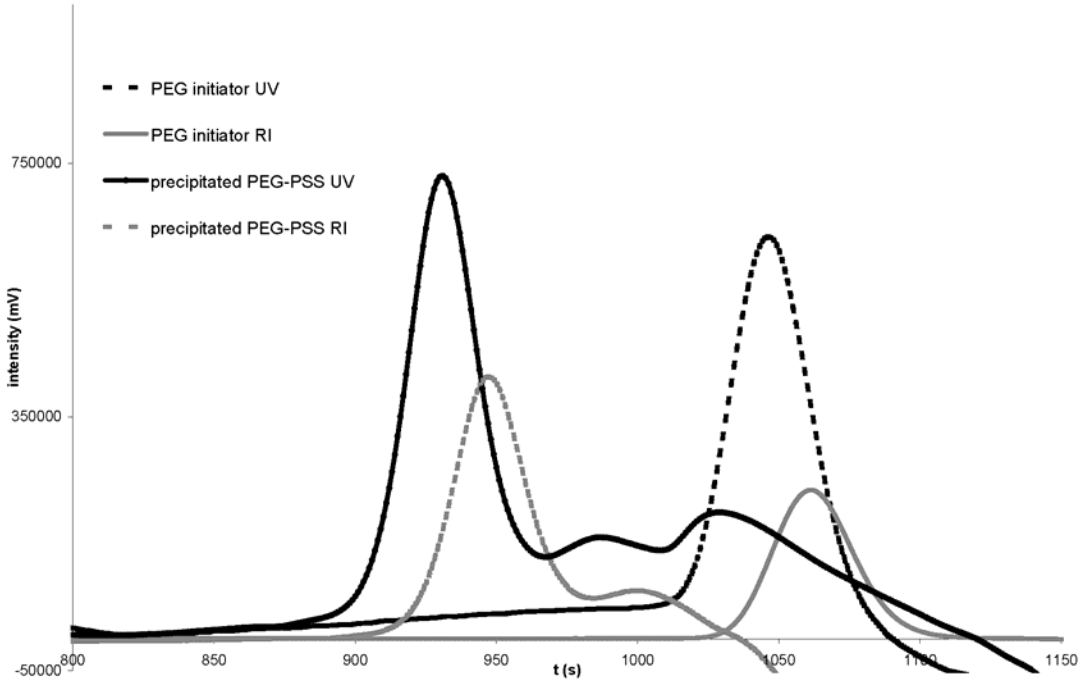

Figure 5.10. *GPC analysis of the polymer mixture obtained after the ATRP of styrene sulfonate ethyl ester using a PEG-based macroinitiator as shown in Scheme 5.5. RI=refractive index detection, UV=UV detection at 254 nm. The UV detector is situated downstream of the RI detector, explaining the shift in the peaks.*

Several observations can be made. The PEG initiator readily adsorbs at 254 nm, which is somewhat surprising. The absorption at lower retention times (signifying a higher molecular weight) indicate that part of the PEG had been functionalized with ESS groups. The crude polymer was precipitated several times, both in methanol and in toluene and centrifuged. This approach did not succeed in purifying the polymer; the traces obtained for precipitated PEG-PSS are identical to those obtained from the crude reaction mixture. Nevertheless, the polymer mixture was deprotected with sodium azide, and dialyzed against pure water, using a dialysis membrane with molecular weight cut off of 3,000. This procedure should remove the oligomeric PSS chains, increasing the relative amount of high molecular weight polymer. This procedure, however, did not yield pure deprotected **11.**

5.2.4 Synthesis of organic block copolymers of PSS *via* modular block coupling

In order to prepare a block copolymer comprising both an ionic and a hydrophobic group for the construction of a mega amphiphile (See Chapters 1 and 7), a polystyrene polymer of high molecular weight (MW 125,000) was prepared using a *tert*-butyl BiB initiator[7]. Subsequently, the *tert*-butyl protecting group was hydrolyzed after which the acid was coupled to 1-azido-3-propylamine. (Scheme 5.6) The success of these reactions could not be determined any way because the resulting mixture had hydrolyzed, forming an inseparable multi-phase system. Large excesses of reagent and long reaction times were therefore applied to ensure complete conversion.

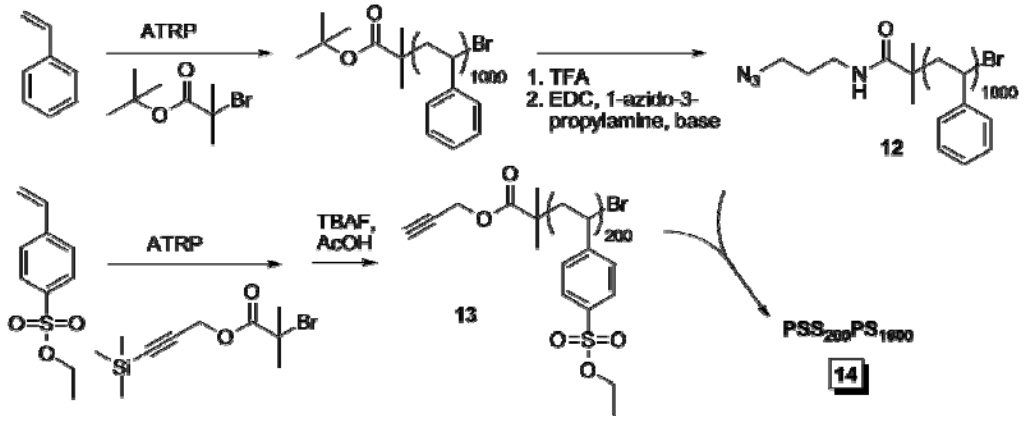

Scheme 5.6. *Synthesis of a high molecular weight polystyrene block (**12**) and subsequent coupling to a polystyrene sulfonate block (**13**) to yield block copolymer **14**.*

Subsequently, polystyrene sulfonate ethyl ester (**13**) was prepared with the help of a TMS protected propargyl-BiB initiator. After the TMS had been removed using a neutral TBAF/AcOH solution, a coupling of the two polymers was attempted. Thus, the compounds were reacted together in a copper-catalyzed "click" reaction by using a 5/95 mixture of water and THF, with an excess of ascorbic acid and copper sulfate. It was checked separately, that the use of TBAF, which had been neutralized with a stoichiometric amount of AcOH, did not hydrolyze the ethyl ester functionalities of the monomer. Care was taken to maintain a low pH (~3) in the mixture in order to prevent the hydrolysis of the ethyl moieties. However, after several hours of reaction, a slurry had formed that did not dissolve in mixtures of THF/water or chloroform/water. GPC analysis of the soluble part of the chloroform mixture revealed only the presence of the

polystyrene part, leading us to conclude that hydrolysis had again taken place, at the acetylene ester moiety. Subsequent attempts to perform this copper catalyzed click reaction in pure chloroform, under the agency of PMDETA and Cu(I)Br, under Schlenk conditions yielded only starting materials, even using different stoichiometric ratios.

5.3 Conclusions and future prospects

We have shown that multifunctional, fluorescent ATRP initiators can be used in the polymerization of styrene sulfonate ethyl ester. Amongst others, fluorescent, polyanionic star-shaped polymers have been synthesized. The synthesis of different types of block copolymers was tried also with varying degrees of success. One important limiting factor was the hydrolysis of the styrene sulfonate ethyl ester moieties of the polymers, which are highly sensitive towards basic conditions. It is suspected that the experimental conditions used in the click reactions also lead to hydrolysis of the esters, but this was not confirmed. It was determined that the preparation of polystyrene-block-polystyrene sulfonate using this methodology is not a viable option, due to the difficulties in detecting and characterizing the polymer.

The methodology to prepare biohybrid block copolymers turned out to be successful, The presence of the DnS-PSS-BSA adduct was proven. This methodology could for example be applied to anchor enzymes onto a solid phase. This could be achieved by the polymerization of styrene sulfonate ethyl ester from a solid phase resin by functionalization of the resin with an initiator, or by coupling the polystyrene sulfonate to the solid resin with the help of click chemistry. Functionalization of the end group with an azide, and subsequent reaction with an enzyme that has been functionalized with an acetylene moiety, would yield the solid phase enzyme. The presence of the polyanionic species would prevent the collapse of the enzyme-polymer hybrid onto the solid carrier, a common problem in current enzyme immobilization techniques. This bioconjugation step may be used to prepare pharmaceutically relevant compounds.

The preparation of block copolymers from polystyrene sulfonate and polystyrene was difficult, since several steps were required to functionalize both ends of each

polymer. Since the success of these manipulations depend on the endgroup functionality, analysis of successful reaction is extremely difficult, since the detection of end-groups in polymer chemistry is much like a "needle in the haystack" problem.

5.4 Experimental section

BSA and GOx were obtained from Sigma. FPLC (SEC) was performed using a Superose 12 PC 3.2/30 analytical column (Amersham/GE biosciences) on a Amersham Ettan system, fitted with a fractionating device, running at 40 µl/min, equipped with UV detection at various wavelengths. Buffers for FPLC were filtered with a Millipore 0.2 µm filter before use and were of identical composition as buffers used to perform reactions. GPC was recorded on a Polymer Labs PL gel 5 µm column with chloroform as the eluent on a Shimadzu 10A LC system and was calibrated with monodisperse polystyrene samples obtained from Polymer Labs. TLC was performed on J.T. Baker Si250F glass TLC plates with a fluorescent impregnation. NMR spectra were recorded on a Bruker DMX 300 MHz or on a Varian DPX 400 MHz machine. Chemical shifts are reported relative to TMS. MALDI-TOF was measured on a Bruker Biflex III spectrometer in the linear mode using ditranol as the matrix. A sample of 10 µl of a dilute solution (~10^{-5} M, equivalent monomer concentration) of polymer was added to an equal amount of matrix solution, and deposited (3 µl) on the MALDI plate. Similar procedures were used for the detection of functionalized porphyrins **1 – 3**.

5.4.1 Synthesis of star shaped polystyrene sulfonate polymers

Tetrakis(phenyl-4-isobromobutyrate)-zinc-porphyrin (1)

To a solution of tetrakis(hydroxyphenyl) porphyrin (45 mg, 0.06 mmol) in 2 ml of pyridine/DCM (1/10, v/v) at -30^{o}C, a solution of 2-bromo-2-methylpropanoyl bromide (isobromobutyric acid bromide) was added dropwise. Sometimes, a green color could be observed in the mixture. After 3 hrs. the reaction was quenched by the addition of dry MeOH (1 ml) followed by stirring at room temperature. After the solvent had been evaporated, the slurry was taken up in DCM and extracted with saturated aqueous $NaHCO_3$ (1 x 50 ml), $NaHSO_4$ (1x50 ml) and brine (1x 30 ml), after which the solution

was dried and evaporated to dryness, yielding pure (**1)** in quantitative yield. Rf 0.8 (DCM). ^{1}H NMR ($CDCl_3$): δ 8.87 (s, 8H, CH pyrrole), 8.25 (d, *J*= 8Hz, 8H, CH arom), 7.57 (d, *J* = 8.4 Hz, CH arom), 2.23 (s, 24 H, CH_3), -2.81 (s, 2H, 2x NH). ^{13}C NMR ($CDCl_3$): The title compound was prepared by dissolving the compound in DCM/MeOH (3/1, v/v, 20 ml) and adding a spatula tip of $Zn(OAc)_2$, of which the excess was removed, after reaction and evaporation of the solvent, by elution over a short plug of silica. (eluent: $CHCl_3$). ^{1}H NMR (400 MHz, $CDCl_3$): δ 9.11 (s, 8H, CH arom porph.), 8.14 (s, 8H, CH phenyl), 7.74 (s, 8H, CH arom phenyl). MS (ACCU-TOF): 1326.9499 (M+H) Calc. 1327.6.

Tetrakis(phenyl-3,5-diisobromobutyrate)-zinc-porphyrin (2)

To a solution of octakis hydroxyphenylporphyrin[8] (100 mg, 0.13 mmol) in THF (50 ml) at 0^{o}C, 3.2 ml of pyridine was added, followed by dropwise dropwise addition of isobromobutyric acid bromide (3.0 ml, 26 mmol) in THF (50 ml). After the reaction was complete, the mixture was quenched by the addition of MeOH (10 ml), after which the solution was stirred for 0.5 h. at room temperature. Subsequently, the solvent was evaporated and the resulting deep purple slurry was dissolved in DCM (20 ml) and an extraction procedure identical to that used in the preparation of **1** was carried out. After evaporation of the solvent the product was dissolved in DCM and a spatula tip of $Zn(OAc)_2$ was added. TLC showed rapid conversion to the zinc coordinated product so the slurry was evaporated and the product was purified by column chromatography (heptane/$CHCl_3$ 50/50, v/v → 10/90, v/v), yielding pure (**2**) (0.14 g, 0.07 mmol, 60%). Rf 0.7 (20% EtOAc/heptane). ^{1}H NMR (400 MHz, $CDCl_3$): δ 9.13 (s, 8H, CH porphyrin); 7.94 (s, 8 x CH Phenyl); 7.49 (s, 4H, 4 x CH Phenyl); 2.12 (s, 46 H, CH_3 ester). MS (MALDI-TOF): 1988.1 (M).

5,10,15-Tris(phenyl-4-dodecyloxy)-20(phenyl-4-isobromobutyrate)-zinc-porphyrin

5,10,15-Tris(phenyl-4-dodecyloxy)-20(phenyl-4-hydroxide)-porphyrin[9] (0.72 g, 0.61 mmol) was dissolved in 50 ml of DCM, after which 40 equiv. of pyridine (2 ml) was added. The flask was cooled to -30^{o}C and a solution of isobromobutyric acid bromide (0.8 ml, 6 mmol) in DCM (20 ml) was added dropwise over a period of 0.5 h. After this

time, the reaction mixture was quenched with dry methanol and the solvent evaporated. The product was co-evaporated with toluene (2 x 50 ml), after which flash silica gel column chromatography ($CHCl_3$) provided the pure product in quantitative yield. (0.95 g, 0.7 mmol). The zinc derivative was obtained by dissolution of the product in DCM/MeOH 1/1, v/v, 30 ml, after which a spatula tip of $Zn(OAc)_2$ was added. The reaction was complete in 30 mins. The product was isolated by evaporation of the solvent and purified by elution over a short silica plug (eluent: toluene). Yield: 0.804 g, 0.57 mmol). ^{1}H NMR ($CDCl_3$): δ 8.97 (m, 6 H, pyrroles), 8.92 (m, 2H, CH pyrroles), 8.21 (d, *J* = 8.0 Hz, 2H, CH arom Ph-initiator); 8.08 (d, *J*=6.4 Hz, 6H, CH arom Ph-tails), 7.52 (d, *J* = 8.2 Hz, 2H, CH arom Ph-initiator), 7.21 (d, *J*=8.4 Hz, 6H, CH arom Ph-tails), 4.17 (m, 6H, 3xCH_2-O), 2.21 (s, 6H, 2xCH_3 ester), 1.92 (m, 6H, 3x O-C$\underline{H}_2$-CH_3), 1.58 (m, 6H, 3x O-C$\underline{H}_2$-CH_2-CH_3), 1.30 (m, 56 H, CH_2 tails), 0.89 (m, 9H, CH_3 tails). MS (MALDI-TOF) 1395.1 ($M^{+\ 79}$Br), M 1396.1 ($M^{+\ 81}$Br). Calc 1394.6 and 1395.6. Polymerization of this compound with SSEt and deprotection of the ethyl functions yields compound **3** (see text).

ATRP using porphyrin initiators

The ATRP reactions were carried out as described in Chapter 4. Polymerization using initiator **1** (molar ratio SSEt:CuBr:Bipy:**1** = 100:2:2:1, 60^{o}C, 1M monomer concentration in propylene carbonate) yielded a polymer with the following characteristics: GPC ($CHCl_3$): MW 43000, PDI 1.6. NMR data were similar to those reported for polymers in Chapter 3. No product could be isolated from the polymerization reaction using **2** as the initiator. The polymerization of styrene sulfonate ethyl ester with **3** as the initiator is described in the text.

5.4.2 Synthesis of biohybrid block copolymers

Functionalization of BSA with an acetylene functionality (5)

In an Eppendorf vial, 50 mg BSA was dissolved in 200 mM phosphate buffer (pH 7.2, 1.5 ml). To this solution, a solution of **4** (10 mg, 7 ·10^{-5} mol) in THF (0.20 ml) was added and the mixture was gently shaken for 48 hrs. The contents of the Eppendorf were subsequently transferred to a dialysis bag (MWCO: 3,000) and extensively dialyzed

against phosphate buffer (20 mM, pH 7.2) to yield **5**. FPLC chromatograms of this compound were identical to those of non-functionalized BSA.

Click reaction of BSA-acetylene (5) with dansyl-PSS-N_3 (6)

A solution of $Cu(OAc)_2$ (10 mg) and sodium ascorbate (10 mg) in 20 mM phosphate buffer (200 µl, pH 7.2) was prepared. A sample of this solution (20 µl) was added to a solution of **5** in phosphate buffer (20 mM, pH 7.2, 10 mg/ml, 1.0 ml). Subsequently, a solution of dansyl-functionalized polystyrene sulfonate (see Chapter 4) (2.2 mg in 200 µl 20 mM phosphate pH 7.2 buffer) was added to the mixture, which was allowed to stand for two days at room temperature. After reaction, the mixture was filtered over a 0.2 µm syringe filter, dialyzed extensively against a phosphate buffer (200 ml 20 mM 0.1 M NaCl pH 7.2), and analyzed by FPLC, UV and SDS-PAGE.

Preparation of GOx – acetylene$_n$ (7)

In a phosphate buffer (pH 7,5, 50 mM, 5 ml), lyophilized GOx (0.073 g, $4.0 \cdot 10^{-7}$ mmol) was dissolved and to this mixture EDC (100 eq., 62 µmol, 0.2 mg) was added. Immediately, 4-pentynoic acid (100 eq., 62 mg, 0.1 mg), dissolved in 0.5 ml of the same buffer, was added to the mixture. The mixture was placed on a roller bank and allowed to stir for 24 hrs at room temperature. Hereafter, the mixture was dialyzed extensively against the same buffer at 4^{o}C (4 x 200 ml).

Preparation of GOx – DNs-PSS$_n$ (8)

To two 1.5 ml batches (*i.e.* samples 1 and 2, see text), obtained from the reaction above, 0.18 µmol of the appropriate dansyl-polystyrene sulfonate-azide (DNs-PSS-N_3) was added. For the 12,000 Da polymer this corresponded to 2.16 mg and for the 16,000 Da polymer to 2.88 mg. The pH was checked to remain at 7.5. Subsequently, a mixture of 12 mg $CuSO_4.5H_2O$ and 13 mg ascorbic acid sodium salt was prepared separately in 0.5 ml distilled water. Samples of this copper solution (50 µl) were added to both protein-polymer mixtures, and the resulting mixtures were allowed to stir for 16 hrs. After this period, the mixtures were dialyzed against phosphate buffer (50 mM, pH 7.5, with 5 mM

EDTA-Na_2, 3 x 200 ml) and the products were analyzed using FPLC and SDS-PAGE (see text).

Polyethylene glycol-polystyrene sulfonate block copolymer (11)

Compound **10** was prepared according to a literature procedure[10]. The preparation of the ATRP reaction of ethyl styrene sulfonate was carried out according to a procedure described in Chapter 4. The following molar ratios were used: SSEt:CuBr:Bipy:Initiator = 150:2:2:1 at 60°C, 1M monomer concentration in propylene carbonate. The initiator, 0.63 g PEG_{25}-BiB (**10**) was dissolved in propylenecarbonate and added to the mixture. Samples were taken at different intervals to determine the conversion. NMR showed that no conversion had taken place within the first 2 hrs., after which the reaction was left to stand overnight. A work up procedure, as described in Chapter 4, was then performed. The yield was not determined, because GPC had shown that the reaction was unsuccessful.

5.5. Notes and references

[1] Webpage:
http://www.kraton.com/content/includes/An%20Intro%20To%20Kraton.pdf
[2] See Chapter 3.
[3] N.S. Hatzakis, H. Engelkamp, K. Velonia, J. Hofkens, P.C.M. Christianen, A. Svendsen, S.A. Patkar, J. Vind, J.C. Maan, A.E. Rowan and R.J.M. Nolte, *Chem. Comm.* **2006**, 2012.
[4] B. Karlen, B.K.B. Lindeke, S. Lindgren, K. Svensson and R.J. Dahlbom, *J. Med. Chem.* **1970**, *13*, 651.
[5] K. Matyaszewski, Y. Nakagawa and C. B. Jasieczek, *Macromolecules* **1998**, *31*, 1535.
[6] P.L. Valint and J. Bock, *Macromolecules* **1988**, *21*, 175..
[7] These experiments were carried out before the extreme sensitivity of the coat protein was established.
[8] Generously provided by A. Deutman.
[9] Generously provided by R. van Hameren
[10] S. Angot, D. Taton and Y. Gnanou, *Macromolecules* **2000**, *33*, 5418.

Chapter 6

Interaction of homopolymers of polystyrene sulfonate with CCMV coat proteins

6.1 Introduction

In Chapter 2, a general description of CCMV was given, and examples of how the virus can be modified were discussed. Until now, only very few studies in the literature have dealt with the problem of controlling assembly behavior and symmetry of the virus particle. It is astonishing, that in a surrounding as crowded as the inside of a (plant) cell, the subtle interactions between the 180 identical subunits and the 4 different RNA strands lead to reproducible self assembly. Several mechanisms have been proposed to explain this phenomenal selectivity, one of which is the presence of a highly conserved RNA structure that resembles a tRNA structure[1]. It would seem likely that the intricate folding patterns of the genetic material has a profound influence on the assembly of the protein subunits around the RNA, or that it serves as a nucleation point for the assembly process at the very least. Studies conducted with another virus related to CCMV, Bromo Mozaic Virus (BMV) have shown that assembly is impossible without the presence of the tRNA-

like structure. However, later research revealed that for CCMV, this is not the case, at least not in vitro.[2] When RNA was genetically engineered to lack the tRNA-like structure, it was found that protein assembly around the RNA was independent of this motif. Thus, although the subunit composition and RNA strand subdivision between several virus particles (i.e. different viral particles contain different strands of RNA) are highly similar, CCMV apparently does not require the tRNA-like strand for assembly, whereas the BMV does. Another striking difference is that CCMV RNA can move from one cell to the other, without its surrounding protein shell, whereas BMV's RNA cannot. Despite the vast number of studies and publications performed on the CCMV, the mechanisms of assembly of the virions *in vivo* remains unclear. For example, the interaction of the protein subunits with the negative charges on the RNA (see Chapter 1) cannot be too strong, because in that case, non-viral assemblies will form, which is detrimental to the survival of the virus. Contrarily, if they are too weak, no particle will form inside the cell, also leading also to the extinction of the virus. The question remains: how does this happen? In order to be able to answer this question it is first important to understand the fundamentals of the "construction scheme" of most spherical viruses. The term "spherical" is not completely correct. The protein subunits of viruses are in fact generally arranged into regular polyhedral structures obeying icosahedral symmetry. This icosahedral symmetry is widespread in spherical viruses.[3] The understanding of the structure of such viruses is based on the Caspar and Klug (CK) ''quasi-equivalence'' principle.[4] Closed icosahedral shells (that is, shells of icosahedral symmetry) can be constructed from pentamers and hexamers by minimizing the number T of nonequivalent locations that protein subunits occupy, with the T-number adopting values of 1, 3, 4, 7, 12, 13,… The T number is given by the formula $T = h^2 + hk + k^2$, where h and k are integers ($h \geq 1$, $k \geq 0$). A spherical arrangement of protein subunits that obeys icosahedral symmetry must therefore always possess 12 pentamers and 10(T-1) hexamers, so that the symmetry around a protein subunit becomes quasi-equivalent when T>1.

The construction of such a polyhedral structure with icosahedral symmetry requires at least three proteins per facet. This is due to the fact that one individual protein does not, in general, display threefold symmetry. It is therefore much easier to employ copies of identical subunits than to synthesize one single protein possessing three-fold

symmetry. It is in fact even thought that a single protein cannot posses three-fold symmetry.

The smallest possible icosahedral viral particle (T=1) is built up from 60 protein subunits (12 pentamers, figure 6.1, left structure) but most viruses have evolved to possess *T* multiples of 60. Since hexameric arrangements cannot themselves bend in space, the presence of pentamers is essential for the curvature of the shell (Figure 6.1.) It can be concluded that lower T numbers imply smaller particles; the presence of pentamers implies a large curvature.

The CCMV virus has 180 subunits, possesses the structure of a *truncated icosahedron* (figure 6.1, top, middle and right structure), and obeys T=3 quasi symmetry, implying that a protein subunit can occupy three different positions with respect to its neighbours.

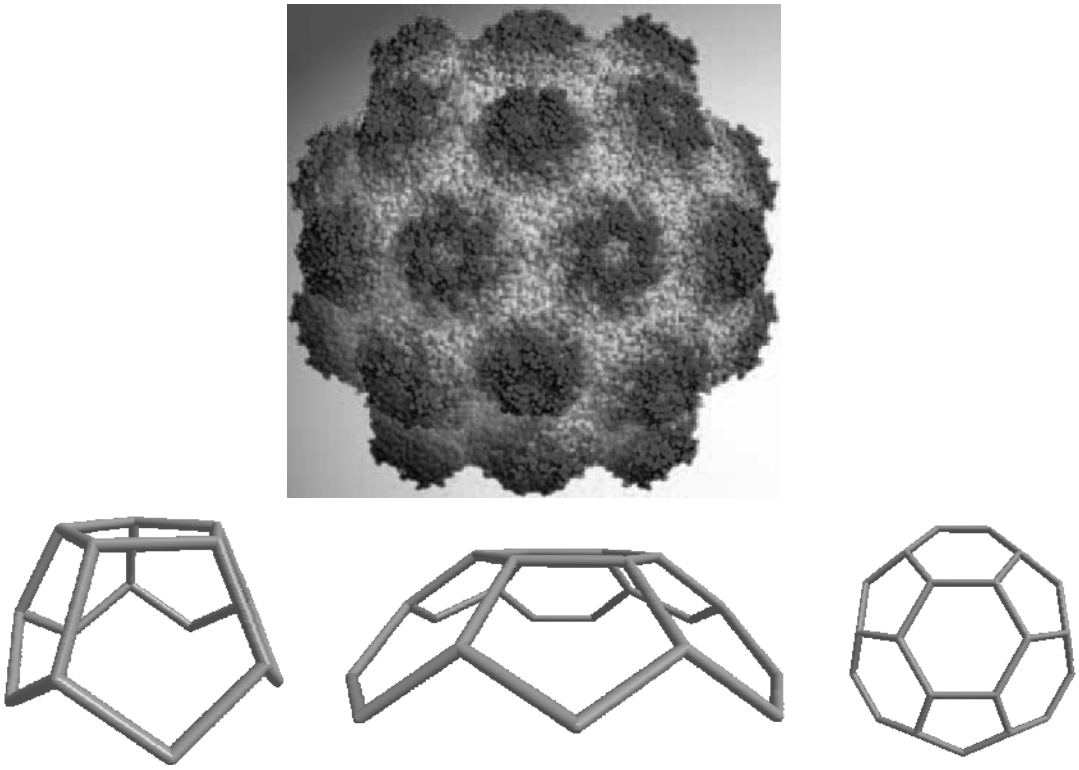

Figure 6.1. *Schematic drawing of the top parts of the polyhedral arrangements of faces which clarifies the high curvature, induced by the pentameric units. Top: schematic reconstruction of the T=3 CCMV virus. Left: the assembly of five pentameric units around a central pentamer, creating a regular dodecahedron which obeys icosahedral symmetry rules. Center: the assembly of three pentameric, and three hexameric units around a central hexameric core, leading to a truncated icosahedron. Right: a top view of the center structure.*

Since the structure on the left (Figure 6.1) possesses maximal curvature and only 12 pentameric faces, it is the smallest viral structure possible (T=1), with three protein subunits arranged around each corner. Each pentameric face contains five protein subunits. In this chapter, this particle is obtained by the interaction of polystyrene sulfonate with the CP dimers. Full construction of the center (and right) structure would yield a T=3 structure, the second-smallest stable structure of icosahedral symmetry.[5] Whenever an icosahedral virus is mentioned, it should be understood that icosahedral symmetry is implied, but that the particle itself does not have a strictly icosahedral shape. It is remarkable that such straightforward considerations can accurately describe the assembly state of such highly complicated virus particles. Several (semi)-stable conformations are known in virology, however, these are almost always induced by non-natural conditions.

In the assembly of CCMV (T=3), recent insights suggest that several protein subunits first form pentamers and hexamers, which then assemble together onto the RNA chains to generate the viral structure. Apparently, the 3' symmetry axis in a hexameric assembly of six subunits, which also contains 6 positively charged protein strands, allows this assembly to be highly specific. So far, however, a detailed description is lacking. For a general understanding of the assembly behavior of this virus and other viruses it is important to study the assembly behavior of the protein subunits under slightly altered assembly conditions. Several computer models have contributed to this understanding. Rudnick et al. have carried out a Monte Carlo simulation of the formation of an icosahedral capsid and have shown that the structures *in vivo* are of a minimal energy configuration.[6] Other, non-icosahedral structures sometimes observed *in vitro* also follow from these calculations. Very recently, theoretical considerations have revealed that viral particles with higher T-value might possess a structure that is nearly icosahedral, but not entirely; the energy levels of these particles, containing a so-called scar, are lower than the corresponding icosadeltahedra.[7] Van der Schoot and coworker have suggested that viral assembly is driven by a subtle equilibrium between attractive hydrophobic interactions and repulsive ionic charges. It is not unexpected that electrostatic repulsions between viral proteins prevents the formation of empty capsids *in vivo*; a charge neutralizing nucleic acid is required to compensate for these repulsive interactions.[8] This

effect can also be achieved by the use of a high salt concentration *in vitro*, as is the case with CCMV CP (see below).

It is known that the assembly of the CCMV CP in the absence of the RNA can yield several morphologies, depending on such variables as the sodium chloride concentration and the presence of divalent cations such as magnesium. (See Chapter 2). It is therefore expected, that different anionic species have a different effect on the assembly. Several decades ago, Bancroft et al. studied the influence of negatively charged species on the assembly behavior of CCMV CP,[9] and found that similar anionic species gave rise to radically different assemblies. Zlotnick et al. have found that the incubation of the CP with double stranded DNA yielded long tubes.[10] Considering these results, and with one of the purposes of this work in mind, being the creation of a mega amphiphile, it was decided to study the interaction of polystyrene sulfonate with the CCMV CP. The synthesis and characterization of the polymers used in this work are explained in Chapter 4.

6.2 Results and discussion

In this Chapter, studies on the interaction of polystyrene sulfonate and CCMV CP are described. Figure 6.2 shows a Transmission Electron Micrograph (TEM image) and a Fast Protein Liquid Chromatography (FPLC) trace of the complete virus particle. FPLC is able to separate proteins and other water soluble macromolecules on the basis of size.

As can be seen from the top and middle elution curves, a (main) elution peak at ca. 1.1 ml can be observed. In the top panel, the complete T=3 virus is shown, and the middle panel shows the empty (T=3) capsid, which also appears at ca. 1.1 ml, implying that the capsid and the complete virus possess similar hydrodynamic radii. The electron micrograps support these observations: the particle in both the top and middle micrograph are equal in size. The difference in staining in the electron micrographs is attributed to the procedure which is used for preparation of the sample: The uranyl acetate used for this purpose cannot penetrate the centre of the particle, if RNA is present. Therefore, only the particles in the middle panel (without RNA) show a dark centre.

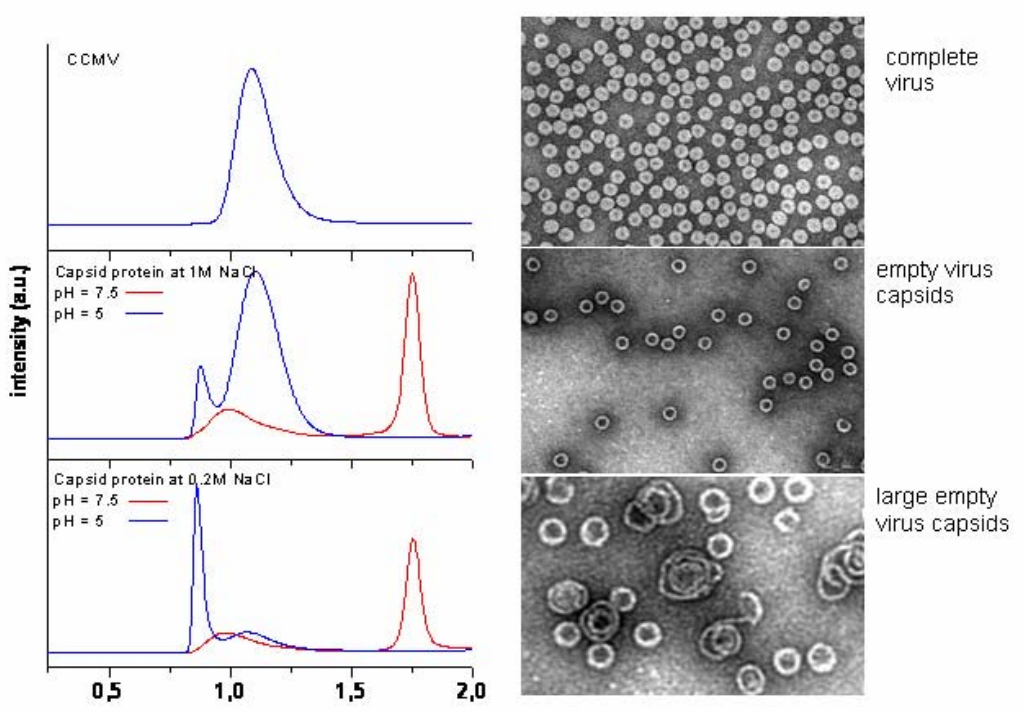

Figure 6.2. *Size exclusion chromatograms and TEM images (negatively stained) of the complete virus (top), the assembly at pH 5 of CCMV CP into empty capsids at 1.0* M *NaCl concentration (as well as the elution of the protein subunits) (middle), and the multi-walled assemblies obtained by pH decrease in a low-salt preparation of the protein at low pH (bottom).*

The empty capsid can be dissociated at higher pH (7.5), whereas low pH (5.0) leads to self assembly. These processes are completely reversible. At pH 7.5, the FPLC curve for the capsid (middle) shows a peak that corresponds to smaller proteins eluting at 1.75 ml. These are the dimeric subunits.

The FPLC curve for the capsid (middle) also shows a peak eluting at 0.9 ml, which is attributed to multi-shelled protein assemblies. This multi-shelled variant is more pronounced, when a lower salt concentration is used, see the bottom right micrograph. Both the middle and the bottom trace also show the elution of the dimeric coat protein (CP) building blocks at 1.75 ml.

Since the use of a low salt concentration (0.2 M NaCl) does not yield the same well-defined particles as the higher (1 M) concentration, it can be concluded that this salt concentration is insufficient to negate the ionic repulsion of the positively charged proteins. The surface charge density of the protein must therefore also be very high.

Subsequently, assembly studies were carried out using the negatively charged polystyrene sulfonate (DNs-PSS) shown in Figure 6.3, which possesses 60 repeat units.

The synthesis of this polymer is described in Chapter 4. It contains a dye function for the purpose of characterization.

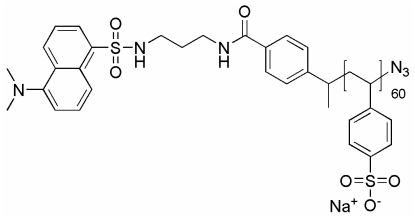

Figure 6.3. *The structure of the polystyrene sulfonate* ***DNs-PSS****, functionalized with a fluorescent probe, as used in this chapter.*

It was reasoned that with this polystyrene sulfonate similar packing might be achieved as with RNA. It is known that the internal pressure in some viruses is exceedingly high, since these species need to inject the RNA/DNA into a cell.[11] This has led to the postulation that the packing density of RNA is very high. Thus, to an aqueous solution 0.5 mg CCMV CP a relatively large quantity of polystyrene sulfonate, corresponding to about 700 negative charges per monomeric subunits, was added. Subsequent lowering of the pH (see Chapter 2) to 5 would then generate the 180 subunit T=3 capsid, filled with the polymer molecules. FPLC chromatograms showed the presence of vast amounts of polymer, see Figure 6.4. The following wavelengths were used for detection: 225 nm (strong absorption of both polymer and protein), 260 (predominantly absorption by protein), and 312 (absorption of the fluorescent dansyl group).

The UV-VIS absorption was so strong that it was initially thought that only polymer (peak at 1.8 ml) was present. It was expected that at least some capsid formation would have taken place. However, at the benchmark elution volume of 1.0 – 1.1 ml no absorption was detected, leading to the conclusion that no assembly had occurred at all, under the influence of the large amount of negative charges. This was surprising, since the natural RNA, which is also negatively charged, does promote assembly. These results led us to conclude that the assembly behavior is controlled in a even more subtle way in the natural virus (see Figure 6.6) than previously thought. Perhaps, the large concentration of polystyrene sufonate had changed the elution volume of the capsid itself.

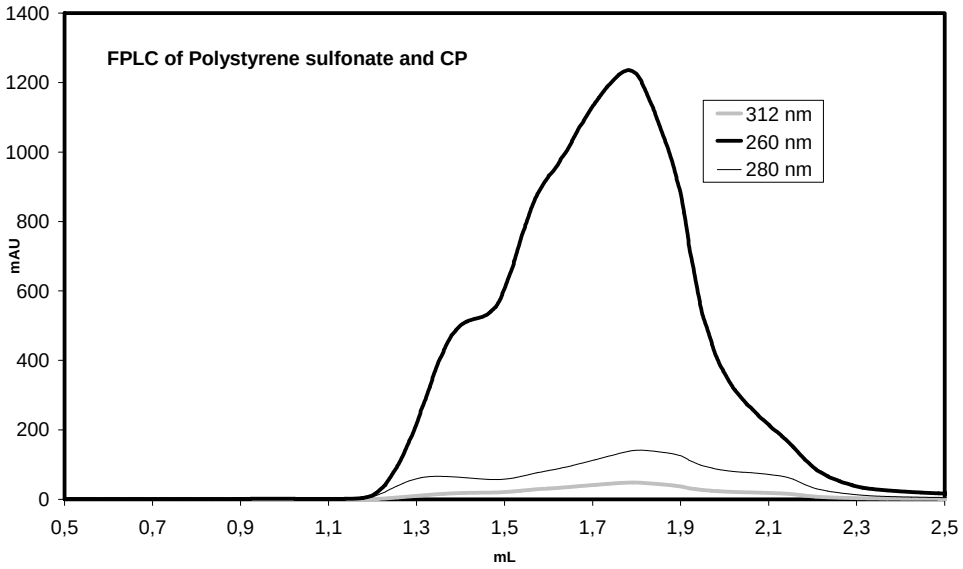

Figure 6.4. *Incubation of CCMV CP with a large excess of polystyrene sulfonate, followed by a lowering of pH to 5, measured at three wavelengths.*

Figure 6.5 shows the elution curves of different concentrations of polystyrenesulfonate. From these curves it can be concluded that the concentration of polymer in the sample does influence the elution volume.

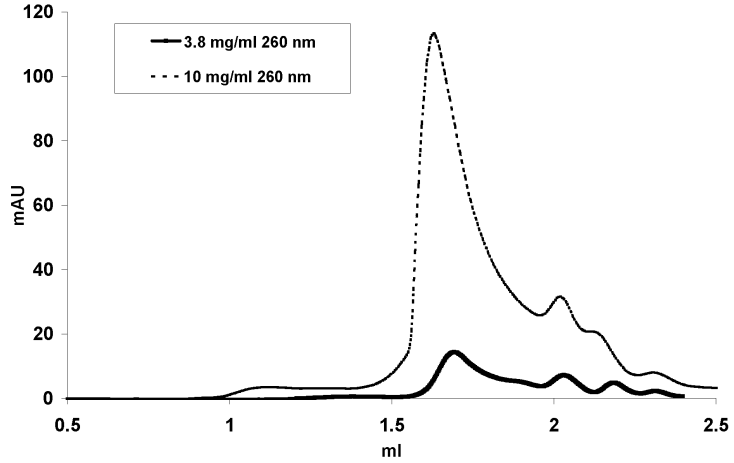

Figure 6.5. *FPLC chromatograms of different concentrations of polystyrene sulfonate.*

When Figures 6.4 and 6.5 are compared, it is clear that there are more peaks than expected for the CP and the PSS. They are probably caused by the presence of various complexes of PSS with CP, i.e. complexes that have different stoichiometric ratios. Since

the results from these experiments were inconclusive, it was decided to investigate the effect of different stoichiometric ratios of polystyrenesulfonate to CCMV CP in more detail. Figure 6.6 shows the FPLC chromatograms of CP, incubated with the different equivalents of fluorescent polystyrene sulfonate (calculated as the ratio of polymer repeat unit per monomeric protein subunit).

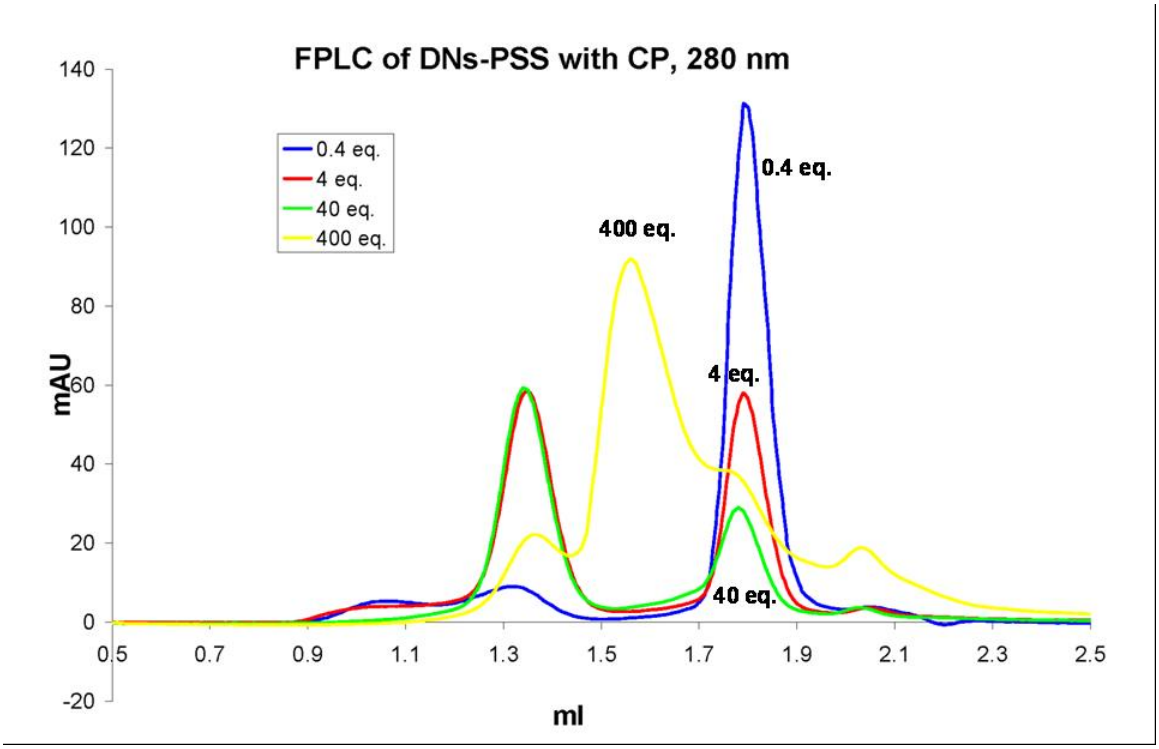

Figure 6.6. *FPLC traces of mixtures containing different ratios of DNs-PSS polymer and CP subunits. The resolution of the FPLC systems does not allow for discrimination between native and degraded CP (see below). Small ratios of DNs-PSS/CP (0.4 and 4) induce formation of two types of particles, with elution volumes of 1.0 ml and 1.35 ml, indicating the presence of T=3 and T=1 protein aggregates. At a ratio of 40 only T=1 particles and free CP are present. Higher ratios of DNs-PSS/CP (400) inhibit particle formation.*

These incubations were performed at pH 7.5, at which all protein is present in its free (dimeric) form. Only two peaks were expected in the FPLC chromatogram; one for the polymer and one for the free CP. Surprisingly, however, for **DNs-PSS**/CP = 0.4, the chromatogram showed the presence of the T=3 assembly (elution at 1.0 ml), and a new assembly, albeit not in high yields, eluting at 1.35 ml. Increasing the ratio of **DNs-PSS**/CP to 4 and then to 40 caused the peak at 1.0 ml to decrease and the one at 1.35 ml to increase. At the ratio of 40 only the assembly eluting at 1.3 ml and free dimeric CP were detected, implying that this ratio is close to the ideal value for formation of this particular assembly. No T=3 capsid formation was detected at all at this ratio. However,

since there was still some free protein left, the exact ratio of polymer to protein is probably somewhat higher. The assembly eluting at 1.35 must correspond to a smaller, T=1 particle (see above and Chapter 2). Increasing the ratio **DNs-PSS**/CP even more (400) yielded these particles as well, but the FPLC trace clearly showed a lower intensity of the 1.35 mL peak, and a large amount of material eluting at 1.6 ml (free DNs-PSS). When the FPLC chromatogram obtained at the ratio of 40 was magnified, very little absorption was observed at 1.6 ml. This implies that at least some, and maybe all of the polymer was incorporated into the new particle. The assembly time did not seem to be an important parameter, since chromatograms obtained from freshly prepared samples and chromatograms of several-day-old samples, did not show any significant difference. Also, the elution times were checked for different concentrations of polymer. These did not change with concentration, so that residual amounts of polymer should still be visible at ca. 1.6 ml. Subsequently, an analysis was made of the relative peak intensities. The peak intensities at a given elution volume, relative to total peak intensities, i.e. the sum of all protein and polymer peak intensities were calculated (Table 6.1). For the T=1 particle, as expected, the highest relative peak intensity was found at the ratio DNs-PSS/CP = 40.

Table 6.1. *Relative intensity of peaks in the FPLC chromatograms of mixtures of polystyrene sulfonate and CCMV coat protein.*

Ratio DNs-PSS/CP	Relative Peak Intensity[a]		
	T=3[b]	T=1[c]	CP[d]
0.4	4	6	90
4	3	48	48
40	0	68	32
400	0	37	63

a) Total intensity (%) based on the peak heights in the FPLC chromatograms detected at λ = 208 nm; b) eluting at v = 1.0 ml, c) eluting at v = 1.35 ml, d) eluting at v = 1.8 ml.

The presence of the fluorescent polymer was checked by comparing the FPLC curves at different wavelengths (Figure 6.7).

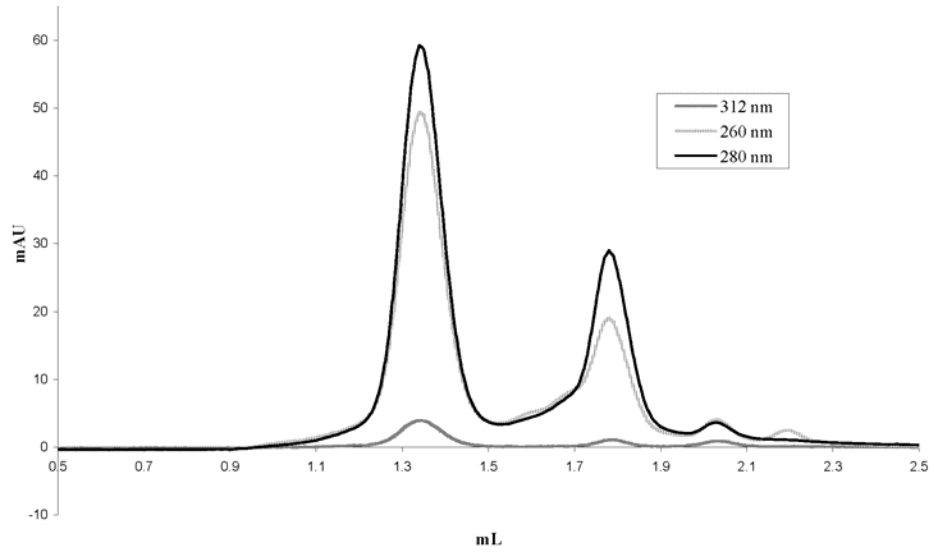

Figure 6.7. *FPLC of the T=1 nanoparticle formed at 40 equivalents of DNs-PSS to CP.*

It can be expected that the UV absorption characteristics of the peak at 1.35 ml differ from those of the peak at 1.8 ml if the polymer is included within the newly formed particle. Separate experiments showed that there is no significant difference between the UV spectra of assembled- and non-assembled coat protein subunits. The areas under the curves recorded at 260 nm (Figure 6.7, predominantly protein absorption) and at 312 nm (predominantly polymer absorption) were divided for each peak. For the peak at 1.35 mL a value of 13 was obtained and for the peak at 1.78 mL a value of 30, indicating a strong absorption increase in the 312 nm wavelength for the T=1 nanoparticle relative to free CP. This in turn indicates that polymer is included. The samples collected from the FPLC experiments were analysed by means of UV-VIS spectroscopy (Figure 6.8).

Figure 6.8 shows that neither the T=3 capsid nor the free protein dimers show significant absorption in the region between 225 and 230 nm, whereas the polymer does. Also, the T=1 nanoparticle shows a large absorption in this region, confirming the encapsulation of the polymer into the T=1 particle. Fractions of the FPLC experiment were subjected to Transmission Electron Microscopy. Figure 6.9 shows the resulting pictures.

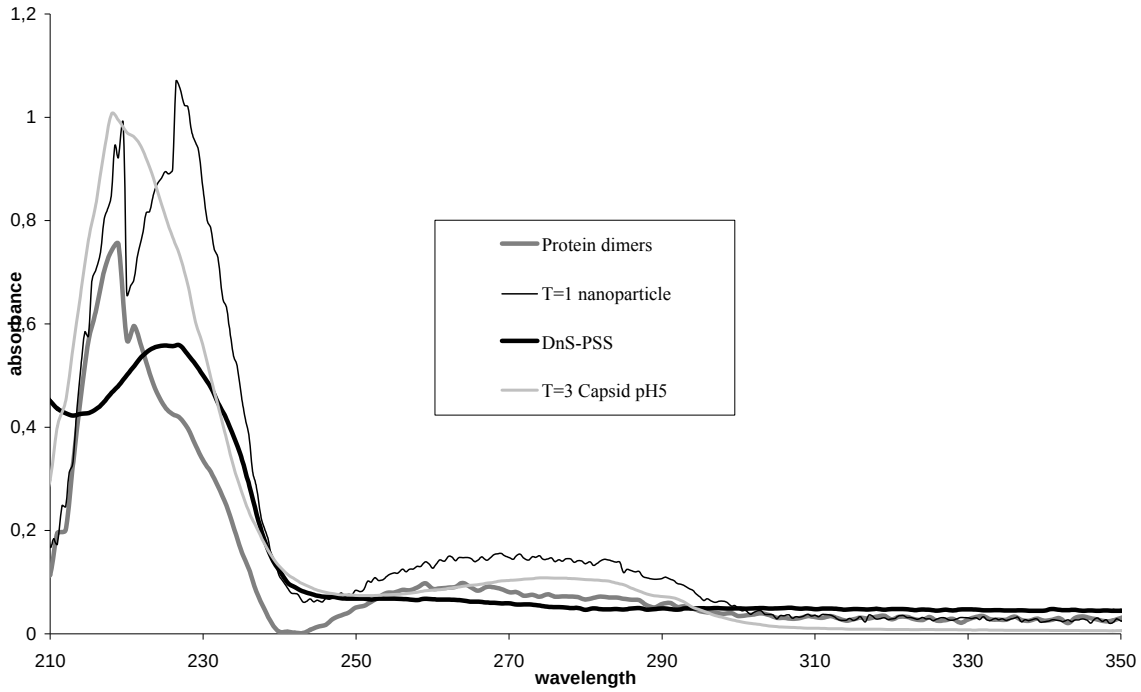

Figure 6.8. *UV spectra of various virus particles. Although the absorption of the dansyl group (ca. 320 nm) can not been seen at the applied concentrations (ca. 0.4 mg/ml polymer), the absorption of the main polymer chain is clearly visible at 225-230 nm.*

The negative staining does not appear to be present inside the protein shell, as the picture on the left shows. However, the right hand picture reveals some staining inside the particle. If the intensity of the staining is compared to that of the empty capsid, (Figure 6.2), the empty capsids show a much higher contrast.

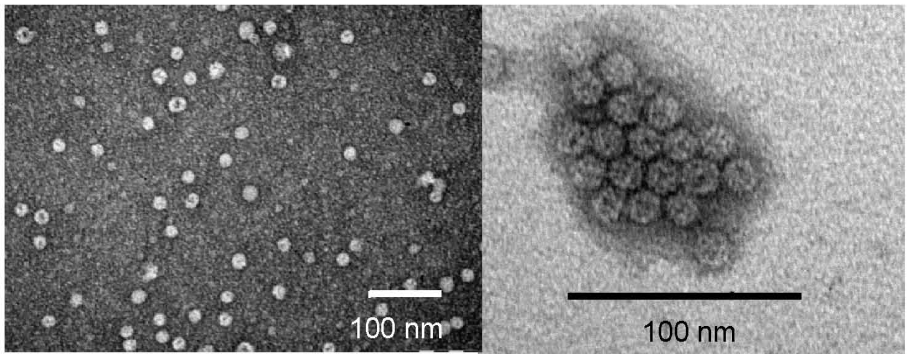

Figure 6.9. *Electron micrographs of the T=1 particles. Left: sample stained with uranyl acetate, showing no inclusion of this staining agent in the particle. Right: assembly of the T=1 particles in a hexagonal fashion.*

The absence of high staining intensity supports the idea that polymer is present within the capsid. Generally speaking, the presence of staining indicates the absence of other species.

The micrograph on the right shows well-defined, monodisperse particles of 16 nm size. The left image shows assemblies that are less well-defined. It is thought that TEM grid preparation (drop casting, drying, staining) is a determining factor for the morphology of the particles. Although the right micrograph shows assembly of viral particles in hexagonal patterns, this tendency was not observed widely on the grid. Most particles were present as separate entities on the grid, as can be seen on the left of Figure 6.9.

If the *individual* particles in the assembly on the right of figure 6.9 are closely studied, some of them look like they have a hexagonal character. When viewed in space-filling models (Figure 6.10, left bottom structure), the hexagonal structure appears, which therefore must be an artefact.

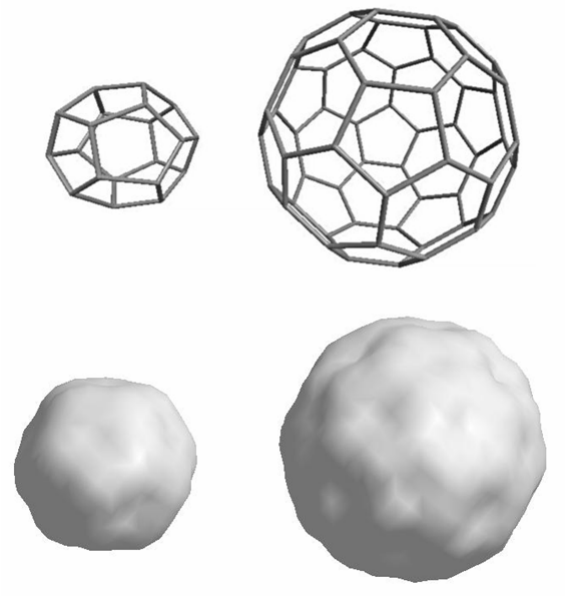

Figure 6.10. *Models of the T=1 particle (left) and the T=3 particle (right). In the space filled model (bottom left) the hexagonal appearance of the T=1 particle can be observed.*

Dynamic light scattering (DLS) measurements were carried out to determine the size of the T=1 particles (Figure 6.11). These experiments confirmed that the particles were smaller than a T=3 particle. A particle with a radius of 9.5 nm was calculated from the measurements, whereas the T=3 particle has a radius of 14 nm.

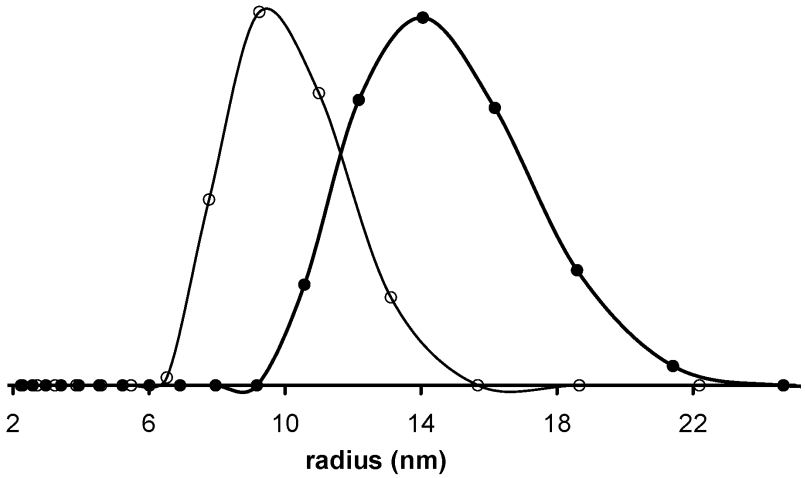

Figure 6.11. *Dynamic light scattering measurements. Hollow circles: T=1 particle. Filled circles: T=3 virus particles.*

The discrepancy between the radii, observed by TEM (8 nm for T=1) and DLS (9.5 nm for T=1) is likely caused by two factors. *(i*) DLS measures the *average* radius of the particle. However, due to the polyhedral nature of the particle, see Figure 6.10, this could lead to an error in the measurements. *(ii*) In DLS the hydrodynamic radius is determined, which could be larger than the radius observed in TEM because of the presence of a water shell. Since the radius, observed for the T=3 particle, is more in accordance with the TEM results, the latter reason is less likely, unless there is a difference in the water layers, surrounding the respective particles. In such a case, the discrepancy is expected to become smaller if the particle size increases.

In a subsequent series of experiments, we investigated the effect of the polymer length on particle formation. It is conceivable that the polymer length affects the aggregation behavior of the protein subunits. Thus, a CP preparation in pH 7.5 Tris buffer was incubated with the same quantities of polymer as described above; for all polymers, care was taken to maintain the same stiochiometry of negative charges per protein subunit as mentioned above. The FPLC results are presented in Figure 6.12.

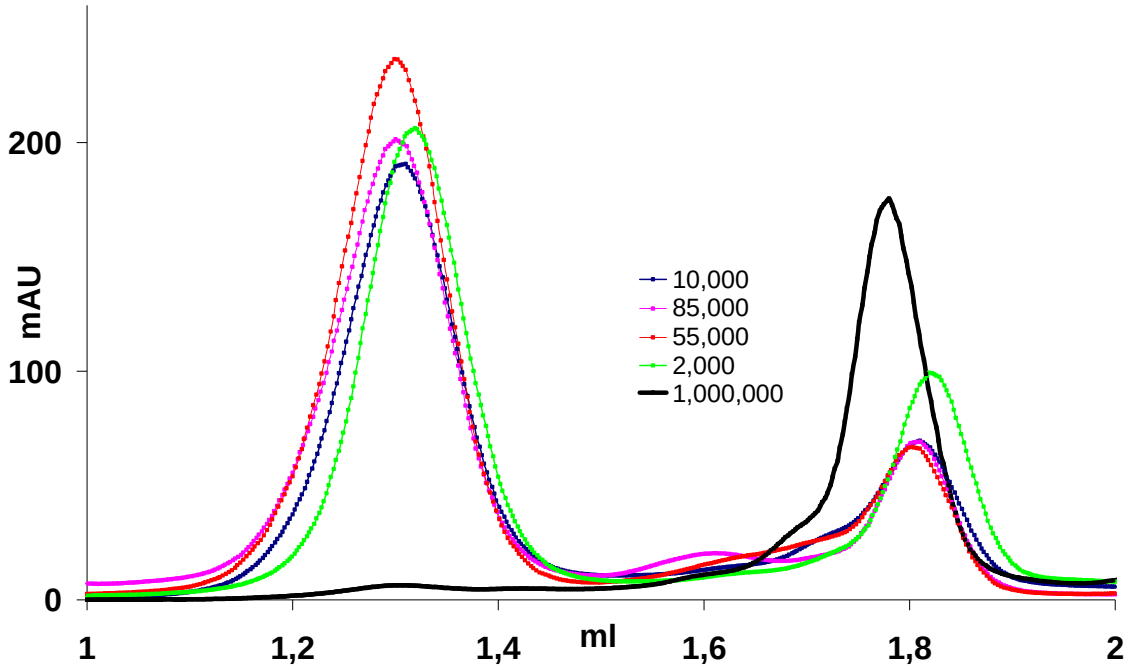

Figure 6.12. *FPLC chromatograms of CP with polystyrene sulfonate polymers of different molecular weight at pH 7.5.*

Figure 6.12 shows that all polystyrene sulfonate polymers give rise to identical particles except one. When PSS of MW 1,000,000 was used for the experiments, no or very little T=1 particles were obtained. Polystyrene sulfonate of this molecular weight possesses ca. 5,000 negative charges (one per repeating unit) whereas the natural RNA has ca. 3,000 negatively charged bases. Hence, the incapability to induce self-assembly around the polymer is probably not due to the large number of negative charges but caused by steric reasons; the polymer simply does not fit inside the capsid. It is possible that the very small amount of T=1 particles in the sample of 1,000,000 MW, arises from the selective encapsulation of the fraction of smaller molecular weight polymers in the polydisperse polymer mixture. A very interesting future experiment would be to incubate the CP with a mixture of PSS of 1,000,000 molecular weight, and another PSS of lower molecular weight. This would presumably result in the selective encapsulation of the smaller polymer species.

The concentration of the polymer inside the T=1 particle was calculated, making the following assumptions: (*i*) The thickness of the protein shell is equal to that of the T=3 particle, and (*ii*) all polymer is encapsulated within the particle. The inner diameter

of the T=1 particle is 11 nm, leading to a volume of 1150 nm^3, which is equal to 1150 • 10^{-24} l. If the presence of 40 equivalents of negative charges per monomeric capsid protein in the T=1 particle is assumed (See Figure 6.6), then 40 • 60 (number of subunits in T=1 particle) = 2400 charges, equal to 2400/6.02 • 10^{23} mol, are present. This amounts to a concentration of ca. 3 M, which is considerably higher than the polymer concentration in solution, implying a strong affinity of the polymer for the capsid protein. Similar calculations carried out for RNA in the T=3 capsid yielded a concentration of only 0.7 M inside the T=3 capsid. These (crude) calculations show that the RNA is, on average, less heavily packed than the polystyrene sulfonate polymer, unless the T=3 particle possesses a RNA-free water pool in the middle of the particle. Preliminary neutron scattering data seems to confirm this hypothesis.[12]

The FPLC fractions containing the DNs-PSS/CP aggregate (pH 7.5) were reinjected on the FPLC column and dialysed to pH 5.0, to see what the influence of pH was on particle formation. Both at pH 7.5 and at pH 5.0 the same particles were detected, and no free CP was observed, implying a high particle stability. This stability was confirmed by the fact that storage at 4^{o}C had no significant effect on the aggregates, as checked by FPLC.

Johnson *et. al.* have reported that the formation of the T=1 particle is rather unlikely, when native CP is used.[13] It is known, that fast adjustment of the pH of a CP solution to 5, at certain salt concentrations yields a mixture of T = 1, 2 and 3 particles. The presence or absence of an N-terminal non-crystalline 34 amino acid segment is believed to be the origin of this behavior. Since the N-terminus of the protein subunits is located on the inside of the virus, the presence of the highly charged segment in that position is thought to favour T=3 formation. The greater folding required to create a pentameric protein aggregate cannot be achieved in this way. Sodium Dodecyl Sulfate – Polyacrylamide Gel Electroforesis (SDS-PAGE) analysis of our T=1 particle with the encapsulated polymer revealed that degraded protein was present (Figure 6.13).

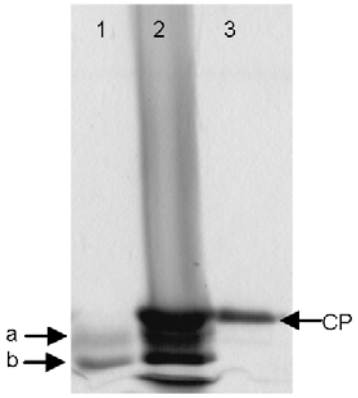

Figure 6.13. *SDS PAGE analysis of the isolated sample of T=1 particle (lane 1), the crude coat protein, as found after some weeks in storage (lane two) and the freshly purified CCMV (lane three). The protein used for the assembly studies had similar degradation patterns as the protein seen in lane one, i.e. degradation had proceeded to some extent. The small molecular weight band at the bottom of lane two may represent the degradation products.*

The degraded products are probably protein subunits missing the first 25 amino acid residues from the N-terminus (NΔ25, arrow *a* in the first lane), and a further degradation product, NΔ41-44, arrow *b*.[13] All three proteins, including the non-degraded species, are observed in the crude CP preparation (lane 2). It is likely that the additional lowest band (corresponding to the smallest molecular weight) in lane 2 is caused by the small oligopeptides that result from the degradation process. This raises the following questions: (*i*) does the T=1 particle still form when all protein is degraded to the NΔ41-44 species and (*ii*) is the formation of the T=1 particle still possible, when the protein is in its natural, non-degraded form? The latter, if true, would be contradictory to the results obtained by Johnson *et. al.* To test this, freshly isolated coat protein was incubated with similar amounts of PSS, after which FPLC and gel electrophoresis were performed. The FPLC chromatograms revealed the same T=1 particle (not shown). Figure 6.14 shows the gel electrophoresis (SDS-PAGE) results. It is clear that some degradation has taken place, but this experiment proves that formation of the T=1 particle is also possible in the presence of non-degraded protein.

The non-degraded protein subunits, present alongside the degraded species, can perhaps adopt a higher folding geometry, possibly because there is ample space to do this, if part of surrounding protein subunits is degraded.

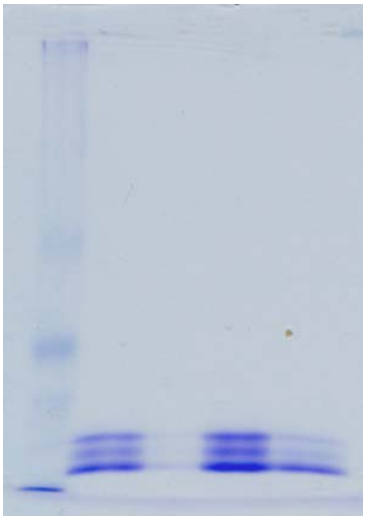

Figure 6.14. *SDS-PAGE gel of the T=1 particle, prepared from freshly isolated CP. Different concentrations of protein are applied at each lane of the gel. Marker (left) moleculair weights not shown, since only the ratio between the spots is relevant for our study.*

The 34 non-crystalline peptide segment is associated with RNA binding since it is rich in arginine and lysine residues. Degradation was found to occur spontaneously; performing the extraction of the virus under as clean as possible conditions (but not sterile) did not prevent the degradation of the N terminus. This has led Johnson et al. to propose that a protease enzyme, responsible for degradation, is co-isolated with the virus.[11] In this connection it should be mentioned that it was observed that the degradation of the protein present in the capsid seems to proceed much faster than that of the protein present in the natural virus. This, in turn, might suggest that the capsid is in equilibrium with the free dimeric subunits, a theory that is confirmed by the fact that in FPLC chromatograms of the capsid at pH 5.0, always some dimeric protein is detected.

Subsequently, in several experiments, it was tried to separate the non-degraded protein from the degraded species in the non-assembled protein preparation. Initially, ion exchange chromatography was attempted using a "super S" negatively charged column. As is mentioned above, the N-terminal peptide sequence contains quite a few lysines and arginines, so a net charge difference is expected. In order to be certain that both degraded and non-degraded proteins species can be detected, a mixture of roughly 1:1 degraded protein and protein from a fresh batch of CP was prepared. Since ion exchange chromatography requires salt-free conditions for the protein, the protein mixture was first dialysed to pH 7.5 with no addition of any NaCl. This procedure, however, caused

precipitation of the protein, as was concluded from visual inspection and from that fact that centrifugation of the mixture and subsequent SDS-PAGE analysis of the supernatant Figure 6.15, lanes 3) failed to show the presence of protein in solution.

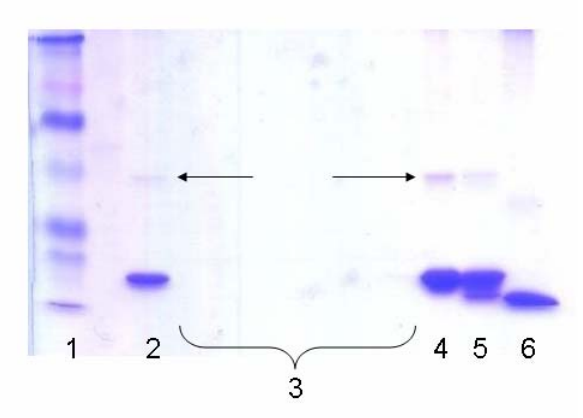

Figure 6.15. *SDS PAGE analysis of CP, dialysed to zero salt concentration. Lane 1: Marker. Lanes 2 and 4: freshly isolated CP in different concetrations. Lane 3: different samples of the supernatant of the CP dialysed to zero salt concentration. Lane 5: mixture of degraded and freshly isolated CP. Lane 6: degraded CP. Arrows: Dimeric protein subunits, as normally found to be stable in solution.*

Subsequently, size exclusion chromatography to separate the two protein subunits was attempted, using a Superdex 75 column. Figure 6.16 shows the chromatograms, obtained from the separation.

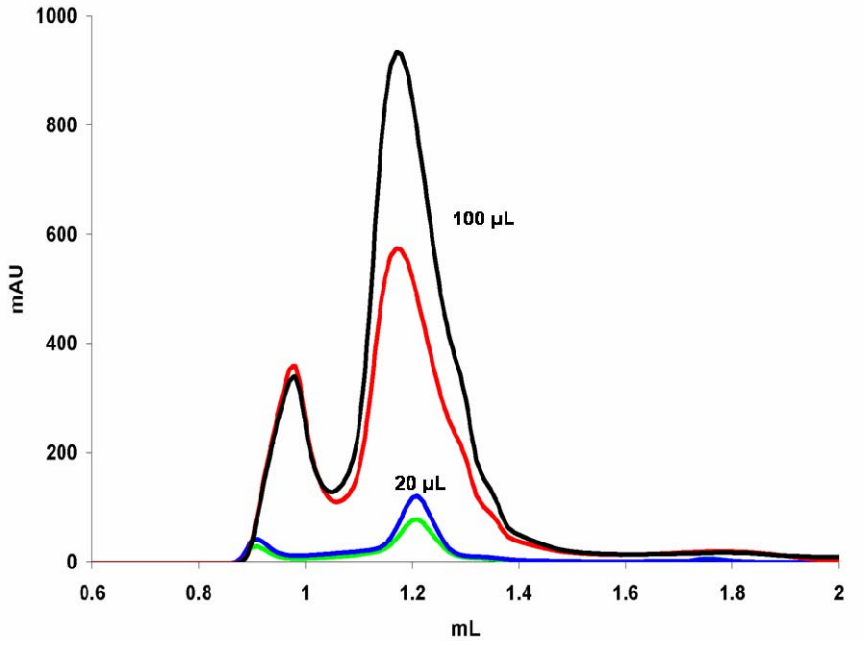

Figure 6.16. *Attempted separation of degraded and non-degraded protein, using a Superdex 75 column.*

Despite the fact that degraded and non-degraded protein do not differ much in molecular weight, a remarkable separation was obtained. Two peaks appeared at 0.9 and at 1.2 ml. Unfortunately, SDS-PAGE analysis of these samples (not shown) revealed the presence of equal amounts of degraded and non-degraded protein in the larger peak at 1.2 ml. When the separation was repeated with a higher sample volume (100 instead of 20 μL), a similar separation was observed, again with degraded and non-degraded CP co-eluting in the peak of 1.2 ml. We believe that the peak at 0.9 ml represents an aggregate, possibly the T=3 capsid, eluting at the separation treshold of the column.

No further attemps were made to separate the degraded and non-degraded products, since in parallel experiments the bacterial synthesis of the CP had proven to be successful (Hendriks from our group, unpublished results). This procedure yields undegraded protein, which is not prone to further degradation, because the protease, responsible for the degradation of the protein isolated from the natural virus, is not present. Preliminary experiments, in which these proteins were incubated with polystyrene sulfonate, revealed the formation of the T=1 particle, but more evidence is required. As a separate observation, it is noted from Figure 6.15 that some of the CP dimer can still be observed in the SDS PAGE gel, which is surprising considering the standard procedure for sample preparation for this technique, which includes boiling the sample in water for about ten minutes in the presence of B-mercaptoethanol and SDS, both strongly denaturing agents. The implication of this fact is that the binding between two subunits is exceedingly strong.

6.3 Conclusions

In this chapter, it is shown that the presence of a negatively charged polymer can induce the self-assembly of CCMV CP even at high pH, yielding a mixture of T=3 and T=1 particles, when very small amounts of polymer are used. When the amount of anionic polymer is increased, the yield of the T=1 particles also increases, the optimum being at 40 equivalents of negative charge per monomeric protein subunit. It is likely that the large curvature needed for the formation of T=1 particles can only be achieved if sufficient ionic interactions are possible with the polymer, which implies a high

concentration of the latter species. At very high polymer concentration, the yield of T=1 particles decreases, and a large peak can be observed, originating from the elution of the polymer itself. The formation of the T=1 particle is independent of the molecular weight, except when the molecular weight is very high: the anionic polymer with 1 MDa molecular weight failed to initiate the self-assembly of the capsid protein. A high molecular weight polymer may cause to much steric hindrance, or the "local" ionic concentration becomes too high, leading to ionic repulsion between two sections in the same polymer chain. The results described in this chapter were published.[14]

Further analyses of the polymer-protein hybrid particles by TEM and DLS showed that they were stable for weeks at 4 ^{o}C. SDS-PAGE analysis of the polymer-protein hybrid particles showed that the capsid protein molecules had partly degraded. Efforts to separate the degraded from the non-degraded proteins were unsuccessful. Further experiments are needed to firmly show that the non-degraded protein forms T=1 particles and to check whether the protein assembly is specific for a low molecular weight anionic polymer, when this polymer is mixed with a high molecular weight one.

6.4 Experimental section

6.4.1 General experimental procedures

All organic solvents were of analytical quality or distilled before use. Buffers were prepared from milliQ grade water with chemicals of analytical or better quality. FPLC(SEC) was performed using a Superose 6 analytical column (Amersham biosciences) on a Amersham Ettan system, fitted with a fractionating device, unless indicated otherwise. Buffers for FPLC were filtered with a Millipore 0.2 μm filter before use. UV-VIS spectra were measured on a Shimadzu UV-300 instrument. TEM grids (Formvar-Carbon) were exposed to an electron discharge treatment, after which 1 μL of sample was put on the grids. After about 1 min. the sample was carefully dried using filter paper. Subsequently, 1 μL of ammonium molybdate (5% w/v) was added and the drying procedure was repeated. SDS-PAGE (10-12 %) was performed using standard Biorad miniprotean equipment and chemicals. Dialysis tubing was obtained from

Spectra/Por and had 12-14 kDa cut-off. Dynamic Light scattering was performed using a Spectra Physics 2000 Argon Ion laser, with λ= 514.5 nm at 200 mW power setting.[15] Data analysis was carried out using the Stokes-Einstein relation in the CONTIN software. Fluorescent polystyrene sulfonate (DNs-PSS) was synthesized according to procedures described in Chapter 4, or obtained from Aldrich and used without further purification

The procedures for the isolation and purification of the CCMV have been described in literature.[16] A detailed description will be given below

6.4.2 Growth of plants and infection

Seeds from the Cowpea plant (*Vigna unguiculata L.,* also known as the black-eyed-pea, US forestry service) were planted to a density of ca. 4 seeds per 100 cm^2 , buried gently at about 1 cm deep in fresh pot soil. A batch of 60 plants will yield between 6 and 10 ml of pure virus solution. The seeds were watered once every two to three days, allowing the soil to be dry to the eye. At ca. 1.5 meters above the plants, 2 standard 600 W growing lights were installed and programmed using a timer to deliver light 16 hours per day. This procedure will yield sprouts in 3 to 4 days. The plants were allowed to mature for 10 to 13 days after seeding, after which they were infected with the CCMV. The primary leaves should at least have grown to a reasonable size (5 cm), before infection can take place. Fresh CCMV (100 μL, 10mg/ml) was ground with two or three fresh plant leaves, using a mortar, a pestle and 1-2 ml of 0.01 M NaH_2PO_4 and 0.01 M $MgCl_2$, pH 6.0 buffer. The leaves were dusted with carborundum (SiC) and, using a finger, the virus solution was rubbed over this surface, infecting every leaf. If leaf damage is too extensive, gentler rubbing should be done with new batches. Less than 5% damaged (completely yellow) leaves should be obtained. After several days the plants showed small yellow spots, which were not very well visible, i.e. from some distance the leaves still looked healthy.

6.4.3 Isolation of CCMV

The plants were harvested after one week and homogenized vigorously for several minutes in an industrial blender, adding ice-cold homogenization buffer (0.2 M sodium acetate, 0.01 M ascorbic acid, 0.01 M disodium EDTA, pH 4.8) to a ratio of about 1 ml buffer per 1 gram of material (note that the total leaf yield needs to be weighed). The homogenate was then squeezed firmly through a double layer of cheese cloth and left for 1 hr. The homogenate was spun for 10 min at 10,000 rpm in Sorvall GSA rotor. To the supernatant 10 % (w/v) polyethylene glycol (PEG, Mw = 6,000) was added while stirring, and the solution was left for 1 h. at 4^{o}C. The mixture was then centrifuged for 15 min at 10,000 rpm in a Sorvall GSA rotor and the supernatant was discarded. The pellet was dissolved in 0.1 M sodium acetate, 1 mM disodium EDTA and 1 mM NaN_3 buffer of pH 5.0 (virus buffer, "**VB**"). At least 5 % of the original homogenization volume was used to redissolve the pellet. Subsequently, the solution was spun for 10 min at 10,000 rpm in Sorvall SS34 rotor and the pellet was discarded. The supernatant was mixed with cesium chloride to obtain a 38.5 % (w/w) solution in VB, and a cesium chloride gradient centrifugation was performed. This solution was centrifuged for at least 16 h at 40,000 rpm in a Beckman VTi65 rotor at 10^{o}C. The tubes were then cut open and the slightly whitish, turbid virus band was collected and dialyzed (3x) against **VB** to remove the CsCl. The UV absorbance at 260 and 280 nm was measured and the ratio A260/A280 was calculated. This value should be between 1.6 – 1.7.

6.4.4 Isolation of coat protein

A virus suspension (~10 mg/ml) was dialysed against an aqueous solution containing 0.5 M $CaCl_2$, 0.05 M Tris-HCl, 0.001 M dithiothreitol (DTT, Cleland's reagent) buffered at pH 7.5, for at least 2 h. at 4^{o}C, but overnight is more practical. Subsequently, the turbid mixture was spun down during 2 hrs. at 40,000 rpm in a Beckman R50Ti rotor at 10^{o}C. The resulting RNA-Ca^{2+} pellet was clear and slightly yellow. The resulting supernatant was dialysed against an aqueous solution containing 50

mM Tris-HCl, 300 mM NaCl, and 1mM DTT at pH 7.5 (capsid buffer, **CB)** for at least 2 changes at 4^{o}C.

6.4.5 Incubation experiments

First, to 0.5 mg CCMV CP in capsid buffer, **CB** (5 mg/ml) a relatively large quantity of polyanion (0.2 mg) was added. Since this procedure did not yield clear results, the protocol was modified in the following way: 0.2 ml of CP in 50 mM aqueous Tris-HCl, 500 mM NaCl, and 1mM DTT at pH 7.5 was incubated with the appropriate solution of DNs-PSS (0.4-400 eq.) which was obtained by dilution of a stock solution. The concentration of the polymer solution was kept such that the dilution of the CP slution was below 10%. The synthesis of DnS-PSS has been described in Chapter 3.

6.5 Notes & references

[1] Y.G. Choi, T.W. Dreher and A.L.N. Rao, *PNAS* **2002**, *99*, 55.

[2] P. Annamalai and A.L.N. Rao, *Virology* **2005**, *332*, 650.

[3] S.C. Harrison in *Fields Virology, eds.B.N. Fields, P.M. Howley, D.E. Griffin, R.A. Lamb, M.A. Martin,B. Roizman, S.E. Straus and D.M.Knipe(Raven, New York)***1990**, *Vol. 2*, 37.

[4] a) D.L.D. Caspar and A. Klug, *Cold spring Harbor Symp. Quant. Biol.* **1962**, *27*, 1; b) J.E. Johnson and J.A. Speir, *J. Mol. Biol.* **1997**, *269*, 665; c) A. Zlotnick, *PNAS* **2004**, *101*, 15549.

[5] The T=2 structure, while not obeying the Caspar-Klug symmetry rules, has been observed in nature, but is not very stable.

[6] R. Zandi, D. Reguera, R.F. Bruinsma, W.M. Gelbart and J. Rudnick, *PNAS* **2004**,*101,* 15556.

[7] A. Iorio and S. Sen, *Science* **2007**,
http://arxiv.org/PS_cache/arxiv/pdf/0707/0707.3690v1.pdf

[8] W. K. Kegel and P. van der Schoot, *Biophysical Journal* **2004**, *86,* 3905.

[9] J. B. Bancroft, E. Hiebert and C.E. Bracker, *Virology,* **1969**, 39, 924. See also Chapter 1.

[10] S. Mukherjee, C.M. Pfeifer, J.M. Johnson, J. Liu and A. Zlotnick, *J. Am. Chem. Soc.* **2006**, *128*, 2538.

[11] D.V. Klinov, N.B. Matsko, A.A. Manykin and V.V. Demin, *Vopr Virusol* **2002.**

[12] Small Angle Neutron Scattering measurements, unpublished results.

[13] J. Tang, J.M. Johnson, K.A Dryden, M.J. Young, A. Zlotnick and J.E. Johnson, *J. Struc. Biol.* **2006**, 154, and references cited.

[14] F.D. Sikkema, M. Comellas-Aragonès, R.G. Fokkink, B.J. Verduin, J.J.L.M. Cornelissen and R.J.Nolte, *Org Biomol Chem*. **2007**, *5*, 54.

[15] R. Fokkink of the Wageningen Agricultural unversity is kindly acknowledged for the DLS measurements.

[16] a) B.J.M. Verduin, *FEBS Lett.* **1974**, *45*, 50; b) J.R.O. Dawson, F. Motoyoshi, J.W. Watts, J.B. Bancroft, *J. Gen. Virol.* **1975,** *29*, 99.

Chapter 7

Interactions of polystyrene sulfonate architectures with the CP of CCMV

7.1 Introduction

One of the goals of the research described in this thesis is the creation of a mega amphiphile through the complexation of the charged part of an amphiphilic polymer within the charged inside of the CCMV capsid. In order to be able to realize this, the assembly mechanisms of the coat protein around the charged polymer and the dependence of this assembly process on the structure of the polymer need to be understood in detail.

In Chapter 6 of this thesis, it was shown that there is a unique interaction of the polystyrene sulfonate polymer with the coat protein of CCMV. Although different molecular weight polymers (MW 2,000 – 85,000 Da) were used, the coat protein always assembled into a 60-dimer T=1 architecture, which is about 3/5 the size of the naturally occurring 90-dimer T=3 icosahedral virus. However, when the polymer had a molecular weight of 1,000,000 Da, no assembly was observed. It was decided to investigate in more

detail the effect of the structure of the polymer on the assembly behavior of CP. The results of these investigations are described in this chapter.

7.2 Results and discussion

In Chapter 5, the synthesis of several polystyrene sulfonate architectures was described. Two of these possessed a star-like architecture, which was achieved by using a porphyrin as a multifunctional ATRP initiator. The structures of these block copolymers are depicted in Figure 7.1.

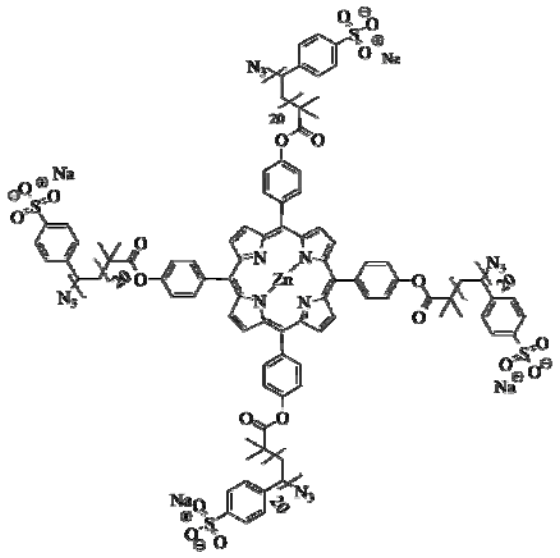

1

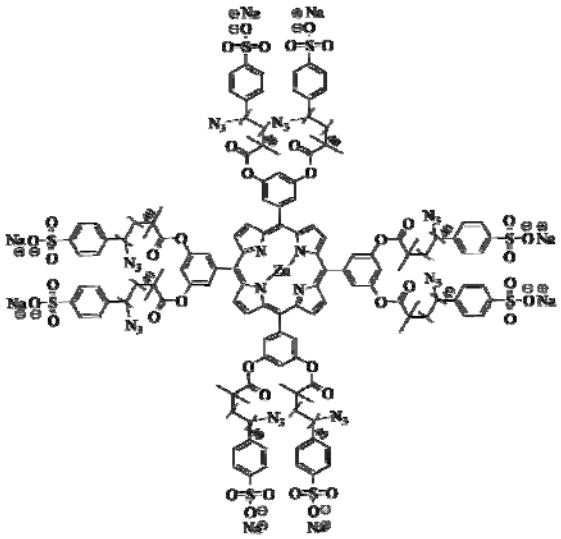

2

Figure 7.1. *The structures of polymers prepared with a symmetrically, 4- and 8- fold functionalized porphyrin initiator. Compound **1** possessed a high polydispersity. The structure of **2** could not be elucidated; see Chapter 5.*

The porphyrin with four polystyrene sulfonate polymers (Figure 7.1, compound **1**) was incubated with CCMV CP in similar quantities as in the experiments described in Chapter 6: to the buffered solution of the CP, 50 equiv. of polymer (defined as the number of polymer repeat units per monomeric coat protein molecule) was added from a concentrated stock solution and the mixture was analyzed by FPLC (Figure 7.2).

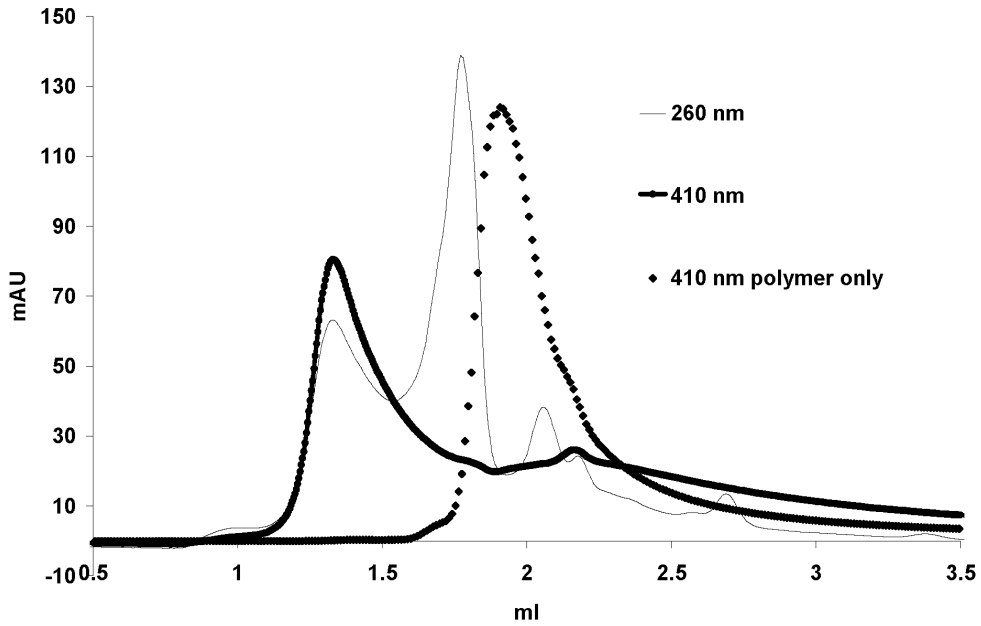

Figure 7.2. *FPLC chromatograms of the reaction mixture obtained after incubation of star-shaped polystyrene sulfonate (**1**) with CCMV CP. The thin grey line represents the elution of the reaction mixture, measured at 260 nm (predominantly protein absorption), and the solid line is the mixture recorded at 410 nm. The dotted curve shows the elution profile of the polymer itself.*

Figure 7.2 reveals that T=1 particles are formed, and the absorption of the porphyrin initiator group in the assembly is clearly observed; the solid trace was recorded at the maximum absorption of the porphyrin moiety (410 nm). This result suggests that the polymer is encapsulated within the protein cage. The dotted curve represents the elution of the polymer alone, which shows a monomodal distribution and a high absorption at 410 nm for the porphyrin moiety.

SDS PAGE experiments performed on the fractions corresponding to the peak at 1.3 ml showed the presence of protein in the aggregate (not shown; see Figure 6.14 for representative traces). The fraction corresponding to the peak at 1.35 ml was isolated and analyzed by UV-Vis spectroscopy, which revealed that the particles had a distinct peak at 420 nm, implying the presence of the porphyrin.

Since it would be interesting to compare these data with those, in which a linear polystyrene sulfonate polymer is encapsulated in the capsid (Chapter 6), calculations on the amount of polymer inside the protein shell were made. However, the accuracy of these calculations was hampered by several factors: *(i*) the exact concentration of the protein preparate was unknown, since there is still a substantial amount of subunit left

(peak at 1.8 ml in the FPLC chromatogram); *(ii*) the molecular weight of the polymer is unknown (see Chapter 5). However, assuming a 50% efficiency in the encapsulation experiments (so that 50% of all the protein is left) and that all polymer is encapsulated, it can be calculated that ca. 300 monomer units are encapsulated within the capsid. If each porphyrin initiator structure (see Chapter 5) is assumed to carry 30 monomer units, then between two and three star-polymer structures are present in each T=1 assembly.

The 8-fold substituted porphyrin-polymer **2** was not studied in the assembly with CP, since its structure could not be sufficiently established.

Further incubation experiments were carried out with polymer **3,** the synthesis of which is also described in Chapter 4.

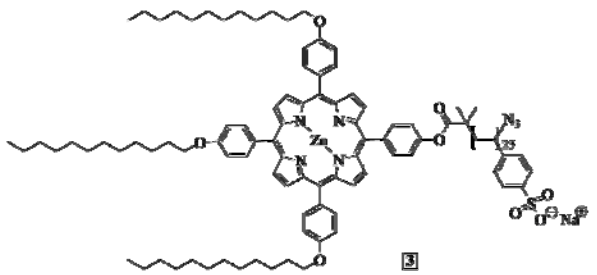

Figure 7.3 *Structure of the amphiphilic polystyrene sulfonate **3** used in the incubation experiments with CCMV coat protein.*

Dissolution of this polymer in water and incubation of the resulting solution with the CCMV CP yielded a precipitate. The color of this precipitate was light purple, suggesting that the protein had co-precipitated with the polymer.

It was then decided to check whether the experiment could be carried out in the presence of an organic solvent. To this end, the sensitivity of the coat protein to THF was tested. Buffer solutions were prepared that contained various amounts of THF (10, 15, 20, and 25% by volume), and samples of the CP were dialyzed against these buffers. In all cases, a precipitate was observed. All samples were centrifuged and the supernatant was analyzed using SDS-PAGE (Figure 7.4).

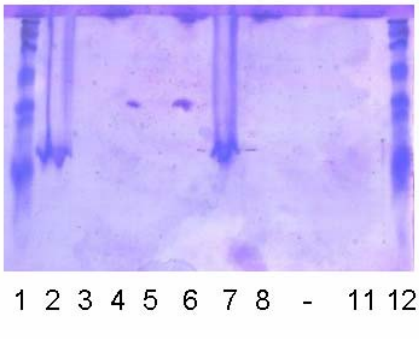

Figure 7.4. *SDS-PAGE analysis of CCMV CP incubated with varying amounts of THF. Lane 1 and 12: markers. Lane 2 and 7: CCMV CP (reference). Lanes 3 - 6 and 8-11: CP dialyzed to buffers containing increased concentrations of THF. Lane 3 corresponds to 10 % THF and this amount increases, up to lane 6 which corresponds to 25% THF. Lanes 8-11 are duplo experiments of this series.*

Although the eletrophoresis gel appears somewhat distorted, from Figure 7.4, lanes 3 through 6, it may be concluded that there is no protein spot present at the same location as in lanes 2 and 7, revealing that all protein has been precipitated. Although the traces and spots in lanes 2 and 7 are distorted due to unknown causes, the presence of CP is unambiguous. However, not even the slightest hint of protein can be found in lanes 3 - 6 and 8 – 11. The spots seen at lanes 5 and 6 are artefacts, probably due to a pollution. The conclusion is that even a low concentration of THF is sufficient to *quantitatively* precipitate the CCMV CP. It is conceivable, that smaller amounts (perhaps 2 - 5%) of THF do not have such a detrimental effect on the solubility of the protein, but this was not investigated further. The solubility of organic amphiphilic block copolymers in water is very low; solubilization, therefore, always requires an organic cosolvent, which, as the experiments above show, is not compatible with the CP. The experiments with polymer **3** were therefore discontinued.

In Chapter 5, the synthesis of a block copolymer (DnS-PSS-BSA), derived from polystyrene sulfonate and bovine serum albumin was described. This was achieved by selective coupling of the polymer, functionalized with an azide, to an acetylene moiety, present on the protein. We were interested to see whether this biohybrid block copolymer would promote the same self-assembly behavior of the CP as homopolymers and polymer **1** (see above) did. To this end the CCMV CP was incubated with a buffered solution of DnS-PSS-BSA[1] and analyzed with FPLC. The Dns-PSS-BSA was dissolved in a concentrated stock solution and samples from this solution corresponding to 20, 60 and

100 equivalents of negative charges per monomeric protein subunit were added to the CCMV CP. In all experiments, a precipitate was formed. The vials were shortly centrifuged and analyzed by FPLC. Figure 7.5 shows the resulting curves.

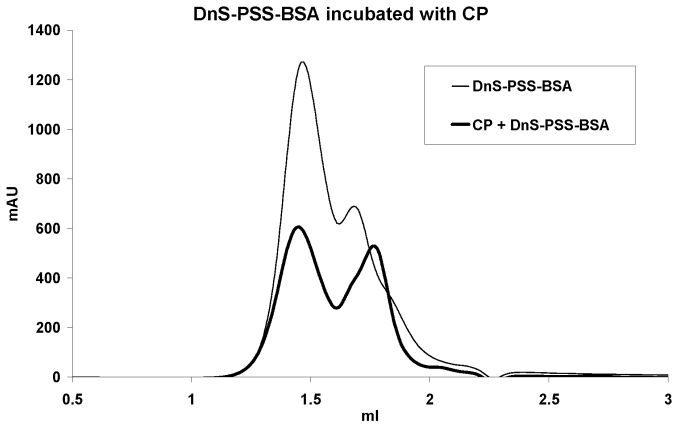

Figure 7.5. *Incubation of CCMV CP with DnS-PSS-BSA with the objective to provoke self assembly.*

The curve for the incubation of the CCMV CP with the polymer/protein (60 equiv., curve is representative for the other experiments) possesses similarities to that of the protein/polymer alone, although a shift can be observed for the peak eluting at 1.7 ml. No larger aggregate (at about 1.35 ml) can be observed, and no significant quantities of coat protein were left in the mixture, as observed by SDS-PAGE. The precipitation of the coat protein is apparently already initiated by the weak hydrophobicity of the BSA.

7.3 Conclusions

In this Chapter efforts are described to generate some form of assembly from CCMV CP and different types of PSS copolymers. It was found that the reduced solubility of the CP- PSS copolymer complexes very severely limits their purification and characterization. Experiments were carried out with small amounts of THF present to increase the solubility of the block copolymers in water already led to precipitates, as did the presence of the slightly hydrophobic protein BSA, which was covalently connected to a polystyrene sulfonate moiety.

It must be concluded from these studies that the future preparation of a mega amphiphile composed of a virus headgroup and a polystyrene sulfonate tail is not possible in this way.

7.4 Experimental section

All buffers were prepared as described in Chapter 6. Analytical characterization techniques were performed as described in the same chapter.

7.4.1 Incubation of CCMV CP with copolymers 1 and 2

To an Eppendorf vial containing 90 µl of coat protein (6 mg/ml), 60 equiv. (styrene-sulfonate monomeric unit to monomeric CP protein subunit) of the desired block copolymer was added. The resulting mixture was analyzed with FPLC. See Chapter 6 for more details on the assembly process and the analysis of the formed T=1 particle.

7.4.2 Incubation of CCMV CP with various amounts of THF

Tris buffers (pH 7.5, 0.5 M NaCl, for other components see Chapter 5) were prepared with varying amounts (10, 15, 20, 25, % v/v) of added THF. A small sample of CCMV CP (200µL, ~5 mg/ml) was transferred into a mini-dialysis Eppendorf vial (molecular weight cutoff = 6-8000) and dialyzed overnight. The Eppendorfs were centrifuged and the supernatant was subjected to SDS-PAGE. All vials showed precipitation before centrifugation. SDS-PAGE analysis was carried out with different concentrations of supernatant. No protein could be detected in this way.

7.4.3 Incubation of CCMV CP with DnS-PSS-BSA polymer/protein biohybrid

To three different samples of CCMV CP at pH 7.5, (90 µl, 4 mg/ml), 25, 75 and 125 µl of a solution containing DnS-PSS-BSA adduct was added. The polymerization degree of the polystyrene sulfonate in the biohybrid block copolymer was 80, and the

concentration of the biohybrid compound was such, that 20, 60 and 100 equiv. of negative charges per monomeric capsid protein subunit were added.

7.5 Notes and references

[1] Dansyl functionalized polystyrene sulfonate – bovine serum albumin adduct. See Chapter 5.

Chapter 8

Polymerization within the CCMV protein cage

8.1 Introduction

Chemical reactions in nature often occur in an enclosed environment, which varies from the cavity of an enzyme to the confinement of a cell.

Organic and polymer chemists also use the principle of confinement to synthesize a wide variety of compounds. For example, polymer beads (e.g. for use as ion exchange resin) can be prepared by polymerizing a monomer and a small amount of crosslinking agent, in the confinement of droplets of an emulsion in water. The size of these beads is dependent on the size of the dispersed droplets. Reactions in the inner compartments of micelles and vesicles have been studied as well. For example, Cuccovia et al. showed that the relative rate of an hydrolysis reaction can be increased by the confinement of a micelle, when compared to the bulk chemical reaction[1]. The micellar environment can be called a catalyst in this case. A vast amount of inorganic nanoparticles has been prepared by coprecipitation using the restricted space in microemulsion systems[2]. A number of methods have been reported for the preparation of enzyme-containing lipid vesicles (liposomes), which are water-soluble enzymes trapped in lipid dispersions that contain an

aqueous space[3]. A review on this topic has been published[4]. Several medical and biochemical applications are possible with these enzyme-containing liposomes.

Most reports on the use of confined spaces for the preparation of compounds, however, employ small cavities such as cage compounds and inorganic complexes[5]. In most cases, the cage-like molecules possess only a single cavity large enough to incarcerate a guest molecule[6]. In our group, a great deal of research effort has been directed towards the preparation of unique glycoluril-based cage structures ("clips") which have shown to possess unique properties[7]. Although some authors describe the encapsulation of a medicinal species using viral cage proteins[8], there are no reports in the literature that deal with synthetic organic species that react on the inside of natural viral cages. In this chapter, efforts are described to perform a photochemical polymerization reaction on the inside of a viral cage.

8.1.1 Photopolymerization

Photopolymerization is defined as the reaction of monomers or macromers to produce polymeric structures by light-induced initiation (excitation of a photoinitiator) followed by polymerization. Fundamental research and practical applications of photopolymerization have evolved significantly over the past decades leading to a better understanding of the mechanisms of the reactions and to numerous industrial and medical applications, such as contact lenses, dental restorations, adhesives, and coatings. All modern integrated circuits are prepared by photopolymerization processes. Photopolymerization reactions usually occur under ambient conditions; they are rapid when compared to thermal polymerizations and the use of a solvent is optional. A proper choice of the monomer and its functionality allow the control over the resulting polymer architecture. Recently, a lot of attention has been focused on the application of photopolymerization in the preparation of materials that are compatible with biological structures[9]. Schubert et al. have investigated the possibilities of incorporating a monomeric anchor on the inside of a vesicle, followed by subsequent photopolymerization. They were thus able to produce stable structures with approximately 100% gel content[10]. A number of studies have been performed to

photopolymerize phospholipids in the interior of the membranes of vesicles[11,12]. The polymerization of liposome-encapsulated hydrophylic monomers by UV light is an important method for the creation of polymer-gel containing vesicles[13]. A disadvantage of such systems is that they often specifically rely on the self-assembly of amphiphilic molecules to generate spherical (or other) structures. Because of this amphiphilic behavior, these systems sometimes possess low biocompatibility.

The project described in this chapter was initiated because it was believed that the confined space of the CCMV capsid shell might have an influence on a polymerization reaction carried out within this capsid. It might be possible that the polydispersity of a polymer synthesized within the capsid is lower than that of the same polymer prepared in bulk solution. This may be the case since reaction kinetics and thermodynamics in a nanoscale environment might be different from those in a micro or macro environment. However, the most conspicuous effect is expected to come from interactions with the inner wall of the viral capsid. This is so, because the photochemical polymerization that was chosen to be studied employs styrene sulfonate sodium salt as monomer. Previous work[14] has shown that the polymer prepared from this monomer, polystyrene sulfonate, has a unique interaction with the capsid shell. Thus, during polymerization, when such interactions start to play a role both the polymerization kinetics and the thermodynamics of the reaction may be changed.

8.1.2 Confined spaces as photochemical environment

In order to realize a polymerization reaction within the CCMV capsid, the compounds, precursors and/or reagents need to be encapsulated first and separated from the excess reagents. Subsequently, external stimuli can be used to start the reaction. A photoinitiator is an excellent means of achieving this: it can be strictly controlled, especially when the photoreactive reagent is sensitive for UV light. The use of other stimuli to start a chemical reaction is limited. One option is an electric potential (and current) to initiate a redox reaction, however, the required oxidizing or reducing reagents will probably disrupt the integrity of the capsid. Addition of a chemical initiator has the disadvantage that the compound must penetrate the protein shell first in order to

commence the reaction. The use of an external magnetic field is a possibility but difficult to realize, although it has been shown that strong magnetic fields can affect the photopolymerization reaction itself[15].

Scheme 8.1 shows the procedures designed to perform a photoinitiated polymerization inside the CCMV capsid.

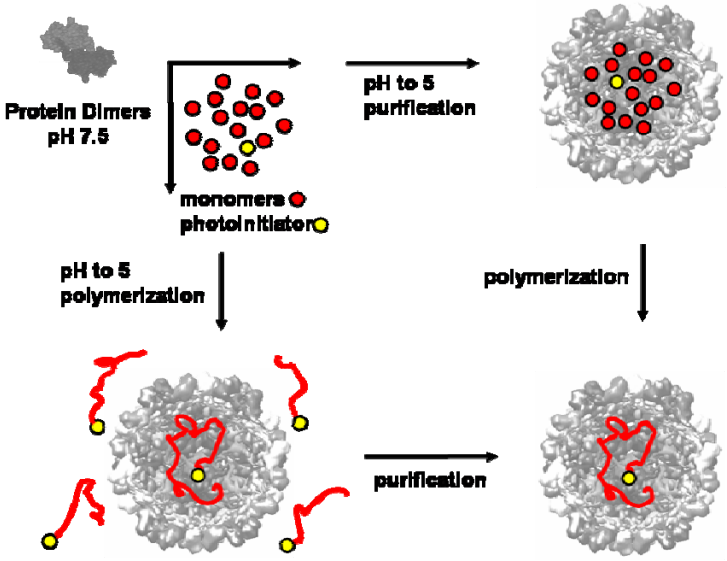

Scheme 8.1. *Different routes to carry out a photochemical polymerization reaction within the CCMV capsid. After inclusion of the desired reagent, the photochemical polymerization can be performed* before *purification or* after *purification.*

After the pH induced encapsulation of the monomer and photoinitiator into the capsid, the polymerization can be performed without separating the capsid from the excess reagents. This will lead to a reaction in which polymers are formed both within the capsid and in the outer aqueous environment. Size exclusion chromatography should be able to separate the polymeric species from the capsid.

Another option is to first separate the capsid from the excess reagent and then perform the photopolymerization reaction. In the following section both routes are described[16].

8.2 Results and discussion

Styrene sulfonate sodium salt was chosen as the monomer for our experiments. Styrene sulfonate is highly soluble in water, has a distinct UV absorption, and, since it is negatively charged, can be expected to have some interaction with the (positively charged) capsid wall, thereby increasing its concentration in the capsid.

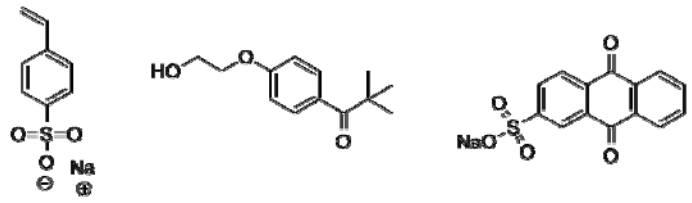

Figure 8.1. *The monomer (styrene sulfonate sodium salt, left), photoinitiator (Irgacure 2959, middle), and anthraquinone sulfonate (right) used in the photopolymerization reaction.*

The industrial photoinitiator Irgacure (Figure 8.1) was used, since it is readily available, slightly soluble in water and has an absorption maximum that lies within the UV range, rendering it insensitive to visible light. This was thought useful, since many manipulations with the protein, monomer and initiator solution are required, before the polymerization can be started. Thus, no reaction would be initiated with visible light, but only with ultraviolet light. The Irgacure initiator is also convenient because the UV absorption maxima of monomer and photoinitiator do not lie at the same wavelength; Irgacure adsorbs at ca. 270 nm, whereas styrene sulfonate possesses a maximum at 225 nm. The presence of the initiator and/or monomer species can be detected in this way.

Initially, a buffered solution of the monomer and Irgacure 2959 were prepared. Since it is known that the protein is insensitive to high salt concentrations (in fact, the CP requires high salt concentrations for its assembly), the concentrations of saline in the CP solution was kept the same as in the monomer and the initiator solution. Thus, in a pH 7.5 buffer (0.05 M Tris.HCl, 0.001 M EDTA, 0.3 M NaCl, 0.01 M $CaCl_2$, 0.02 mM PMSF[17]), monomer was dissolved to a concentration of 0.5 M, as well as the photoinitiator Irgacure (1.6 mM). Subsequent dialysis of a preparation of CCMV coat

protein using this buffer yielded a clear, viscous, slightly yellow solution. After some time (several hours), however, a precipitate was observed. SDS PAGE analysis revealed that no protein was left in the supernatant. Therefore, the saline concentration was lowered. The resulting preparation using 0.3 M monomer and no NaCl was stable, when left at pH 7.5 for several hours. However, a subsequent slow decrease of the pH of the buffered solution to 5.0, using HCl (0.5 M) led to a precipitate in the dialysis bag, albeit to a considerably smaller degree. It was thought that the presence of the photoinitiator (1.6 mM), which is not readily soluble in water, was the origin of this effect.

Therefore, in later experiments, the photoinitiator was replaced by the more soluble anthraquinone sulfonate. Also, assembly of the protein subunits could be achieved by a slow pH reduction of the protein sample in the Eppendorf vial itself. This was done by the slow addition of very small amounts of glacial acetic acid under vigorous stirring, alleviating the need for a pH 7.5 buffer with its concomitant large monomer concentration. In this way, the styrene sulfonate consumption was reduced.

Dialysis of a solution in which monomer was encaged in the closed capsid (pH 5) against a pH 5 buffer without monomer was found to effectively remove the monomer from the capsid, leading to the conclusion that the photochemical reaction must take place with the presence of monomer both on the inside and on the outside of the capsid. Therefore, the sample, after incubation with the monomer, was not dialyzed for purification, but irradiated immediately so that polymerization would take place both on the outside and on the inside of the capsid (compare Scheme 8.1). In separate experiments, the monomer was photopolymerized in the *absence* of protein. All these reactions were carried out using Irgacure as the photoinitiator and were analyzed with the help of FPLC (Figure 8.2). The left curve in Figure 8.2 represents CCMV itself. The figure on the right is a control experiment involving monomer and initiator in the absence of the protein. The fractions obtained from this chromatography experiment were analyzed by ^{1}H-NMR. The fraction corresponding to a 1.5 ml elution time was expected to contain polystyrene sulfonate. However, ^{1}H-NMR only showed the presence of the solvent, even when the spectrum was recorded at a high sample concentration and with long acquisition times. NMR analysis of the large fraction eluting at 2.8 ml revealed the presence of monomer.

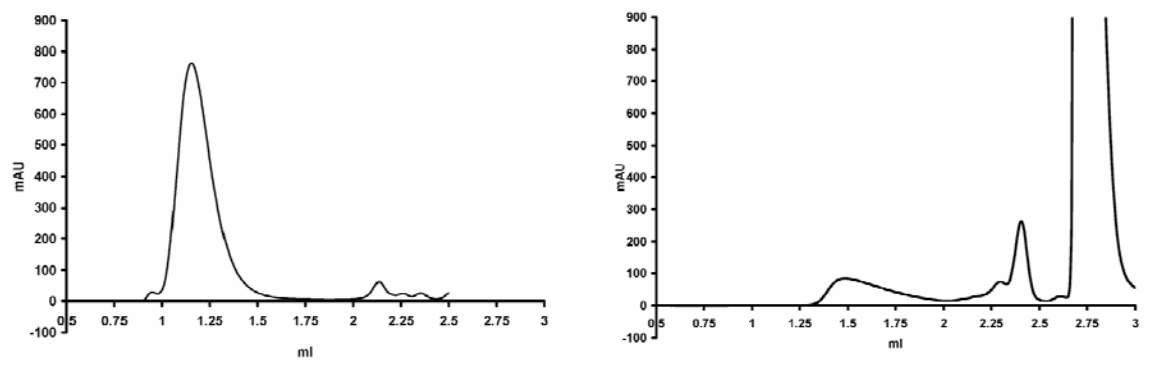

Figure 8.2. *Left: pure CCMV. Right: irradiation experiment involving the monomer and photoinitiator in the absence of protein. All curves were recorded at 260 nm.*

We tentatively concluded that it is possible with this size exclusion material, to separate the monomer from the polymer, although this was not confirmed by NMR. Subsequently, FPLC chromatograms were taken from the polymerization experiments in the presence of the CCMV capsid (Figure 8.2).

Inspection of Figure 8.3 reveals that little capsid is present. Only in the enlarged chromatogram (Figure 8.3, right), assembled protein shows up at 0.9 and 1.1 ml. The small peaks at 1.1 and 1.3 ml probably correspond to T=3 and T=1[18], respectively. The same observations were made for a sample that had not been irradiated, meaning that the chromatogram for a non-irradiated sample is virtually identical to that of an irradiated one. The relative UV absorptions for the set of peaks between 0.9 and 1.5 ml are also virtually identical, when irradiated and non-irradiated samples are compared. The UV absorption at 225 nm, however, is higher than would be expected for protein alone. This additional absorption could indicate the presence of either monomer or polymer.

It is possible, that oligomers of polystyrene sulfonate co-elute with the capsid protein or that the presence of the large amount of negatively charged polymer leads to aggregation with the individual coat protein units, thus inhibiting any assembly of the capsid. It cannot even be excluded that the peak eluting at 0.9 ml is an unknown assembly particle, eluting at the exclusion limit of the column. SDS PAGE analysis (not shown) did not show the presence of coat protein at 0.9 and 1.3 ml, but this may be due to the low

concentration of the material. The above results are not conclusive and more data are needed before any conclusion can be drawn.

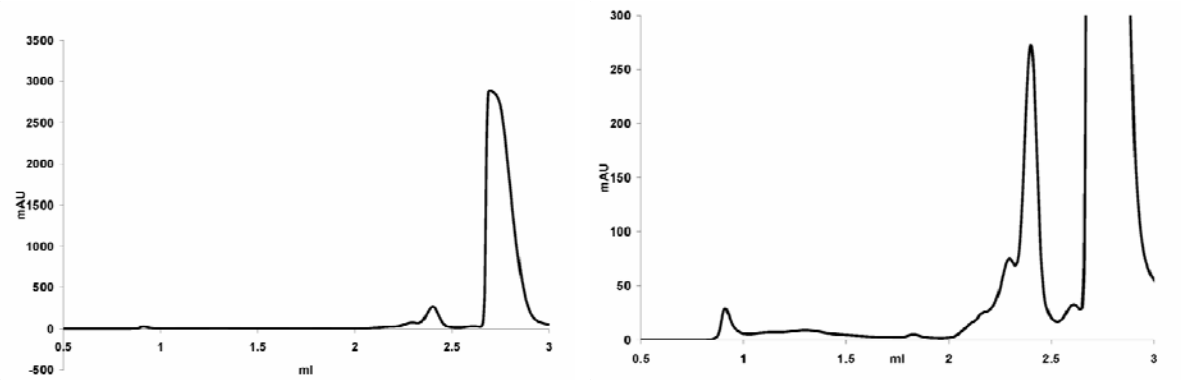

Figure 8.3. *Left: FPLC chromatogram taken from a polymerization experiment containing monomers, initiators and CCMV capsid. Right: magnification of the chromatogram. A solution of CCMV protein at pH 7.5 was incubated with buffers containing the appropriate concentrations of photoinitiator and monomer at pH 7.5, after which a small amount of glacial acetic acid was added to the sample solution in the Eppendorf vial lowering the pH to 5.0. The solution was degassed by bubbling the solution with argon and subsequently irradiated with broad spectrum UV radiation with a maximum of 405 nm, for 20 seconds.*

In order to investigate whether the negative charge of the monomer and the formed polymer would influence the outcome of the assembly reaction, the styrene sulfonate monomer was replaced by the neutral monomer hydroxyethylacrylate (HEA). Furthermore, in order to facilitate detection by UV absorption, some of this monomer used was functionalized with a dansyl group, see Figure 8.4.

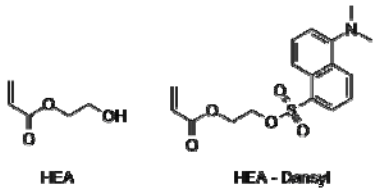

Figure 8.4. *Structure of hydoxyethylacrylate (HEA) and its dansyl[19] derivative.*

A further motivation for choosing dansyl-functionalized HEA is the fact that the sidechain glycol ester functions will show up more clearly in the ^{1}H-NMR spectrum, thus facilitating the detection of the product when compared to polystyrene sulfonate. It was also envisaged that poly hydroxyethylacrylate dissolves in (polar) organic solvents, thus enabling GPC measurements after the reaction mixture had been freed of protein and extracted with organic solvent. In order to investigate the sensitivity of the protein

towards the presence of the HEA, samples of CCMV CP were incubated with buffers, in which various concentrations of HEA and HEA-dansyl were dissolved. It was expected that the presence of large amounts of the monomer would induce the precipitation of the protein. However, this was not the case: the limit for precipitation appeared to be approximately 20 g/l. This value is not very accurate and depends strongly on, amongst others, the saline concentration (0.3 M was used) as well as the concentration of protein (3-5 mg/ml). Subsequently, in order to determine the molecular weight of the polymer obtained when the polymerization was carried out under the chosen conditions, several blank polymerization experiments were performed using a solution of 10 g/l (86 mM) HEA and anthraquinone sulfate as the initiator. The resulting reaction product was analyzed with FPLC. Figure 8.3 shows the chromatograms of the monomer (left) and the polymer after photopolymerization (right), both in the absence of capsid. In both preparations, 0.05 g/l of the dansyl-HEA was added to the mixture. Unfortunately, even small amounts of this substance did not dissolve, even after ultrasound treatment. Its use, therefore, was abandoned.

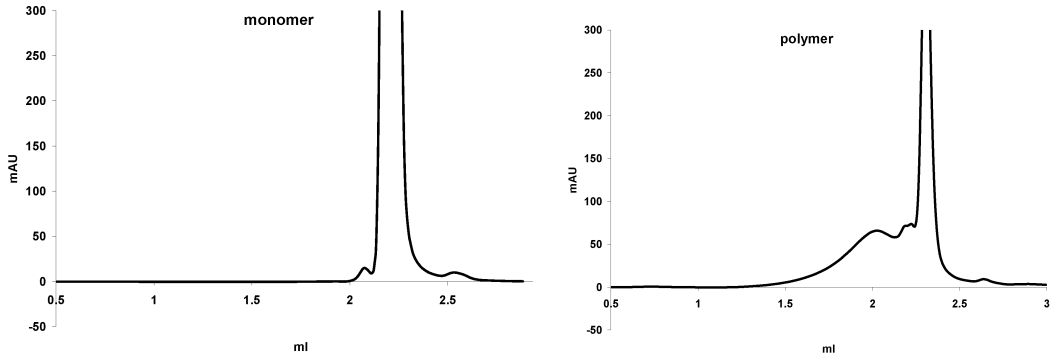

Figure 8.5. *FPLC traces of HEA monomer in pH 7.5 buffer (left) and photopolymerized products (right). All curves were recorded at 260 nm.*

From the chromatograms in Figure 8.5 it can be concluded that photopolymerization does take place. The fractions corresponding to the peak between 1.5 and 2.1 were collected, concentrated and analyzed by ^{1}H-NMR spectroscopy, but no signals were observed. Subsequently, FPLC experiments were carried out again and the resulting fractions were extracted with chloroform, dried, concentrated and analyzed again with NMR. Again, no signal was obtained. Also, in GPC experiments, no polymer

was found. Subsequent experiments with 100 g/L HEA (0.83 M) did show polymer signals in ^{1}H-NMR spectra after isolation of the samples by FPLC. However, as mentioned above, the limit at which the protein precipitates is ±20 g/L. Therefore, these concentrations cannot be used in experiments with the capsid protein. The inability to detect the polymer by ^{1}H NMR after purification with FPLC was disappointing, since it was thought that this technique would be the most sensitive tool to determine the presence of polymer.

Although the detection of the polymer after purification by FPLC was difficult, it was decided to perform the polymerization of the monomer encapsulated in the capsid.

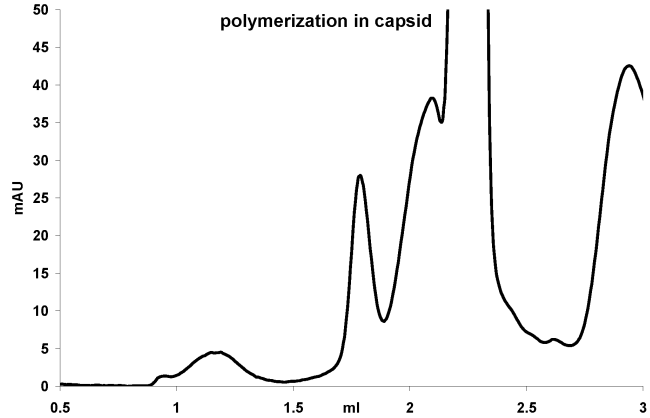

Figure 8.6. *FPLC chromatogram of the photopolymerization reaction of HEA in the CCMV capsid. Detection was at 225 nm. Reagents and conditions: Concentration of HEA, 86 mM, anthraquinone photoinitiator 3.8 mM dissolved in a pH 5.0 buffer (see experimental section).*

Figure 8.6 shows the FPLC chromatogram that was obtained after irradiation of HEA encapsulated in the CCMV capsid. FPLC chromatograms, which were taken from monomer that was encapsulated in the capsid, without subsequent irradiation, did show significant amounts of capsid, as well as the polymer eluting at approximately 2.0 ml. Although the typical peak at an elution volume of 1.1 ml is present, the intensity of this peak is so low, that no NMR spectra could be recorded. This chromatogram was also recorded at 225 nm, a wavelength where the protein adsorbs very strongly. The conclusion was that the concentration of the capsid was too low to be detected. It is possible, that the peak observed at 1.8 ml is due to the protein subunits, but this was not verified.

8.3 Conclusions

The first series of experiments, involving the polymerization of styrene sulfonate encapsulated in CCMV, did yield some virus particles after purification. The concentration of product was so low, that virtually no analysis could be performed to check whether the particles contained monomer or polymer. UV analysis on the fractions with the correct elution volume did suggest the presence of either monomer or polymer, but the result was not conclusive. It is very problematic to detect the presence of any polymer that is formed within the capsid, since the quantities are minute. MALDI-TOF mass spectroscopy on the samples would be a possibility, but the charged nature of the polymer may cause problems in the analysis. A method to detect the presence of polymer, and possibly to analyze its polydispersity, is the isolation of the capsid by multiple FPLC runs, followed by either elution over a small, strongly acidic ion exchange column or the addition of a strong acid to the sample. Both methods serve to protonate the polystyrene sulfonate, which then can be isolated and analyzed by MALDI-TOF MS[20].

Preliminary calculations were carried out showing that ca. 800 styrene sulfonate molecules can be expected to be encapsulated in the capsid, if a concentration of approximately 0.5 M is used in the experiments, and only statistical inclusion is taken into account. This quantity would seem sufficient to allow a polymerization reaction to take place.

Attempts to polymerize a neutral HEA monomer within the capsid were not successful either; in this case, the capsid protein may have been denatured by the presence of the more hydrophobic polymer. It may also be the case that the monomer and corresponding polymer interfere with the assembly behavior. This interference is somewhat unexpected, since in the purification of the virus, large quantities of polyethylene glycol are used to precipitate the virus. The polarity of poly HEA should be within the same order of magnitude as that of polyethylene glycol, therefore small amounts of this polymer were not expected to have such a dramatic effect on the assembly of the capsid or the denaturation of the capsid protein.

The general conclusion of this chapter is that photopolymerization within the CCMV capsid may have taken place, but that more data are required to prove the

formation of polymer. Future experiments may include the synthesis of a genetically modified coat protein, which bears an azide moiety that is only located on the inside of the capsid. Coat proteins containing such azide functions are currently being prepared in our group. This azide may be selectively reacted with an acetylene that bears a (photo)initiator via a "click" reaction. Subsequent incubation and polymerization of this initiator would yield a (photo)polymerization reaction similar to the one described in this chapter, but with two essential differences: the polymer is now attached to the protein and no polymerization occurs on the outside, which will facilitate the purification of the product. Research in this direction is currently underway.

In later experiments, Dr. dela Escosura of our group prepared capsids, which probably contained polystyrene sulfonate oligomers by using similar conditions as described in this work. He was able to show, by using non-denaturing agarose gel electrophoresis, that capsids containing this polymer migrated towards the cathode of the electrophoresis setup, while empty capsids did not. The preliminary conclusion of his work is that the capsid wall acts as a template for the polymerization process, leading to oligomers instead of high molecular weight polymers[21].

8.4 Experimental section

All chemicals were of analytical grade or better quality and were used without further purification. For further information regarding analytical techniques (FPLC), see Chapter 5. The following procedure was used for the photopolymerization of the charged monomer: a 50 µl sample of CCMV CP at pH 5.0 was dialyzed against a pH 7.5 buffer (0.05 M Tris, 0.1 M styrene sulfonate sodium salt, 0.2 M NaCl, 1 mM EDTA.2Na, 10 mM $CaCl_2$, 0.2 mM PMSF, and 3.8 mM anthraquinone sulfonate) at 4^{o}C (thus containing the monomer and photoinitiator in the appropriate concentrations). The molecular weight cut off (MWCO) of the dialysis bag was 12,000. Subsequently, the pH of the entire solution was lowered to 5.0 using the dropwise addition of aqueous 3 M AcOH, requiring only ca. 1 ml in total. This solution was left for at least 1 h., after which the contents of the dialysis bag were transferred to an Eppendorf vial. A dialysis step at this time would allow the monomer to diffuse out of the capsid. Using a fine needle, argon gas was

bubbled through the solution for 30 min. at 4°C. Then, the solution was irradiated for 20 s using a high intensity glass fiber optic UV lamp with a radiation maximum of 405 nm. Subsequently, the mixture was transferred to a dialysis bag with a MWCO of 1,000,000 and dialyzed extensively against a pH 5.0 buffer (0.05 M NaOAc, 1 mM EDTA.2Na, 0.3 M NaCl, 10 mM $CaCl_2$, 0.2 mM PMSF), in an attempt to remove the polymers, present outside the capsid. This turned out to be a very sluggish process. Several days of dialysis with several dialyzate changes did not efficiently remove the polymers, present on the outside of the capsid. The dialyzed mixtures were then analyzed using FPLC.

8.5 Notes and references

[1] L.M. Gonçalves, T.G. Kobayakawa , D. Zanette, H. Chaimovich and I.M. Cuccovia, *J. Pharmac. Sciences* **2008**, 22.

[2] See Chapter 8 for extensive literature overview.

[3] D.M. Vriezema, M. Comellas Aragones, J.A.A.W. Elemans, J.J.L.M. Cornelissen, A. E. Rowan and R.J.M. Nolte, *Chem. Rev.* **2005,** *105*, 1445.

[4] P. Walde and S. Ichikawa, *Biomolecular Engineering* **2001**, *18*, 143.

[5] M. Yoshizawa, Y. Takeyama, T. Okano and M. Fujita, *J. Am. Chem. Soc* **2003**, *125*, 3243 and references therein.

[6] For example C.J. Kuehl, Y.K. Kryschenko, U. Radhakrishnan, S.R. Seidel, S.D. Huang and P.J. Stang, *Proc. Natl. Acad. Sci.***2002**, *99*, 4932; C.J. Kuehl, T. Yamamoto, S.R. Seidel and P.J. Stang, *Org. Lett.* **2002,** *4,* 913; S.-S. Sun and A.J. Lees, *Chem. Comm.* **2001**, 103.

[7] A.E. Rowan, J.A.A.W. Elemans and R.J.M. Nolte, *Acc. Chem. Res*. **1999**, *32*, 995.

[8] C. Flynn, *Acta Materialia* **2003**, *51*, 5867.

[9] a) S.H. Dickens, J.W. Stansbury, K.M. Choi and C.J.E. Floyd, *Macromolecules* **2003,** *36,* 6043; b) G. Kloosterboer, *Adv Polym. Sci.* **1988,** *84,* 1; c) K.S. Anseth, J.A. Burdick, *MRS Bull.* **2002,** *27*, 130; d) J.P. Fisher, D. Dean, P.S. Engel and A.G. Mikos, *Ann. Rev. Mater. Res.* **2001,** *31*, 171; e) C. Decker, *Polym. Int.* **1998**, *45,* 133; f) K.S. Anseth, A.T. Metters, S.J. Bryant, P.J. Martens, J.H. Elisseeff and C.N. Bowman, *J. Controlled Release* **2002,** *78,* 199; g) K.S. Anseth, S.M. Newman and C.N. Bowman, *Adv. Polym.*

Sci. **1995,** *122*, 177; h) C. Decker, *Acta Polym.* **1994,** *45*, 333; i**)** M.A. Carnahan, C. Middleton, J. Kim, T. Kim, M.W. Grinstaff, *J. Am. Chem. Soc.* **2002**, *19*, 5291.

[10] O. Stauch, T. Uhlmann, M. Fröhlich, R. Thomann, M. El-Badry, Y-K Kim and R. Schubert, *Biomacromolecules* **2002**, *3*, 324.

[11] J. Hotz and W. Meier, *Langmuir* **1998**, *14*, 1031.

[12] a) S.L. Regen, B. Czech and A. Singh, *J. Am. Chem. Soc.* **1980**, *102*, 6638;

b) J. Fendler, *Science* **1984**, *223*, 888.

[13] W. Meier, *Chem. Soc. Review.* **2000**, *29*, 295.

[14] See Chapters 6 and 7.

[15] D.S. Bag and S. Maiti, *J. of Pol. Science, Part A: Polymer Chemistry* **1998**, *36*, 1509.

[16] For detailed information on the assembly behavior of CCMV, see Chapter 1.

[17] PMSF = phenylmethanesulfonyl fluoride, which functions as protease inhibitor.

[18] See Chapter 6.

[19] Dansyl = "dimethylaminonaphtyl sulfonyl" (5-(dimethylamino)naphthalene-1-sulfonyl-). This compound was synthesized according to a literature procedure: C-H. Cho, H-S. Yun and K. Park, *J. Org. Chem.* **2003**, *68*, 3017.

[20] R. Arakawa, S. Watanabe and T. Fukuo, *Rapid Comm. in Mass Spectr.* **1999**, *13*, 1059.

[21] A. de la Escosura Navaso, unpublished results.

Chapter 9

Inorganic nanoparticles inside viral protein cages

9.1 Introduction

Ever since the discovery that the properties of nanosized materials can be different from those in bulk[1], the preparation of such nanomaterials in well-defined form is one of the objectives of modern chemistry. Nanoparticles are often synthesized from solution. For example, the synthesis of catalytic metal nanoparticles from aqueous solutions can be achieved by the reduction of a metal salt[2]. These reactions often require a stabilizing agent, *i.e.* an organic capping agent to prevent aggregation of the nanoparticles formed[3]. A large variety of metal oxides has been prepared in this relatively simple way and these synthetic procedures have been extensively reviewed by Cushing et al.[4] Another widely employed method to synthesize nanoparticles is the sol-gel process, which involves the immobilization of a solvated metal precursor in a gel, followed by the ageing of the gel and subsequent drying[5]. These procedures lead to the dispersion of nanoparticles in a gel matrix, known as xero- or aerogels.

Microemulsions have also been extensively used in the synthesis of inorganic nanoparticles (see below)[6]. Usually, two different reagents are separately "dissolved" in microemulsions and subsequently added to one another, leading to a statistically

controlled formation of nanoparticles. The use of dendrimers to template the formation of CdS nanoparticles has also been reported[7].

The synthesis and properties of the well-known magnetic compound Prussian blue ((MFe(III)[Fe(II)CN$_6$]) (M = NH$_4$, Li, Na, K)) have been studied for over 300 years. The first report dates from 1704, when a German draper boiled beef blood in a strongly basic medium and obtained, presumably to his astonishment, a blue coloration. An equally simple method is still used today to demonstrate the formation of Prussian blue; it involves the deposition of a few crystals of potassium hexacyanoferrate (II) on one side, and a few crystals of iron(III) chloride on the other side of a petri dish, followed by careful wetting. The formation of crystalline material in the middle can then be observed after a while.

Prussian blue is a molecular magnetic material, meaning that below a certain temperature T_c (the Curie or critical temperature, 5.6 K for bulk preparations of this compound[8]) it displays ferromagnetism. A large variety of different structures and concomitant magnetism of compounds related to Prussian blue are known[9]. The synthesis of these compounds, which often have paramagnetic metals as contributing ions, is no more complicated than the precipitation reaction of two compounds in the petri dish experiment mentioned above. A great advantage is that the magnetic properties of the compounds of the Prussian blue family can be tuned by changing the (paramagnetic) transition metals in the compound. A large variety of magnetic materials can be prepared in this way, leading to, for example, in the case of CsMn(II)[Cr(III)CN$_6$], Curie temperatures above that of liquid nitrogen (T_C = 90 K)[10]. A lot of attention has been directed towards understanding the correlations between the crystalline structure and the magnetic properties of the Prussian Blue family[11]. Surprisingly, relatively few studies have focused on the understanding and control of the growth and assembly mechanisms of Prussian Blue, although some papers on the growth of Prussian Blue crystals in Langmuir monolayers have been published[12]. Nanosized particles of "classical" Prussian blue have been synthesized by Mann et al., who used microemulsions in which two photosensitive precursors, ammonium hexakiscyanato iron (III) and ammonium bis oxalato iron (III), were incorporated[13]:

$$(NH_4)_3[Fe(III)(CN)_6] + (NH_4)_3[Fe(III)(C_2O_4)_3] \rightarrow (NH_4)Fe(III)[Fe(II)CN)_6$$

Upon photoirradiation, the oxalic acid anion reduces the iron (III) to iron (II), which then reacts with the iron cyanide complex to form the aforementioned Prussian blue. In this way, 16 nm crystals of narrow polydispersity (σ = 2.7 nm) were generated, which evolved into superlattice structures. Photoirradiation in the bulk led to very disperse and large particles (100 – 250 nm). The synthesis of these Prussian Blue nanoparticles was thus controlled by the spatial confinement of the microemulsion. No other chemical precondition, except the concentration of the reagents was required for synthesis of these particles. Another important point is that both reagents are not reactive towards each other without an irradiation step. Therefore, the reaction can be initiated at will. It was thus envisaged that Prussian Blue would make an ideal model reaction to test the use of the cavity of the CCMV capsid as a nanoreactor for the preparation of nanoparticles. Experiments towards this goal are presented in this chapter.

Not much is known in the literature about the synthesis of inorganic nanoparticles with the help of biomolecules or biomolecular systems. The first such report dates only from 1991, when Meldrum et al. reported the synthesis of iron sulfides and amorphous manganese and uranyl compounds inside the cage of the protein ferritin[14]. The ferritin effectively served as a spatially constrained medium for particle growth. Mirkin et al. found that DNA oligomers, attached to the surface of a gold nanoparticle could direct the self assembly of these gold nanoparticles in solution[15]. Viruses have also been applied to direct the growth of nanoparticles: Dujardin used the Tobacco Mosaic Virus, a long and stiff rod-like virus, to create of long cylindrical aggregates of Pt and Au[16]. Certain microorganisms known for their reductive power have similarly been employed in the synthesis of crystalline iron salts[17]. Finally, it is worth mentioning that gold can be extracted from the soil with the help of plants, a process that is applied commercially[18]. This extraction of gold salts from the soil results in nanoparticle formation in the plant stems.

The viral cage of CCMV (See Chapter1) is ideal for biomineralization reactions, at least in principle, because the reversibility of capsid formation implies easy access to the interior of the virus. As explained before, this behavior can be controlled by applying a simple change in pH. Thus, incubation with precursors that can produce the desired

metal or metal oxide after reaction is easily achieved in this manner, as has been reported by Douglas and Young, who synthesized tungsten and vanadium derived nanoparticles inside CCMV[19] by incubation of the pH 6.5 gated form of the virus with inorganic precursor ions. These ions reacted subsequently under the influence of the pH drop to slowly form crystalline tungstate and vanadate species. Very recently, the same authors reported the preparation of a gadolinium structure, consisting of the CCMV capsid with Gd ions bound to the inside[20]. If Gd ions are coordinated to a macromolecular structure, their magnetic relaxation is enhanced. Thus, coordination to protein subunits inside a viral particle may be successful as high relaxivity Magnetic Resonance contrast agents. A drawback of this system is the unknown effect of calcium ions that might compete with the Gd for the binding pockets in the protein; the fact that both calcium and gadolinium coordination relies on the presence of positively charged ammonia groups on the inside of the protein makes that this is generally not applicable.

In order to be able to tune the size and shape of any nanoparticle, synthesized within a confined space, it is of paramount importance to exert control over the inclusion and reaction procedures. For example, if two components are mixed and react immediately, this is disadvantageous since the exact size and stoichiometry can no longer be controlled. If it therefore preferable to set in some way the point in time at which the reaction starts. Figure 9.1 illustrates this principle for the preparation of Prussian Blue nanoparticles inside the CCMV capsid.

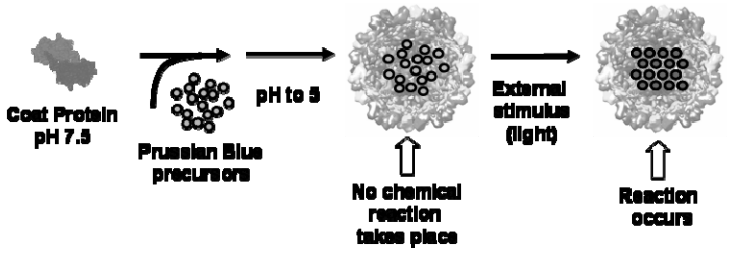

Figure 9.1. *Schematic procedure for the synthesis of nanoparticles inside the CCMV capsid. Key point is the external stimulus, which starts the reaction.*

A possibility to do this is by using an external stimulus. In the case of the synthesis of Prussian blue this stimulus is light. It was therefore decided to include the water-soluble Prussian blue precursors $(NH_4)_3[Fe(III)(CN)_6]$ and

$(NH_4)_3[Fe(III)(C_2O_4)_3]$ inside the CCMV capsid and to induce reaction of the two components by irradiation. Experiments of this type to synthesize Prussian blue nanoparticles, enclosed within the viral protein shell of CCMV, are described in this chapter.

9.2 Results and discussion

Before performing experiments with the precious CCMV proteins, the formation of Prussian blue was investigated in bulk. Since it is known that the ammonium iron cyanate is significantly more stable than the potassium salt of the Prussian blue, the precursors for the photochemical reaction were prepared in the following manner:

$$2\bullet(NH_4)_3[Fe(C_2O_4)_3] + K_3[Fe(CN)_6] \rightarrow K_3[Fe(C_2O_4)_3](s) + (NH_4)_3[Fe(CN)_6](aq) + (NH_4)_3[Fe(C_2O_4)_3](aq)$$

The solid potassium salt was removed from the reaction mixture either by filtration or by centrifugation. The soluble ammonium salts are the precursors for the photochemical reaction. The concentrations of these precursors was 1.0 M Subsequent irradiation with visible light (a simple light bulb) for one night yielded a dark blue mixture that was analyzed with UV-VIS. Figure 9.2 shows the UV-VIS spectra of the mixture as a function of time.

Irradiation of the precursor salts in a 1 M concentration using a normal 200 W light bulb for three days was not sufficient to complete the reaction (Figure 9.2 (top)). It was therefore decided to use a 405 nm laser for the experiments. This proved to be successful; a very rapid emergence of a broad peak at ~700 nm was detected. Transmission electron microscopy analysis of the material irradiated in bulk showed amorphous particles of ca. 1 μm size, which is in contrast with results obtained in the literature[13], where 100 nm sized particles were reported to be formed.

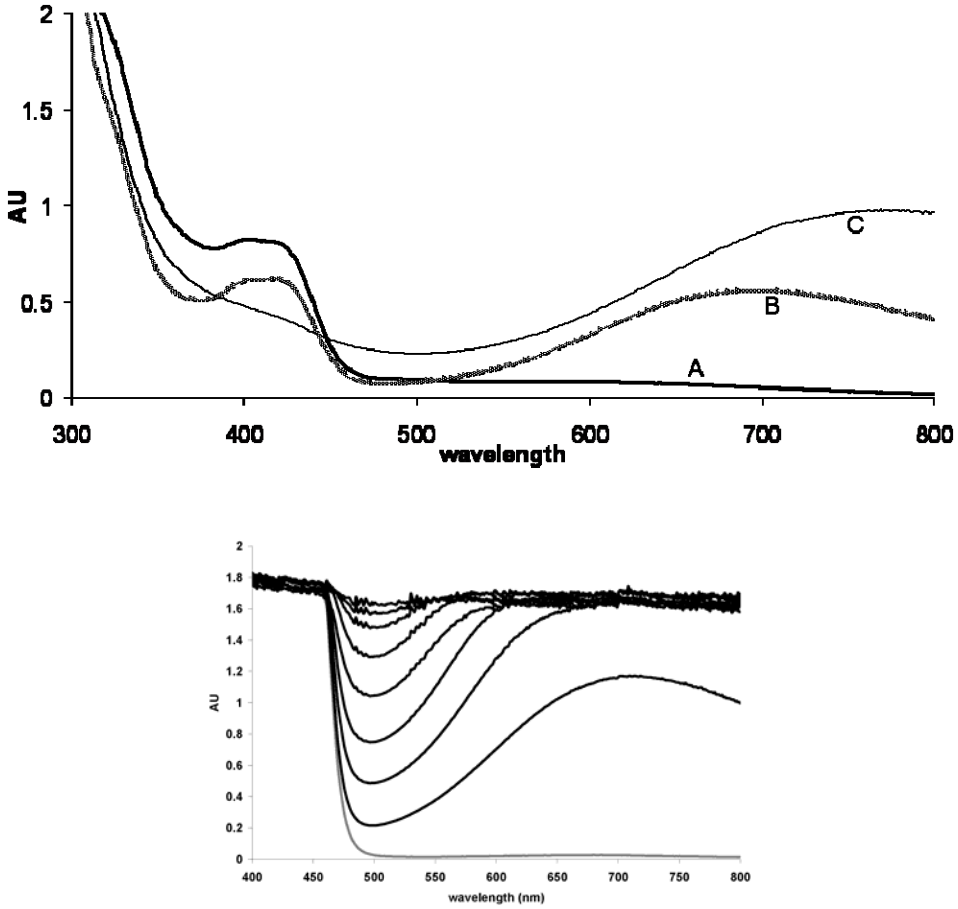

Figure 9.2. *Top: UV-VIS spectra of the Prussian blue precursors and the reaction product after irradiation. All concentrations are 1 mM A) UV-VIS spectrum of Prussian blue precursors; B) reaction mixture irradiated for >48 h. C) Reaction mixture irradiated for 105 h using a standard 200 W light bulb. Bottom: UV-VIS spectra of a concentrated mixture of Prussian blue precursors taken at two minute intervals showing a sharp increase of the absorption at 700 nm. The grey trace indicates the absorption spectrum of the starting material.*

Since our bulk experiments were carried out in a buffer identical to the one which is used for the manipulation of the CCMV protein, it is possible that the salts (NaCl), coordinating agents (EDTA) and the pH of the buffer have influenced the crystal growth.

9.2.1 Prussian blue nanoparticles inside the viral capsid

Initially, a solution of coat protein (CP) at pH 7.5 was incubated with a solution of Prussian blue precursors, at a 0.1 M concentration of the salts. In order to close the capsid shell, the pH was subsequently lowered by dialysis against a pH 5.0 buffer that did not contain any precursors. This procedure proved to be problematic, because the precursors

were dialyzed out of the closed shell. It was therefore decided to employ the following procedure. A given volume of capsid protein (CP) was incubated with the Prussian blue precursors at pH 7.5, where no assembly is expected to occur. To this solution, a 0.2 M acetic acid solution was slowly added over a period of 10 min. allowing the pH to slowly reach the final value of 5.0. The use of the relatively high concentration of acid prevented the large dilution effect, usually observed with dialysis, to take place. The slow addition was deemed to be necessary, as it is known that rapid pH changes give rise to kinetically controlled architectures such as multi-shelled or tubular particles. The thus obtained solution of pH 5 was irradiated with the help of a 405 nm laser beam, which very rapidly led to the formation of a distinct blue color. The reaction mixture was centrifuged to remove the solid material, which was formed outside the CCMV shell, and analyzed with Fast Protein Liquid Chromatography (FPLC), UV-VIS, Transmission Electron Microscopy (TEM), and Atomic force microscopy. Figure 9.3 shows the FPLC traces of the different preparations.

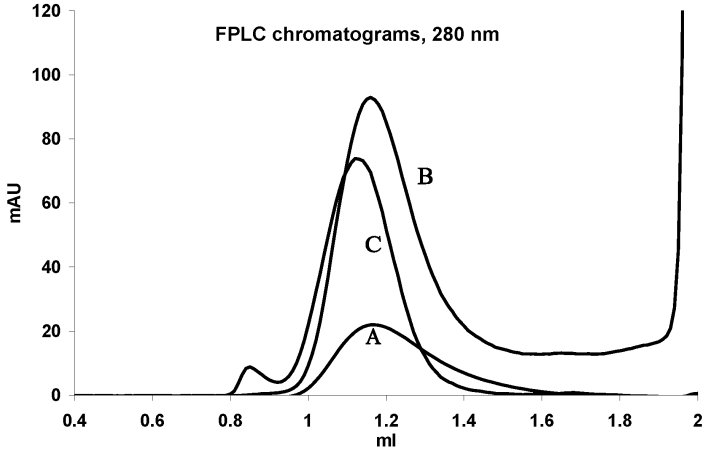

Figure 9.3. *FPLC chromatograms, measured at 280 nm. A: CCMV capsid (blank experiment). B: Capsid containing Prussian blue precursors. The sharp increase at 1.9 ml is due to the non-encapsulated precursors. C: Capsid with Prussian blue nanoparticles after purification. For reaction conditions, see text and experimental section.*

At a retention volume of 1.1 - 1.2 ml a peak representing the CCMV capsid with the Prussian blue nanoparticles inside, can be observed. A much larger peak, corresponding to the green Prussian blue precursors is seen at a retention time of 2.0 ml. It is possible that there is some of the free dimeric coat protein left, which shows up at 1.7-1.8 ml. The purified sample (curve C) does not exhibit the peak at 2.0 ml,

corresponding to the precursors. The fractions corresponding to the individual peaks in Figure 9.3 were collected and analyzed by UV-VIS spectroscopy. Figure 9.4 shows the resulting spectra.

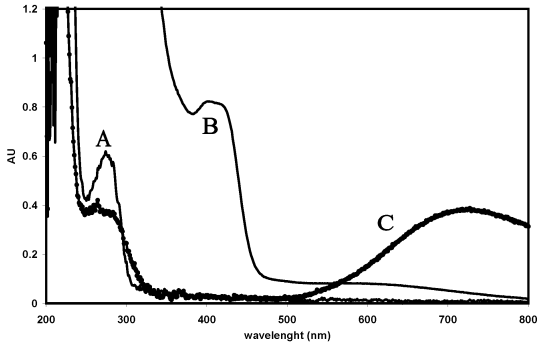

Figure 9.4. *UV-VIS absorption curves. A: CCMV capsid (blank experiment). B: Prussian blue precursors in the presence of capsid. C: Capsid with Prussian blue nanoparticles.*

In this figure, the typical absorption for the protein at 260-280 nm is present (curves A and C). This absorption cannot be observed in curve B because of the large concentration of Prussian blue precursors. The absorption of the Prussian blue precursors is not visible in curve C, indicating their absence. By contrast, the broad absorption at about 720 nm in curve C is indicative of the presence of Prussian blue. The co-elution of the Prussian blue with the capsid in FPLC suggests that the solid species is included inside the protein shell. Additionally, the FPLC fractions corresponding to the capsid had a distinct blue color.

After these initial experiments a more simple method was used to separate the capsid with the solid Prussian blue from the non-reacted low molecular weight Prussian blue precursors. To this end, a small column was filled with Sephadex G 100 and charged with the reaction mixture, after it had been centrifuged. A neat separation was obtained as can be seen in Figure 9.5.

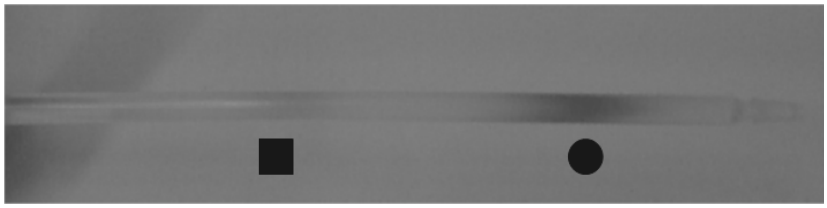

Figure 9.5. *Sephadex G 100 column showing the very efficient separation of the components shortly after the column was charged with the reaction mixture (see text). The column (ca. 0.5 cm in diameter) is eluted from left to right. The square represents unreacted precursor and the circle the CCMV capsid with Prussian blue.*

The capsids containing Prussian blue were analyzed after purification by TEM. It is common, in the study of viruses and virus-like particles to employ a negative staining agent, which is often uranyl acetate or ammonium molybdate sulfate[21] to visualize the particles. Accordingly, some of the grids were stained.

Figure 9.6 shows several TEM micrographs obtained from these experiments, where A and B are pictures of non-stained samples.

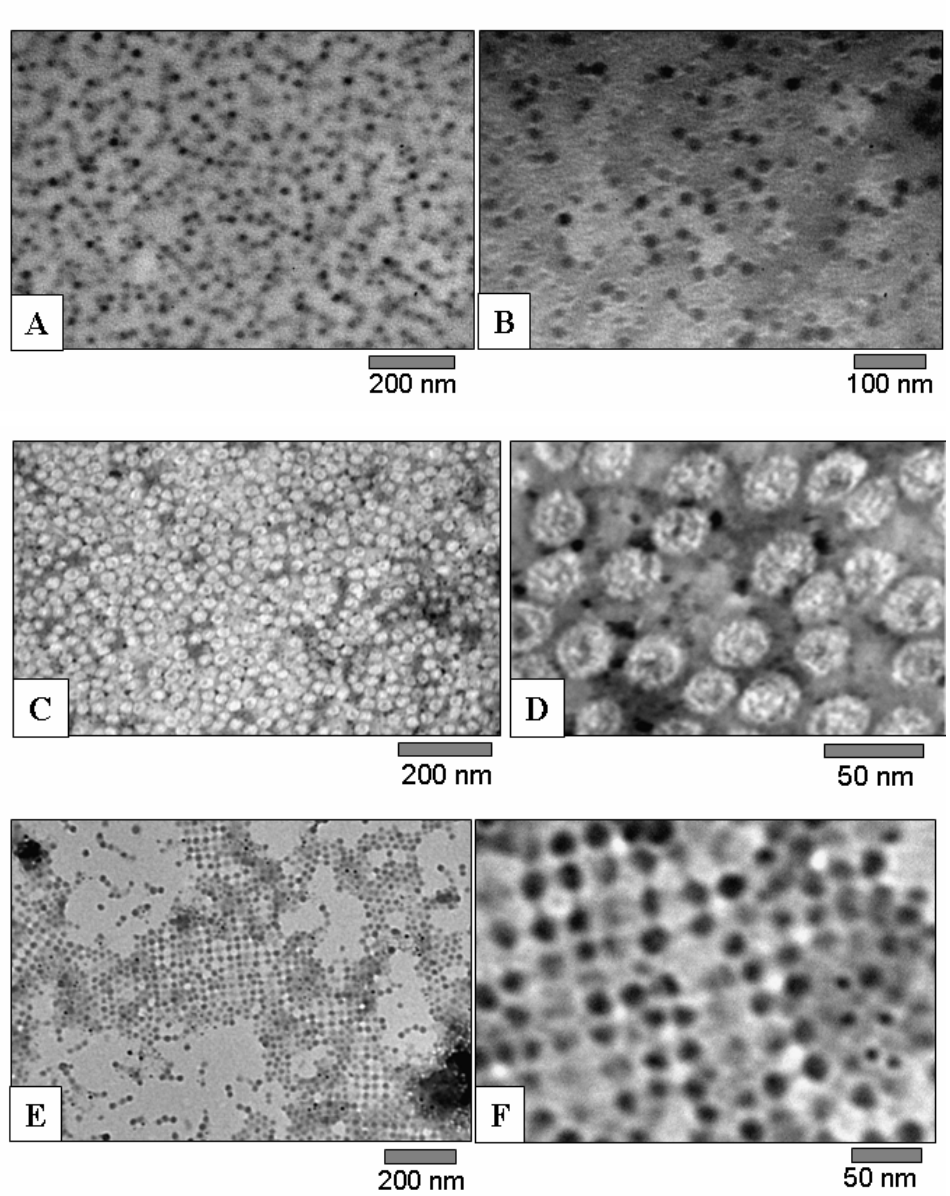

Figure 9.6. *TEM micrographs obtained from irradiated CCMV particles. A and B: non-stained grids. C and D: grids stained with uranyl acetate. E and F: grids stained with ammonium molybdate.*

Micrographs A and B show monodisperse particles, which were visible everywhere on the grid. Both grids were not stained. The contrast therefore comes from the iron, present in the capsids. When zoomed in (B), the protein shell is just visible as smaller rings of higher transmission. A size distribution analysis on 80 particles yielded a mean diameter of 18.6 ± 1.7 nm, which is in agreement with the known inner diameter of the capsid[22]. Figure 9.7 (left) shows the size distribution curve. Negative staining with 1 % uranyl acetate gave the micrographs that can be observed in image Figure 9.6C and 9.6D. The inside of the capsid gives no or little contrast, when compared to images A and B, but the protein shell is now visible. Monodisperse capsids are observed. This proves that the incubation with the iron salts followed by irradiation does not affect the protein subunits and the assembly process.

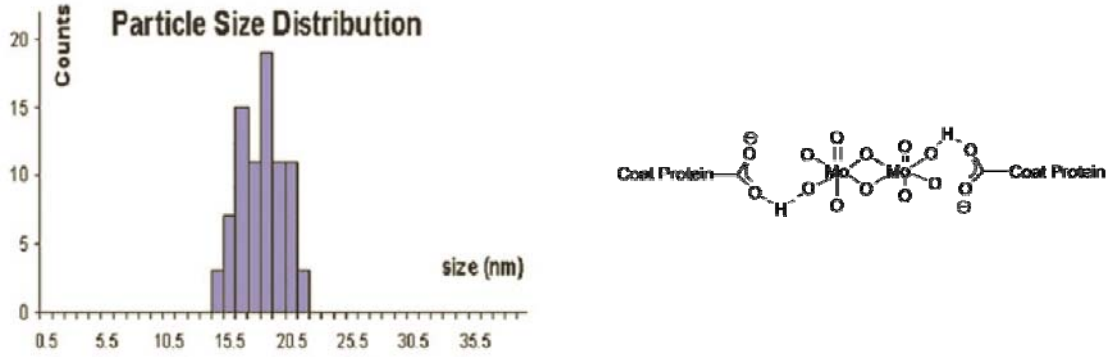

Figure 9.7. *Left: Size distribution of the CCMV – PB particles. Right: Proposed interactions between two neighboring coat proteins in separate capsids, as mediated by molybdate species.*

Another series of newly prepared samples were stained with ammonium molybdate. Again, the monodisperse particles were observed, but now assembled in arrays. Although hexagonal patterns can be discerned, the preference seems to be an organization in cubic arrays (Figure 9.6 E and F). Whether or not this is a consequence of the presence of ammonium molybdate is currently under investigation. It is possible that a discrete $Mo_7O_{24}^{6-}$ species, which is present in the staining, can serve as a bridging anionic species between neighboring capsids, forcing the particles to self-assemble into hexagonal and cubic patterns. A structure as shown in Figure 9.7 (right) may be feasible. An interesting consequence of the above is that such structures might form in solution, leading to 3-dimensional architectures, if the molybdate species is present.

Still another set of samples was prepared in a similar manner as described above. The incubation of CP with PB precursor, followed by irradation and purification again yielded the CCMV-PB nanoparticles. After staining these particles with ammonium molybdate, now hexagonal patterns were observed, in contrast to the results mentioned above. Figure 9.8 shows the corresponding micrographs.

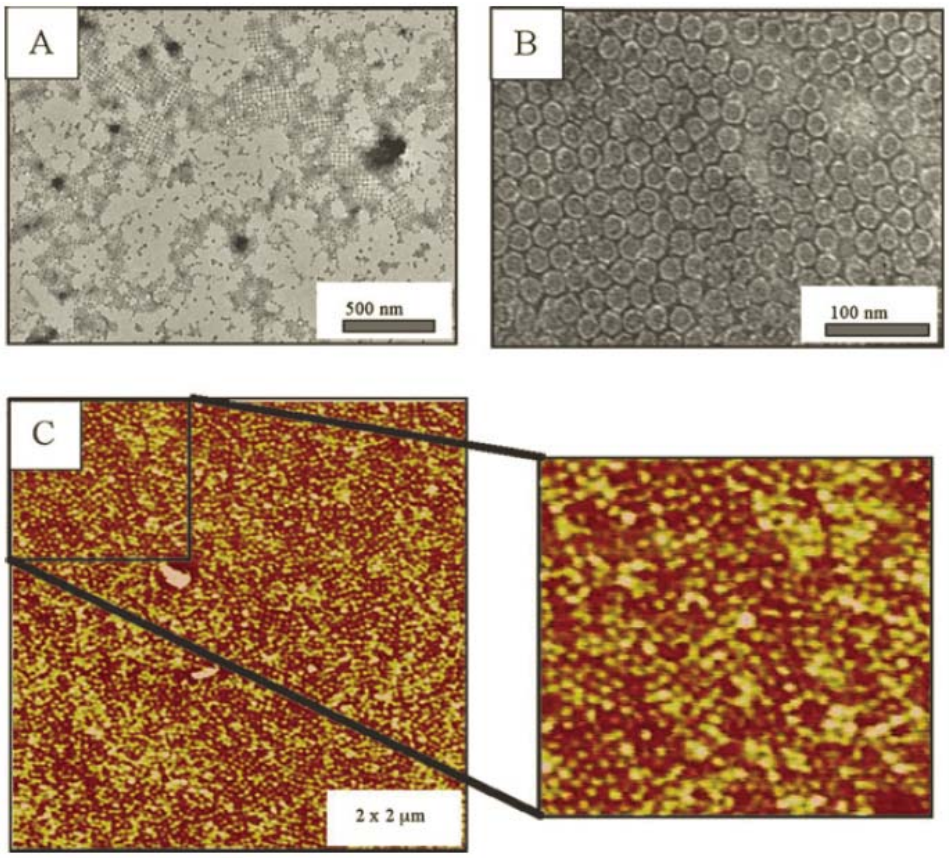

Figure 9.8. *TEM and AFM micrographs. A and B: electron micrographs of CCMV-PB stained with ammonium molybdate, showing hexagonal patterns. C: AFM micrographs.*

Also, AFM experiments were performed on the last set of examples. The AFM micrograph in Figure 9.8C was obtained by incubating a hydrophilic mica surface with the CCMV Prussian blue nanoparticles. The same arrangement of virus particles as observed in Figure 9.8 A,B can be seen. The magnetic properties of these particles are currently under investigation.

9.3 Conclusions

In this chapter, we have shown that monodisperse Prussian blue nanoparticles can be prepared inside the capsids of CCMV by mixing capsid protein (CP) with the Prussian blue precursors at pH 7.5 followed by acidification of the sample to pH 5.0 and irradiation with visible or UV light. FPLC, in combination with UV-VIS analysis have provided unambiguous evidence for this. The purification of these bio-inorganic particles by Sephadex column chromatography was very straightforward and the procedures could probably be scaled up without problems. Preliminary experiments suggest that simply incubating the intact capsid (at pH 5.0) with the Prussian blue precursors, followed by irradiation yields the same results as incubation at high pH followed by the closing of the capsid by addition of acid.

Electron microscopy has revealed that an electron dense inorganic species of 18 nm diameter was confined within the CCMV capsid. Electron microscopy also revealed that the biohybrid species organize themselves in certain patterns on a surface. This process, which yielded both hexagonal and cubic structures, seems to be dependent on the presence of ammonium molybdate [$(NH_4)_6Mo_7O_{24}.4H_2O$] as a staining agent, although this requires further study. Atomic force microscopy also showed the presence of hexagonal and cubic patterns on a mica surface, suggesting that the self organization is independent of the type of surface. The determination of the magnetic properties of the biohybrid particles is currently under investigation.

An interesting possibility is to align the particles under the influence of a magnetic field, forcing them further into a lattice structure. A disadvantage is that Prussian blue only becomes ferromagnetic at temperatures lower than the Curie temperature, which is ca. 5K, depending on the size of the particle. Other molecular magnetic materials may be better suited for this alignment. Investigations along this line are ongoing.

9.4 Experimental section

9.4.1 General experimental procedures

All FPLC chromatograms were taken using buffers of the following composition: 50 mM sodium acetate or Tris-HCl, 500 mM NaCl, and 1mM DTT at pH 7.5 (Tris) or pH 5.0 (sodium acetate). The column was a Superose 6 3/100 column (Amersham biosciences) with a 20 μL injection volume. In some cases, the injection loop was changed to 100 μL in order to be able to purify more of the virus. Sephadex 100 columns were prepared according to the manual of the manufacturer and run with identical buffers as the FPLC. Spin dialysis Eppendorfs were obtained from BIORAD and had a molecular weight cut off of 3,000. All chemicals used for the preparation of buffers were of analytical quality, and buffers were prepared from ultrapure (MilliQ) water. UV-VIS spectra were recorded on a Cary 50 UV-VIS spectrophotometer, for which appropriate baselines were measured first. Transmission Electron Microscopy (TEM) was performed as follows: a copper TEM grid which was coated with Formvar (polyvinylformate) was subsequently provided with a hydrophylic layer of carbon in a glow discharge apparatus and 5 μL of the desired sample was applied onto the grid. After leaving the sample for 1 min., excess liquid was drained off using a scrap of filter paper. 1 μl of ammonium molybdate (5% w/v) or uranyl acetate (5% w/v) was then applied and the drying procedure was repeated.

9.4.2 Preparation of Prussian blue precursors

Ammonium iron (III) oxalate ($(NH_4)_3[Fe(C_2O_4)_3]$. $3H_2O$ (2.57 g, 6 mmol) was dissolved in hot MilliQ grade water (3 ml, 50^oC) and to this solution, K_3FeCN_6 (0.98 g, 3 mmol) was added. The mixture was vigorously stirred for 40 min. and sonicated for 2 min. at this temperature. The mixture was cooled in the dark and subsequently filtered to remove the precipitated $K_3Fe(C_2O_4)$ from the solution. Before use, the mixture was centrifuged at 13,000 rpm in a bench top centrifuge for 10 min. to remove any residual solid.

9.4.3 Preparation of Prussian blue nanoparticles in CCMV capsids

To a solution of CCMV CP (200 μL, 4 mg/ml in pH 7.5 0.1 M Tris buffer, 0.5 M NaCl), the Prussian blue precursor solution was added (20 μL) resulting in a solution containing 0.1 M precursor components. The mixture was slowly acidified with several drops of 0.2 M acetic acid solution. Alternatively, the mixture was dialyzed against a pH 5.0 acetic acid (0.01 M) buffer containing 0.5 M NaCl. This appeared not to be a successful procedure due to the almost complete removal of the iron salts. Later experiments showed that the capsid particles were permeable to the low molecular weight precursors, so that simple incubation at pH 5.0 was sufficient for the preparation of the capsids with the incorporated precursor compounds. The mixture was then irradiated with a high powered (200 W) conventional desk lamp or with a 405 nm laser. The latter procedure proved to be more efficient. Subsequently, after the photochemical reaction, all samples were centrifuged for 15 min. at 13,000 rpm in a desk-top centrifuge and analyzed by FPLC. The attempted separation with spin-dialysis Eppendorfs vials turned out to be unsuccessful; the dark-blue solution was placed on a centrifugation device that had been flushed with pH 5.0 buffer two times before use. After 20 min. of gentle centrifugation, the eluate did not show any capsid. Further elution and longer centrifugation times did not lead to improvement. The most efficient preparation of the Prussian blue nanoparticles in the CCMV capsid is therefore as follows: the Eppendorf containing the pH 5.0 CP solution in the presence of the Prussian blue precursors was irradiated with the 405 nm laser for 1 h. Thereafter, the Eppendorf vial was centrifuged at 10,000 rpm in a desktop centrifuge for 3 min., and irradiated once more. This sequence was repeated twice and the sample was transferred to a preparative Sephadex G-100 column (approximately 8 mm in diameter and 15 cm long), and this column was eluted with the pH 5.0 buffer. A very distinct separation was observed between the Prussian blue containing capsids and the green low-molecular weight precursor components, which eluted much later.

9.5 Notes and references

[1] S. Deka and P.A. Joy, *Materials Chemistry and Physics* **2006**, *100,* 98 and references stated therein.

[2] a) K.J. Klabunde (ed), R.S. Mulukutla in *Nanoscale Materials in Chemistry,* Wiley-interscience, New York, **2001**; b) B.F.G. Johnson, *Top Catal.* **2003**, *24*, 147.

[3] J. Turkevich, P.S. Stevenson and J. Hillier, *Discuss. Faraday Soc.* **1951**, ***5***, 209.

[4] B.L. Cushing, V.L. Kolesnichenko and C.J. Connor, *Chem. Rev*, **2004**, *104*, 3893.

[5] L.L. Hench and J.K. West, *Chem. Rev*. **1990**, *90*, 33.

[6] V. T. Liveri, in *Nano-surface chemistry*, M. Rosoff (ed); Dekker, New York, **2001**.

[7] R.C. Hedden, B.J. Bauer, A.P. Smith, F. Gröhn and E. Amis, Polymer, **2002**, *43*, 5473.

[8] P.H. Zhou and D.S. Zue, *J. App. Phys* **2004**, *96*, 610.

[9] a) S. Ferlay, T. Mallah, R. Ouahès, P. Veillet and M. Verdaguer, *Nature* **1995**, *378*, 701 ; b) S. Ohkoshi, Y. Abe, A. Fujishima and K. Hashimoto, *Phys. Rev. Lett.* **1999**, *82*, 1285.

[10] W.D. Griebler and D. Babel, *Z. Naturforschung,* **1982**, *87b*, 832.

[11] M. Verdaguer, A. Bleuzen, V. Marvaud, J. Vaissermann, M. Seuleimann, C. Desplanches, A. Scuiller, C. Train, R. Garde, G. Gelly, C. Lomenech, I. Rosenman, P. Veillet, C. Cartier and F. Villain, *Coord. Chem. Rev.* **1999**, 190.

[12] a) S. Ravaine, C. Lafuente and C. Mingotaud, *Langmuir* **1998,** *14*, 6347 ; b) R. Saliba, B. Agricole, C. Mingotaud and S. Ravaine*, J. Chem. Phys. B* **1999**, *103*, 9712.

[13] S. Vaucher, M. Li and S. Mann, *Angew. Chem.* **2000**, *112*, 10.

[14] F. C. Meldrum, V. J. Wade, D.L. Nimmo, B. R. Heywood, S. Mann, *Nature* **1991**, *349*, 684.

[15] R. Elghanian, J.J. Storhoff, R.C. Mucic, R. L. Letsinger and C.A. Mirkin, *Nature* **1996**, *382*, 607.

[16] E. Dujardin, C. Peet, G. Stubbs, J. N. Culver and S. Mann, *Nano Lett.* **2003**, *3*, 413.

[17] Y. Roh, R. J. Lauf, A. D. McMillan, C. Zhang, C. J. Rawn, J. Bai and T. J. Phelps, S*olid State Comm.* **2001**, *118*, 529.

[18] B.I.A. McInnes, C.E. Dunn, E.M. Cameron and L.J. Kameko, *Geochem. Explorer* **1996**, *57,* 227.

[19] T. Douglas and M. Young, *Nature* **1998**, *393,* 152.

[20] M. Allen, J.W.M. Bulte, L. Liepold, G. Basu, H.A. Zywicke, J.A. Frank, M. Young and T. Douglas, *Magnetic Resonance in Medicine* **2005**, *54,* 807.

[21] M. Arif Hayat, *Principles and Techniques of electron microscopy* **2000**, Cambridge University Press, ISBN 0521632870; see also Chapter6.

[22] J.E. Johnson and J.A. Speir, *J. Mol. Biol.* **1997**, 665.

Summary

This thesis describes experiments in the area of supramolecular chemistry, involving the Cowpea Chlorotic Mottle Virus (CCMV) and various polymers and inorganic compounds. CCMV exhibits, like most viruses, a highly organised structure. It is a plant virus consisting of 180 identical protein subunits, which form a spherical architecture that encapsulates RNA. The protein subunits are arranged in a pattern with icosahedral symmetry and the viral structure is highly conserved. One important property of the virus is its possibillity to disassemble into separate protein subunits and RNA. The RNA can be separated from the protein, and the protein subunits can be re-assembled into similar structures as the natural virus. This opens the way to include foreign species into the virus.

Up to now, most studies on viruses have focused on their morphology and their interaction with living matter. Only recently, it was realized that viruses can be seen as monodisperse (bio-) nanoparticles. As a result, scientists working in the areas of supramolecular chemistry and nanotechnology are now using the viral structure as a template for the preparation of new nanoscopic architectures.

Chapter 1 is an introductory chapter in which the scope of this thesis is placed in a broader perspective and the initial goal of the work is explained. The latter involves the construction of a so-called mega amphiphile or mega-surfactant containing a virus particle as head group and a large hydrophic polymer as tail. To this end a block-copolymer composed of a hydrophobic and a negatively charged domain will be co-assembled with the separate protein subunits of the CCMV, the idea being that the virus particle will assemble specifically around the negatively charged domain of the block-copolymer.

In Chapter 2 the CCMV is introduced and an overview of the literature, in which the virus is studied as a nanoscopic particle instead of as a pathogen, is presented. The assembly and disassembly mechanisms are discussed, as well as the various methods that have been reported in the literature for the modification of the viral structure.

Chapter 3 describes the preparation of novel polyisocyanides that can be used, at least in principle, for the construction of the above mentioned mega amphiphile. Given the size of the (virus) headgroup of the mega amphiphile long and bulky polymers with hydrophobic properties are required. Several polyisocyanides with apparent molecular weights of more than 3 million have been prepared.

In Chapter 4 the synthesis of polystyrene sulfonate polymers equipped with a fluorescent group by Atom Transfer Radical Polymerization (ATRP) is described. The idea is that the CCMV protein molecules can assemble around such negatively charged polymers and block-copolymers, because the inside of the virus is positively charged Much attention has been given to the preparation of a suitable fluorescent initiator for the ATRP reaction and to the polymerization conditions. Also the deprotection and purification of the polymer have been studied in detail.

Since it was envisaged that the structure of the polymer would have a great influence on the assembly behaviour of the CCMV protein subunits several negatively charged polymers with varying architectures were synthesized. The results of these studies are described in Chapter 5. These architectures include a star-shaped polystyrene sulfonate, which was prepared by using a tetra- functional porphyrin initiator. Also, attempts to synthesize high molecular weight block copolymers *via* modular block coupling are reported. This chapter futhermore describes an architecture in which a protein is covalently attached to a polystyrene sulfonate polymer.

In Chapter 6 studies on the interaction of homopolymers of polystyrene sulfonate (prepared according to methodologies described in Chapter 4) with the CCMVsubunits are presented. The most relevant conclusions of these studies are that self assembly of the CCMV protein molecules around a polystyrene sulfonate species leads to particles with a smaller diameter than the particles of the natural virus. The influence of the stoichiometry and the molecular weight of the polymer on the virus assembly has been investigated and the results indicate that, regardless of the molecular weight of the polymer, the same smaller particle is obtained. It was shown that high polymer to CCMV protein ratios inhibit particle formation. The obtained polystyrene-CCMV particles were studied by electron microscopy and chromatographic methods, and it was shown that the polymer is incorporated into the virus particle.

Chapter 7 describes similar experiments as reported in Chapter 6, but now with polymers of different architectures. In general , the obtained particles are smaller than the natural virus particle. However, due to the increased hydrophobic character of some of the polymers, often precipitation of the protein was observed.

Attempts to photopolymerize a styrene sulfonate monomer within the cavity of the CCMV are discussed in Chapter 8. It was envisaged that the polymerization reaction inside

the nanoscopic shell of the virus might be influenced by the spatial confinement. Although several polymerization routes were explored, no evidence of a succesful polymerization could be obtained.

Finally, in Chapter 9, the preparation of monodisperse inorganic nanoparticles using CCMV as a template is described. To this end, a solution containing Prussian Blue precursor salts was encapsulated into the CCMV capsules and irradiated. This led to the formation of Prussian Blue nanoparticles of well defined size (18 nm) incorporated inside the CCMV.

Samenvatting

Dit proefschrift beschrijft experimenten die zijn uitgevoerd op het gebied van de supramoleculaire chemie, waarbij gebruik gemaakt is van het Cowpea Chlorotic Mottle Virus (CCMV) en diverse polymeren alsmede anorganische verbindingen. CCMV is, zoals veel andere virussen, sterk georganiseerd, waarbij 180 identieke eiwitmoleculen zich spontaan assembleren tot een bol-achtige structuur met icosahedrale symmetrie, waarin het genetische materiaal, RNA, zit opgesloten. Een belangrijke eigenschap van het virus, waarvan in dit onderzoek gebruik gemaakt wordt, is de mogelijkheid om het *in vitro* te ontleden in de samenstellende eiwitten en het RNA. De eiwitten kunnen van het RNA worden gescheiden en op eenvoudige manier opnieuw worden geassembleerd in deeltjes met een vergelijkbare structuur als het virus.

In het verleden is het meeste onderzoek aan virussen uitgevoerd met als doel het bestuderen van de morfologie van deze deeltjes en hun interacties met levend materiaal, de pathologie. Het idee, dat virussen kunnen worden gezien als monodisperse (bio)nanodeeltjes, is pas recentelijk opgevat. Daarom worden virussen op dit moment door onderzoekers op het gebied van de supramoleculaire chemie en door nanotechnologen meer en meer gebruikt om nieuwe nanoscopische structuren te maken.

In hoofdstuk 1 is gepoogd het onderzoek, dat in dit proefschrift is beschreven, in een breder perspectief te plaatsen. Ook wordt in dit hoofdstuk het oorspronkelijke doel van de studie nader toegelicht, namelijk de constructie van een z.g.n. mega-amfifiel (een zeep-achtige verbinding), opgebouwd uit een virus en een lang polymeer. Hiervoor moet een blokcopolymeer, samengesteld uit een hydrofoob en een negatief geladen segment, worden samengebracht en geassembleerd met de afzonderlijke viruseiwitten. Het idee hierbij is dat het virusdeeltje zich zal groeperen rond het negatief geladen gedeelte van het blokcopolymeer en zo het mega-amfifiel zal vormen.

Het CCMV wordt in Hoofdstuk 2 beschreven , en de literatuur, waarin het virus wordt wordt toegepast als nanoscopisch deeltje (en niet als pathogene verbinding) wordt besproken. De verschillende assemblage- en de-assemblage-mechanismen, die zijn voorgesteld voor het CCMV, worden hierbij in ogenschouw genomen. Ook passeren diverse technieken, waarbij het deeltje wordt gemodificeerd, de revue.

Hoofdstuk 3 beschrijft de synthese van nieuwe hydrofobe polymeren van isocyaniden, die mogelijk gebruikt kunnen worden voor de constructie van het bovengenoemde mega-amfifiel. Gezien de relatief grote omvang van de virale structuur zijn hiervoor lange polymeren nodig . De syntheses van verschillende polymeren van isocyaniden met een molecuulgewicht van meer dan 3 miljoen, worden in dit hoofdstuk beschreven.

Een belangrijke kenmerk van het CCMV is het feit dat de binnenzijde van het virus positief geladen is. Deze positieve lading zorgt voor een attractieve interactie met het negatief geladen RNA. Omdat het doel van het onderzoek ondermeer de bestudering van de zelf-assemblage van viruseiwitten rondom het negatieve gedeelte van een amfifiel blok-copolymeer is, werd besloten om in eerste instantie de interactie van een negatief geladen homopolymeer met deze eiwitten te bestuderen. De synthese van zo'n polymer, namelijk polystyreensulfonaat voorzien van een fluorescerende groep, wordt in hoofdstuk 4 beschreven. Voor de bereiding van het polymeer is gebruik gemaakt van Atom Transfer Radical Polymerization (ATRP). Er wordt veel aandacht besteed aan de synthese van een geschikte fluorescente initiator, alsook aan de manier waarop de polymerisatie moet worden uitgevoerd en onder welke reactiecondities. Verder krijgt de ontscherming en opzuivering van het negatief geladen fluorescente polymeer de nodige aandacht.

Het is te verwachten dat de structuur van het polymeer van invloed is op het assemblagegedrag van de CCMV-eiwitten. Met het oog hierop zijn negatief geladen polymeren met een uiteenlopende structuur gesynthetiseerd. Dit onderzoek wordt in hoofdstuk 5 beschreven. Zo is een sterk fluorescente, ster-vormig polystyreensulfonaat gesynthetiseerd door gebruik te maken van een viervoudig-functionele porfyrine initiatorverbinding. Ook worden in dit hoofdstuk pogingen beschreven om via een modulaire aanpak blok-copolymeren met een hoog molekuulgewicht te synthetiseren. Tenslotte omvat het hoofdstuk een studie betreffende de synthese van een bio-hybride polymeer, opgebouwd uit een eiwit, dat covalent gekoppeld is aan polystyreensulfonaat.

Hoofdstuk 6 heeft als onderwerp de interacties tussen polystyreensulfonaat (de synthese hiervan is beschreven in hoofdstuk 4) en de manteleiwitten van het CCMV. De meest opvallende conclusie van dit onderzoek is dat de assemblage van de eiwitten rondom de negatief geladen polymeermoleculen leidt tot een virusdeeltje met een kleinere afmeting dan dat van het natuurlijke virus. De invloeden van de stoichiometrie en het molekuulgewicht op het assemblageproces zijn onderzocht en het blijkt dat deze geen effect hebben op de

grootte van het virusdeeltje. Bij grote overmaat aan polystyreensulfonaat wordt de vorming van de deeltjes geremd, zoals ook het geval is wanneer het polystyreensulfonaat een zeer hoog molekuulgewicht heeft. De verkregen virusdeeltjes zijn bestudeerd met elektronenmicroscopie en chromatografische methodieken en er kon bewezen worden dat het polymeer opgesloten zit in de virus-eiwitstructuur.

In hoofdstuk 7 worden experimenten beschreven, die vergelijkbaar zijn met die in hoofdstuk 6, maar nu met negatief geladen polymeren, die een andere structuur bezitten (zie hiervoor hoofdstuk 5). In het algemeen worden dezelfde typen virusdeeltjes waargenomen als beschreven in hoofstuk 6, namelijk deeltjes met een kleinere afmeting dan die van het natuurlijk voorkomende virus. Een nadeel is dat door het grotere hydrofobe karakter van sommige van de polymeren vaak precipitatie van de viruseiwitten plaatsvond.

Hoofstuk 8 beschrijft pogingen om een fotopolymerisatie uit te voeren in de holte van het lege CCMV deeltje. Doel was te onderzoeken of de polymerisatiereactie zou worden beïnvloed door de beperkte ruimte in het virusdeeltje. Om dit te bereiken werden diverse negatief geladen monomeren ingesloten in de virusmantel, waarna er bestraling met UV-licht plaatsvond. Hoewel er verscheidene pogingen zijn ondernomen, kon er geen bewijs worden gevonden voor een succesvolle polymerisatiereactie.

Als laatste wordt in hoofdstuk 9 een onderzoek beschreven naar de bereiding van monodisperse, anorganische nanodeeltjes met gebruikmaking van het CCMV als template. Een oplossing bestaande uit reagentia die bij bestraling met UV-licht Pruisisch Blauw vormen, werd ingesloten in de CCMV capsule en bestraald. Dit leidde tot de vorming van nanodeeltjes met een afmeting van 18 nm, welke waren opgesloten in de virus-capsule.

Dankwoord

Zoals het een fatsoenlijk proefschrift betaamt, volgt aan het einde ervan een dankwoord. Om te beginnen uiteraard mijn dank richting Roeland Nolte voor het aannemen van een student uit Leiden die eigenlijk niks met polymeerchemie of met supramoleculaire chemie te maken had gehad. Mijn directe begeleider, Jeroen Cornelissen, heeft eigen initiatief en vrijheid altijd hoog in het vaandel gehad, waarvoor dank, maar was ook altijd bereid om te sparren (is dit een goed woord?) over de materie wanneer dat noodzakelijk was. Een compleet nieuwe richting is met dit onderzoek opgestart, wat nog al eens voor eigenaardige problemen zorgde. Bijvoorbeeld, op welke locatie gaan wij een broeikas inrichten waarin wij onze plantjes gaan laten groeien? Voor het opzetten van dit virus-onderzoek is Marta onmisbaar geweest. Hoewel op dit moment het groeien van de planten en de isolatie van het virus relatief eenvoudig is, heeft zij verreweg het grootste deel daarvan voor haar rekening genomen. Martin, bedankt voor de steun bij de neutronenbegeleiding! Désirée, Jacky en Peter, zonder jullie steun was het een stuk ingewikkelder geworden. Alan, talks with you were always interesting. Veel heb ik veel gehad aan mijn studenten, Martijn, en Isabel. I hope that everything in Spain is fine!

Voorts gaan alle collega's, waarvan er nu veel tot mijn vriendenkring horen, mij aan het hart. Lee en Hefziba, (mooi hoe veel vrienden tegenwoordig samenwonen), Dennis en Paula, Matthijs en Irene (nog gefeliciteerd met jullie huwelijk!), Hans en Sandy, Dani en Daniel, Michal, Kasper, Erik, Joe, Hoogboom, Edward, Paul en iedereen die ik nog vergeet. Vele ander collega's ben ik dankbaar voor hun inbreng (anders 2x input), zowel op inhoudelijk als op sociaal vlak: Capo, Nikos, Henri, Joost, Ton, Pieter, Ruud, Richard, Onno, Heather, Kelly, thanks for all the input, both socially and for the chemistry! Andrès, thanks for all the discussions, including some heated ones!

Alex heb ik gevraagd een van mijn Paranimfen te zijn… Wie weet wat voor vragen ik aan je ga doorspelen! Mijn andere paranimf Victor, dank je wel voor alles, dude.

Mijn andere vrienden in Leiden waren altijd bereid om een biertje te pakken als ik ernaartoe (naar deze stad?) ging, bedankt voor alle gezelligheid, mannen! We moesten snel maar weer eens een lang weekend op reis. Ik kom ook weer snel eens een casino-clusje draaien.

Sinds januari 2008 werk ik bij KEMA Nederland, bij een afdeling die zich voornamelijk bezighoudt met innovatie. Alle collega's bedankt! Het is een zeer vruchtbaar jaar geweest, met door de week energieinnovatie en in het weekend soft-matter-chemie.

Toute la Famille Française, merci pour les week-ends; Francoise, tu prends soin de ma petite fille n'importe quand on demande, merci pour ça ! Gros bisous á Mamie Jeanne. Jean-Luc, tu nous prêtes ta maison dans les vacances, c'est génial pour l'été, doeidoei ! Cees, veel geluk in Hongarije.

Carla, Doetze, Arjan, Wouter en Lizeth, mijn famiglia, jullie hebben mij altijd gesteund in de keuzen die ik maakte, waarvoor dank. Veel liefs aan allen.

Uiteindelijk mijn twee kleine meisjes, Aurélie en Inès. Heerlijk om zo samen met de liefdes van mijn leven te zijn! Op dit moment is een tweede meisje onderweg, en aan mijn beide dochtertjes (een stoeiend op de bank, de ander stoeiend in mama's buik) draag ik dit werk op.

Curriculum Vitae

Friso Doetze Sikkema werd op 27 juli 1976 geboren in Ellecom, Gelderland. Hij bezocht het Thomas á Kempis college in Arnhem, waar hij in 1995 zijn VWO-diploma behaalde. Na een korte uitstap Technische Natuurkunde in Delft, begon hij in september 1996 aan de studie Scheikunde in Leiden. Naast zijn studie is Friso actief lid geweest van de studentenvereniging Augustinus. Van 1999 tot 2001 heeft hij een onderzoeksproject uitgevoerd bij de groep Bio-Organische Chemie van de onlangs overleden Prof. Dr. J.H. van Boom; de groep staat tegenwoordig onder leiding van Prof. Dr. H. Overkleeft en Prof. Dr. G. A. van der Marel. In dit onderzoek, dat in samenwerking met Unilever Research werd uitgevoerd, werd onderzocht op welke wijze de Mitsunobu-reactie kan worden aangewend in de synthese van suiker-aminozuuradducten. De studie heeft geresulteerd in twee publicaties en een afstudeermanuscript met als titel: “Use of the Mitsunobu reaction and nitrobenzenesulfonamide activated amino acids in organic synthesis”.

Na het behalen van zijn doctoraal-diploma Scheikunde in 2003 is Friso begonnen met zijn promotieonderzoek aan virusdeeltjes in de groep van Prof. Dr. R.J.M. Nolte. De resultaten van dit onderzoek worden in dit proefschrift beschreven.

Sinds januari 2008 is Friso Sikkema werkzaam bij KEMA Nederland, waar hij betrokken is bij innovaties op het gebied van energie. Hij is daar momenteel leider van diverse projecten.

List of publications

Friso D. Sikkema, Isabel Ayora González, Jeroen J.L.M. Cornelissen and Roeland J.M. Nolte, Well-defined heterotelechelic poly(p-styrenesulfonate) synthesised by atom transfer radical polymerization for the preparation of a bioconjugate, *submitted*.

Andrès de la Escosura, Martijn Verwegen, Friso D. Sikkema, Marta Comellas-Aragonès, Andrei Kirilyuk, Theo Rasing, Roeland J. M. Nolte and Jeroen J. L. M. Cornelissen, Viral capsids as templates for the production of monodisperse Prussian blue nanoparticles, *Chem. Commun*., **2008**, 1542–1544.

J.J.L.M. Cornelissen, I.C. Reynhout, A.J. Dirks, F.D. Sikkema, M. Comellas Aragones, A. de la Escosura Navazo, R.J.M. Nolte, Virus capsid proteins as building blocks for nanoreactors and new materials, *PMSE*, 97, 299, **2007**

Friso D. Sikkema, Marta Comellas-Aragonès, Remco G. Fokkink, Benedictus J. M. Verduin, Jeroen J. L. M. Cornelissen and Roeland J. M. Nolte, Monodisperse polymer–virus hybrid nanoparticles, *Org. Biomol. Chem.*, **2007**, *5*, 54–57**.**

John J. Turner, Friso D. Sikkema, Kees Erkelens, Gijs A. van der Marel, Herman S. Overkleeft, Jacques H. van Boom and Mark Overhand, Novel Reversed Chain Modified Oligopeptides via Sequential α-N-Mitsunobu Condensation of a Functionalized C-glycoside, *Chemistry Letters,* **2004**, *33*, 468.

J.J. Turner, F.D. Sikkema, D.V. Filippov, G.A. van der Marel, J.H. van Boom, Synthesis of β-Lactams via Ring Opening of a Serine Derived Aziridine, *Synlett* **2001,** 1727–1730.